THE MARINE BIOGEOCHEMISTRY OF MOLYBDENUM

By

Caroline Beth Tuit

B.S., Chemistry and Geology
Beloit College, 1996

Submitted in partial fulfillment of the requirement for the degree of

Doctor of Philosophy

at the

MASSACHUSETTS INSTITUTE OF TECHNOLOGY
and the
WOODS HOLE OCEANOGRAPHIC INSTITUTION

February, 2003

Signature of Author

_____

Joint Program in Marine Geology and Geophysics
Massachusetts Institute of Technology and
Woods Hole Oceanographic Institution
January, 2003

Certified by

_____

Gregory E. Ravizza
Assistant Professor Geology and Geophysics
SOEST-University of Hawaii
Thesis Supervisor

Accepted by

_____

Daniel C. McCorkle
Chair, Joint Committee for Marine Geology and Geophysics
Woods Hole Oceanographic Institution

THE MARINE BIOGEOCHEMISTRY OF MOLYBDENUM

by

Caroline B. Tuit

Prevailing wisdom holds that the vertical distribution of molybdenum (Mo) in the open ocean is conservative, despite Mo's important biological role and association with Mn oxides and anoxic sediments. Mo is used in both nitrogenase, the enzyme responsible for N_2 fixation, and nitrate reductase, which catalyzes assimilatory and dissimilatory nitrate reduction. Laboratory culture work on two N_2 fixing marine cyanobacteria, *Trichodesmium* and *Crocosphaera*, and a marine facultative denitrifier, *Marinobacter hydrocarbanoclasticus,* showed that Mo cell quotas in these organisms were positively correlated with Mo-containing enzyme activity. Mo concentrations in *Crocosphaera* dropped almost to blank levels when not fixing N_2 suggesting daily synthesis and destruction of the entire nitrogenase enzyme and release of Mo. *Trichodesmium* cultures, however, retained a pool of cellular Mo even when not fixing N_2. Colonies of *Trichodesmium* collected in the field have Mo:C tenfold higher than seen in culture, these Mo:C ratios were reflected in SPM samples from the same region. Fe:C ratios for Trichodesmium were between 12-160 μmol:mol in field and culured samples. The Fe:C ratio of *Crocosphaera* was established to be 15.8±11.3 under N_2 fixing conditions. Mo cellular concentrations in cultured organisms were too small to significantly influence dissolved Mo distributions, but may slightly affect Suspended Particulate Matter (SPM) distributions. Mean SPM Mo:C ratios were slightly elevated in regions of N_2 fixation and denitrification..

A high precision (±0.5%) isotope dilution ICP-MS method for measuring Mo was developed to re-evaluate the marine distribution of Mo in the dissolved and particulate phase. Mn oxides were not found to significantly influence either the dissolved or SPM Mo distribution. Dissolved Mo profiles from the Sargasso and Arabian Sea were conservative. However, dissolved Mo profiles from the Eastern Tropical Pacific showed both depletion and enrichment of dissolved Mo possibly associated with interaction of Mo with coastal sediments. Dissolved Mo profiles in several California Borderland Basins showed 1-2 nM Mo depletions below sill depth. A more focused study of water column response to sediment fluxes using the high precision Mo analyses is necessary to determine whether these phenomena are related.

Dedication

To my parents

Acknowledgments

Producing a Ph.D. thesis is a long and arduous process that would impossible without the support of friends and colleagues. First, I must thank Greg Ravizza, my advisor, for his patience and support. He has been a wonderful example of scientific generosity, integrity and civility. His boundless enthusiasm and willingness to let me roam far from his usual stomping grounds in pursuit of the interesting question, and to support those travels with multiple grant applications, was critical for the completion of this thesis. I could not have asked for a better mentor, colleague or role model.

I am indebted to the members of my thesis committee, John Waterbury, Jim Moffett, Rob Sherrell, and Ed Boyle. John, in particular has been exceedingly generous with his time, laboratory space and equipment, and his cultures. I want to thank Dan McCorkle for serving as the chair of my defense (and my generals) and for his insightful comments. He has been a source of support and advice throughout my time at WHOI.

I want thank many people from the scientific community. Here at WHOI I have joined working with many groups. The noble metals group (Bernhard Peuker-Ehrenbrink, Tracy Abbruzzese, Jurek Blusztajn, Alberto Saal, and Deb Hassler) is where I started out working on platinum and palladium, and in whose lab I continued to work, gradually filling up as much space as I possibly could. I want to thank them for their patience, and company in the late nights. The Moffett group is where I first learned that microbes are powerful. I want to thank Kathy Barbeau, Liz Kujawinski, and Mak Saito for their friendship, practical assistance and advice. The Waterbury/Webb lab succeeded in turning a geochemist in to a passable (in bad lighting) microbiologist. Freddie Valois always knew where whatever that thing was and Eric Webb has been a great sounding board and source of advice. This thesis would not have been possible with out the many colleagues who gave me samples (Chris Measures and Sue Vink, Eric DeCarlo and Maureen Conte), lent me equipment (Alan Fleer, Joe Bonaventurra helped me with analyses (WHOI ICP-MS facility, VIMS Analytical Services Center, Julie Palmieri, Matt

Allen, and Tom McCollum) or allowed me to hitch a ride on their cruises (Jim Moffett, Mark Altabet, Joe Montoya, Chuck Fisher).

I want to thank the Joint Program students that have supported me throughout out the last 6 years. Those students who came be for me and showed it could be done: Kirsten, Claudia, Mak, Kathy, Liz, Anne and Jen. I am truly appreciative of my housemates and office mates through the years Jen, Danny, Matt, Sherri and Carolyn and Mark Behn,my one and only classmate. Thesis Support (Ana, Anna and Joanna) provided the outlet this last year much less grueling. Ana, Mike, Carolyn and Robyn were life saviors during the final printing and collating battle.

I am particularly grateful to my parents, Mom and Rollie and Dad and Rhoda for their love, encouragement and pride. My sister Lisa and brother-in-law James have been great mentors throughout my graduate education. They have set an example of scholarship to which I only hope to aspire. I need to thank Matt for his love and understanding. I have treasured our time together.

This work was funded by a grant from the National Science Foundation (#OCE-0096453) and the WHOI Academic Programs Ocean Ventures Fund. I have also been supported through WHOI by a NSF coastal traineeship #DGE-9454129, by the US GS Cooperative Agreement #USGS-00HQAGOO1 and by WHOI Academic Programs.

TABLE OF CONTENTS

LIST OF TABLES

TABLE OF FIGURES

CHAPTER 1. INTRODUCTION TO THE MARINE BIOGEOCHEMISTRY OF MOLYBDENUM

1.1 Preface

Molybdenum (Mo) is an essential micronutrient, required in a variety of enzymes that catalyze oxygen transfer reactions such as nitrate reduction, as well as nitrogen fixation (Stiefel 1996). Despite its important biological role, Mo has been classified as a conservative element in seawater, similar to the major salts. This classification is based on early studies of the distribution of Mo in the Atlantic and the Pacific, which determined that the Mo concentration in seawater was extremely high (107 nM) and invariant with salinity (Collier 1985; Morris 1975; Prange and Kremling 1985). Collier (1985) saw salinity normalized Mo concentration variations in the upper 300m suggestive of Mo cycling but because these variations were not resolvable at 4-sigma level he concluded that the profiles were conservative. These early studies of Mo in seawater had measurement uncertainties (2.5 to 10 nM) larger than the total concentration range of many biologically critical trace metals (Fe, 0-1 nM ;Zn, 0-10 nM ;Cd, 1-1.2 nM). These high measurement uncertainties may have obscured any biological signature. The high concentration of Mo and its perceived conservative behavior has led to a lack of interest in pursuing the biogeochemical role of Mo in the surface ocean.

The goal of this thesis was to seek evidence of non-conservative behavior of Mo in seawater and to determine what, if any, effect biological utilization has on Mo distribution in seawater. Chapter 2 describes a high precision method for determining Mo concentration in seawater as well as methods for determining trace quantities of Mo, Rb, Mn, Fe, and Al in microbial cells and marine suspended particulate matter. Chapter 3

applies the Mo seawater method to a survey of 13 water column profiles from the Arabian Sea, Sargasso Sea and Eastern Pacific Ocean. Chapter 4 examines diel Mo cycling in 2 nitrogen fixing cyanobacteria, *Trichodesmium erythaeum* and *Crocospheara watsonii*, in response to nitrogen fixation activity. Chapter 5 reports the Mo concentration of suspended particulate matter in regions influenced by Mo enzyme activity. And finally, experiments comparing Mo cellular concentration during growth on oxygen and nitrate for a facultative marine denitriying bacterium, *Marinobacter hydrocarbanoclaticus*, are presented in Appendix 1.

Table 1.1 Marine Molybdenum Budget (after Morford and Emerson 1999)

	Mo Flux (10^8 mol yr^{-1})	References
Sources		
River	1.8	(Martin and Meybeck 1979)
Dust	n	
Continental Margin Sediments (O_2 penetration †1 cm)	0.08-0.17	(Morford and Emerson 1999)
Hydrothermal	n	
TOTAL SOURCES	**1.88-1.97**	
Sinks		
Oxic Sediments (Carbonates and red clays)	0.9	(Bertine and Turekian 1973)
Continental Margin Sediments (O_2 penetration †1 cm)	n	
Anoxic Sediments	0.2-0.8	(Bertine and Turekian 1973; Manheim 1974)
Mn nodules and metalliferous sediments	n	(Manheim 1974)
Hydrothermal	0.04 0.17	(Trefry et al. 1994)
TOTAL SINKS	**1.1-1.9**	

n=negligible

1.2 Molybdenum Geochemistry

The marine geochemical cycle of molybdenum was first examined by Bertine and Turekian (1973) and Emerson and Huested (1991) and most recently by Morford and Emerson (1999). Rivers provide the major source of Mo to the oceans, the oceanic residence time based on the riverine flux is 800 kyr (Morford and Emerson 1999). Anoxic sediments, though only 0.3% of the total oceanic area, are a major sink for Mo, accounting for up to 40 % of the total Mo riverine input. Sedimentary Mn oxides, which cover a much larger geographic range, are a less understood Mo sink. Mo is scavenged from bottom waters into the sedimentary Mn oxide cap. However, upon sediment burial, Mn oxide reduction remobilizes Mo to the pore waters. In the pore waters, Mo either diffuses downwards to be precipitated in the anoxic portion of the sediments or upwards where it is either scavenged again by Mn oxides or if the Mn oxides cap is thin enough (depth of O_2 penetration in sediments $\leq$ 1 cm: Morford and Emerson 1999) Mo can escape back into bottom waters. These reducing sediments (O_2 penetration $\leq$ 1 cm) are generally found on continental margins. It is possible that variations in bottom water redox conditions could lead to rapid release of Mo to bottom waters due to Mn oxide reduction.

Mn oxide cycling can influence the distribution of trace elements in the water column as well as in pore waters and sediments. Though Mo is generally not scavenged by particles in the water column, it is strongly associated with Mn oxides in sediments. Many marine Mn oxide nodules, crusts and sediments have a Mn:Mo molar ratio of 1.1 x 10^{-3} (Manheim 1974; Shimmfield and Price 1986). By extrapolating this ratio to Mn oxides precipitated in the open ocean we can estimate the amount of Mo that could be

removed via Mn oxidation. Rates of Mn oxidation in the Sargasso Sea are less than 0.09±0.01 nM/d at 100 m depth (Sunda and Huntsman 1988) and would not produce resolvable depletions in Mo dissolved concentrations. However, in coastal regions and stratified water columns, rates of Mn oxidation can be several orders of magnitude higher than those seen in the Sargasso (Martin and Knauer 1982; Moffett 1997) and may play a significant role in controlling Mo distributions.

The mechanism controlling Mo incorporation into Mn oxides is unknown. Very recently, data on Mo isotope fractionation in Mn oxides have shown similar fractionations in natural Mn nodules and Mn oxides chemically precipitated in the laboratory, implying that Mo incorporation into Mn oxides is an abiotic process (Arnold and Anbar pers com.). In sediments, Mn oxidation is autocatalytic, the presence of fresh Mn oxide surfaces enhances further Mn oxidation (Hem 1978). Water column Mn oxides, which are formed by microbial precipitation of amorphous Mn oxide on an organic matrix, may not scavenge Mo in the same way.

Mo is also enriched in anoxic sediments. In enclosed basins, such as the Cariaco Trench and Saanich Inlet, sediment Mo concentrations can be as high as 140 $\mu g\ g^{-1}$ and may lead to depletion of water column distributions by 10-30% (Berrang and Grill 1974; Colodner et al. 1995). Mo has been proposed as a tracer of ocean anoxic events in sediment cores (Dean et al. 1999; Emerson and Huested 1991). In the open ocean Mo enrichments in sediments are highest in regions with low oxygen in bottom waters and high organic carbon flux (Zheng et al. 2000). Molybdenum enrichment in anoxic sediments appears to occur primarily at the sediment water interface rather than by a water column process and seems to be related to sulfide availability (Francois 1988; Helz

and Adelson 1997). Zheng et al. (2000) have identified two sulfide thresholds for Mo scavenging by sediments, 0.1 M sulfide likely initiates the coprecipitation of Mo-Fe-S phases and scavenging of Mo by organic matter, and 100 M sulfide seems to initiate direct Mo sulfide precipitation. The first sediment phase seems to be very sensitive to changes in the redox conditions and is easily released to bottom waters if sediments are exposed to higher concentrations of oxygen, causing oxidative burn down (Zheng et al. 2000). The second form of sedimentary Mo may be less labile. Uptake of Mo from sediments can influence water column distributions in anoxic basins but it remains to be seen if uptake and release of Mo from sediments can influence the regional distribution of dissolved Mo in the open ocean.

1.3 Mo Biology

Much effort has been expended in recent years to understand the near surface biogeochemical cycling of limiting trace metals, but very little is understood about how organisms regulate readily abundant micronutrients. When faced with a sufficient supply of a trace metal, organisms have the option of only consuming just enough to satisfy their current needs or to indulge in luxurious consumption. Determining what strategy an organism employs and how the availability of other nutrients affects those strategies relies on evaluating both metal cellular concentrations and enzymatic demands. Mo is an essential micronutrient for most marine phytoplankton and bacteria, but it is not a major player in cellular metabolism. Unlike Fe which is commonly modeled using a single Fe:C ratio (Archer and Johnson 2000; Johnson et al. 1997) Mo:C ratios in marine particulate matter may be determined by specific enzymatic demands that vary

significantly between ocean regions. Whether Mo consumption is luxurious or subsistence level can be determined by comparing measured rates of processes catalyzed by Mo-containing enzymes to Mo cellular concentrations in culture and field samples.

Mo is found in two types of enzymes, 1) those based on a substituted pterin molecule which mediate oxygen transfer reactions (Table 1.1), and 2) nitrogenase, where it resides in the MoFe cofactor. This thesis focuses on the aspects of Mo utilization associated with the N cycle: nitrate reductase, which converts NO_3^- to NO_2^- or NH_3 (Raven 1988), and nitrogenase, the enzyme responsible for reduction of N_2 to NH_3.

Table 1.2 Some oxygen transfer enzymes (Mo pterin cofacter)[a]

Nitrate Reductase	$NO_3^- + 2H^+ + 2e^- = NO_2^- + H_2O$
Sulfite oxidase	$SO_3^{2-} + H_2O = SO_4^{2-} + 2H^+ + 2e^-$
Formate dehydrogenase	$HCOOH = CO_2 + 2H^+ + 2e^-$
CO dehydrogenase	$CO + H_2O = CO_2 + 2H^+ + 2e^-$
Dimethylsulfoxide (DMSO) dehydrogenase	$(CH_3)_2SO + 2H^+ + 2e^- = (CH_3)_2S + H_2O$
Trimethylamine N-oxide reductase	$(CH_3)_3NO + 2H^+ + 2e^- = (CH_3)_3N + H_2O$
Biotin sulfoxide reductase	Biotin sulfoxide $+ 2H^+ + 2e^-$ = biotin $+ H_2O$
Xanthine oxidase	Xanthine $+ H_2O$ = uric acid $+ 2H^+ + 2e^-$

[a](Lippard et al. 1994)

N_2 fixation supports phytoplankton growth in much of the oligotrophic ocean. Its significance is spatially and temporally variable. Some factors that have been identified as important influences on N_2 fixation activity include fixed nitrogen concentrations, surface temperature and Fe availability (Karl et al. 2002). Calculations of Mo requirements based on enzyme activity imply that cells fixing N_2 require significantly more Mo than cells growing on NO_3^- which require more Mo than cells growing on NH_4^+ at the same rate of nitrogen assimilation (Sanudo-Wilhelmy et al. 2001; Sprent and Raven 1985). Estimates of Fe requirements for growth increase in a similar pattern as well (Rueter et al. 1992; Sanudo-Wilhelmy et al. 2001; Sprent and Raven 1985). This could lead to significant enrichment of Mo in suspended particulate matter in regions where N_2

fixation is an important source of fixed nitrogen in surface waters. Current estimates of N_2 fixation are based on indirect measurement of nutrients (Gruber and Sarmiento 1997; Karl et al. 1997; Karl et al. 2002) or direct measurements of N_2 fixation at sea (Lipschultz and Owens 1996). There is significant uncertainty is associated with both these approaches. The most recent studies agree that global N_2 fixation has been grossly underestimated; total estimates of N_2 fixation (100-200 Tg yr^{-1}) now approach estimates of for denitrification (Karl et al. 2002). If Mo concentrations in particulate matter correlate with N_2 fixation, Mo enrichment may provide an alternate method for estimating N_2 fixation rates.

Nitrate reduction, the first step in the denitrification pathway, may also play a role in the biological cycling of Mo. Nitrate reductase is required by all organisms that utilize nitrate as an N source (assimilatory nitrate reduction). It can also be used as an oxidant for ATP generation in oxygen depleted regions (dissimilatory nitrate reduction). The Mo requirement for organisms obtaining N via assimilatory nitrate reduction is less than those relying on N_2 fixation (Flynn and Hipkin 1999; Sanudo-Wilhelmy et al. 2001). However, in suboxic regions of the water column, where dissimilatory nitrate reduction is the primary metabolism, Mo requirements may be much larger than where it is used only in its role for nitrogen assimilation.

The overarching hypothesis of this work is that Mo distribution in seawater is influenced by the biological and geochemical processes described above and therefore should not be considered a conservative element. Additional questions that derive from trying to understand these processes include:

- What is the Mo requirement for N_2 fixation and respiratory nitrate reduction and how are the rates of these processes related to the Mo concentration in cultures and field samples of N_2 fixing and in cultures of denitrifying bacteria?
- Can the flux of Mo to and from anoxic sediments influence the distribution of dissolved Mo?
- Does the Mo and Mn relationship seen in sediments hold for microbially produced authigenic Mn oxides in the water column and if so can the cycling of Mo with Mn oxides affect the distribution of dissolved and particulate Mo?
- Does the Mo content of suspended particulate matter reflect regional importance of Mo-containing enzymatic processes?

The work presented here only just begins to elucidate the marine biogeochemistry of Mo. It will be the work of many researchers and years before we know as much about Mo biogeochemistry as we do for other biologically important trace metals. In the end, I hope this thesis demonstrates that Mo biogeochemistry is a fertile field, long overlooked, that we now have the ability to examine.

1.4 References

Archer, D. E., and K. Johnson. 2000. A Model of the iron cycle in the ocean. Global Biogeochemical Cycles **14:** 269-279.

Berrang, P. G., and E. V. Grill. 1974. The effect of manganese oxide scavenging on molybdenum in Saanich Inlet, British Columbia. Marine Chemistry **2:** 125-148.

Bertine, K. K., and K. K. Turekian. 1973. Molybdenum in marine deposits. Geochimica et Cosmochimica Acta **37:** 1415-1434.

Collier, R. W. 1985. Molybdenum in the Northeast Pacific-Ocean. Limnology and Oceanography **30:** 1351-1354.

Colodner, D., J. Edmond, and E. Boyle. 1995. Rhenium in the Black Sea; comparison with molybdenum and uranium. Earth and Planetary Science Letters **131:** 1-15.

Dean, W. E., D. Z. Piper, and L. C. Peterson. 1999. Molybdenum accumulation in Cariaco Basin sediment over the past 24 k.y.; a record of water-column anoxia and climate. Geology (Boulder) **27:** 507-510.

Emerson, S. R., and S. S. Huested. 1991. Ocean Anoxia and the Concentrations of Molybdenum and Vanadium in Seawater. Marine Chemistry **34:** 177-196.

Flynn, K. J., and C. R. Hipkin. 1999. Interactions between iron, light, ammonium, and nitrate: Insights from the construction of a dynamic model of algal physiology. Journal of Phycology **35:** 1171-1190.

Francois, R. 1988. A study on the regulation of the concentrations of some trace metals (Rb, Sr, Zn, Pb, Cu, V, Cr, Ni, Mn and Mo) in Saanich Inlet sediments, British Columbia, Canada. Marine Geology **83:** 285-308.

Gruber, N., and J. L. Sarmiento. 1997. Global patterns of marine nitrogen fixation and denitrification. Global Biogeochemical Cycles **11:** 235-266.

Helz, G. R., and J. M. Adelson. 1997. Geochemical methods for investigating past changes in Chesapeake Bay. 35.

Hem, J. D. 1978. Redox Processes at Surfaces of Manganese Oxide and Their Effects on Aqueous Metal-Ions. Chemical Geology **21:** 199-218.

Johnson, K. S., R. M. Gordon, and K. H. Coale. 1997. What controls dissolved iron concentrations in the world ocean? Marine Chemistry **57:** 137-161.

Karl, D., R. Letelier, L. Tupas, J. Dore, J. Christian, and D. Hebel. 1997. The role of nitrogen fixation in biogeochemical cycling in the subtropical North Pacific Ocean. Nature **388:** 533-538.

Karl, D. and others 2002. Dinitrogen fixation in the world's oceans. Biogeochemistry **57:** 47-109.

Lippard, S. J., J. M. Berg, and G. Klatt. 1994. Principles of Bioinorganic Chemistry. University Science Books.

Lipschultz, F., and N. J. P. Owens. 1996. An assessment of nitrogen fixation as a source of nitrogen to the North Atlantic Ocean. Biogeochemistry **35:** 261-274.

Manheim, F. T. 1974. Chap. 42. Molybdenum. *In* K. H. Wedepohl [ed.], Handbook of Geochemistry. Springer-Verlag.

Martin, J. H., and G. A. Knauer. 1982. Manganese Cycling in Northeast Pacific Equatorial Waters. Journal of Marine Research **40:** 1213-1225.

Martin, J. M., and M. Meybeck. 1979. Elemental Mass-Balance of Material Carried by Major World Rivers. Marine Chemistry **7:** 173-206.

Moffett, J. W. 1997. The importance of microbial Mn oxidation in the upper ocean: a comparison of the Sargasso Sea and equatorial Pacific. Deep-Sea Research Part I-Oceanographic Research Papers **44:** 1277-1291.

Morford, J. L., and S. Emerson. 1999. The geochemistry of redox sensitive trace metals in sediments. Geochimica et Cosmochimica Acta **63:** 1735-1750.

Morris, A. W. 1975. Dissolved Molybdenum and Vanadium in Northeast Atlantic Ocean. Deep-Sea Research **22:** 49-54.

Prange, A., and K. Kremling. 1985. Distibution of dissolved molybdenum, uranium and vanadium in Baltic Sea waters. Marine Chemistry **16:** 259-274.

Rueter, J. G., D. A. Hutchins, R. W. Smith, and N. L. Unsworth. 1992. Iron nutrition of Trichodesmium., p. 289-306. *In* E. J. Carpenter, D. G. Capone and J. G. Rueter

[eds.], Marine Pelagic Cyanobacteria: Trichodesmium and Other Diazotrophs. Kluwer Academic Publishers.

Sanudo-Wilhelmy, S. A. and others 2001. Phosphorus limitation of nitrogen fixation by Trichodesmium in the central Atlantic Ocean. Nature **411:** 66-69.

Shimmfield, G. B., and N. B. Price. 1986. The Behavior of molybdenum and manganese during early sediment diagenesis-offshore Baja California, Mexico. Marine Chemistry **19:** 261-280.

Sprent, J. I., and J. A. Raven. 1985. Evolution of Nitrogen-Fixing Symbioses. Proceedings of the Royal Society of Edinburgh Section B- Biological Sciences **85:** 215-237.

Stiefel, E. I. 1996. Molybdenum bolsters the bioinorganic brigade. Science **272:** 1599-1600.

Sunda, W. G., and S. A. Huntsman. 1988. Effect of Sunlight on Redox Cycles of Manganese in the Southwestern Sargasso Sea. Deep-Sea Research Part a-Oceanographic Research Papers **35:** 1297-1317.

Trefry, J. H., D. B. Butterfield, S. Metz, G. J. Massoth, R. P. Trocine, and R. A. Feely. 1994. Trace metals in hydrothermal solutions from Cleft Segment on the southern Juan de Fuca Ridge. Journal of Geophysical Research, B, Solid Earth and Planets **99:** 4925-4935.

Zheng, Y., R. F. Anderson, A. van Geen, and J. Kuwabara. 2000. Authigenic molybdenum formation in marine sediments; a link to pore water sulfide in the Santa Barbara Basin. Geochimica et Cosmochimica Acta **64:** 4165-4178.

CHAPTER 2 METHODS OF DISSOLVED AND PARTICULATE MOLYBDENUM ANALYSIS

Abstract

Methods have been designed for the determination of molybdenum (Mo) in seawater, phytoplankton and marine particulate matter by both Isotope Dilution (ID) and the Standard Addition (SA) analysis using an Inductively Coupled Plasma Mass Spectrometry (ICP-MS). The Mo in seawater ID method includes a chelex pre-concentration step and offers a significantly more precise (±0.5% 1sd.) technique than have been employed in the literature thus far. The ID method for cells and particulate matter simultaneously determines the Fe and Mo concentrations while correcting for molecular and isotopic interferences and mass bias issues that often limit the accuracy of these analyses in solid samples. The SA method for Mo analysis in particulate matter and phytoplankton cells offers a means of simultaneously determining Fe, Rb, and Mn, for comparison to Mo. ID and SA analyses of Mo and Fe are within ±10% of each other for most samples. These methods represent a significant improvement in the ability to measure Mo precisely and accurately in environmental samples

2.1 Introduction and Method Intercomparison

Precise determination of molybdenum (Mo) concentrations in natural materials was critical for the completion of this thesis. This chapter is devoted to a description of the methods used for the analysis of Mo in seawater, microbial cells and suspended particulate matter (SPM). Previous methods of seawater analysis employed a variety of separation, preconcentration and analysis techniques including co-precipitation with cobalt-APDC followed by Atomic Adsorption Spectrometry (AAS) (Collier 1985), chelation with anion resin separation followed by AAS (Riley and Taylor 1968) or X-ray Fluorescence (XRF) (Prange and Kremling 1985), solvent extraction using 8-hydroxyquinoline followed by Graphite Furnace(GF) AAS (Berrang and Grill 1974), catalytic current polagraphy or High Resolution Inductively Coupled Plasma Mass Spectrometry (HR-ICPMS) using standard curves (Sohrin et al. 1998; Sohrin et al. 1999), and direct Isotope Dilution Inductively Coupled Plasma Mass Spectrometry (ID-ICPMS)

with no separation step (Colodner et al. 1995; Nameroff 1996). None of these methods produce concentration data with precisions better than ± 2.5 %. They are unable to resolve variations less than 4 nM in amplitude. Given that the total concentration range of many biologically important trace element, such as Fe(0-0.8 nM), Cu (0.6-6 nM), Mn (0.1-0.9 nM), Zn (0-8 nM) or Cd (0-1.2 nM) (Nozaki 1996), is close to this range, current Mo measurements techniques could not hope to resolve biologically relevant variations. Below I outline a method for analysis of Mo in seawater via (ID-ICPMS) including a Chelex column separation step that achieves a precision of ±0.5 % based on replicate analyses.

As discussed in Chapter 1 there are very few analyses of Mo in phytoplankton, either natural or culture populations. Outlined below is the method used to measure trace metals and nutrients in samples of cultured and natural populations of phytoplankton and Suspended Particulate Matter (SPM) collected on filters. Mo and Fe were analyzed by both Isotope Dilution (ID) and Standard Addition (SA) ICPMS. Additional trace metals (Mn, Al, Rb) and were measured by SA-ICPMS. Samples were analyzed for N and C using a CHN analyzer.

2.2 Sample Preparation

2.2.1 Solutions, Plastic ware, Standards and Spikes

Solutions were prepared with Milli-Q 18.2 MΩ water (Q-H_2O). All sample processing was done using trace-metal grade (Seastar or Optima) HCl, HNO_3, HF, and

H_2O_2. Concentrated NH_4OH was prepared by two-bottle (2B) distillation of Reagent grade NH_4OH. Stock solutions of trace-metal reagents were stored in Teflon bottles.

All HDPE plastic ware was cleaned by leaching with 10% reagent grade HCl for at least 5 days, rinsed three times with Q-H_2O and dried in a laminar flow hood before use. Teflon vials (Savillex) for particulate matter analysis were cleaned by soaking in 10% reagent grade HCl then 10% reagent grade HF each for 24 hours. Vials were capped and individually leached with concentrated Optima HNO_3 at 120°C, rinsed three times with Q-H_2O then leached again with concentrated Optima HNO_3 and HF in 10:1 ratio. Vials were rinsed again and then given a final leach for 4 hrs at 120°C with 950 µL HNO_3 and 50 µL HF, the same conditions as a sample digestion. The final HNO_3/HF leach is diluted ten-fold and stored for vial blank analysis. Osmotics polycarbonate membrane filters and Pall Gelman Supor filters were used to collect cultured cells and natural particulate matter for metal analysis. Filters were cleaned in 10% Optima HCl overnight at 60°C, rinsed with Q-H_2O and allowed to soak for an hour at 60°C, then rinsed 5 times with Q-H_2O and stored in pH 2 water.

Standard solutions were diluted from Specpure or Alfa Aesar ICP-MS standard solutions. Concentrations of diluted standards were determined gravimetrically. The ^{95}Mo isotope spike was purchased from Oak Ridge National Laboratory as a metal powder and dissolved in 10% HNO_3. The ^{57}Fe spike was provided by J. Dahmen of Merck KgaA as a solution in 5% nitric acid (Dahmen et al. 1997). Spike concentrations and abundances were determined by reverse isotope dilution. Natural and spike abundances for elements of interest are presented in Table 2.1.

Table 2.1 Isotopic abundances of natural metal and enriched isotope spikes for trace metal measured via ICPMS.

Element	Isotope	Enriched Spike Abundance (%)	Natural Isotope Abundance (%)	Method
Al	27		100	Standard Addition
Mn	55		100	Standard Addition
Fe	54	5.845	5.85	Isotope Dilution and
	56	2.119	91.75	Standard Addition
	57	91.754	2.12	
	58	0.282	0.28	
Rb	85		72.16	Standard Addition
	87		27.83	
Mo	92	0.23	14.84	Isotope Dilution and
	94	0.56	9.25	Standard Addition
	95	96.45	15.93	
	96	1.42	16.68	
	97	0.48	9.55	
	98	0.69	24.14	
	100	0.17	9.62	
In	115		100	

2.2.2 Seawater Collection, Separation and Preconcentration.

Seawater samples for dissolved molybdenum analysis were collected using either a standard shipboard Niskin bottle rosette deployed by hydrowire or in trace metal clean Go-Flo bottles deployed on a clean Kevlar line. Water samples from the Arabian Sea collected from the similar depths (88 and 100 m, respectively) in both Go-Flo and Niskin bottles show less than 0.3% difference. Go-Flo and Niskin collected water samples from a Pacific profile (9°50'N 104°15'W) collected in 2001, however, shows an offset of 1.2 nM. There may be a small amount of Mo contamination associated with sampling method. When possible, both filtered and unfiltered seawater samples were collected and analyzed. Filtered samples were passed through 0.2 μm syringe or inline filter. Both

filtered and unfiltered seawater samples were acidified to pH 2 with Optima HCl at sea and/or frozen and acidified on shore.

Our methodology differs from ICPMS methods commonly employed for Mo because it includes a separation and preconcentration step. Mo separation and preconcentration is not required for low (greater then ±2.5%) precision ID-ICPMS analyses of natural waters (Colodner et al. 1995; Nameroff et al. 1995; Zheng et al. 2000), but in order to increase precision and accuracy it is necessary to reduce interferences and matrix effects associated with seawater salts. This was accomplished by using a Chelex ion exchange procedure to purify Mo.

In the lab, 5-10 mL aliquots of pH 2 seawater are weighed into an acid cleaned 20 mL HDPE vial and spiked with approximately 0.05 g of 675 ppb ^{95}Mo spike solution weighed from a dropper bottle and with 200 µl 30% hydrogen peroxide. The peroxide is added to ensure all of the Mo is in the molybdate form, not associated with any organic ligands. Spiked samples are heated gently (<95°C) for at least 8 hours. The gentle heating and peroxide treatment is intended to facilitate isotopic equilibration of spike and sample Mo. Table 2.2 shows that a sample of Sargasso Seawater measured with or with out peroxide added yielded the same concentration within error. However, since organic ligand concentration could vary significantly among samples, and the addition of peroxide does not significantly raise the sample blank, peroxide addition was continued in all sample measurements. More significant was the effect of gentle overnight heating on isotope equilibration. Samples spiked and run on the same day have greater variability compared to replicate samples allowed to equilibrate overnight. This

discrepancy is possibly due to preferential loss or retention of spike or sample during column ion exchange. After equilibration, small losses during ion exchange separation do not adversely affect our results.

Table 2.2 Spike and sample equilibration tests

Sample	Treatment		Concentration (nmol/kg)
	H_2O_2	Overnight heating	
Sargasso Sea, 10m	+	+	114.5 ± 0.4 (n=4)
	+		135.9 ± 32 (n=2)
Sargasso Sea, 200m	+	+	114.8 ± 0.5 (n=3)
	+		113.1 (n=1)
Sargasso Sea, 125m	+	+	110.75 ±0.16 (n=2)
		+	110.74 (n=1)
Column Blanks	+	+	0.84±0.74 (n=24) ng
		+	0.47±0.28 (n=4) ng

Mo is separated from sea salts using a Chelex (Biorad Chelex, 100-200 mesh) ion exchange resin procedure (Riley and Taylor 1968). The Chelex is cleaned using a method modified from (Price et al. 1991). Cleaning reduces the procedural Mo blank and removes any extra organic ligands, which can interfere with ICPMS uptake and analysis. To clean Chelex soak for 4 hrs in methanol, then overnight in 2 N HCl and then for a week in 2 N 2B NH_4OH. All leaches use 200 mL solution per 40 g Chelex and are soaked in a clean Pyrex beaker. Chelex is recovered and rinsed in an acid cleaned sintered glass filter rig and rinsed with 2 L Q-H_2O between each leach.

Columns are prepared by adding 2-3 mL of Chelex to a 5 cm long acid cleaned polyethylene column with a acid cleaned polyethylene funnel, tip and frit. Chelex is rinsed with 10 mL of Q-H_2O. It is then washed with 3 10 mL aliquots of 2 N 2B NH_4OH and rinsed again with 3 10 mL aliquots of Q-H_2O. Chelex is then converted to the acid

form by washing with 5 mL 2 N HNO_3, the Chelex volume shrinks by half and is rinsed again with 3 10 mL aliquots of Q-H_2O. At this point the column is ready to use.

The spiked sample is removed from the hot plate, allowed to cool, and run through the prepared column. Mo is retained on the Chelex and the columns are washed with 10 mL of Q-H_2O to remove salts. Molybdenum is eluted in 5 mL of 2 N NH_4OH and collected in a cleaned HDPE vial. Sample is gently dried down completely in a flow box to remove NH_4OH and diluted to about 5 mL in 10% HNO_3. Following column separation, mass spectra on the ICP-MS are typically free from isobaric interferences. The total recovery of Mo from the column in the NH_4OH fraction is >85% (Figure 2.1).

2.2.3 Particulate Matter Analyses

Samples of particulate matter, either cells collected from laboratory cultures, *Trichodesmium* colonies picked from net tows or suspended particulate matter collected with in situ pumps, were collected on filters. Cultures and *Trichodesmium* field samples were collected on acid cleaned 47 mm polycarbonate membrane filters (Osmotics). Pore size varied from 0.2 μm to 5.0 μm according to application (Table 2.3). Prior to use filters are rinsed in the filter holder with sterile seawater or media to neutralize the filter after storage in a dilute HCl solution (pH 2). Samples of cells were collected by filtering a known volume of culture or number of colonies onto a filter, using an acid cleaned Teflon filter holder. Filters were transferred to an acid cleaned polycarbonate Petri dish sealed in Ziploc bags and frozen for storage.

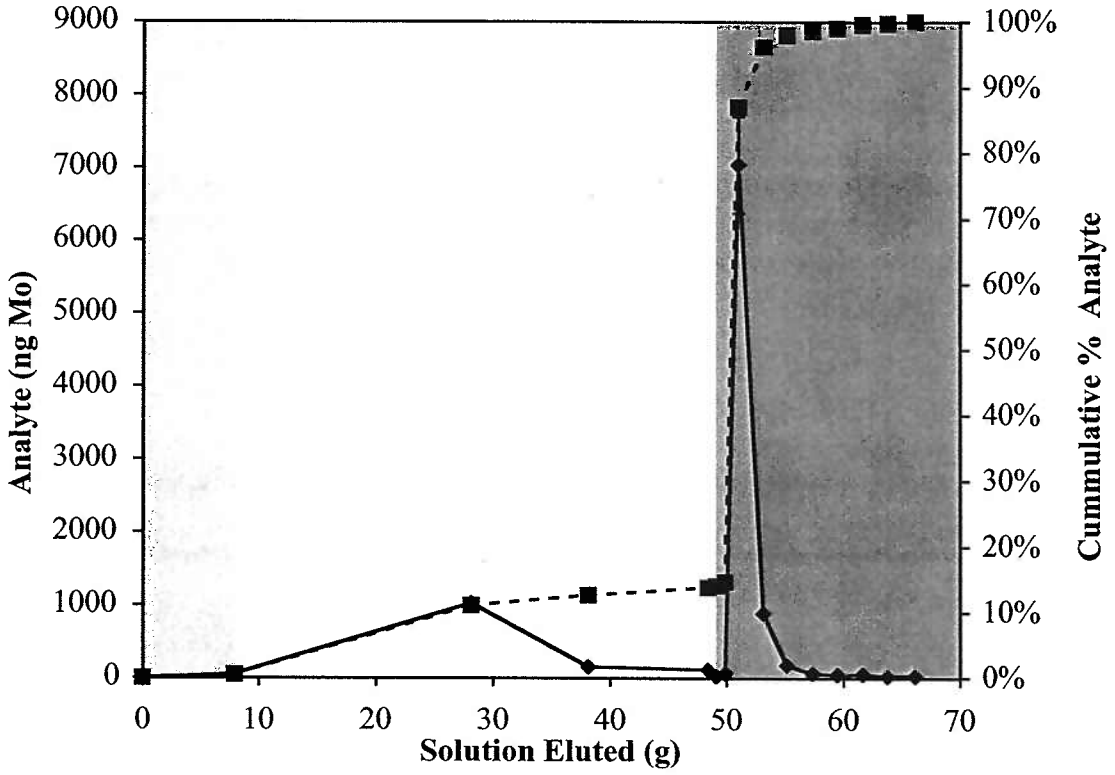

Figure 2.1 Graph of Mo (ng) eluted from Chelex column (solid diamonds) and cumulative percent total analyte Mo (solid squares) versus grams of eluent. Light gray area indicates pH2 seawater sample spiked with 1000 ng of AESAR ICPMS standard Mo and allowed to equilibrate over night to ensure measurable quantities of Mo in each fraction. White area indicates Q-H2O rinses and dark gray area indicates 2 N NH4OH. <1% of Mo is not retained on the column and approximately 12% is removed during rinses to remove salts. >85% of Mo is eluted with the NH4OH and recovered for analysis.

Table 2.3 Filter types and applications used for trace metal analyses

Application	Filter type	Filter Diameter	Pore size
		mm	µm
Cultures			
Crocosphaera	Polycarbonate	47	0.45
Trichodesmium	Polycarbonate	47	5.0
Natural samples			
Suspended particulate matter	Supor	142	0.45
Trichodesmium	Polycarbonate	47	5.0

Suspended particulate matter samples were collected with the McLane in situ pumps (discussed in detail in Chapter 5). These pumps were battery operated and programmable. They were deployed inline on 7.5 to 15 m of trace metal clean Amsteel line with stainless steel shackles. The amount of water was determined by a flow meter on the pumps. Trace metal concentrations were reported in terms of grams per liter of seawater. The filter used for trace metal analysis was a 142 mm 0.45 µm Supor filter. It was cleaned using the same method as the polycarbonate filters. Filtered samples were also stored frozen.

Samples collected on Supor and polycarbonate filters for metals analysis were refluxed with acid to dissolve particulate matter and cells. A known fraction of the filter area was removed using a stainless steel scalpel to cut the filter. For the 47mm polycarbonate filters half of the filter was used for each analysis, but for the Supor filters an acrylic form was used as a cookie cutter to remove a 2.5 by 5 cm rectangle. Stainless steel scalpels have been shown not to significantly increase filter blanks (Cullen et al., 1999). The piece of filter was then placed on the side of a 20 mL Savilex Teflon vial, loaded side out. 950 µL HNO_3 and 50 µL HF were added to the bottom of the vial which

was then tightly capped and place on an 120°C hot plate for 4 hrs. Vials were weighed before and after leaching to determine loss of acid during heating. The sample was diluted ten-fold by addition of Q-H_2O and decanted into a cleaned HDPE vial for storage until analysis.

There are several types of blanks associated with this procedure. Vial blanks were determined for each Teflon vial individually by performing a 950 µL HNO_3 and 50 µL HF leach exactly as if it were a sample before each vial was used. Filter blanks were determined for each filter type by leaching clean unused filters. There were also Media, Seawater or Dip blanks which take into account possible blank contributions from culture media, seawater and filter apparatus, respectively. These are the most representative blanks for these procedures. Media, Seawater and Dip blanks will be discussed in depth in the chapters relevant to each procedure.

2.3 Instrumental Analysis

2.3.1 Inductively Coupled Plasma Mass Spectrometer (ICP-MS)

All trace metal concentrations were determined by isotope dilution (ID) or standard addition (SA) and analyzed by inductively coupled plasma mass spectrometry (ICP-MS) using WHOI's Finnigan Element with a MCN-6000 desolvating nebulizer and a autosampler. The Finnigan Element is a magnetic sector high mass resolution ICP-MS; the operating conditions are listed in Table **2.4**.

Table 2.4 Operating conditions for the Finnigan Element ICP-MS

Ar Cooling Gas Flow	12-14 l min^{-1} optimized daily
Ar Sample gas flow	0.9-1.2 L min^{-1} optimized daily
Ar Auxiliary gas Flow	1.10 L min^{-1} optimized daily
Nebulizer	100 µL/min Elemental Scientific PFA Nebulizer with a CETAC MCN-6000 desolvator
	Ar Sweep gas (3.0-5.5 l min^{-1}) and N_2 gas flow (0.01-0.04 L*min^{-1}) optimized daily
	Spray Chamber temperature 100°C; Desolvator Temperature 160°C
RF power	1200-1400 W optimized daily
Detector voltage	-2000 V
Lenses	Optimized daily to maximize intensity of ^{115}In or ^{238}U and separation of ^{56}Fe and ^{40}Ar-^{16}O in medium resolution
Sample and skimmer cones	Ni cones cleaned and replaced daily
Resolution mode	Low for Mo, In and Rb, Medium for Fe, Mn, Al
Scanning mode	Peak jumping

For analysis the sample, diluted in 10% HNO_3, was sprayed into the MCN-6000 desolvating nebulizer via a PFA nebulizer at a rate 100 µL/min. The MCN-6000 removes water vapor and allows the sample to be introduced to the torch as a dry aerosol. Use of a desolvating nebulizer increases ionization efficiency, stability and sensitivity, but may also increase machine blanks unless the MCN-6000 is acid cleaned prior to each analysis day. In the torch, the sample is ionized and then passes through the nickel sampler and skimmer cones into the transfer optics of the analyzer. The cones were cleaned and changed daily. In the analyzer the ions are attracted and accelerated by the high voltage of the extraction lens. The ion beam is shaped and focused by the transfer optics onto the entrance slit. It then passes through the magnetic sector, which separates

out the ions by mass charge ratio, followed by the electronic sector, for energy separation and energy focusing. The ion beam is then passed through the exit slit and detected by an electron multiplier. Ion currents are reported in counts per second and detected in pulse counting mode for intensities less than $5x10^6$ cps. Higher intensities are quantified as an analog signal.

The ICP-MS is mass calibrated daily using a multi-element standard with masses ranging from ^7Li to ^{238}U. The Finnigan Element software uses a proprietary algorithm to mass calibrate the magnet. This is sufficient for many elements, but does not always find the peak tops for molybdenum. In order to obtain a mass calibration that allows Mo isotopes to be measured on the flat top of the peak rather than the peak shoulder a second mass calibration step was required (Figure 2.2). A Mo standard is measured separately and used to correct the initial multi-element mass calibration. Previous software version 1.75 for the Finnigan Element required that the Mo standard mass calibration be added manually to the mass calibration. However the latest software version 2.14 allows calculation of a mass offset, the difference between the peak top as determined from the mass calibration and the peak top as measured by the sample method. The mass offset is calculated from a standard run using the sample method but with larger mass windows in order to capture the whole peak. The mass offset is then incorporated into the method and applied to all samples measured. Mass offset and manual mass calibration techniques markedly improve the quality and stability of the Mo mass calibration.

For analysis of Mo and Rb the ICP-MS is run in low-resolution mode, but for Mn, Fe and Al medium resolution must be used to exclude interferences. Resolution (R) is

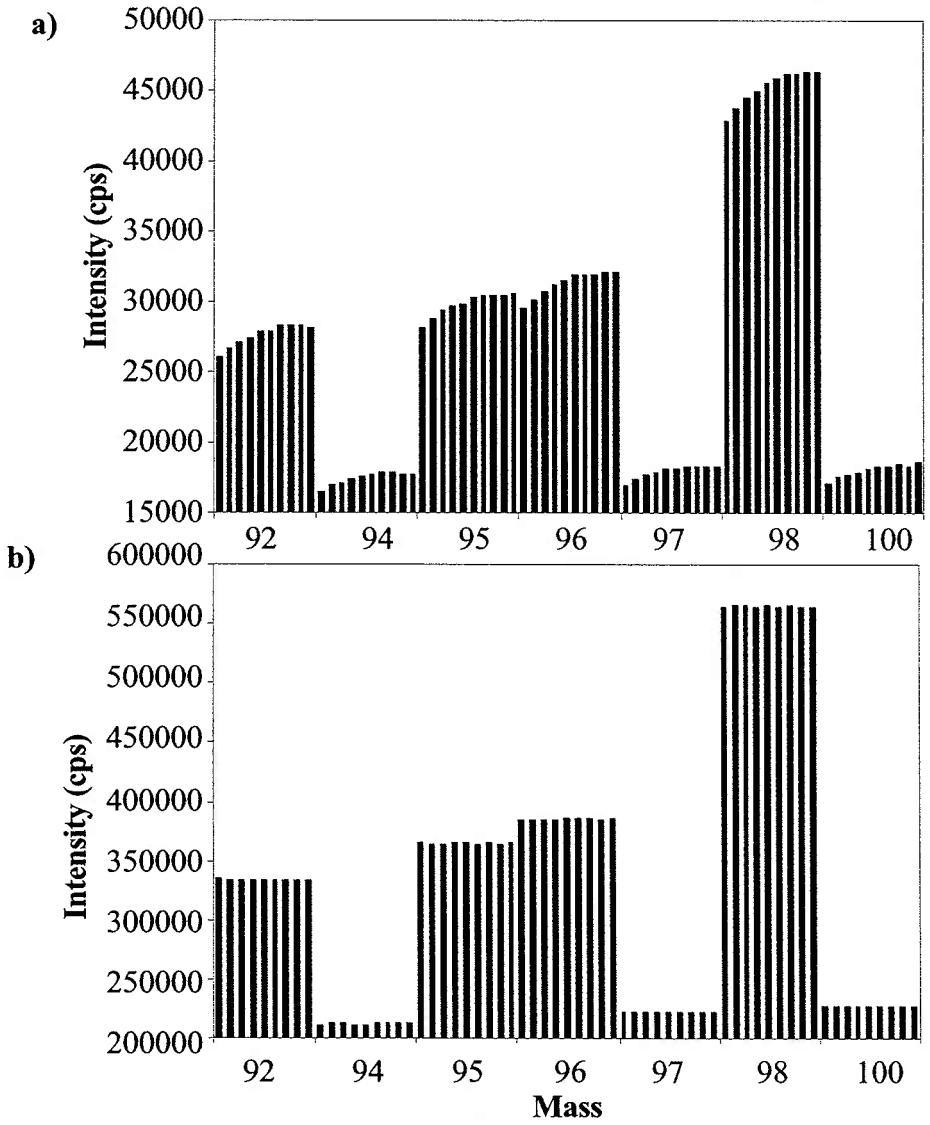

Figure 2.2 Comparison of Mo standards run before (a) and after (b) manual Mo mass calibration or mass offset correction.

defined in a Magnetic Sector ICPMS as the center mass of the peak divided by the width of the peak at 5% of the peak height. Mass resolution is determined by the width of the entrance and exit slits through which the ion beam passes and for the Element is available in low (160 μm; R=300) medium (16 μm; R=3000) and high (5 μm; R=10000). Increasing the resolution allows separation of molecular interferences with overlapping or tailing peaks, such as $^{40}Ar^{16}O$ on ^{56}Fe (Figure 2.3). However the decrease in slit size decreases the overall transmittance of ions and thus lowers sensitivity. For example, indium was used as an internal standard and was measured in both low and medium resolution for all standard addition samples. Count rates in medium resolution were approximately 100,000 cps/ppb, compared to 2,000,000 cps/ppb for the same solution measured in low resolution.

Acquisition schemes and parameters for the ID and SA methods are presented in Tables **2.5, 2.6 and 2.7.** The mass range is the total width of the peak and the mass window is the percentage of the center of the peak collected. The samples per peak is the number of masses analyzed in that mass range. Ratios are determined by rapid scanning from one mass to the other. For isotopes within +15% amu of the magnet mass, the mass at which the magnet is set to measure sometimes called the rest mass, the Element performs a rapid electronic scan varying the voltage on the lenses to control what mass ions hit the detector. But for masses greater than 15% amu apart the voltage on the magnet must be changed to jump masses. The settling time is the amount of time spent letting the magnet and lenses stabilize at to the new mass before collecting data. This

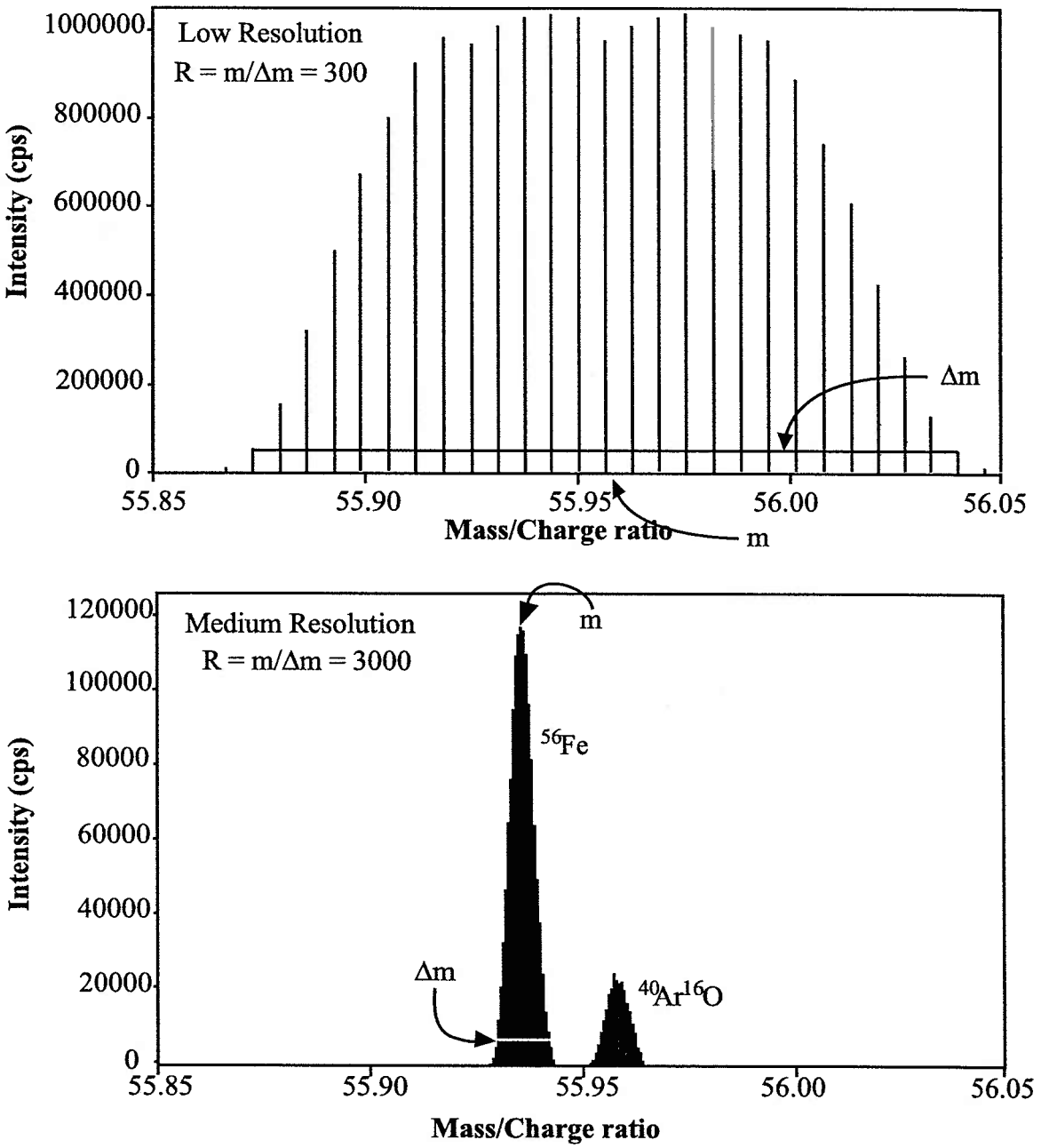

Figure 2.3 Comparison of 56Fe and 40Ar16O peaks as measured in a 1 ppb Fe standard solution with Low (a) and Medium (b) resolution. Resolution (R) is defined as the center mass of the peak (m) divided by the width of the peak at 5% of the maximum peak height (Δm). 56Fe and 40Ar16O peaks that are unresolved in low resolution can be easily distinguished with medium resolution. Notice the approximately 12-fold drop in 56Fe intensity with increasing resolution

time must be longer after a magnet jump than after an electronic jump because the magnet takes longer to stabilize than the lenses.

The sample time is the amount of time spent collecting counts on that mass. The Element has 1 discrete dynode electron multiplier that is set to detect ions in either as a pulse counting or analog signal. The software enables the user to set possible detection modes, pulse counting, analog or both. Analog mode is less precise at low intensities due to higher background counts. For this study, most data was collected in pulse counting mode, but for isotopes known to occasionally exceed counting signal intensities the detection mode is set to both (allowed to switch between analog and counting) in order not to lose data.

Each run reports the average of a specified number of passes; multiplied together they give the total number of scans performed. For low resolution work the mass window and samples per peak are small and sample only the flat top of the peak. Ratios are determined by taking the ratio of each channel for each run, creating a matrix of 200-500 ratios. The average of the block of ratios is determined and the all ratios over three standard deviations away from the mean are discarded and the average recalculated. This process is repeated iteratively until the ratio converges. Generally only 1-4 ratios out of 200 ratios were discarded.

For medium resolution the window is large with a higher number of samples per peak in order to describe the whole peak and the make sure that there is no significant overlap with other peaks. Each sample mass is averaged for the total number of scans, in

order to get a smooth average peak shape. Ratios are determined using the maximum peak height of the averaged peak.

Total dwell time, or time spent collecting data on a mass, can be determined by multiplying the percent mass window by the samples per peak by the sample time by the total number of scans. For example, mass 96 as measured using the seawater Isotope Dilution method (Table 2.5) has a total dwell time of

2% mass window* 500 samples * 0.003 sec *20 runs * 50 passes = 30 sec

The average intensity on mass 96 for a 1 ppb standard Mo solution is about 500,000 cps which equals a total of 15 million counts over the course of a single analysis. Counting statistics give a standard deviation of the square root of the total counts or 0.03%. As expected all measured standard deviations for blanks, standards and samples are larger than counting statistics.

Table 2.5 Isotope dilution acquisition scheme for seawater analyses.

Isotope	Mass Window	Mass range	Samples per peak	Magnet Mass	Settling Time	Sample Time	Detection Mode
	%	amu		amu	sec	sec	
Low resolution							
^{90}Zr	2	89.902-89.908	500	98.905	0.300	0.0010	Counting
^{92}Mo	2	91.904-91.910	500	98.905	0.001	0.0030	Counting
^{94}Mo	2	93.902-93.908	500	98.905	0.001	0.0030	Counting
^{95}Mo	2	94.903-94.909	500	98.905	0.001	0.0030	Counting
^{96}Mo	2	95.901-95.908	500	98.905	0.001	0.0030	Counting
^{97}Mo	2	96.903-96.909	500	98.905	0.001	0.0030	Counting
^{98}Mo	2	97.902-97.909	500	98.905	0.001	0.0030	Counting
^{100}Mo	2	99.904-99.911	500	98.905	0.001	0.0030	Counting
^{101}Ru	2	100.902-100.909	500	98.905	0.001	0.0010	Counting
Globals							
	Runs			20			
	Passes			50			

Table 2.6 Isotope dilution acquisition scheme for cells and particulate matter

Isotope	Mass Window	Mass range	Samples per peak	Magnet Mass	Settling Time	Sample Time	Detection Mode
	%	amu		amu	sec	sec	
Low resolution							
^{90}Zr	2	89.902-89.908	500	98.905	0.300	0.0010	Counting
^{92}Mo	2	91.904-91.910	500	98.905	0.001	0.0030	Counting
^{94}Mo	2	93.902-93.908	500	98.905	0.001	0.0030	Counting
^{95}Mo	2	94.903-94.909	500	98.905	0.001	0.0030	Counting
^{96}Mo	2	95.901-95.908	500	98.905	0.001	0.0030	Counting
^{97}Mo	2	96.903-96.909	500	98.905	0.001	0.0030	Counting
^{98}Mo	2	97.902-97.909	500	98.905	0.001	0.0030	Counting
^{100}Mo	2	99.904-99.911	500	98.905	0.001	0.0030	Counting
Medium Resolution							
^{7}Li	20	7.016-7.016	10	7.016	0.300	0.0010	Counting
^{56}Fe	120	55.924-55.946	25	55.935	0.100	0.0600	Both
^{57}Fe	120	56.924-56.947	25	55.935	0.001	0.0600	Both
^{238}U	20	238.043-238.059	10	238.051	0.010	0.0010	Counting
Globals		Low Resolution			Medium Resolution		
	Runs	20			20		
	Passes	10			5		

Table 2.7 Standard addition acquisition scheme for particulate matter

Isotope	Mass Window	Mass range	Samples per peak	Magnet Mass	Settling Time	Sample Time	Detection Mode
	%	amu		amu	sec	sec	
Low resolution							
^{7}Li	10	7.0115-7.017	50	7.016	0.300	0.0050	Counting
^{85}Rb	10	84.898-84.926	100	84.912	0.300	0.0050	Both
^{95}Mo	10	94.890-94.922	100	84.912	0.001	0.0050	Counting
^{97}Mo	10	96.890-96.922	100	84.912	0.001	0.0050	Counting
^{115}In	10	114.885-114.923	100	114.904	0.100	0.0050	Counting
Medium Resolution							
^{7}Li	10	7.016-7.016	30	7.016	0.300	0.0100	Counting
^{27}Al	150	26.975-26.988	30	26.982	0.050	0.0100	Both
^{55}Mn	150	54.924-54.952	30	54.938	0.050	0.0100	Counting
^{56}Fe	150	55.921-55.949	30	54.938	0.001	0.0100	Both
^{57}Fe	150	56.921-56.950	30	54.938	0.001	0.0100	Counting
^{115}In	150	114.875-114.933	30	114.904	0.100	0.0100	Counting
^{238}U	10	238.047-238.005	30	238.051	0.300	0.0100	Counting
Globals		Low Resolution			Medium Resolution		
	Runs	50			50		
	Passes	1			1		

2.3.2 *Isotope Dilution*

Isotope Dilution is known to be one of the most precise and accurate methods for determining element concentration. Following isotopic equilibration, it is a method that is relatively insensitive to matrix effects, variable instrumental sensitivity and any minor samples losses during handling. However, it requires at least two isotopes that are free of molecular or uncorrectable isobaric interferences. For this reason the ID method could only be employed to measure Mo and Fe for this study (Table **2.1**). In the ID method, a known mass of an isotopic spike, artificially enriched in a less abundant natural isotope, is added to a known mass of sample assumed to have a natural isotopic composition. The sample is well mixed to ensure that the spike and sample equilibrate isotopically. The resulting mixture has a new isotope ratio that is determined by the atom ratio of the spike to sample (Figure 2.4.) All measured ratios for the new mixture will fall along a mixing line determined by a straight line between standard and spike in two ratio space (Figure 2.5). Deviations from this line, caused by mass bias or interferences can be identified and corrected as discussed in the next sections.

The concentration of the sample is calculated from the measured spike sample ratio, $R_m^{i/j}$, the measured ratio of isotopes i (spike mass, ^{95}Mo and ^{57}Fe) to j (standard mass, ^{96}Mo and ^{56}Fe). The sample-spike mole ratio is calculated using the isotope dilution equation:

$$N_{sm}/N_{spk} = \left(Ab^{i}_{spk} - R^{i/j}_{m} Ab^{j}_{spk}\right)/\left(Ab^{j}_{sm} R^{i/j}_{m} - Ab^{i}_{sm}\right) \qquad \text{eqn. 2.1}$$

where the subscripts sm and spk stand for sample and spike, respectively. N is the number of atoms in moles, and Ab is the abundance of isotope i or j in the spike or

the sample. The mole ratio is converted to sample concentrations in parts per billion (ppb) by:

$$C_{sm} = \left(C_{spk} M_{spk} AW_{sm}\right) / \left(M_{sm} AW_{spk}\right) \times \left(N_{sm} / N_{spk}\right) \qquad \text{eqn. 2.2}$$

where C, M and AW are the element concentration (ppb), mass (g) and atomic weight (g/mol), respectively, in the sample and spike.

A precise and accurate determination of the concentration requires a precise and accurate determination of R_m. The propagation of error on the sample through the ID equation, assuming that the isotopic abundances of the spike and sample are well known, is

$$s^2(N_{sm}) = s^2(N_{spk}) + f^2(R_m) s^2(R_m) \qquad \text{eqn. 2.3}$$

where s is the standard deviation and $f(R_m)$ is the error multiplication factor for R_m (Heumann 1988). Assuming that $s(N_{spk})$, the error on spike addition, is negligible, the first term in equation **2.3** drops out. The $f(R_m)$ function below can be minimized by optimizing the ratio of spike added to sample (Heumann 1988)

$$f(R_m) = \frac{\left[\left(i/j\right)_{sm} - \left(i/j\right)_{spk}\right] R_m}{\left[R_m - \left(i/j\right)_{sm}\right]\left[R_m - \left(i/j\right)_{spk}\right]} \qquad \text{eqn. 2.4}$$

By combining equations **2.1** and **2.4** we can solve for the range of N_{sm}/N_{spk} ratios where $f(R_m)$ is at a minimum. In this minimum, $f(R_m)$ is close to 1. The minimum is a broad feature encompassing almost an order of magnitude in N_{sm}/N_{spk} ratios (Figure 2.6). Equivalent optimal R_m range from 6 to 10 for $^{95}Mo/^{96}Mo$ and from 1.6 to 0.14 for $^{57}Fe/^{56}Fe$. For most samples in this thesis analyzed by ID spike sample ratios are within

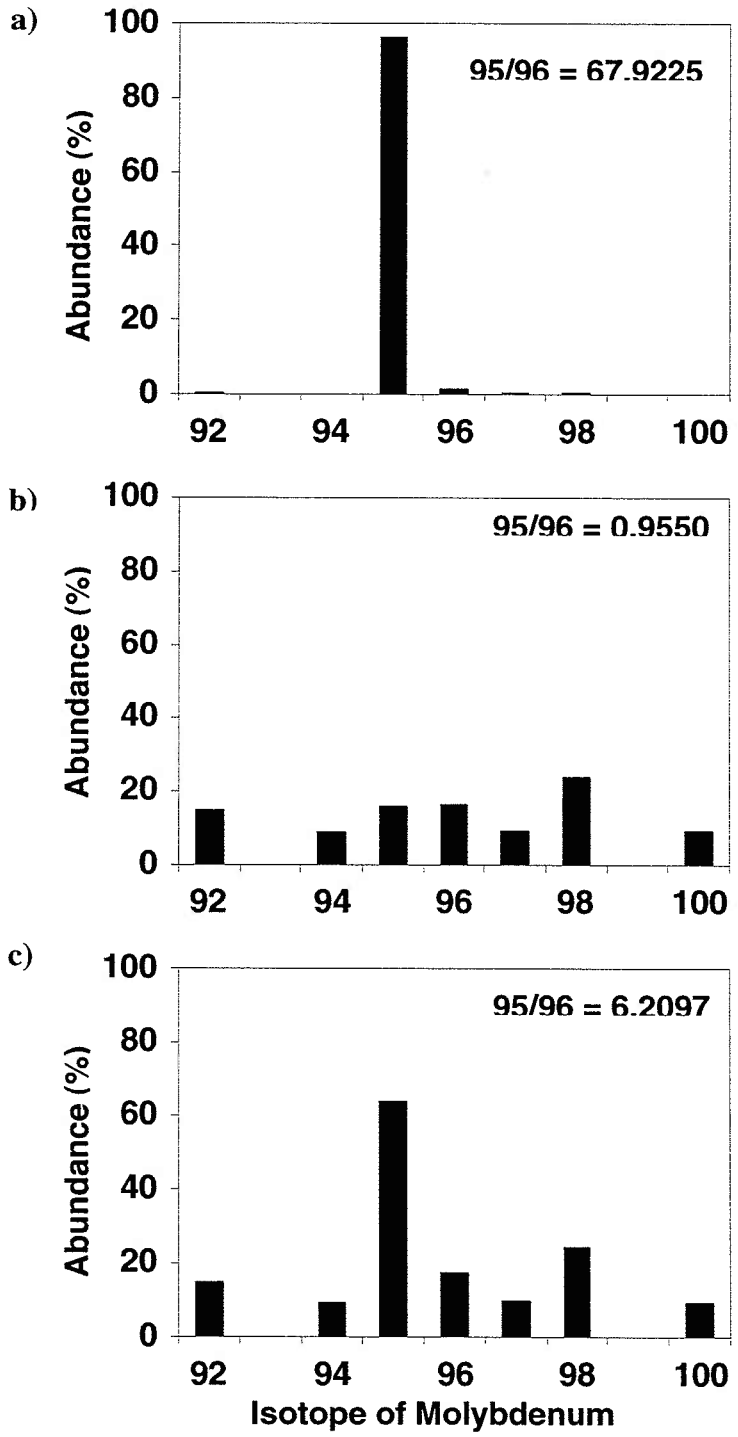

Figure 2.4 Histogram of spike (a) and natural (b) isotope abundances and a mixture (c) of 50% each with calculated 95/96 Mo isotope ratios.

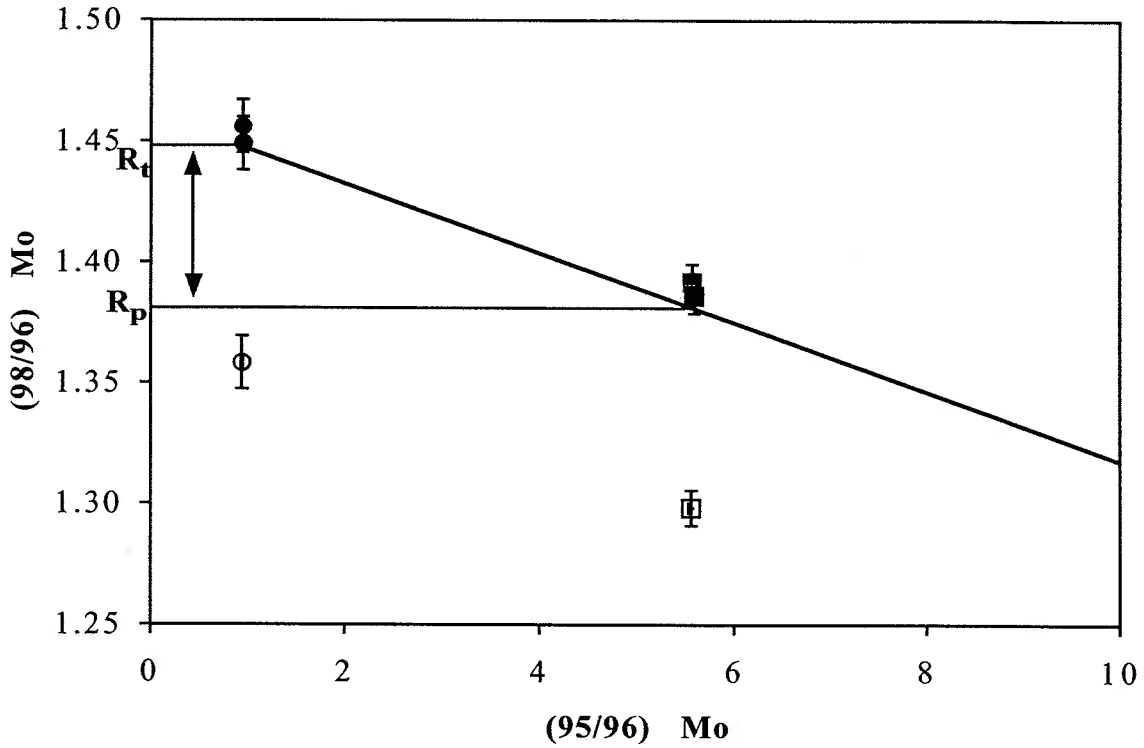

Figure 2.5 A plot of the spike-sample mixing line in two ratio space. Dark line represents the spike-sample mixing line, spike end member is off scale. Representative standard (circles) and sample (squares) measurements are shown for measured (open symbols) Zr interference corrected (gray symbols) and mass bias corrected (black symbols). Notice how corrections progressively move ratios back onto the spike-sample mixing line. Lines labeled Rt and Rp indicate the natural and projected isotope ratios, respectively. Rp for 98/96 is calculated by projecting the 95/96 measured and interference corrected ratio (gray square) to the spike sample mixing line. This is a one step calculation where Rp corresponds the actual 98/96 of the spike sample mixture, subsequent iterations do not significantly alter the calculated ratio. The difference between Rt and Rp (arrows) represents the contribution of the spike solution on non-spike masses.

a)

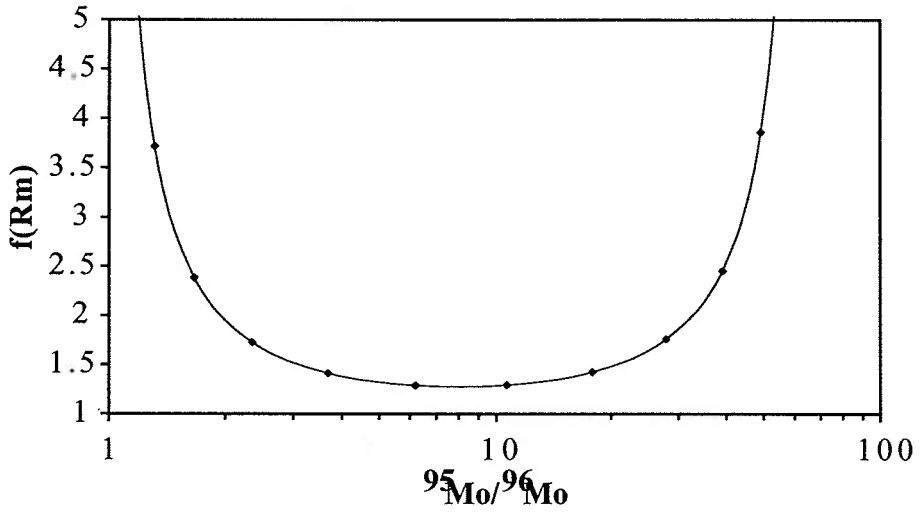

b)

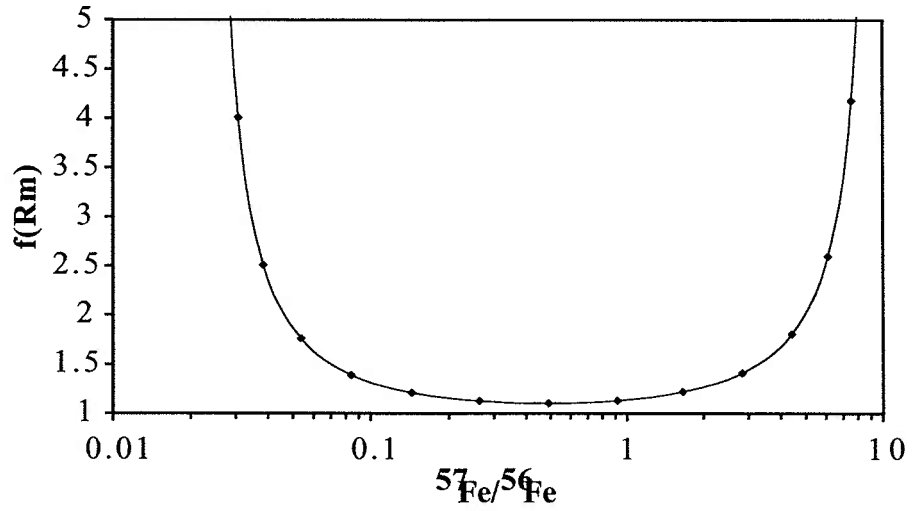

Figure 2.6 Plots f(Rm) versus the Nsm/Nspk ratio. The minimum represents the optimal range in Rm for a) Mo (6 to 10) and b) Fe (1.6 to 0.14).

these ranges. Error associated with weighing of spike and sample is negligible; therefore the propagated error on the individual measurements is approximately equal to 10% of the error on the measured ratio.

2.3.5 Standard Addition

A standard addition method was developed to measure Mo, Fe, Rb, Al, and Mn in SPM, natural Trichodesmium populations or cultured organisms collected on filters. The objective is to be able to quantify contributions of Mo and Fe in SPM from dissolved salts, terrestrial dust, Mn oxides and calculate biogenic Mo by difference. Rb, Mn, and Al are predominantly associated with dissolved salts, Mn oxides and terrestrial dust of SPM respectively and have relatively constant ratios to Mo and Fe in those materials, and therefore they can be used to calculate Mo and Fe contributions from those fractions.

Standard addition is a less precise method of determining concentrations than ID, however, provided there are no spectral interferences it can be used to measure mono-isotopic elements such as Mn and Al. Mo and Fe were measured by SA as well as ID to provide an additional check on data quality. Figure 2.7 shows a comparison of the two methods. All standard addition solutions were prepared with a final concentration of 1 ppb In. In acts as an external standard and is used to correct for sensitivity drift and matrix effects. Two types of multi-element standards were developed and used depending on which type of filter sample particles were analyzed. Standard solution concentrations are list in Table 2.8

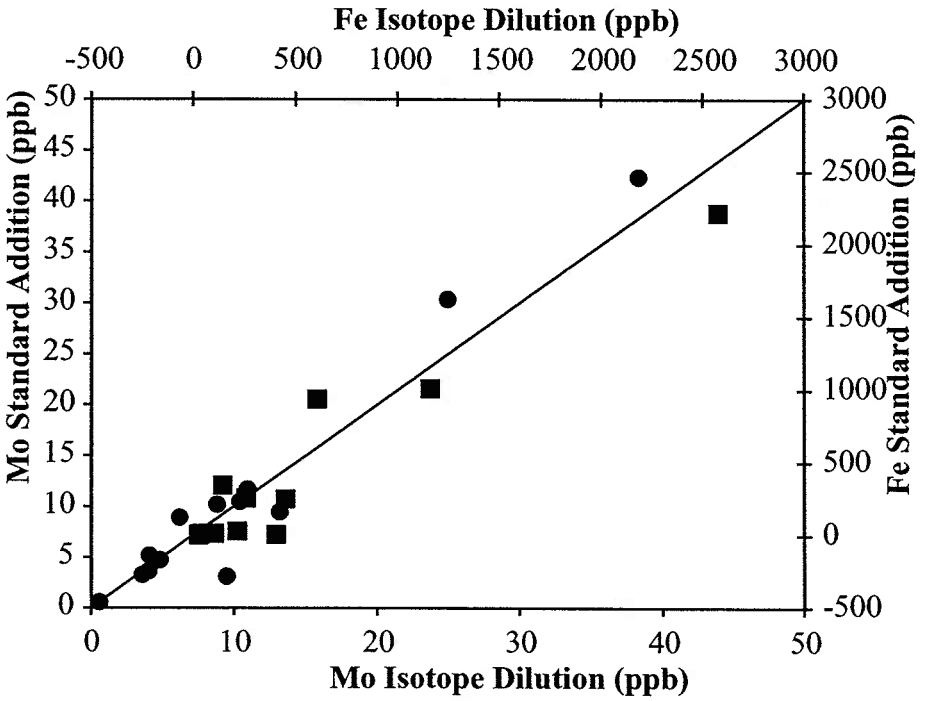

Figure 2.7 Comparison of sample and blank solutions measured via isotope dilution v. standard addition for Fe (squares) and Mo (circles) 1:1 line plotted for comparison.

Table 2.8. Standard solution concentrations

Element Standard	Polycarbonate Filter Standard Solution (ppb)	Supor Filter Standard Solution A (ppb)	Supor Filter Standard Solution B (ppb)
Mo	11.6	6.46	5.61
Rb	2.28	22.7	21.8
Mn	6.34	214	184
Fe	71.2	479	371
Al	36.1	348	335

A four point standard additions curve was created for each sample with 100 μL sample, 200 μL 10 ppb In standard, 0, 20, 50 or 100 μL of the appropriate metal standard and enough 10% HNO3 to make up the volume to a total of 2000 μL. Additions are determined by weight as well as volume to correct for inaccuracies in pippetting. Samples are alternated with acid blanks and standards monitor instrument blanks and mass bias, respectively. The SA ICP-MS method is presented in Table 2.7.

To calculate the concentration of these metals in the sample solution, we first determine the concentration of Mn, Al, Fe, Mo and Rb standard added to each vial from weights or volumes of standards added and the total weight or volume. Approximately 1 ppb final concentration In is added to each vial and the signal of each metal measured, I^M, is divided by the signal of In in that sample, I^{In}, to normalize out discrepancies in sensitivity. In order to account for small differences in the amount of In added, the metal/In intensity ratio is divided by the total In added determined by weight, [In]. This ratio is plotted versus $[M]_{add}$, the concentration of metal standard added to the solution measured, and should give a straight line with the equation.

$$\frac{I^M}{\left(\frac{I^{In}}{[In]}\right)} = m * [M]_{add} + b \qquad \text{eqn. 2.5}$$

An example is given in figure 2.8. The slope of the line, m, is determined by the concentration of the standard and should be the similar for all samples, depending on matrix effects. The intercept of the line will increase with increasing sample concentration. The concentration of the sample solution is then calculated as the intercept divided by the slope of the line.

2.3.3 Mass Bias in high precision samples

A critical factor in determining accurate isotope ratios is a reliable method of determining instrumental mass bias. Mass bias is the deviation of measured isotope values from the natural isotopic ratios. During instrumental analysis by ICP-MS heavier isotopes are preferentially detected. Mass bias for Mo and Fe is on the order of 0.5 and 2 %/amu, respectively. In low precision samples, when the error on the ratio far exceeds the magnitude of mass bias, correcting for mass bias is not critical, but when precision is high, mass bias can lead to a systematic error in analyses unless corrected. There are two approaches to making mass bias corrections, internal and external. External mass bias corrections are based on measurements of standard solutions with known natural isotopic composition. These solutions are used to determine a linear fractionation factor, k (%/amu)

$$k = \left(\frac{R_m}{R_{true}} - 1\right) \Big/ \Delta m \qquad \text{eqn. 2.6}$$

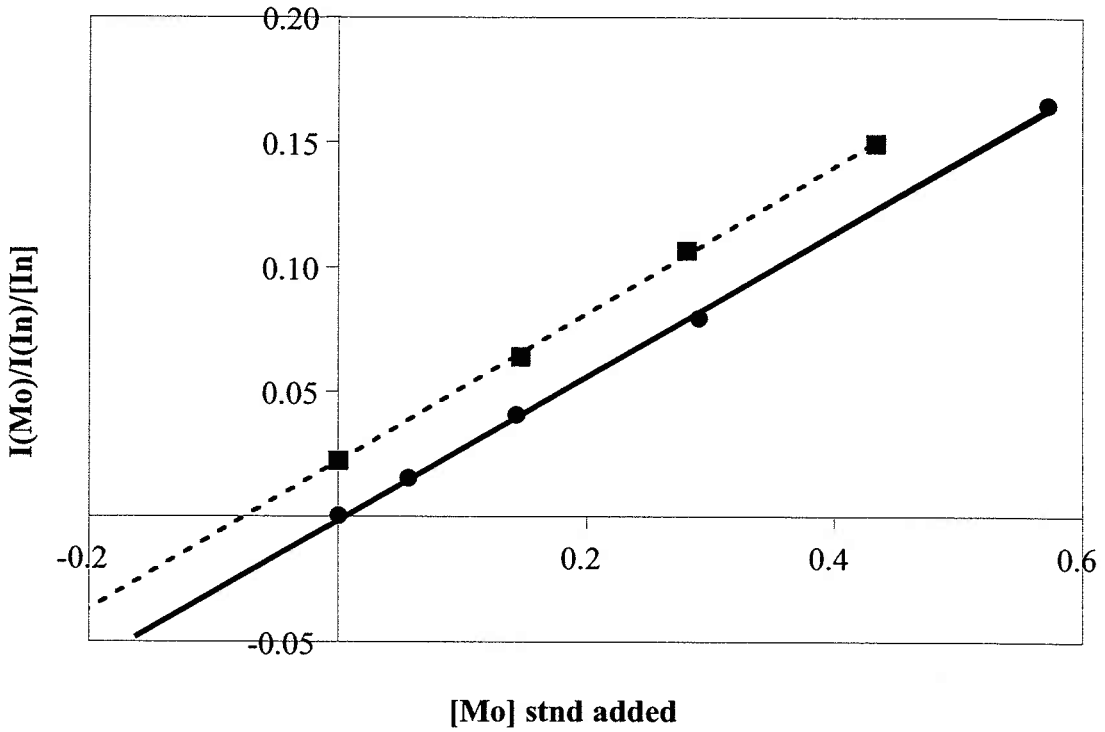

Figure 2.8. Example of Standard Addition lines for a sample (squares) and a standard curve (circles). Slopes are 0.295 and 0.287 for sample and standard, respectively, with intercepts of 0.0219 and 0.0008. The r2 for each line is 0.999.

Where R_{true} and R_m are the true (natural, non-fractionated) and measured ratios, respectively, and Δm is the mass of the isotope in the numerator minus the mass of the isotope in the denominator (i.e. for 95/96 Δm is –1). Alternating sample and standards are run and the k of the bracketing standards is used to correct the samples. This is the scheme used for Fe analyses. The problem with the use of external mass bias correction factors is that mass bias can vary considerably (~1%/amu) over the course of a day and from standard to sample due to different rates of sample uptake or matrix effects.

Conviently for elements like Mo, which have a plethora of isotopes, we can calculate an internal mass bias correction factor during the analysis of each sample. This is determined from equation 2.5 similar to the external fractionation factor. Figure 2.9a shows a plot of R_m/R_t versus Δm of the unspiked masses for a standard and a sample solution (open symbols). While the standard has good correlation coefficient and an intercept of close to 1, the spiked sample has a poor correlation coefficient and a depressed intercept. This is due to the small contributions of non-spike masses in the spike. To correct for this spike contribution, the R_m of 95/96 is projected onto the spike sample mixing line for each ratio and the true isotopic ratio for the mixture is determined called R_p, projected (Figure 2.5). The solid symbols in Figure 2.9a show R_m/R_p plotted versus Δm of the unspiked masses for the same standard and a sample solution as the open symbols. The R_m/R_p gives a higher fractionation factor with a better correlation coefficient. When the fractionation factor determined by the projected ratios is applied it give ratios are with in 0.2% of normal for both standard and sample (Figure 2.9b) This

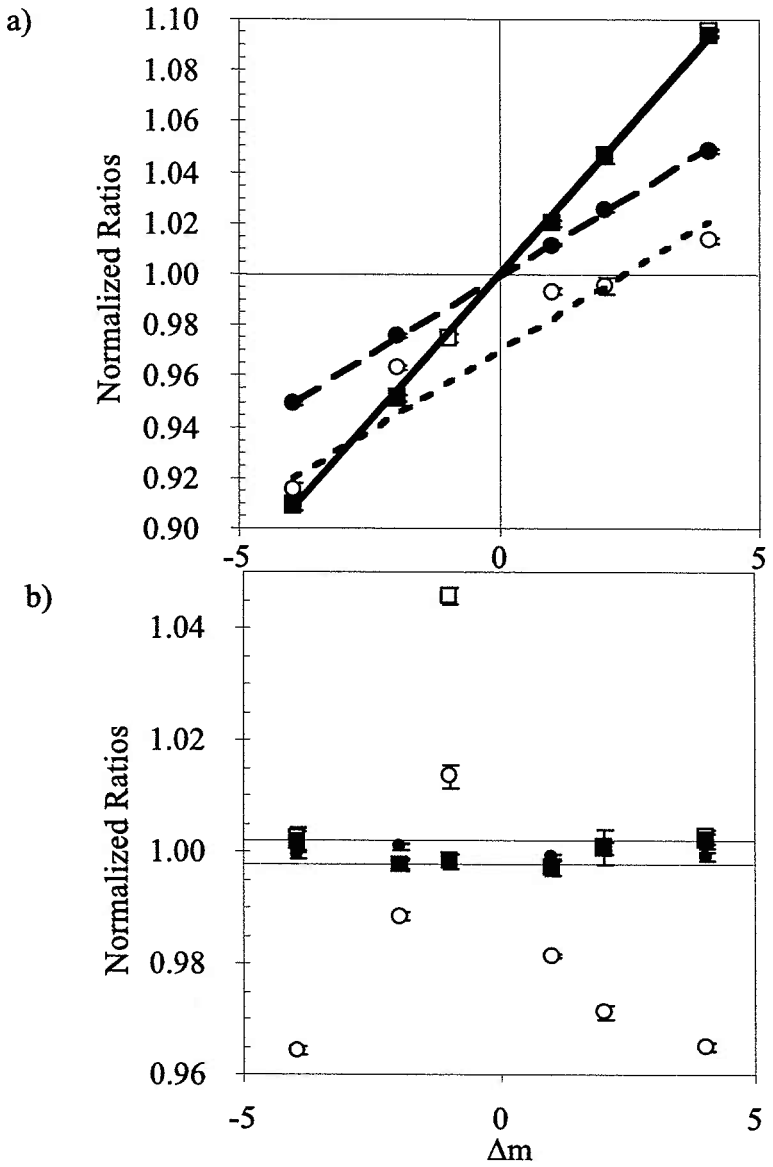

Figure 2.9 a) Plot of Rm/Rt versus Δm of the unspiked masses for a standard (open squares) and a sample solution (open circles). The spiked sample has a poor correlation coefficient and a depressed intercept. This is due to the small contributions of non-spike masses in the spike. To correct for this spike contribution, the Rm of 95/96 is projected onto the spike sample mixing line for each ratio and the true isotopic ratio for the mixture is determined called Rp, projected (Figure 2.3). The solid symbols show Rm/Rp plotted versus Δm of the unspiked masses for the same standard and a sample solution as the open symbols. Both sample and standard show better correlation and a n intercept closer to 1. b) Plot of mass bias corrected normalized ratios for samples and standard shown in (a) demonstrates that using Rp rather than Rt normalized ratios to determine fractionation coefficient improves the precision of the mass bias correction. All corrected isotopes fall within ±0.2% of normal values.

calculation can be repeated iteratively using the new projected ratio, but for all but the most severely over spiked samples one iteration suffices.

2.3.4 Interferences

A major source of systematic error in both ID and SA methods is caused by isobaric and molecular interferences. Table 2.9 lists the possible interferences on the masses of elements of interest to this study. Interferences can be categorized as isobaric and molecular. Isobaric interferences can be corrected by monitoring an additional interference free mass of the interfering element. The major isobaric interferences are (Zr and Ru for Mo; Sn for In; Cr and Ni for Fe.) The equation used to correct measured intensities at Mo mass 96 is:

$$I_{corr}^{96} = I_{m}^{96} - \left(Ab_{ave}^{^{96}Zr} \Big/ Ab_{ave}^{^{90}Zr} \right) \times I_{m}^{90} \qquad \text{eqn. 2.7}$$

where I is the intensity in counts per second of the mass of interest as directly measured (m) and Ab_{ave} is the natural isotopic abundance of the isotope in superscript. All other isobaric corrections follow the same format. In general, Zr interferences on Mo in water samples were below 5% of the measured intensity, though it could exceed 50% for some particulate samples. In water samples the source of Zr was from Pyrex beakers used to clean Teflon, and was substantially reduced by avoiding glassware in the cleaning steps.

Table 2.9 Isobaric and Molecular interferences.

	Mass (Ab%)	Isobaric Correction	Magnitude of Correction	Possible Molecular Interferences			
Al[a]	27			Cr++	C-N	B-O	Be-O
	(100)			Fe++			
Mn[a]	55			Cd++	K-O	Cl-	Ar-NH
	(100)			Pd++	Ar-N		
Fe[a]	56			Cd++	Ar-O	K-O	Ar-NH
	(91.72)			Sn++	Ca-O	Cl-OH	
	57			Sn++	K-O	Ca-O	K-O
	(2.20)			Cd++	Ar-F	Ar-O	Ar-OH
Rb[b]	85			Ar-Ti	Ga-O	Yb++	Er++
	(72.17)			Ar-Sc	Zn-O		
Mo[c]	92	^{92}Mo=	Seawater ^{92}Zr = 0.7-14%	Ar-Fe	Se-O	As-O	Os++
	(17.84)	I_m-^{90}Zr*17.15/51.45	Cells ^{92}Zr =1.5-8.0%	Ar-Cr	Ge-O	W++	
			Particulate ^{92}Zr = 18-63%				
	94	^{94}Mo=	Seawater ^{94}Zr = 1.0-21%	Ar-Fe	Se-O	Ge-O	Os++
	(9.25)	I_m-^{90}Zr*17.38/51.45	Cells ^{94}Zr = 2.4-11%	Ar-Cr	Br-N	Ar-Ni	
			Particulate ^{94}Zr = 25-71%				
	95			Ar-Mn	Br-O	Se-O	Os++
	(15.92)			Ar-Co	Se-O	Br-N	Pt++
	96	^{96}Mo=	Seawater ^{96}Zr = 0.1-1.8%,	Ar-Fe	Se-O	Br-O	Pt++
	(16.68)	I_m-^{90}Zr*2.80/51.45	Cells ^{96}Zr = 2.9-19%,	Ar-Ni	Br-N	Br-OH	Os++
		-^{101}Ru*5.52/17.0	Particulate ^{96}Zr = 0.2-1.1%,				
			Seawater, Cells and				
			Particulates				
			^{96}Ru<0.001%				
	97			Ar-Co	Br-O	Br-OH	Pt++
	(9.55)			Ar-Fe	Se-O		
	98	^{98}Mo=	Seawater, Cells and	Ar-Ni	Se-O	Br-OH	Pt++
	(24.13)	I_m-^{101}Ru*1.88/17.0	Particulates	Ar-Fe	Br-O	Hg++	
			^{98}Ru<0.002%				
	100	^{100}Mo=	Seawater, Cells and	Ar-Ni	Sr-O	Br-OH	Hg++
	(9.63)	I_m-^{101}Ru*12.60/17.0	Particulates	Ar-Zn	Se-O		
			^{100}Ru<0.001%				

a)Molecular interferences are all removed by using medium resolution of 3000. b) Measured in low resolution but molecular interferences are minimal due to inhibition of oxide formation by use of the desolvating nebulizer and the relatively minor abundance of Sc, Ti, Yb and Er in seawater and particulate matter compared to dissolved Rb. c)Measured in low resolution, corrected for isobaric interferences and monitored for molecular interferences by using spike-sample mixing plots or comparing measured ratios to natural ratios.

For the particulate samples there was a significant contribution of Zr from the filter blanks as well as in the sample itself and could not be eliminated. Table 2.9 lists isobaric corrections and the range in relative magnitude of each correction for particulate and seawater samples.

Molecular interferences include argides, nitrides, oxides and hydrides of lower mass metals. The formation of molecular interferences depends on the chemistry of the plasma formed in the ICPMS torch and the concentration of the metals and other matrix elements in the sample solution. There is no simple mathematical way to correct for molecular interferences. Hydrides and oxides can be minimized with the use of a desolvating nebulizer to remove the water. Argides form with the sample gas and cannot be removed, but ^{40}Ar-^{16}O, a major interference at ^{56}Fe can be resolved away by measuring Fe at medium mass resolution.

Samples with unresolvable molecular interferences can be identified and eliminated by constructing spike-sample mixing diagrams. When three isotopes were available, ratio-ratio plots (Figure 2.5) were used to monitor data quality and to check for molecular and isobaric interferences. Figure 2.5 illustrates the effect of Zr interferences on Mo ratios. These plots are constructed on the theory that, since all sample ratios are mixtures of spike and natural compositions, all of the ratios measured must fall on a line between natural isotopic composition and the isotopic composition of the spike. Samples that do not fall on the mixing line are subject to isobaric or molecular interferences and do not give reliable concentrations. Most molecular interferences could be projected back to the mixing line by using the equation 2.5, but if the interference exceeded 30% of

the measured intensity the correction often fell short of the mixing line. Ratios subject to molecular interferences could not be corrected. All data presented here are within one standard deviation of the mixing line.

2.4 Results and Discussion

2.4.1 Precision and Accuracy

As discussed above, the precision and accuracy of isotope dilution techniques rely on precise and accurate determination of isotope ratios. Greater precision is required to determine small variations in dissolved Molybdenum in seawater than is necessary to measure larger variations and concentrations in cells and particulate matter. Our ability to make precise and accurate isotope ratio measurements of Mo is demonstrated by our accumulated standard analyses of $^{95}Mo/^{96}Mo$, the isotope ratio used in concentration calculations: 0.9549 ± 0.0018 (1SD = 0.19%; n = 350) after correction for instrumental mass bias (Figure 2.10). The accepted value is 0.955022 (Lee and Halliday 1995).

Accuracy and precision of dissolved Mo analyses can be demonstrated several ways: analysis of certified reference standards, comparison with other researchers results, or replicate analyses. We measured the NASS 5 certified standard seawater and obtained 92.0±0.8 nmol/kg (not salinity normalized), which is within error of the certified value (100±10 nmol/kg). However, NASS 5 like most seawater standards is poorly constrained for Mo and so is not a very rigorous test. Collier (1985) reported a mean Mo concentration of 107 nM ± 2.3% (1 s.d.) for two Pacific profiles normalized to 35‰ salinity. A comparison of our salinity normalized seawater measurements from the

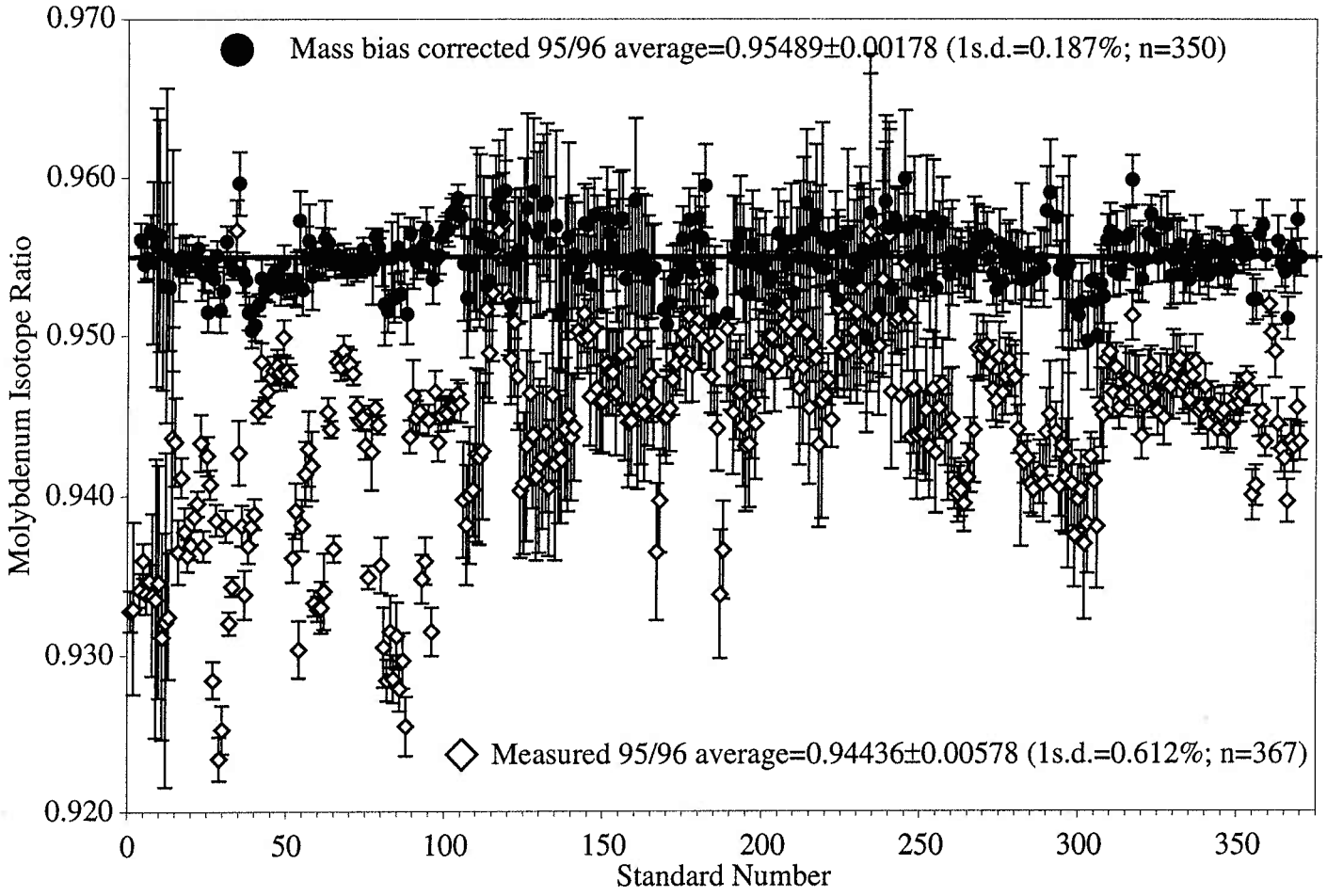

Figure 2.10 Plot of 95/96 Mo ratios from over 350 standard analyses run over the course of 3 years on the WHOI magnetic sector ICPMS. Open diamonds show measured, interference corrected ratios. Filled circles indicate mass bias corrected ratios. The thick black line is the accepted value of 0.955022 (Lee and Halliday 1995)All error bars are one standard deviation measurement errors. The average mass bias corrected ratio id 0.9549 ± 0.0018 (1SD = 0.19%).

Atlantic (107.5 nM ± 0.5%; 1 s.d.; n=17). and Pacific samples below 200m (108.5 nM ± 0.8%; 1 s.d.; n=8) shows a good agreement with Collier and argues strongly for the accuracy of this method. All seawater analyses in this study were measured in duplicate or triplicate to provide a rigorous measure of external precision. The average standard deviation on replicate analyses is ±0.46 %. This excludes replicates that had obvious contamination (single samples that differed significantly from triplicate analyses) or interference problems as discussed in the previous section.

For cell and particulate matter samples, higher concentrations and larger variations between samples do not require as precise analyses. This allows use of the less precise standard addition method. Accuracy is demonstrated by determination of trace metals in a certified reference standard (Table 2.10). All of these analyses were within 3.4% of the certified values. There is greater discrepancy between the measured and uncertified values. Rb, in particular is over 33% different from the reference value.

Table 2.10 Certified Sediment Standard analyses

	NIST Estuarine Sediment Standard 1646a		
	Certified values	**Measured values**	**% Difference**
Aluminum (%)	2.297	2.24	2.5
Iron (%)	2.008	1.94	3.4
Manganese (ppm)	234.5	222	2.3
	Uncertified values		
Rubidium (ppm)	38	25	33
Molybdenum (ppm)	1.8	1.6	11

2.4.2 Blanks and Detection Limits

Instrument blanks were monitored by running 10% HNO_3 interspersed with samples during every ICP-MS run. Mo, Rb and In blanks associated with the instrument

were negligible compared to average sample intensities. However, instrument contributions on Fe, Al, Mn and Zr could be significant. Fe, as the most contamination prone of these elements, was monitored closely and blank levels were determined prior to each days run. If levels were unacceptable (>10% of the intensity measured in a 1 ppb Fe standard), steps were taken to reduce blank either by changing the cones or cleaning the MCN-6000 or increasing sample concentration. The average instrument blank was determined for each run and subtracted from samples.

Procedural blanks were determined for seawater and particulate matter analyses. Blanks for dissolved seawater Mo associated with the column procedure averaged 1.04±0.73 nmol/kg and always less than 0.7% of total analyte used for seawater analyses. For particulate matter collected on filters and dissolved via refluxing leach, filter blanks were analyzed as discussed in section 2.2.3. These blanks and detection limits are shown in Table 2.11.

Table 2.11 Filter blanks and detection limits.

Blanks	Mo	Rb	Al	Mn	Fe
Polycarbonate filters (n=5; ng/filter)	0.30±0.05				9.4±3.2
Detection limit (ng)[a]	0.15				9.6
Supor Filters (n=4; ng/filter section)	0.42±0.35	1.3±1.3	74±40	3.6±1.8	29±25
Detection limit (ng)[a]	1.1	1.7	120	5.4	75

[a]etection limits are equivalent the 3 time the standard deviation of the blank

2.5 Conclusions

ICP-MS is an important analytical tool for the analysis of biologically relevant trace metals in seawater, particles and cultured cells. It's precision and accuracy is limited by interfering molecular and isobaric species, but these problems can be

overcome by careful selection of isotopes monitored, utilization of higher mass resolution methods and careful cleaning or preconcentration steps to remove interfering elements. These advances allow for greatly improved precision and accuracy of Mo concentration in environmentally relevant materials.

2.6 References

Berrang, P. G., and E. V. Grill. 1974. The effect of manganese oxide scavenging on molybdenum in Saanich Inlet, British Columbia. Marine Chemistry **2:** 125-148.

Collier, R. W. 1985. Molybdenum in the Northeast Pacific-Ocean. Limnology and Oceanography **30:** 1351-1354.

Colodner, D., J. Edmond, and E. Boyle. 1995. Rhenium in the Black Sea; comparison with molybdenum and uranium. Earth and Planetary Science Letters **131:** 1-15.

Cullen, J.T., and R.M. Sherrell.1999. Techniques for determination of trace metals in small samples of size-fractionated particulate matter: phytoplankton metals off central California. Marine Chemistry **67**:233-247.

Dahmen, J., M. Pflugger, M. Martin, and L. Rottmann. 1997. Trace element determination of high-purity chemicals for the processing of semiconductors with high-resolution ICP-mass spectrometry using stable isotope dilution analysis (IDA). Fresenius Journal of Analytical Chemistry **359:** 410-413.

Heumann, K. G. 1988. Isotope dilution mass spectrometry. In Inorganic Mass Spectrometry, p. 301-376, Inorganic Mass Spectrometry. John Wiley.

Lee, D.-C., and A. N. Halliday. 1995. Precise determinations of the isotopic compositions and atomic weights of molybdenum, tellurium, tn nd tungsten using ICP magnetic sector multipl collector mass spectrometry. Internaltional Journal of Mass Spectrometry and Ion Processes **146/147:** 35-46.

Nameroff, T. J. 1996. Suboxic trace metal geochemistry and paleo-record in continental margin sediments of the eastern tropical North Pacific. University of Washington, Seattle, WA, United States.

Nameroff, T. J., M. Kondo, J. W. Murray, and Anonymous. 1995. The geochemistry of cadmium, molybdenum, rhenium, uranium, and vanadium in the oxygen minimum zone of the eastern tropical North Pacific. AGU 1995 spring meeting. American Geophysical Union, 1995 spring meeting **76:** 320.

Nozaki, Y. 1996. A fresh look at Elements Distribution in the North Pacific. EOS. www.agu.org/eos_elec/97025e.html (posted 05/1997).

Prange, A., and K. Kremling. 1985. Distibution of dissolved molybdenum, uranium and vanadium in Baltic Sea waters. Marine Chemistry **16:** 259-274.

Price, N. M., L. F. Andersen, and F. M. M. Morel. 1991. Iron and Nitrogen Nutrition of Equatorial Pacific Plankton. Deep-Sea Research Part a-Oceanographic Research Papers **38:** 1361-1378.

Riley, J. P., and D. Taylor. 1968. The use of chelating ion exchange in the determination of molybdenum and vanadium in seawater. Analytica Chimica Acta **41:** 175-178.

Sohrin, Y. and others 1998. Determination of trace elements in seawater by fluorinated metal alkoxide glass-immobilized 8-hydroxyquinoline concentration and high-resolution inductively coupled plasma mass spectrometry detection. Analytica Chimica Acta **363:** 11-19.

Sohrin, Y., M. Matsui, and E. Nakayama. 1999. Contrasting behavior of tungsten and molybdenum in the Okinawa Trough, the East China Sea and the Yellow Sea. Geochimica et Cosmochimica Acta **63:** 3457-3466.

Zheng, Y., R. F. Anderson, A. van Geen, and J. Kuwabara. 2000. Authigenic molybdenum formation in marine sediments: A link to pore water sulfide in the Santa Barbara Basin. Geochimica Et Cosmochimica Acta **64:** 4165-4178.

CHAPTER 3 NON-CONSERVATIVE MOLYBDENUM BEHAVIOR IN SEAWATER

Abstract

This study re-examined the dissolved distribution of Molybdenum (Mo) in the world ocean using high precision (±0.5%) isotope dilution ICP-MS analyses. Thirteen profiles were measured, four from the California Borderland Basins, seven from the Eastern Equatorial Pacific and one each from the Arabian and Sargasso Seas. The average salinity (35 ppt) normalized concentration of Mo for the Arabian Sea and Sargasso Sea profiles were 107.78±0.32 and 107.50±0.34 nmol kg^{-1}, respectively. These values were in agreement with previous measurements of the Mo concentration of seawater. The Eastern Tropical Pacific profiles however show both enrichment and depletion (up to +5 and –3 nmol kg^{-1}) of water samples after salinity normalization. These deviations from the Mo salinity trend suggest that Mo behavior is non-conservative in the Equatorial Pacific. Several mechanisms capable of causing non-conservative behavior were evaluated. Neither uptake of Mo by bacteria and phytoplankton or scavenging of Mo by Mn oxide particles can sequester enough Mo to deplete the dissolved phase. Profiles from the Santa Barbara and San Nicholas Borderland Basins showed Mo depletions in waters below sill depth of up to 2.5 nmol kg^{-1} relative salinity. Uptake of Mo from coastal anoxic sediments is likely the cause of Mo in stratified basins. However, the flux of Mo in or out of sediments required to support the propagation of these features into the open ocean where the Eastern Tropical Pacific depleted and enriched profiles were measured appears to be unreasonably large. The mechanism causing non-conservative variations of Mo is still at large.

3.1 Introduction

The distribution of Mo in seawater was initially examined in the mid-1970's and 1980's (Collier 1985; Morris 1975; Prange and Kremling 1985; Sohrin et al. 1989). These studies conclude that that Mo is broadly conservative in seawater, similar to the other transition metals present in seawater primarily as oxyanions (U, Re, W and V). This conclusion implied that biological utilization did not significantly influence the water column distribution of Mo. However, Mo is an essential micronutrient intimately involved in the nitrogen cycle. It is used in nitrogenase, the enzyme responsible from nitrogen fixation and nitrate reductase, the first step of the denitrification pathway. Estimates of the rates of marine nitrogen fixation and denitrification have increased

significantly in recent years (Capone 2001; Capone and Montoya 2001; Falkowski et al. 1998; Gruber and Sarmiento 1997). These developments provide motivation for revisiting the distribution of Mo in seawater as a possible tracer of processes important to the nitrogen cycle.

The goal of this work was to reevaluate the conclusion that Mo behaves conservatively in seawater. To accomplish this goal, improved methods for the analysis of Mo in seawater that take advantage of improvements in ICPMS technology were developed and implemented. Water column samples were collected from oceanic regions where processes that might cause Mo to behave non-conservatively are active. These processes include biological utilization of Mo in association with nitrogen fixation and nitrate reduction, as well as abiotic cycling of Mo in association with water column Mn oxides and reducing sediments. The specific study sites are: the Sargasso Sea, a region of nitrogen fixation (Gruber and Sarmiento 1997; Lipschultz and Owens 1996; Michaels et al. 1996; Orcutt et al. 2001); the Arabian Sea, an area of water column denitrification and Mn oxide cycling (Gruber and Sarmiento 1997; Lewis and Luther 2000; Naqvi 1994); the Eastern Tropical Pacific, a zone where low oxygen conditions on the coast produce highly Mo enriched anoxic coastal sediments as well as near shore denitrification and Mn oxidation (Codispoti and Packard 1980; Deutsch et al. 2001; Gruber and Sarmiento 1997; Johnson et al. 1996; Nameroff 1996); and the California Borderland basins a series of silled basins characterized by variable bottom water oxygen concentrations, a setting that highlights Mo interaction with sediments (Zheng et al. 2000).

3.1.1 Previous analyses of Mo in seawater

Results of earlier work on the distribution of Mo in the open ocean are consistent with conservative behavior of this element. Analyses of Mo in Atlantic (Morris 1975) and Pacific samples (Collier 1985; Morris 1975) do not reveal any resolvable structure in the vertical distribution of Mo in the water column. When normalized to a salinity of 35 ppt these profiles give average Mo concentrations of 107.6±3.4 nmol kg^{-1} (±1sd; Collier 1985) and 110.5±8.7 nmol kg^{-1} (±1sd; Morris 1975). Data from the Baltic Sea show a linear correlation of Mo concentration with salinity over the range of 2 to 16 ppt with a projected concentration of 107.6 at 35 ppt (Prange and Kremling 1985). Mo concentrations resulting from these studies agree within analytical uncertainty. These data sets were determined by preconcentration using either a coprecipitation or a chelating resin method and were analyzed via atomic adsorption spectroscopy. Analytical uncertainties associated with these methods ranged from ±2 to 10% or ±2 to 11 nmol kg^{-1} (±1sigma). These large uncertainties overlap the entire concentration range of most biologically important metals (Fe 0-1 nM; Zn 0-10 nM; Cd 0-1.2 nM) and may have obscured non-conservative behavior associated with biological or sedimentary processes. Despite ±2% standard deviation, Collier's (1985) North East Pacific profile shows tantalizing near surface variations (Figure 3.1). However Collier concluded that the profiles were conservative because the peaks do not exceed four standard deviation in amplitude. This conclusion was consistent with Mo's relatively high concentration in seawater and the high solubility of the molybdate (MoO_4^{-2}) anion, the likely species of Mo in oxic seawater. More recent measurements of Mo in seawater that have been

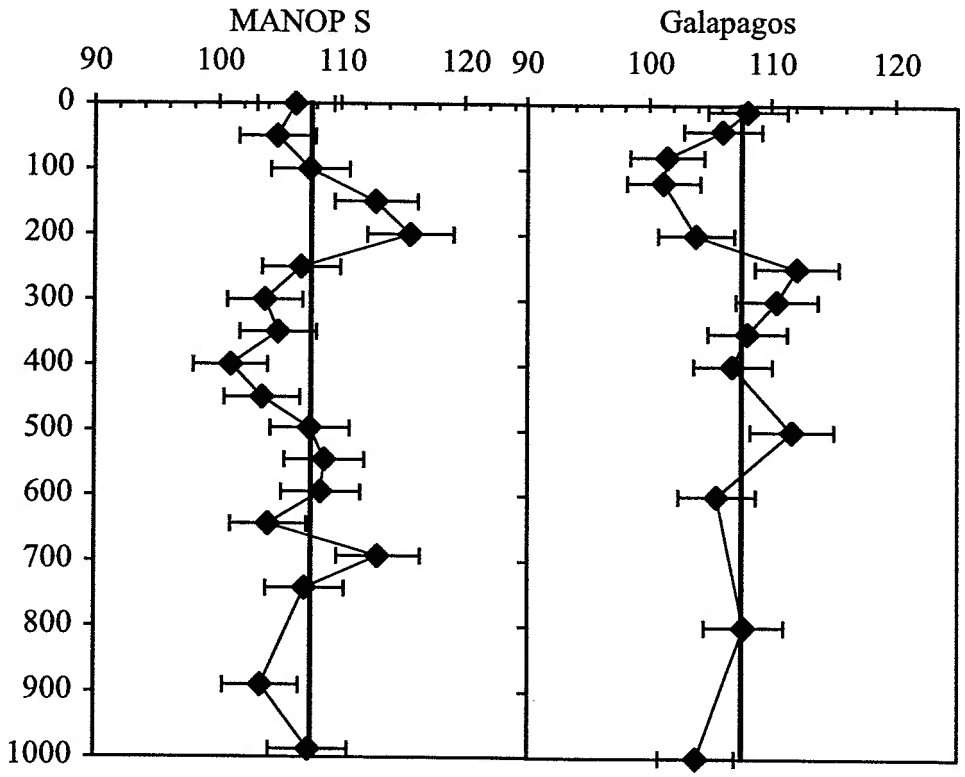

Figure 3.1 Salinity-normalized profiles of dissolved Mo (filled diamonds) from 2 Pacific sites replotted from Collier (1985). Error bars are ± 2.5 nM (1sd). Subtle variations in dissolved Mo occur in the upper water column.

made by isotope dilution and analysis of diluted seawater via ICPMS, without a preconcentration step do not yield more precise data (Nameroff, 1996: ±5%; Sohrin et al.1989: ±6%; ±1sd).

3.1.2 Biological utilization of Mo

Although direct analyses of seawater Mo have not yielded evidence of large variations of Mo concentration in seawater, utilization of Mo by biota for enzymatic processes is a potentially important mechanism for depleting Mo in the water column. Mo enzymes catalyze both oxidation and reduction reactions, and Mo valances in these enzyme systems include Mo (VI), Mo (V) and Mo (IV). In the marine environment the most important of the Mo enzymes are likely nitrogenase, the enzyme responsible for the reduction of N_2 to NH_3, and assimilatory and dissimilatory nitrate reductase, an enzyme required for the reduction of NO_3^- to NO_2^- for nitrogen uptake or as an electron sink (Raven 1988). Mo utilization in other enzymes, such as DMSO reductase, responsible for DMS production in the ocean (Stiefel 1996) may also impact marine Mo behavior. The amount of Mo in phytoplankton and bacteria is not well known (Table 3.1). The average value for phytoplankton appears to be about 2 to 2.5 ppm or about 0.6 μmol Mo: mol C (Martin and Knauer 1973). The Mo content of phytoplankton may depend strongly on enzymatic requirements. Recent measurements of Mo:C ratios in nitrogen fixing (Tuit 2003 Chapter 4) and denitrifying organisms (Tuit 2003 Appendix 1) vary significantly with Mo enzyme activity. These estimates allow an assessment of whether these processes can lead to depletion or enrichment of dissolved Mo the water column.

Table 3.1 Molybdenum in Particulate Matter

Sample	Mo g g^{-1}	Mo:C (μmol:mol)	Cellular Concentration (fg $cell^{-1}$)	Ref.
Phytoplankton	$2x10^{-6}$	0.56		a
N_2 fixing cyanobacteria		0.06-1.33	0.0015-.44	b
Denitrifying bacteria		0.48	0.000116	b
UCC	$2x10^{-6}$			c

[a]Martin and Knauer 1973 [b]Tuit 2003 [c]Taylor and McLennan 1985

3.1.3 Geochemical controls on Molybdenum Distribution

Numerous studies of Mo in marine sediments have documented processes that can give rise to Mo depletion and enrichment in pore waters and associated sediments. Analogous processes operating in the water column, as well as benthic fluxes of Mo in and out of the sediment, could potentially produce non-conservative distributions of Mo that are unrelated to utilization of Mo in specific enzymes. Geochemically, Mo is enriched in sedimentary Mn oxides and may be involved in Mn cycling in the water column (Berrang and Grill 1974; Francois 1988; Shaw 1988; Shaw et al. 1990). It is also highly enriched in anoxic sediments and has been proposed as a tracer of ocean anoxia (Dean et al. 1999; Shaw et al. 1990). These processes must be evaluated and shown to be unimportant before non-conservative distributions of Mo in the water column can be unequivocally linked to biological utilization of these element.

Prior studies clearly demonstrate that Mo is commonly associated with Mn oxides in a variety of oxic to suboxic sedimentary settings: at the chemocline of stratified basins (Berrang and Grill 1974; Colodner et al. 1995), sediments and sediment pore waters (Shimmield and Price 1986; Shaw et al. 1990), and in Mn crusts (Manheim 1974). Many sedimentary marine Mn oxides exhibit a similar molar ratio of Mo:Mn of $1.1x10^{-3}$

(Manhiem, 1974; Shimmield and Price, 1986.). This corresponds to an effective concentration of roughly 1000 ppm Mo in pure MnO_2, a 500-fold enrichment relative to the Mo concentration commonly assumed for continental detritus (approximately 2 ppm: Taylor and McLennan 1985). The mechanisms that underlie the association of Mo with sedimentary Mn oxides are not understood. Nor has it been determined whether the Mo enrichment seen in sediment environments also occurs in Mn oxides produced in the water column. These Mn oxide particles are produced by very different processes (i.e. photo-reduction: (Sunda and Huntsman 1988), and microbially mediated oxidation: (Tebo and Emerson 1986)) rather than the autocatalytic oxidation that forms sedimentary Mn oxides (Hem 1978; Wehrli et al. 1995). If the large enrichment factor holds true for authigenic Mn oxides associated with suspended particulate matter, Mn cycling in the water column could dramatically influence Mo dissolved distribution.

Mn oxides may affect the Mo dissolved Mo budget in two ways. First, authigenic Mn oxides formed in the water column may preferentially scavenge Mo. Second, dissolution of Mn oxides near the sediment-water interface can release Mo to pore waters and allow Mo to flux back out of the sediment into bottom water (Shaw et al. 1990). This process is likely to occur under non-steady state conditions in which shoaling of the oxygen penetration depth has resulted in dissolution of Mo-enriched Mn-oxides. Evidence for Mo cycling with Mn oxides in the water column can be found in two recent coastal studies. Zheng et al. (2000: Santa Barbara Basin) saw enrichments of both Mo and Mn in sediment trap brines and suggested that Mn cycling may have had a role in delivering Mo to the trap. Nameroff et al. (2000: Western Mexican Margin) also saw

elevated non-lithogenic Mo and Mn concentrations in trap samples. The ratio of total Mo:Mn in the Nameroff et al. (2000) trap samples was between 0.0012 and 0.0046 g g^{-1} within in range of the 0.002 seen in Mn oxides, but the ratio in the Zheng samples was high and extremely variable. These data suggest that Mn oxides may effect the distribution of particulate and possibly dissolved Mo.

In addition to exhibiting an affinity for Mn oxides, Mo is also strongly enriched in anoxic coastal sediments. These sediments, though only 0.3% of the total oceanic area, are the major sink for Mo, accounting for approximately 60 % of the total Mo riverine input (Bertine and Turekian 1973; Emerson and Huested 1991). Mo is enriched in sediments underlying the Oxygen Minimum Zone (OMZ) on the coast of Mexico (Nameroff 1996), California (Zheng et al. 2000) and Oman (Morford and Emerson 1999). In enclosed basins, such as the Cariaco Trench and Saanich Inlet sediment concentrations can be as high as 140 μg g^{-1} and may lead to depletion of water column distributions by 10-30% (Berrang and Grill 1974; Colodner et al. 1995; Crusius et al. 1996; Francois 1988). Molybdenum enrichment appears to occur primarily at the sediment water interface and in pore waters rather than by a water column process and seems to be related to sulfide availability (Francois 1988; Helz and Adelson 1997). Mo can also be released from anoxic sediments when sediments are exposed to higher concentrations of oxygen in overlying waters causing oxidative burn down (Zheng et al. 2000). Whether the flux of Mo out of sediments due to oxidation is enough to enrich overlying waters is unknown. Uptake of Mo from sediments can influence water column distributions in

confined basins but it remains to be seen if these processes can influence the distribution of Mo in the open ocean.

3.2 Methods

3.2.1 Sample Collection and Storage

To survey the distribution of Mo in the world oceans a suite of seawater profiles were examined from the California Borderland Basins, the Eastern Equatorial Pacific, the Sargasso Sea and the Arabian Sea. These regions were chosen to address specific aspects of Mo biogeochemistry. The Sargasso Sea was chosen to represent a region influenced by surface nitrogen fixation. The California Borderland Basin profiles focus on the potential influence of sediments on Mo distribution. The Arabian Sea profile examined an area of in situ water column denitrification and Mn oxide cycling. The Eastern Tropical Pacific, a region where ocean circulation and high productivity combined to produce low oxygen conditions, combines the influences of highly Mo enriched anoxic coastal sediments as well as near shore denitrification and Mn oxidation in the water column. Station locations are shown in Figure 3.2. Table 3.2 lists the location, sampling techniques and researchers who collected the samples for each site, as well as auxiliary data available in Appendix 2. During the initial phase of this work samples were collected on cruises of opportunity where it was not possible to collect filtered samples suitable for trace metal analysis. Similar to previous work (Collier 1984) it was assumed initially that the particulate contribution was negligible and that total Mo in a seawater sample and dissolved Mo were essentially equivalent. In addition it was also assumed

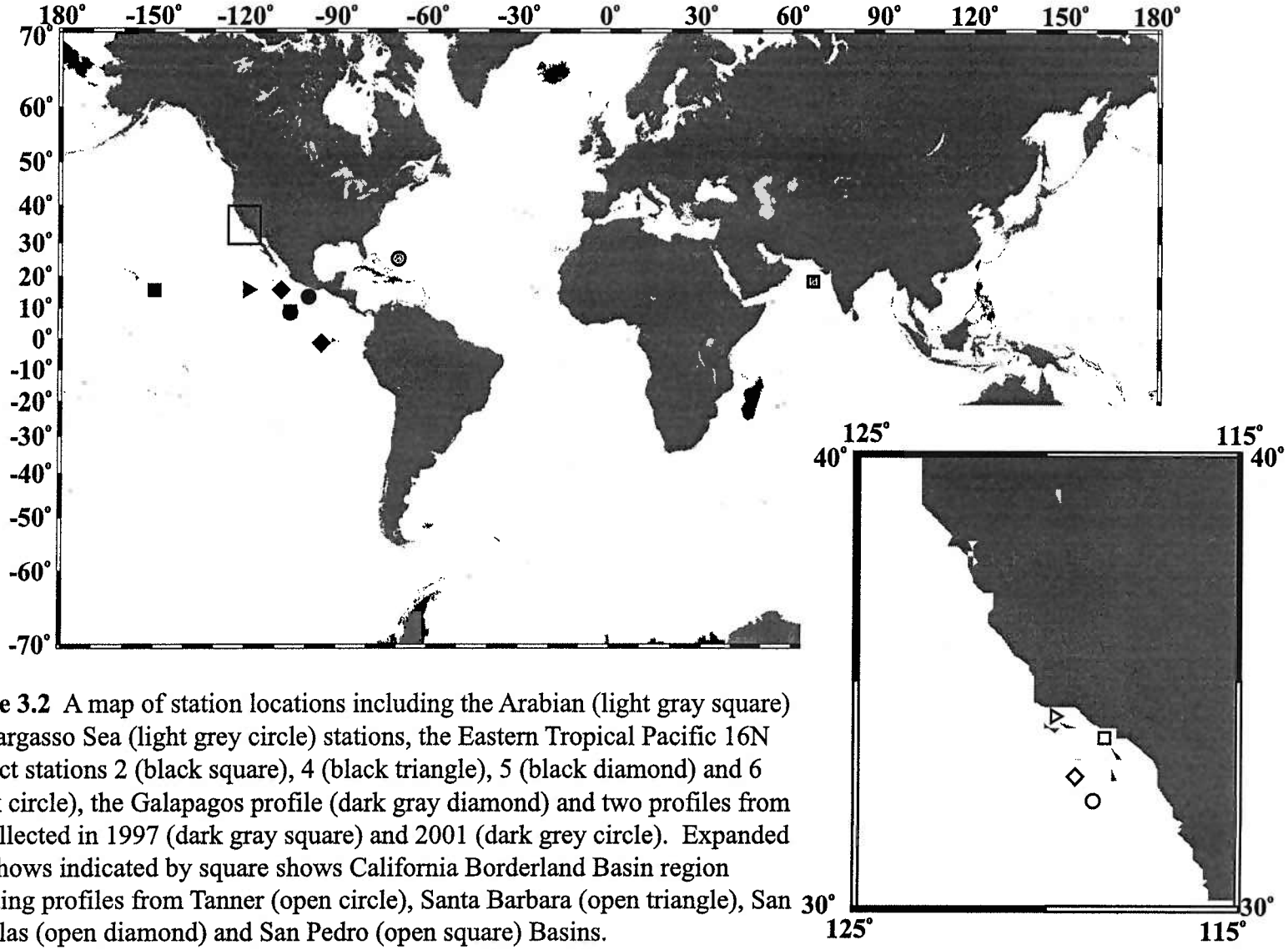

Figure 3.2 A map of station locations including the Arabian (light gray square) and Sargasso Sea (light grey circle) stations, the Eastern Tropical Pacific 16N transect stations 2 (black square), 4 (black triangle), 5 (black diamond) and 6 (black circle), the Galapagos profile (dark gray diamond) and two profiles from 9N collected in 1997 (dark gray square) and 2001 (dark grey circle). Expanded area shows indicated by square shows California Borderland Basin region including profiles from Tanner (open circle), Santa Barbara (open triangle), San Nicholas (open diamond) and San Pedro (open square) Basins.

Table 3.1. Station locations and available data.

Profile	Lat	Lon	Date	Dist from coast (km)	Sample Collection Technique	Collected by	Auxilary Data
Arabian Sea	19 10 N	67 10 E	Jul 1995		CTD unfiltered & Go-Flo filtered	a	Sal, Temp, O2, Nutrients, Mn
Sargasso Sea	25 59 N	70 04 W	Mar 1998		Go-Flo filtered	e	Sal, Temp, O2, Nutrients
Eastern Tropical Pacific Ocean							
Transect 2	16 00 N	150 00 W	Jun 2000	5550	CTD filtered and unfiltered	b	Sal, Temp, O2, Nutrients, Mn
Transect 4	16 00 N	119 00 W	Jun 2000	2250	CTD filtered and unfiltered	b	Sal, Temp, O2, Nutrients, Mn
Transect 5	16 00 N	107 00 W	Jun 2000	960	CTD filtered and unfiltered	b	Sal, Temp, O2, Nutrients, Mn
Transect 6	15 00 N	98 00 W	Jun 2000	540	CTD filtered and unfiltered	b	Sal, Temp, O2, Nutrients, Mn
Galapagos	1 S	95¡W	Nov 1992	1500	CTD unfiltered	c	Sal, Temp, O2, Nutrients,
9N	9 49 N	104 15 W	Dec 1997	2110	CTD filtered and unfiltered	c	Sal, Temp, O2,
9N	9 49 N	104 15 W	Dec 2001	2110	CTD & GoFlo filtered	e	Sal, Temp, O2, Nutrients
California Borderland Basins							
Santa Barbara	34 13 N	120 02 W	Jul 2001		CTD filtered	d	Sal, Temp, O2
San Nicholas	33 01 N	119 03 W	Jul 2001		CTD filtered	d	Sal, Temp, O2
San Pedro	33 35 N	118 32 W	Jul 2001		CTD filtered	d	Sal, Temp, O2
Tanner	32 59 N	119 45 W	Jul 2001		CTD filtered	d	Sal, Temp, O2

[a]Chris Measures and Sue Vink [b]Eric DeCarlo [c]Ravizza [d]Ravizza and Haupert [e]This Study

that samples for Mo analysis could be collected from a conventional Niskin rosette system without contamination. These assumptions were found to be generally correct by were comparing filtered and unfiltered Niskin samples, as well as samples collected using Go-Flo bottles and Niskin rosettes.

3.2.2 *Mo Analyses*

Mo concentrations were determined by isotope dilution (ID) and analyzed by inductively coupled plasma mass spectrometry (ICP-MS). The sample handling scheme differed from those commonly employed for Mo analyses because it used an ion exchange Mo preconcentration and separation step. ICP-MS Mo analyses of natural waters at low precision do not require preconcentration (Colodner et al. 1995; Nameroff 1996) but higher precision analyses benefit from the separation of Mo from the seawater matrix. For the high precision procedure, samples, either unfiltered or filtered through a 0.2μm filter, were acidified to pH 2 at sea and stored for analysis on shore. In the lab, an aliquot of seawater was spiked with an isotopically enriched ^{95}Mo spike (96.45% ^{95}Mo: Oakridge National Laboratory), treated with 300 μl hydrogen peroxide and heated gently for at least 12 hours to allow for spike sample equilibration. The peroxide treatment was designed to ensure that all Mo existed as molybdate, to facilitate spike-sample equilibration and improve yields. The spike solution concentration was calibrated against a Specpure™ plasma standard (Alpha Aesar, nominal accuracy ±0.3%). Typically, 15 ml of seawater were used per analysis, although as little as 250 μl could be analyzed to achieve the same precision. Because spike and sample equilibrated prior to the ion exchange separation, non-quantitative recovery of Mo from the ion exchange column did

not adversely affect results. Nevertheless experiments performed to monitor the efficiency of Mo recovery indicated yields over 80%. The Mo ion exchange separation was performed using a chelex ion exchange resin procedure (modified from Riley and Taylor 1968). The chelex was cleaned using the Price et al. (1989) method to reduce the procedural Mo blank and clogging of the instrument uptake system with by organic matter. Blanks associated with the procedure were typically 0.67±0.33 ng (n=47) total analyte or between 0.2 and 0.5%. This limited measurement precision.

Following column separation, mass spectra on the ICP-MS were typically free from isobaric interferences, and several independent isotope ratios could be monitored as internal measures of instrumental mass bias (discussed in depth in Tuit 2003 chapter 2). In plasma source mass spectrometry, heavy ions are preferentially extracted into the mass analyzer. In the Mo mass range, mass bias effects were on the order of 1-2 % per amu. To obtain accurate isotope dilution data, corrections must be made to compensate for this effect. Because Mo has seven stable isotopes it was possible to make mass bias corrections on a sample by sample basis, using the non-spike masses, thus eliminating uncertainty due to fluctuations in machine mass bias common in plasma source mass spectrometers. Non-spike masses were corrected for small contributions from isotopic impurities in the ^{95}Mo spike and fitted with a linear mass bias equation. This allowed precise and accurate corrections for this effect to be made, which were essential for high precision concentration determinations. Counting statistics associated with the isotope ratio measurements had 2 sigma standard errors of ±0.1-0.2%.

To assess the reliability of the mass bias correction and procedural blanks, duplicate or triplicate analyses were performed on over 80% of the samples. The mean difference between replicate analyses was 0.5%. As the analyses reported here were preformed over the course of several years, duplicates from different profiles were reanalyzed together to make sure that there were no systematic offsets.

Table 3.3 shows that replicates from the Sargasso Sea, 9N 1997 and the Go-Flo samples from the Arabian Sea reproduced within the 0.5% 1sd precision that was normal for replicate analyses in this study. The only samples that failed to reproduce well were the surface Niskin samples from the Arabian Sea. The Arabian Sea unfiltered Niskin samples run in 1999 had larger standard deviations associated with error in measuring the sample ratio and unusually high Mo concentrations, particularly the two samples from 50 m. The high values seen for the Niskin samples from the surface Arabian Sea are therefore interpreted to be spurious and may be the result of laboratory contamination during the analysis.

Table 3.3 Replicate analyses.

Profile	Depth	Data	Concentration (nmol kg^{-1})	% 1sd	Average (nmol kg^{-1})	% 1sd
Arabian Sea Go-Flo	51	Sep-99	112.05	0.62%	112.18	0.38%
Arabian Sea Go-Flo	51	Sep-99	111.82	0.74%		
Arabian Sea Go-Flo	51	Feb-02	112.66	0.03%		
Arabian Sea Go-Flo	88	Sep-99	112.31	0.92%	112.75	0.37%
Arabian Sea Go-Flo	88	Sep-99	112.81	0.84%		
Arabian Sea Go-Flo	88	Feb-02	113.13	0.04%		
Arabian Sea Niskin	10	Sep-99	118.02	0.70%	116.44	2.37%
Arabian Sea Niskin	10	Sep-99	118.04	0.84%		
Arabian Sea Niskin	10	Feb-02	113.26	0.04%		
Arabian Sea Niskin	50	Sep-99	118.08	2.10%	119.43	6.19%
Arabian Sea Niskin	50	Sep-99	127.41	4.12%		
Arabian Sea Niskin	50	Feb-02	112.81	0.03%		
Arabian Sea Niskin	100	Sep-99	112.57	0.81%	112.66	0.69%
Arabian Sea Niskin	100	Sep-99	111.93	0.74%		
Arabian Sea Niskin	100	Feb-02	113.49	0.04%		
Sargasso Sea	300	Feb-02	112.08	0.03%	112.43	0.43%
Sargasso Sea	300	Feb-99	112.77	0.01%		
2N 1997	72	Feb-02	107.92	0.03%	107.70	0.29%
2N 1997	72	Aug-99	107.48	0.08%		

3.3 Results

3.3.1. Galapagos profile

The first profile measured for this study was collected on a cruise of opportunity in 1992 (Figure 3.3). The samples were collected unfiltered using a Niskin rosette and were acidified at sea. This profile and all subsequent Mo profiles unless otherwise stated are plotted normalized to a salinity of 35 ppt using the equation. The total range in salinity for the profile was 34.554 to 35.084 ppt.

$$C_{\text{Salinity Normalized}} = C_{\text{Measured}} \times \frac{35 \text{ ppt}}{\text{Sample Salinty}}$$

Conservative elements vary directly with salinity, thus any Mo concentration variations that persist after normalizing Mo concentrations to a constant salinity highlight non-conservative behavior. The Galapagos profile shows two distinct peaks in Mo concentration at 40 and 160m separated by a minimum at 100m. The profile is enriched in the upper 200m relative to the average Mo concentration of 107.6 nmol kg^{-1} at 35 ppt but approaches the conservative concentration at depth. The total range in concentration is 6.5 nmol kg^{-1} with an average concentration of 109.26±0.76 nmol/kg (±2 times the standard error (2se)). Additional analyses available for this profile included nutrients and CTD data. The upper Mo peak at 40 m is coincident with the fluorescence maximum. The primary nitrite maximum (80 m) and the Mo minimum (100 m) are quite close to each other and are directly underlain by the second Mo peak. These data first drew our attention to the possible link between Mo and denitrification, a microbial process catalyzed by a Mo bearing enzyme. It motivated acquisition of other profiles from the Arabian sea, document Mo variations in a region of pronounced denitrification (Gruber and Sarmiento 1997), and the Sargasso sea, a zone of active nitrogen fixation, a biological processes thought to require the largest biological Mo demand (Sanudo-Wilhelmy et al. 2001; Sprent and Raven 1985)

3.3.2 Arabian Sea

The Arabian Sea profile was collected as part of the JGOFS program (R/V Thomas G. Thompson 1995 Process 4 station N7) by Chris Measures and Sue Vink (Figure 3.4). The majority of the samples was collected unfiltered using a standard Niskin bottle rosette and was acidified at sea. Several depths near the surface (16m, 51m

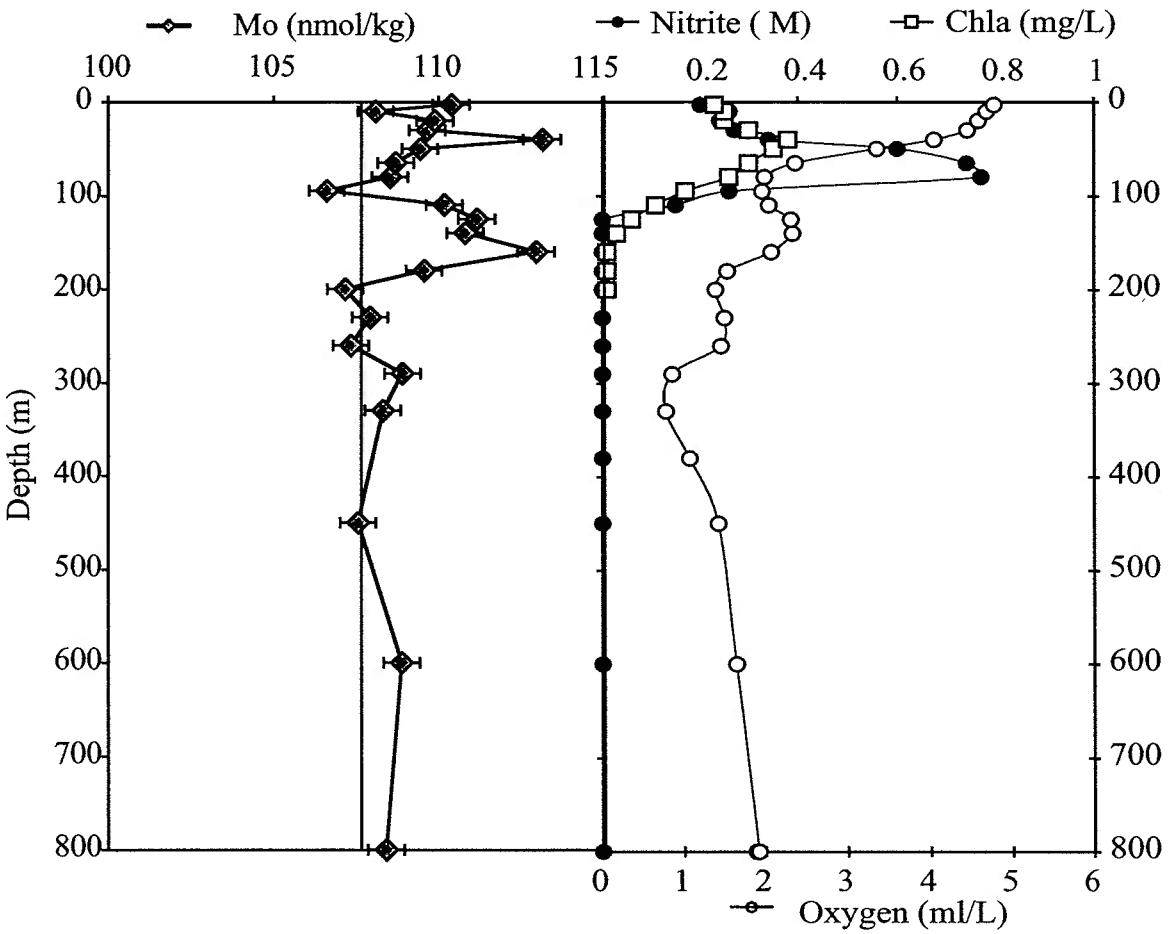

Figure 3.3 Galapagos station 1S 95W profiles of unfiltered niskin samples for Molybdenum (grey diamonds) Nitrite (filled circles) Oxygen (open circles) and fluorescence (open squares) collected in 1992. Molybdenum concentrations were normalized to a salinity of 35 ppt. The straight line at 107.6 nmol/kg represents the nominal salinity normalized Mo concentrationfrom Collier (1985). This same line is shown for reference in all subsequent Mo concentration profiles. Error bars on Mo are –0.5%. Mo concentrations are enriched in surface waters but approaches conservative values at depth.

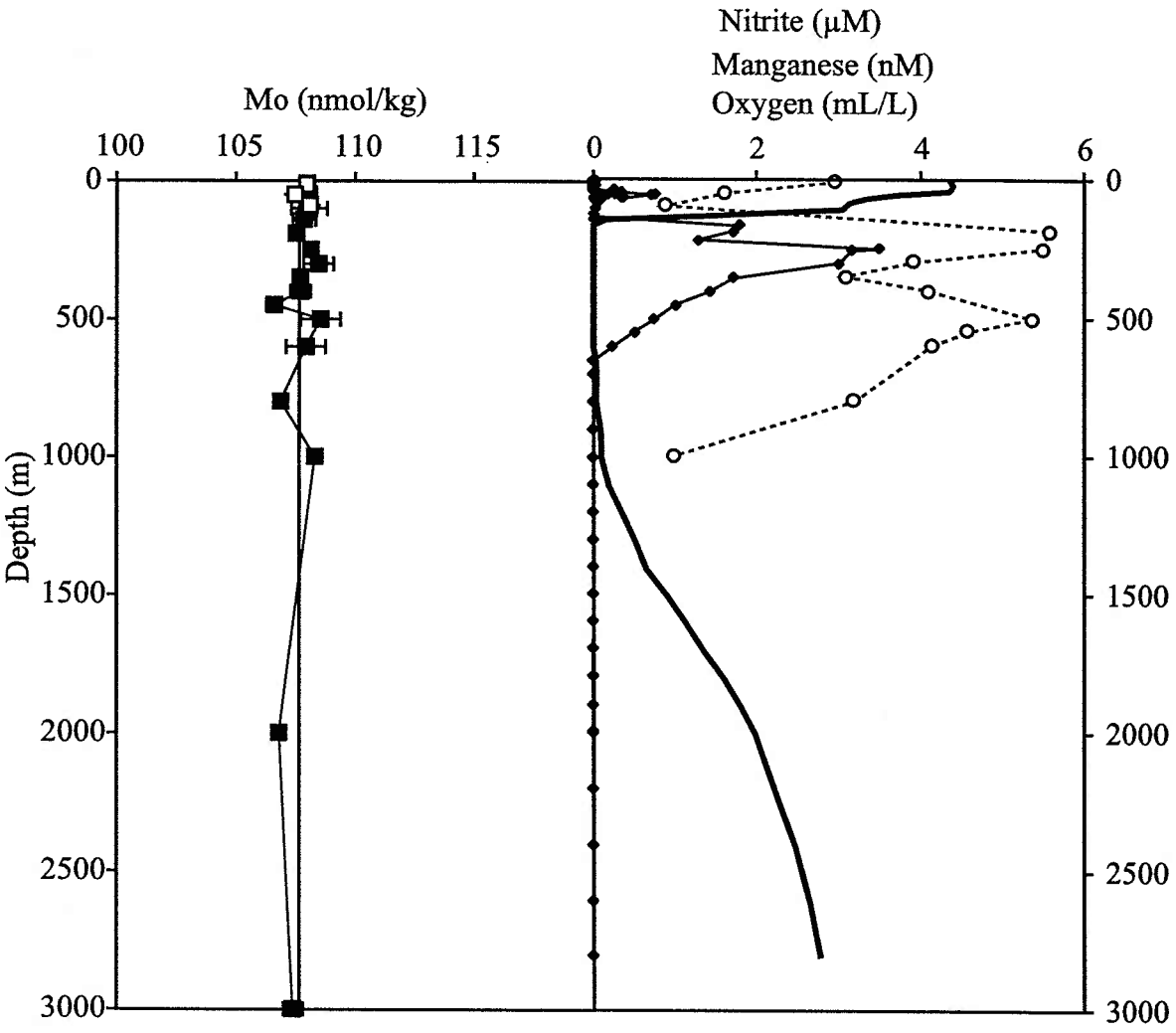

Figure 3.4 Profiles of unfiltered Niskin samples for Mo (black squares), filtered Go-Flo samples for Mo (open squares), Nitrite (black diamonds) Oxygen (thick line) and Manganese (open circles) from the Arabian Sea JGOFS N7 station 19°10N 67°10W collected in 1995. Molybdenum concentrations are normalized to a salinity of 35 ppt. The straight line at 107.6 nmol/kg represents the nominal conservative value of Mo. Error bars on Mo represent average replicate precision. Mo concentration averaged 107.8+/-0.6 nmol/ kg 2se. Concentrations appeared conservative throughout the profile. Go-Flo and niskin samples agree within error suggesting the Mo can be collected without contamination using a niskin rosette.

and 88m) were also collected using Go-Flo bottles and trace metal clean techniques. The Go-Flo samples were filtered and acidified at sea. After excluding initial (Sept 99) analyses of the rosette samples from 16m and 51 m (Table 3.3), which we believe were contaminated, there is agreement between the filtered Go-Flo samples and the unfiltered Niskin, samples. This implies that Mo, unlike many other trace metals, can be collected without obvious contamination using a Niskin rosette. The Arabian Sea profile was conservative over a relatively large salinity (34.7-36.7 ppt) range. The average salinity normalized concentration was 107.78±0.32 nmol kg^{-1} (2se) which agrees with the conservative value established by previous studies (Collier 1985; Morris 1975; Prange and Kremling 1985). The fact that Mo concentration variations spanning a 5 nmol range are well correlated with salinity demonstrates that the methodology developed in this study can resolve Mo concentration variations at the 1 nM level.

The Arabian Sea is a complex region possibly influenced by both in situ denitrification or Mn cycling processes. Despite high concentrations of both nitrite (nearly 4 μM (Morrison et al. 1998; Morrison et al. 1999)) and Mn (1 nM to > 5 nM: S. Vink pers.comm. unpublished data) indicating active denitrification and an Mn oxide cycling, there is no correlation between dissolved Mo and nitrite or Mn concentrations. In addition, trace element distributions may also be influenced by coastal sediments due to a strong oxygen minimum zone. Molybdenum is enriched in Oman (Morford and Emerson 1999) and Indian (Sirocko 1995) margin sediments, but not on the Pakistani margin (Crusius et al. 1996) despite similar oxygen concentrations and organic carbon deposition conditions.

3.3.2 Sargasso Sea

The Sargasso Sea profile was collected in March 1998 (Oceanus 318 Station 001) at 25°60N and 70° 04'W (Figure 3.5). These samples were collected using trace metal clean techniques. They were passed through a 0.2 μm pore size filter and acidified at sea. All samples were screened for Zn, a particularly contamination prone element, by cathode stripping voltammetry (Saito 2001).

At the Sargasso Sea station the mixed layer depth was 80m and strong nutrient depletion over this depth interval indicates long term surface stratification. There was nearly complete depletion of nitrate + nitrite in the mixed layer (3-4 nM from 0-80m depth, rising to 1716 nM at 125m. K.K. Cavender-Bares et al. (2000). The nitrogen fixing cyanobacterium *Trichodesmium* was abundant at the sea surface during the cruise and the low nitrate concentrations suggested significant N-fixation at this station. However, the salinity normalized dissolved Mo profile concentration is 107.50±0.34 (2se) nmol kg^{-1} for upper 300 m, excluding one near surface outlier (Figure 3.5) The absence of dissolved Mo concentration variations at the ± 0.5% level shows that there is no resolvable depletion in dissolved Mo in the presence of active nitrogen fixation.

3.3.3 Eastern Equatorial Pacific Profiles

Six additional profiles were measured in the Eastern Equatorial Pacific. Two profiles over the 9N vent field on the east Pacific Rise (9 49N, 105 15W) were collected on cruises of opportunity, the first in December of 1997 (R/V Atlantis 3-11) and the second on a return cruise in December of 2001 (R/V Atlantis 7-5). Four additional

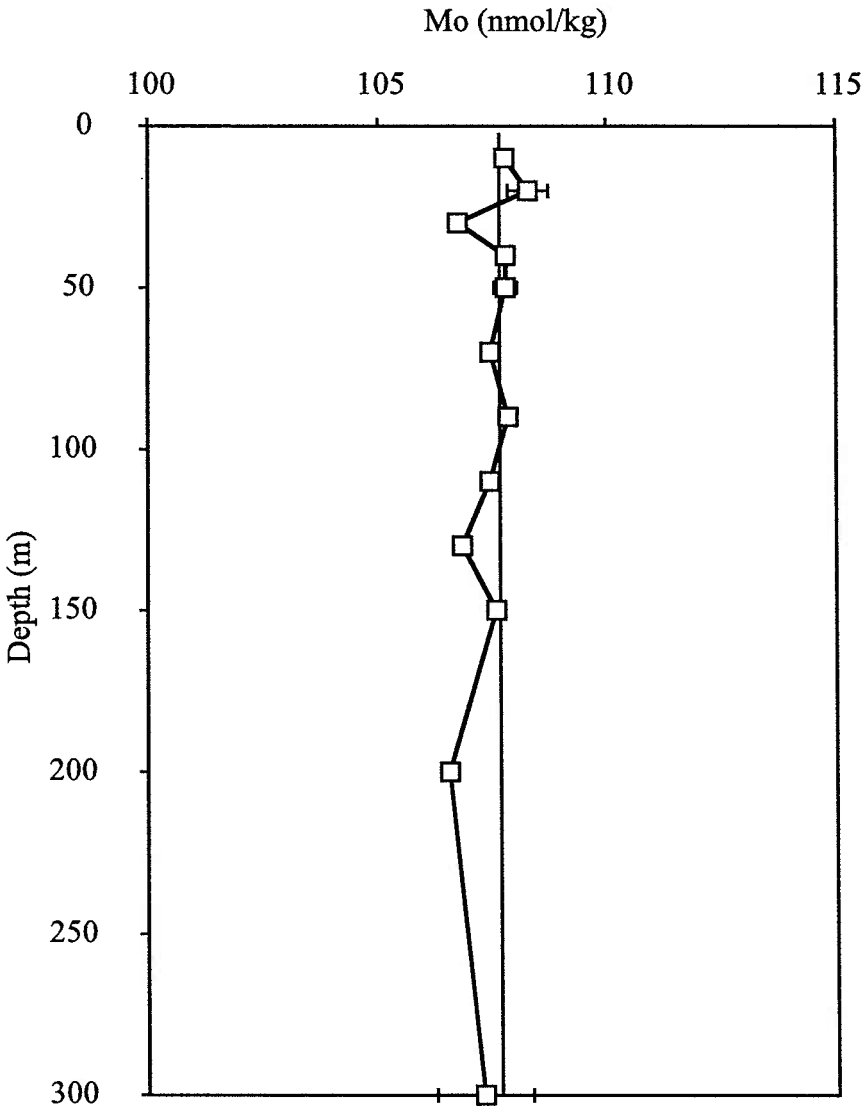

Figure 3.5 Profile of filtered go-flo samples for Mo (open squares) from the Sargasso Sea 25°60N 70°04W collected in 1998. Molybdenum concentrations are normalized to a salinity of 35 ppt. The straight line at 107.6 nmol/kg represents the conservative value of Mo. Error bars on Mo indicate average replicate precision. Mo concentration averaged 107.6±0.6 (2se) nmol/kg. Concentrations appeared conservative throughout the profile despite low nitrogen concentrations and the presence of nitrogen fixing cyanobacteria.

profiles were investigated from a transect along 16N latitude from Hawaii to the coast of Mexico collected by Eric DeCarlo in May 2000.

The 9N 1997 profile was collected using a Niskin bottle rosette. The profile has a surface minimum with a peak at 62 m and another local minimum at 120m. Between 120 and 300m there were a series of one point maxima and minima (Figure 3.6). The average salinity normalized concentration of the profile was 108.77±0.64 nmol kg^{-1} (2se). There were no nutrient data available for this profile, which made the peaks difficult to interpret. The majority of the profile was enriched relative to average seawater concentrations, similar to the Galapagos profile.

The 9N 1997 profile was predominantly unfiltered, though several filtered samples were available from the near surface. Filtered and unfiltered samples were within error of each other with one exception. A single filtered sample analyzed in duplicate from 162 m yielded an unusually low Mo concentration (95.4±1.7 nmol kg^{-1}: ±1 sd). This filtered sample was approximately 11 nmol kg^{-1} lower than the unfiltered samples from similar depths. The sense of the deviation was the opposite from what would be predicted by Mo contamination of the sample. The difference between filtered and unfiltered implies a particulate Mo concentration that is 2 orders of magnitude larger than the highest measured particulate Mo concentrations (Tuit 2003; Chapter 5). No other filtered sample in any of the profiles measured exhibited such a large divergence between coordinate filtered and unfiltered samples. One possible explanation of this large discrepancy is that contamination with another metal, such as Mn, resulted in molecular interferences on the spike mass (Note that $^{55}Mn^{40}Ar$ is isobaric with the ^{95}Mo

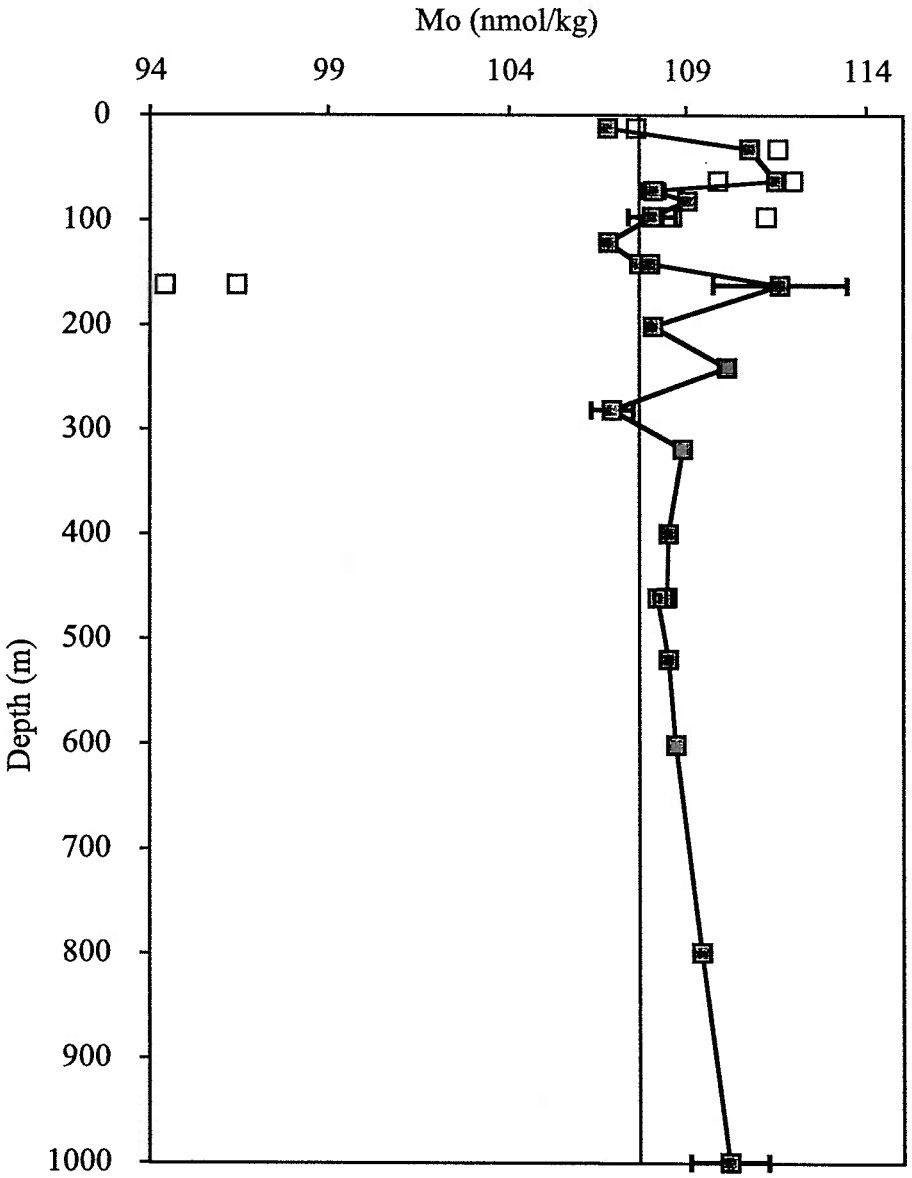

Figure 3.6 Mo profile from analyses of unfiltered niskin samples (grey squares) and filtered niskin samples (open squares) from the Pacific 9°49N 104°15W collected in 1997. Molybdenum concentrations are normalized to a salinity of 35 ppt. The straight line at 107.6 nmol/kg represents the nominal conservative value of Mo. Error bars on Mo indicate average replicate precision.

spike). This would result in an erroneously low Mo concentration. Excluding this low outlier, filtered and unfiltered samples are within error of each other.

For the 9N 2001 profile both filtered Niskin and filtered Go-Flo samples were analyzed. The depth of the Go-Flo samples were not well constrained when collected; nutrient data suggest that some bottles were triggered much closer to the surface than expected. The Go-Flo depths reported here are based on correlation of the dissolved nutrient data between the Niskin and Go-Flo samples. The salinities for the Go-Flo data based on this depth have large uncertainties. To avoid incorporating this uncertainty into the Go-Flo and Niskin, samples were compared without salinity normalization (Figure 3.7). The Go-Flo samples have Mo concentrations that are within error of the Niskin samples. However, some surface samples collected with Go-Flo bottles are on average 1.2 nmol kg^{-1} lower (Figure 3.7), implying that samples collected using the Niskin rosette employed on this cruise were slightly contaminated with respect to Mo. Regardless of any possible contamination of Niskin samples, the whole profile is depleted relative to average seawater by 0.5 to 1.0 nmol kg^{-1} except for the three Niskin samples at 50 80 and 120m that were systematically enriched in Mo relative to the Go-Flo samples (Figure 3.8). The average concentration was 106.46±0.26 (2se) nmol kg^{-1}, at least 1.41 nmol kg^{-1} lower than the concentration measured at the 9N site in 1997. The deep water (>2000m) samples from the Pacific (106.5±0.8 nmol kg^{-1}: 9N 2001) are within error of the deep Arabian Sea samples (107.4±0.4 nmol kg^{-1}). A full suite of nutrient data was measured for this profile, but Mo variations did not correlation with any nutrient profile.

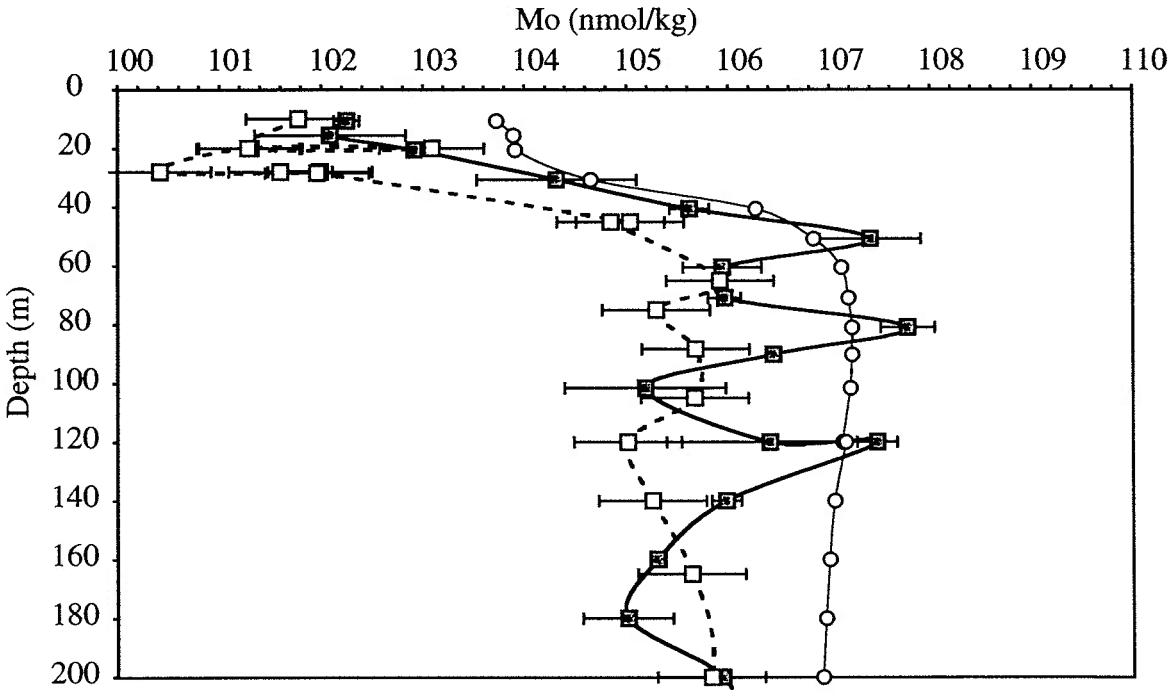

Figure 3.7 Mo profile of filtered Niskin samples (grey squares) and filtered Go-Flo samples (open squares) from the Pacific 9°49N 104°15W collected in 2001. Due to the poor depth control on the Go-Flo samples, the salinity values for these samples imprecise. To allow comparison of the Mo concentrations with out adding additionally uncertainty due to salinity these data were not salinity normalized. Open circles represent Mo concentration calculated from salinity using the Mo salinity relationship of Prange and Kremling (1985). Error bars on Mo indicate average replicate precision. Go-flo samples are lower than niskin samples by 1-2 nM in the upper 50m.

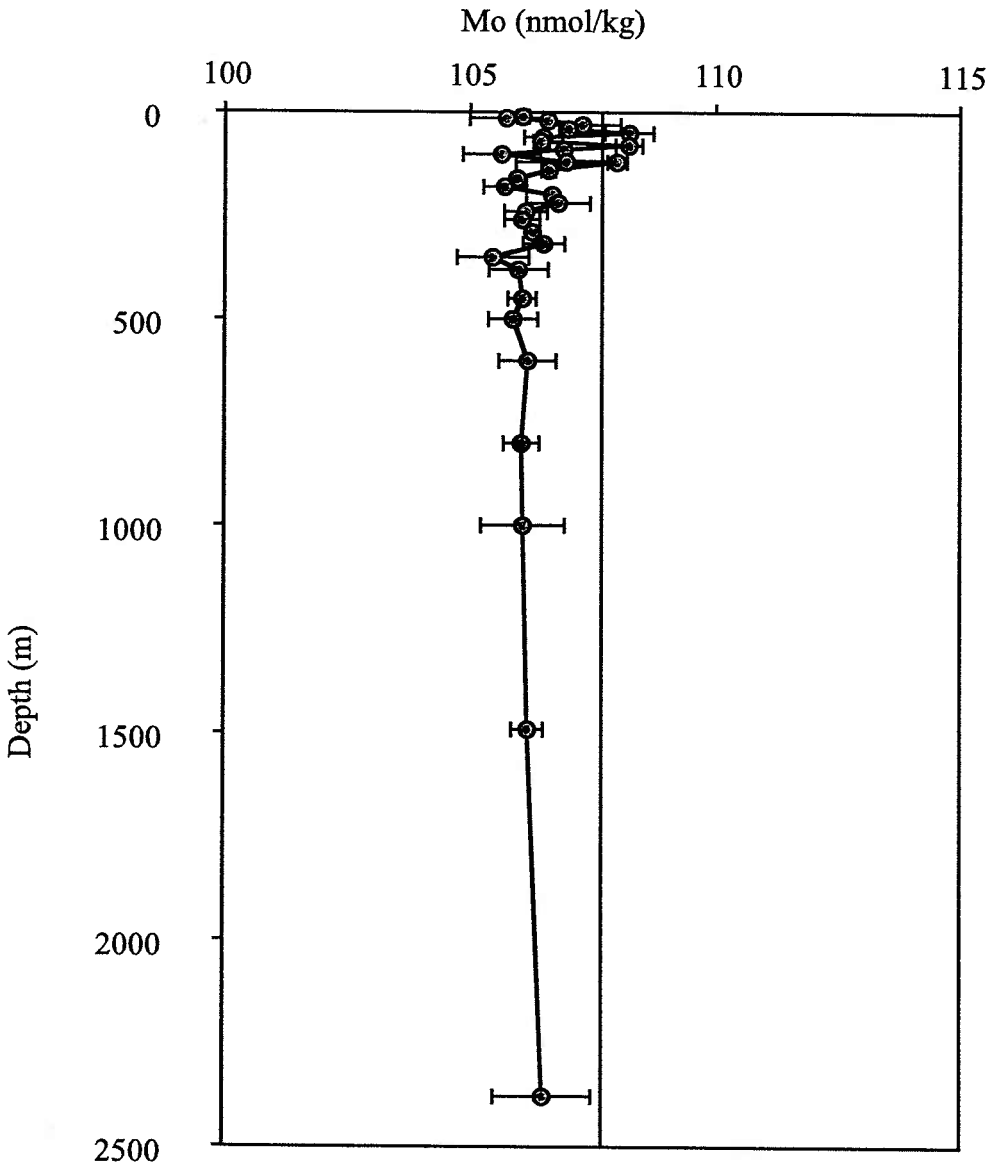

Figure 3.8 Mo profile of filtered niskin samples (grey circles) from the Pacific 9°49N 104°15W collected in 2001. Molybdenum concentrations are normalized to a salinity of 35 ppt. The straight line at 107.67 nmol/kg represents the nominal conservative value of Mo. Error bars on Mo indicate average replicate precision.

Both filtered and unfiltered Niskin samples were analyzed for the 16N transect (Figure 3.9). The unfiltered samples were slightly less depleted in Mo than the filtered samples relative to average seawater concentration (Table 3.4). The concentration ranges of filtered and unfiltered profiles overlap for all of the stations except 6, the closest to the coast (Figures 3.9 and 3.10). Profile 6 was collected during a storm that disturbed the water column and may have resuspended particles from the coastal region, which may be the cause of the slightly more elevated concentrations in the unfiltered samples. Nutrient data (nitrate, nitrite, ammonia, phosphate and silica: Popp) and trace metal (Fe and Mn: DeCarlo) were available for the 16N transect. The 16N transect did not show correlations with any dissolved species.

Table 3.4 Salinity Normalized Molybdenum Concentrations from the 16N Transect

Profile (lat, lon)	Filtered nmol kg^{-1} (2se)	Unfiltered nmol kg^{-1} (2se)
6 (15N 98W)	105.95 (0.38)	107.50 (0.80)
5 (16N 107W)	106.55 (0.31)	106.84 (0.53)
4 (16N 119W)	106.33 (0.27)	106.65 (0.46)
2 (16N 150W)	106.15 (0.35)	106.88 (0.71)

3.3.4 California Borderland Basins

Profiles were taken from several of the California borderland basins, from the RV Point Sur in July of 2001 focusing on the bottom waters (Figure 3.11). Samples were collected using a Niskin rosette, and were filtered and acidified at sea. Whole water column profiles were collected from San Pedro and Tanner Basins. Both profiles had a surface maximum followed by a minimum at 15 to 25 m. Mo concentrations in the mid-

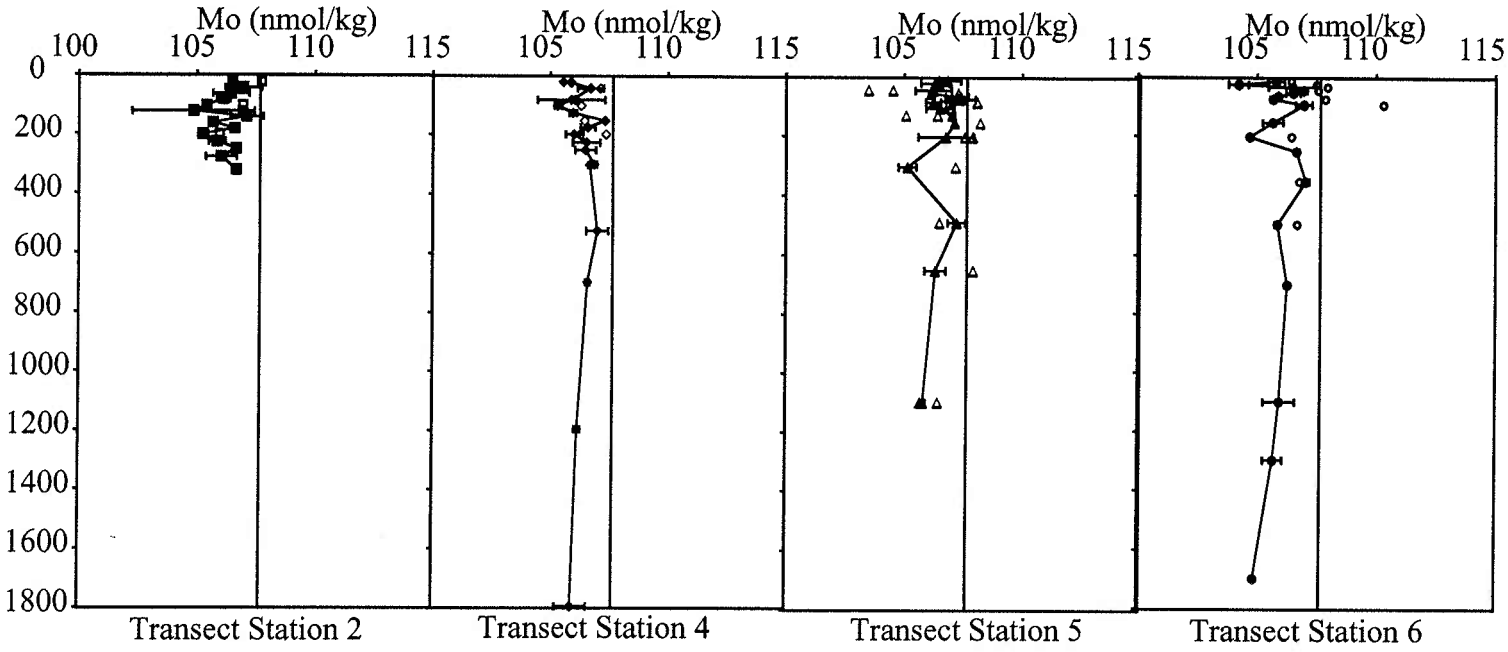

Figure 3.9 Mo profiles of unfiltered niskin samples (open symbols) and filtered niskin samples (closed symbols) from a transect from Hawaii to the coast of Mexico collected in 2000 by Eric DeCarlo. Molybdenum concentrations are salinity normalized to 35ppt. Error bars on Mo indicate average replicate precision. The straight line at 107.67 nmo/ kg represents the nominal conservative value of Mo.

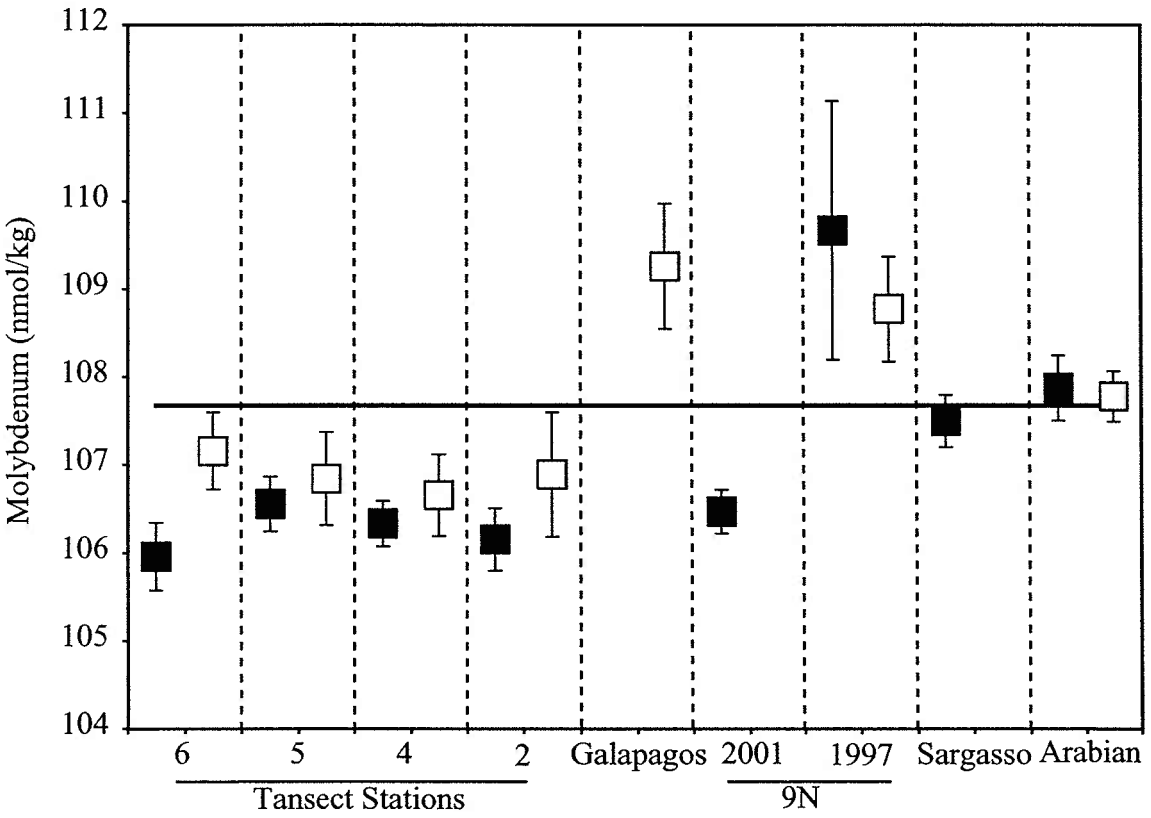

Figure 3.10 Chart of average salinity normalized concentrations separating filtered (filled squares) and unfiltered (open squares) data sets. Error bars represent 2 times the stnadrd error. The solid line represents the average Mo concentration of seawater. The Arabian Sea and Sargasso profiles are equivalent to the average seawater value. The 16N transect and the 9N 2001 profiles are all depleted through out, while the 9N 1997 and Galapagos profiles are enriched. Unfiltered samples tend to have larger variability than the filtered samples, perhaps do to particle contributions.

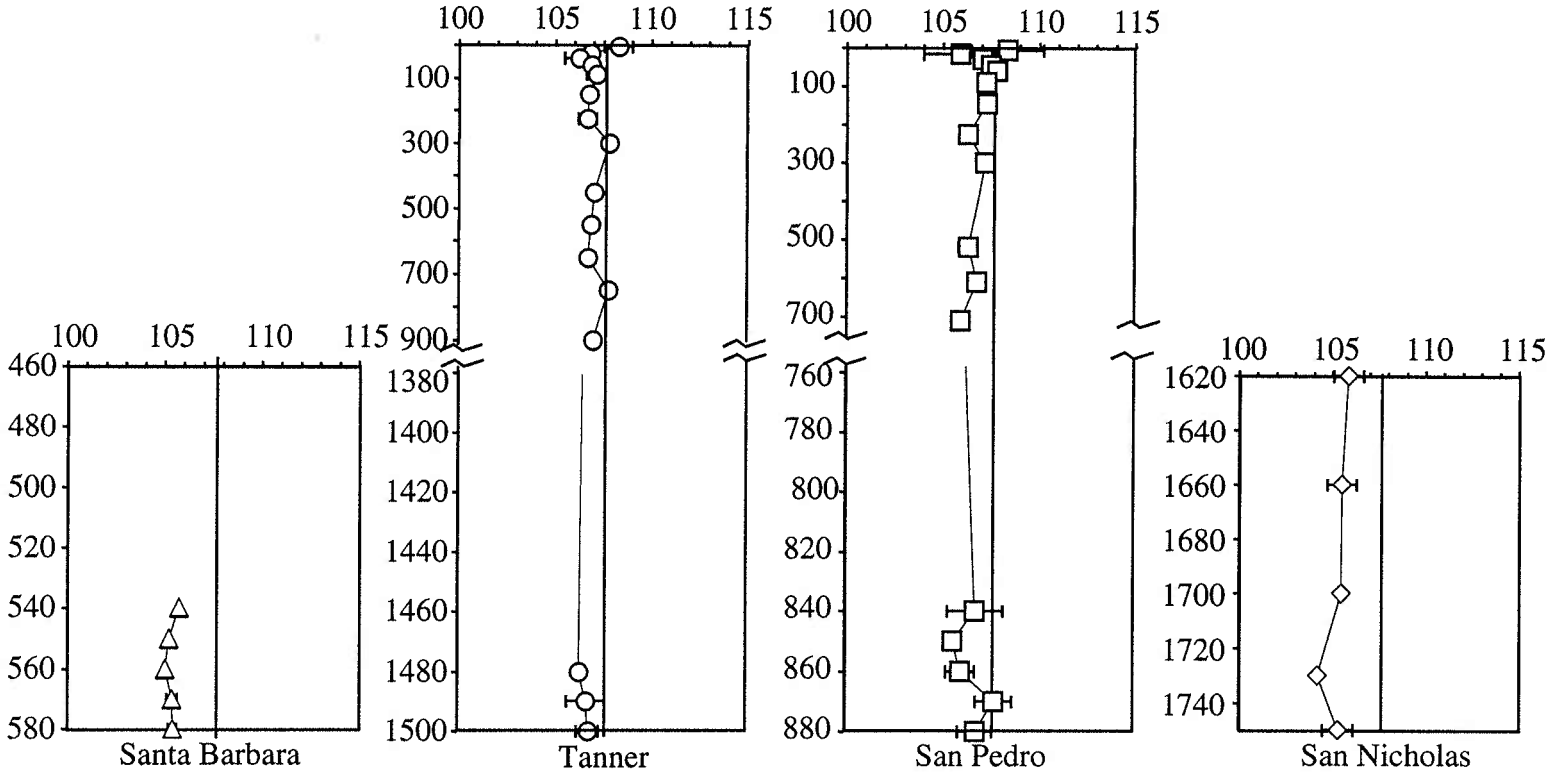

Figure 3.11 Profiles of filtered niskin samples for Mo from 4 California Borderland Basins, Santa Barbara (triangles), Tanner (circles), San Pedro (squares) and San Nicholas (diamonds) collected in 2001. Molybdenum concentrations are salinity normalized to 35ppt. Error bars on Mo indicate average replicate precision. The straight line at 107.6 nmol/kg represents the conservative value of Mo. Profiles focus on the bottom 120m of each basin. Upper water column samples were available for Tanner and San Pedro (note break in scale).

Depths, above sill depth and below surface peaks were within error of average seawater salinity normalized concentrations. Bottom water samples in these basins ranged from conservative to depleted. Table 3.5 lists bottom water characteristics for each basin. Santa Barbara and San Nicholas bottom waters are depleted on the order of 1-2 nM. There is no correlation between bottom water oxygen concentrations or gradients as measured during sample collection and Mo concentrations. San Pedro for instance has relatively low bottom water oxygen concentration but is not depleted in Mo relative to it's own upper water column samples or samples from mid depth on the Tanner profile which were collected at similar depths to the shallower San Pedro bottom waters.

Table 3.5 Salinity-normalized Molybdenum Concentrations

Basin	Basin Depth (m)	Sill Depth (m)	Depth Range (m)	Molybdenum nmol kg^{-1} (2se)	Oxygen µmol kg^{-1} (2se)
San Nicholas	1760	1100	1620-1750	105.29 (0.56)	17.7
Santa Barbara	580	475	540-580	105.37 (0.23)	3.4
San Pedro	880	740	840-880	106.67 (0.94)	3.9
			30-710	106.93 (0.37)	
Tanner	1500	1165	1480-1500	106.56 (0.29)	21.7
			40-900	106.99 (0.27)	

3.4 Discussion

3.4.1 Data Quality.

Possible contamination during sampling and long term accuracy of the analytical methods are critically important aspects of the data quality that must be considered prior to interpreting the Mo seawater data. Some of these samples were collected using Go-Flo

bottles and trace metal clean techniques, while others were collected using the more common, but contamination prone, Niskin bottle rosette. Mo is found in many lubricants used on ships. Samples were collected and measured over a five year period, therefore effects of sample storage and long term accuracy of the Mo concentration measurements must be considered. To compare these profiles we must also evaluate what, if any effect collection method had on sample concentration.

Several lines of evidence suggest that the enrichments and depletions seen in the profiles are not due to analytical or instrumental phenomena such as variable blank or mass bias. Over 80% of the samples in this study were duplicated and 60% were triplicated. Sample replication is the basis of all error bars plotted. Replicates of samples measured years apart are within ±0.5% error of each other (Table 3.3). Samples from different profiles prepared in the same column batch and analyzed in the same ICPMS run preserve the relative concentration differences (Table 3.3). Both aspects of the composite data set indicate that the long term precision of the method is approximately ± 0.5 nM. These results also argue against evaporation during storage causing the enrichment in the older profiles.

It is unlikely that an acid soluble particulate Mo in unfiltered samples is responsible for a systematic offset between filtered and unfiltered analyses. Particulate (>0.45 μm) Mo concentrations in the Pacific range between 1.7-16.6 pmol L^{-1} at 9N and between 0.4-51.6 pmol L^{-1} off the California coast (Tuit 2003, Chapter 5). If the particulate Mo were all acid soluble, it would lead to a maximum increase of 0.005%, a difference that cannot be resolved by this method. However there are some indications

that particulate matter may be more significant in some sites or at individual depths. Figure 3.9 compares the average filtered and unfiltered salinity-normalized profile concentrations. The unfiltered samples from the 16N transect were slightly enriched relative to the filtered samples for the entire transect. Unfiltered profiles also tend to reproduce less well and therefore have larger analytical uncertainties. In most cases the unfiltered average salinity-normalized profile concentrations were within 2 standard error of the filtered, the exception was the station 6 of the 16 N transect. Station 6, the nearshore (500 km) station was collected during and after a storm and may have experienced some sediment resuspension driving up the particulate load. These data show that the contribution of particulate Mo to the total Mo inventory of seawater is of local significance at most, and is in general negligible.

Contamination during sample collection must still be considered. Mo is found in many lubricants used on research vessels including WD-40 and Moly Lube. The agreement between Go-Flo and Niskin samples from the Arabian Sea suggested that Mo was less susceptible to contamination than other trace metals when collected via a Niskin rosette. Go-Flo samples from the 9N 2001 profile are slightly lower (1-2 nM) relative to the Niskin-collected samples suggesting that there may be a slight contamination in these Niskin samples. The 1-2 nM discrepancy between the Go-Flo and Niskin samples implies that the depletions maybe even greater than suggested by the Niskin data.

Could sample contamination cause the enrichments seen in the Galapagos and 9N 1997 samples? Figure 3.12 compares the deep water concentrations of both 9N profiles and the Galapagos profiles. The CTD rosette on the Atlantis was used to collect both the

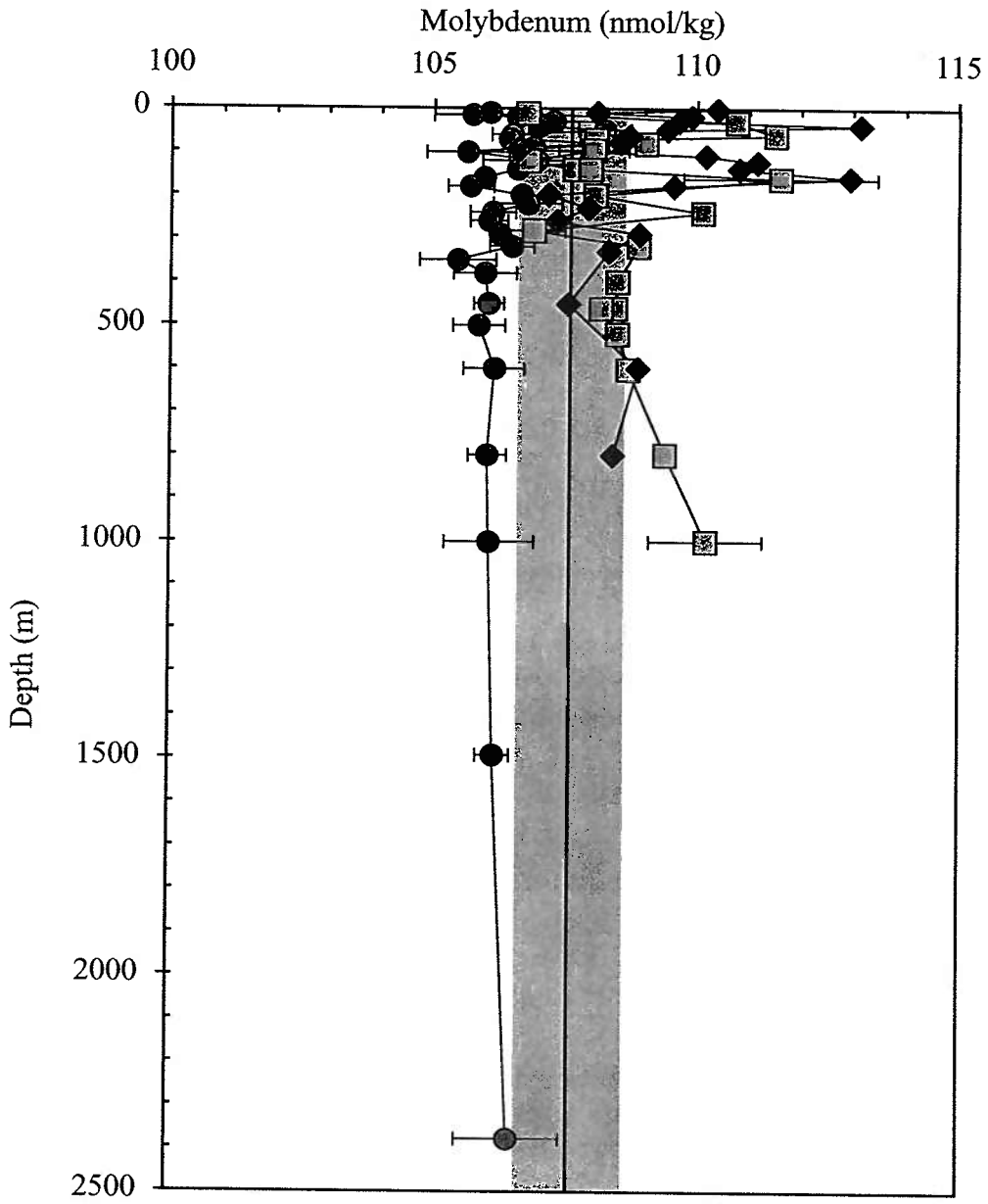

Figure 3.12 A plot pf the Galapagos (diamonds) 9N 1997 (squares) and 9N 2001 (circles) Mo concentration profiles. Molybdenum concentrations are normalized to a salinity of 35 ppt. The straight line at 107.6 nmol/kg represents the nominal conservative value of Mo. Error bars on Mo represent average replicate precision. This figure emphasizes the descrepnacy in deep water concentrations between theses profiles. The shaded region represents the range in the Arabian and Sargasso Sea data.

enriched profile from 9N 1997 and the depleted profile from 9N 2001, albeit 4 years apart. The difference in deep water concentrations between the 9N samples is 4.1 nM at 1000 m, twice that of the discrepancy between Go-Flo and Niskin bottle collected samples in 2001. This would require a significant contamination source. The fact that surface peaks in both the 9N 1997 (Figure 3.6) and Galapagos (Figure 3.3) profiles are defined by multiple points and exhibit smooth shapes consistent with the operation of diffusive processes suggests that these features are real and not due to random contamination.

Contamination from the Niskin rosettes cannot be precluded. If Niskin contamination is the cause of the enrichments seen in the Galapagos and 9N 1997 profiles, it suggests that the entire Pacific is depleted in Mo. This implies a significant sink for Mo in the Eastern Tropical Pacific. If the enrichments are real it implies a significant and episodic source of Mo to the Pacific. Subsequent discussions address the possible mechanisms that could cause Mo depletion or enrichment.

3.4.2. Non-conservative Mo behavior.

A dissolved element is designated as conservative by default; the designation means that within the precision of the measurement techniques used and the suite of samples measured, the concentration element of interest is co-varies with salinity. There are three different criteria that are used to test for conservative behavior, lack of variability in salinity normalized profiles, lack of differences in deep water concentrations and a strong correlation with salinity. If a sample suite, measured by a given analytical method, passes all of these tests it is termed conservative. If an element

fails any one of these tests has been proven non-conservative. Previous work on Mo, with measurement errors ranging from ±2 to 10%, did not show resolvable concentration differences in vertical profiles or a contrast in concentration between Pacific and Atlantic deep waters. In this section, I make the case that previous studies were not of high enough precision to reveal non-conservative behavior and discuss evidence for non-conservative behavior seen in this study.

The most rigorous test for non-conservative behavior is demonstrating concentration variations that do not co-vary with salinity. Water column profiles can miss subtle variations due to under-sampling. Discrepancies between ocean basin deep water dissolved concentrations only evolve if the distribution is related to particle formation and regeneration, which enrich or deplete bottoms waters along the long slow pathway of the global conveyor belt. Lack of differences in deep-water dissolved concentrations cannot preclude non-conservative behavior related to point sources such as shallow coastal anoxic sediments, which may not influence deep-water concentrations.

The data currently available in the literature for open ocean profiles of dissolved Mo do not provide a strong basis for determining whether or not Mo behaves non-conservatively in the open ocean. Figure 3.13 shows a plot of Mo versus seawater for several studies, along with the Prange and Kremling (1985) low-salinity Baltic Sea trend extended to relevant salinities for reference. Prange and Kremling's (1985) data set from the Baltic Sea does show a strong correlation (r^2=0.85) between Mo and salinity, however these samples span a low and large range in salinity (2-16 ppt). The Baltic Sea is a region where the most prominent characteristic of the hydrography is mixing of fresh and

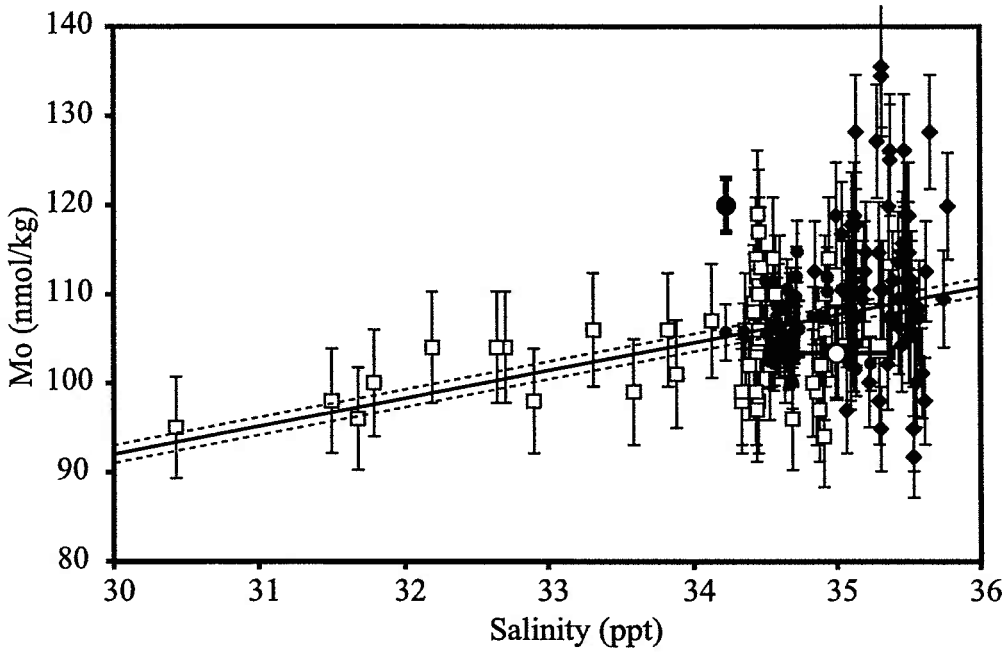

Figure 3.13 Molybdenum v. Salinity diagram for Mo profiles from the literature. Individual analyses from the Sea of Japan (open squares: Sohrin et al, 1999), North Atlantic Ocean (black diamonds: Morris, 1975) and the Eastern Tropical Pacific (grey circles: Collier 1985). Average data sets from Santa Barbara Basin (black circle: Zheng et al. 2000) and Pacific coast of Mexico (open circle: Nameroff et al. 1996). Errors on the individual analyses represent measurement replication precision. Thick error bars on average data sets represent 1 sd of the whole profile. The solid line is the projection of the Mo versus salinity trend measured at lower salinities in the Baltic Sea (Prange and Kremling 1985: Mo nmol kg-1=3.13*salinity ppt-1.88). The area between the two dotted lines represents ±1 nmol/kg (2sd) for this study. These data sets have r-squared correlation coefficients of less than 0.15.

saline waters. Thus these results from the Baltic Sea can only be used to argue that Mo behaves conservatively upon dilution associated with fresh water input. Generalizing these results to the behavior of Mo in the entire open ocean is inappropriate. None of the open ocean studies have Mo versus salinity r^2 correlation coefficients greater than 0.1. Though many of these samples fall on the Prange and Kremling (1985) Mo versus salinity trend, due to the large analytical uncertainty associated with the data it is impossible to demonstrate or preclude a strong correlation of Mo concentration and salinity.

Examining the co-variation of Mo and salinity for the data collected during this study provides evidence for regions of both conservative and non-conservative distributions of Mo given the precision of this method. The Sargasso and Arabian Sea profiles appeared to be broadly conservative with depth when normalized to 35 ppt salinity (Figures 3.4 and 3.5). When plotted versus salinity they form a linear array with a r^2 of 0.86 (Figure 3.14) and a slope of 2.88±0.18 within error of Prange and Kremling's (1985) 3.10±0.10 slope from the Baltic. All of the Arabian and Sargasso Sea samples are within 2 sd of the Mo versus salinity trend of Prange and Kremling (1985). The salinity normalized concentration for the Sargasso and Arabian Sea data set is 107.6± 0.4, which is in agreement with previous studies (Collier 1984; Morris 1975; Prange and Kremling 1985). These data establish a Mo versus salinity trend that defines conservative behavior for Mo in the open ocean measured with precision of ±0.5 %.

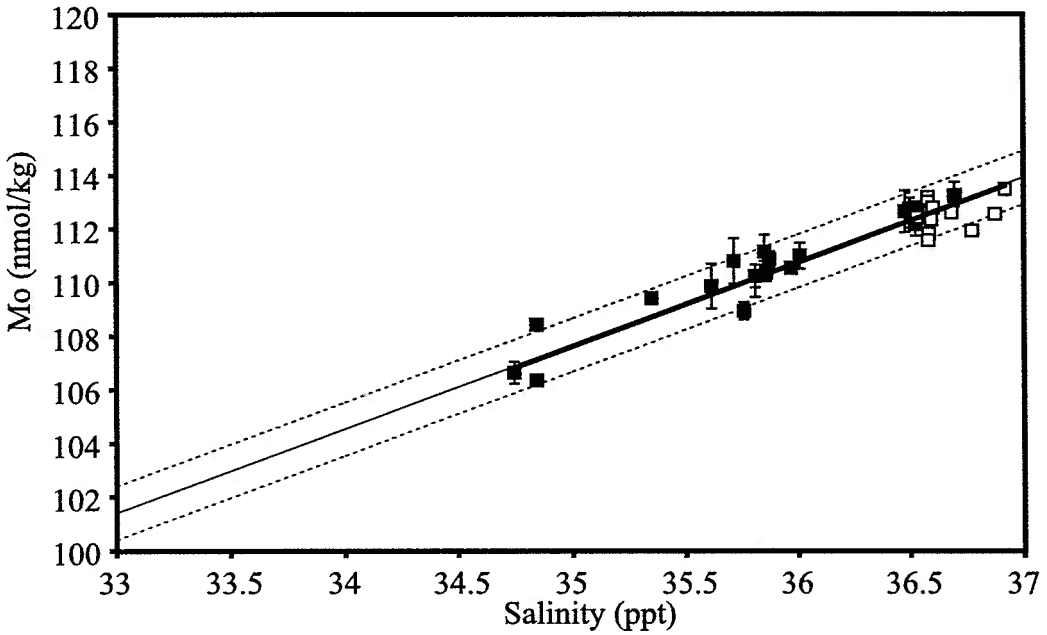

Figure 3.14 Molybdenum versus Salinity diagram for the Arabian Sea (filled squares) and Sargasso Sea (open squares) profiles. Note smaller range in axes than figure 3.9. Error bars from replicate analyses. The solid line is the Mo versus salinity trend measured at lower salinities in the Baltic Sea (Prange and Kremling 1985: Mo nmol/kg=3.13*salinity ppt-1.88). Dotted lines indicate the average 2 sd error bars (± 1nmol/kg). Any analysis within 2 sd of the line is considered to be conservative. The thick line is the regression through the Arabian and Sargasso Sea data set. This line is within error of the Baltic Sea trend (Mo nmol kg-1=3.12*salinity ppt-1.80). The r-squared correlation coefficient was 0.86. This tight correlation of Mo concentration with salinity indicates that these profiles are conservative.

The California Borderland Basin profiles show both conservative and depleted characteristics (Figure 3.13). These samples were collect in Niskin bottles and filtered. The mid-depth (above basin sill depth and below mixed layer) samples of the Tanner and San Pedro Basin profiles are correlated with salinity. They can be fit by line with a slope of 2.60±0.31 nM Mo (salinity ppt)$^{-1}$ giving an r^2 of 0.79. This slope is within error of the slope seen for the Arabian and Sargasso Sea data. The bottom waters (from below sill depth) from the San Nicholas and Santa Barbara basin are depleted by 1 to 3 nM relative to both the Arabian and Sargasso trend and the trend of the mid-depth samples from Tanner and San Pedro Basins. This suggests the depletions occur in the isolated waters of the basins rather than prior to spill over of ambient waters into the basin. The sediments of the Santa Barbara basin are enriched in Mo, suggesting that they are a sink for Mo.

Profiles of Mo from stations in the Equatorial Pacific display non-conservative distributions of Mo (Figure 3.15,16). These data do not conform to the same Mo-salinity relationship established in the Sargasso and Arabian Sea. Samples from all these profiles deviate from the conservative trend by more than ±2 sd. In Mo v. salinity space the Pacific profiles fall into two broad categories. The Galapagos and 1997 9N profile are both enriched with regards to salinity, while the 16N transect and the 2001 9N profile are depleted (Figure 3.16). The profiles are enriched or depleted throughout the entire upper 2000m. The peaks measured are not large; their diffusive lifetime is only on the order of 30-60 days (Figure 3.17). An in situ mechanism may be required to maintain the concentrations anomalies. There does not appear to be enriched bottom water to balance

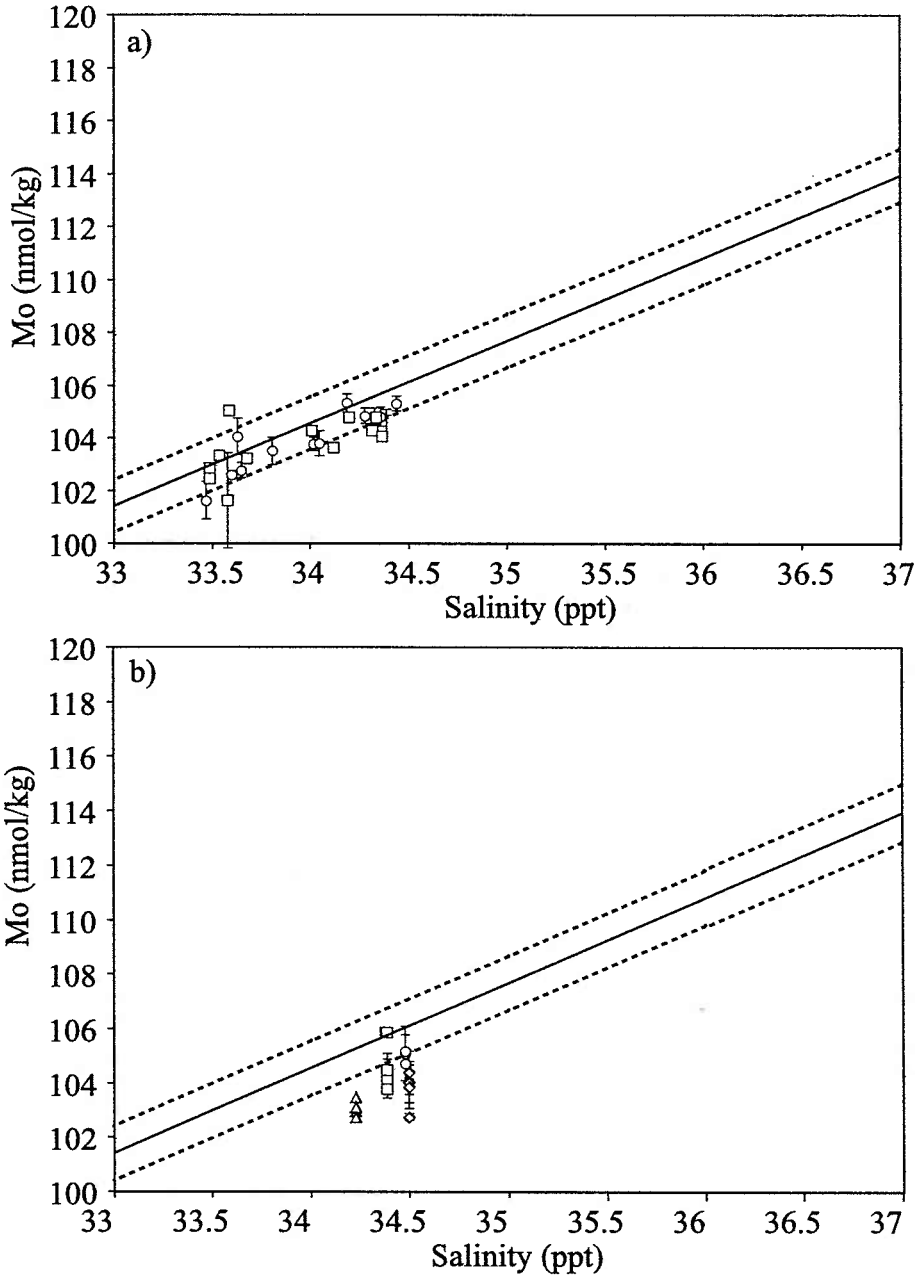

Figure 3.15 Molybdenum versus Salinity diagram for the California Borderland Basins Santa Barbara (triangles), Tanner (circles), San Pedro (squares) and San Nicholas (diamonds) a) water column above sill depth and b) bottom 120m. Error bars from replicate analyses. The solid line is the Mo versus salinity trend from the Arabian and Sargasso Sea extended for the entire salinity range. Dotted lines indicate the average 2 sd error bars (+/- 1nmol/kg). Any analysis outside of the 2 sd field is considered to be non-conservative. Bottom waters of the Santa Barbara and San Nicholas Basins are depleted in Mo relative to salinity

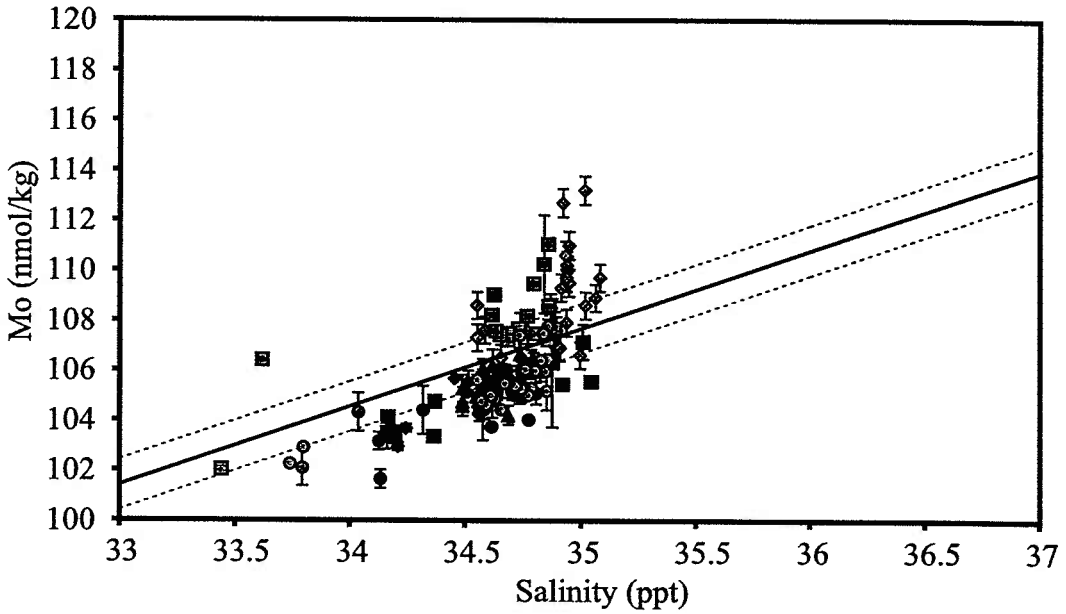

Figure 3.16 Molybdenum versus Salinity diagram for the Pacific Galapagos (grey diamonds), 9N 1997 (grey squares), 9N 2001 (gery circles), and transect station 2 (black squares), 4 (black diamonds), 5 (black triangles) and 6 (black circles) profiles. Error bars from replicate analyses. The solid line is the Mo versus salinity trend from the Arabian and Sargasso Sea extended for the entire salinity range. Dotted lines indicate the average 2 sd error bars (± 1nmol/kg). Any analysis outside of the 2 sd field is considered to be non-conservative. The 9N 1997 and Galapagos profiles are enriched above the line, while the 9N 2001 and the 16N transect are depleted.

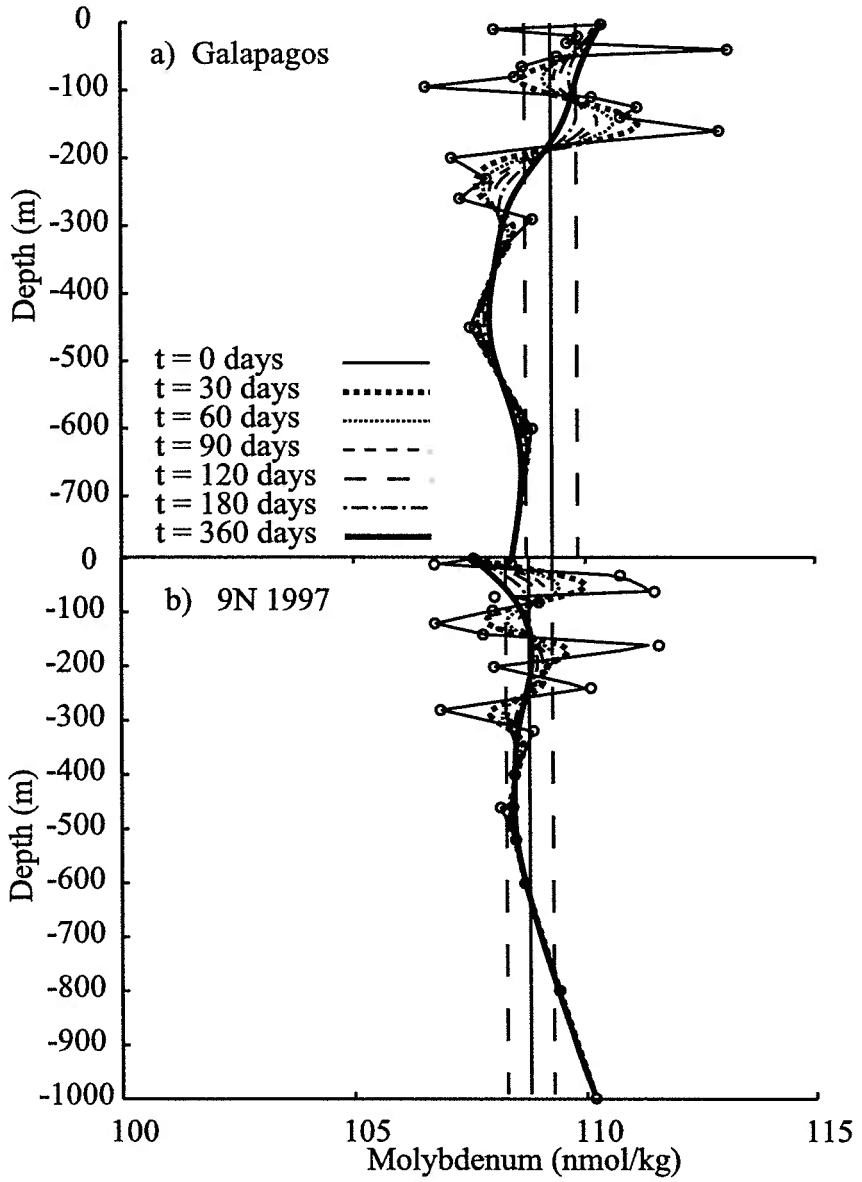

Figure 3.17 Model results from a simple one dimension vertical advection diffusion model used to determine the life time of Mo concentration anomalies in the absence of Mo fluxes. 1 Profiles from the Galapagos (a) and 9N 1997 (b) used as examples. The profiles were allowed to diffuse from initial measured conditions represented by the circles for a total of 360 days. The model equation was $dC/dt=D_V(dC^2/d^2z) + v_V(dC/dz)$, where D_v, the vertical diffusion rate, was 1 cm^2 s^{-1} and v_V, the vertical advection rate, was 0.23 μm s^{-1}. Diffusion profiles plotted for initial conditions (thin solid line) 30 days (thick dotted line) 60 days (thin dotted line) 90 days (small dash line) 120 days (large dash line) 180 days (dot-dash line) and 360 days (thick line). The straight solid line represents the average concentrations of the profile and the straight dashed lines are the 1 sd error bars (± 0.5 nmol/kg).

a depleted surface waters, such as is seen for most nutrients. This suggests that the processes causing non-conservative behavior are not simply vertical and one dimensional, lateral processes may be important as well. Possible causes of Non-conservative distributions of Mo in the Pacific are discussed below.

3.4.3. Uptake by biota

Mo cell quotas and Mo/carbon ratios determined in culture experiments described in Chapter 4 indicate that export of biologically fixed Mo is unlikely to produce depletions or enrichment of dissolved Mo as large as those documented in the Pacific. The average concentration of Mo in plankton is <2 $\mu g\ g^{-1}$ dry weight (Martin and Knauer 1973), similar to the average crustal concentration. Mo is utilized for specific enzymatic systems and its cellular concentration appears to be tightly tied to enzymatic activity. Nitrogen fixing cyanobacteria, for instance, in culture experiments (Tuit 2003; Chapter 4) take up Mo only when actively fixing nitrogen and release a large portion of that Mo back into seawater when not fixing nitrogen. The Mo:C ratios of nitrogen fixers can range from approximately twice that of bulk phytoplankton to about an order of magnitude less (Table 3.1) Since most nitrogen fixing phytoplankton fix nitrogen during only a portion of a the day, either nocturnally or diurnally but not both, this can lead to rapid exchange of Mo between the dissolved and particulate phase, limiting phytoplankton's ability to deplete dissolved Mo. Assuming a high cell density of 10^6 cells ml^{-1}, the order of magnitude of living cells in seawater (Landry and Kirchman 2002), N_2 fixing phytoplankton would correspond to a maximum particulate Mo concentration of $4.7*10^{-2}$ nmol kg^{-1} from a liter of seawater. These concentrations are

small compared to dissolved Mo concentration. The export flux of Mo from surface waters supporting significant N fixation can be estimated as between 0.05 and 1.04 μmol Mo m^{-2} yr^{-1}, using the BATS average particulate organic carbon flux at 150 m (Steinberg et al. 2001) and Mo:C ratios of bulk phytoplankton and N_2 fixers. Averaged over the upper 150 m this flux would deplete the dissolved concentration by a maximum of 0.0069 nmol Mo L^{-1} yr^{-1}. This is not resolvable by current methods. These results imply that nitrogen fixation as a process could not cause depletions in dissolved Mo. Thus both the culture experiments in chapter 4 and the conservative behavior of Mo seen in the Sargasso Sea profile, despite low surface nitrate+nitrite concentrations and the presence of Trichodesmium colonies, indicate that the distribution of dissolved Mo is not influenced by N-fixation.

The cellular Mo concentrations of denitrifying bacteria are also very small, but they may not be as variable on a diel timescales. Assimilatory nitrate reductase is used to uptake nitrogen for growth and therefore likely has a constant demand in organisms using nitrate as their nitrogen source but may vary with the availability of other nitrogen sources. Mo concentration in facultative dissimilatory denitrifiers appears to be linked to the regulation of nitrate reductase by oxygen availability (Tuit, 2003 Appendix 1). These heterotrophic bacteria use oxygen as a terminal electron acceptor, but when oxygen concentrations become very low in the OMZ nitrate becomes the primary electron acceptor. Using the cellular concentration of Mo in a denitrifier we can estimate the amount of Mo the organisms would sequester in the particulate phase. If denitrifying bacteria were present in seawater at a concentration of 10^6 cells mL^{-1} the Mo requirement

would be $1.2*10^{-4}$ nmol L^{-1}, not likely to deplete the dissolve phase. The Mo:C ratio of suspended particulate matter in the Pacific increase with depth peaking at about 7 μmol Mo:mol C at 300 m coincident with the OMZ and the nitrite maximum (Tuit 2003, Chapter 4). Still, to appreciably deplete the dissolved Mo phase there would need to be a much larger formation and removal of particulate organic carbon from the OMZ than is reasonable for this cold non-productive region.

3.4.4 Cycling with Mn Oxides

Molybdenum has been shown to be enriched in sedimentary Mn oxides with a relatively constant ratio of Mo:Mn ratio of 0.0011 mol Mo:mol Mn (Manhiem, 1974; Shimmield and Price, 1986). Whether Mo is similarly associated with authigenic Mn produced in the water column is unknown. Should this ratio hold true for Mn oxides produced in the water column it may have large effect on Mo distribution. At rates of particulate Mn formation common in the open ocean (0.033 ± 0.003 μmol Mn L^{-1} yr^{-1} at 100m depth in the Sargasso: Sunda and Huntsman 1988) it is unlikely this process would influence the dissolved Mo distribution. Near shore in the Pacific, particulate Mn formation estimates are much higher and vary by up to an order of magnitude through the oxygen minimum zone (Martin and Knauer 1995; Johnson et al. 1996). The highest rates are observed below the oxygen minimum zone. For the Vertex II site the particulate Mn formation rates of 4.0 to 1.2 μmol kg^{-1} yr^{-1} have been observed below 900m (Martin and Knauer, 1984). Given the sedimentary Mo: Mn ratio this would result in the scavenging of 3.7-14.6 nmol Mo kg^{-1} yr^{-1}, which may significantly affect Mo dissolved concentrations.

Two lines evidence argue against Mo being scavenged by Mn oxides in the water column. First, the dissolved phase variations of Mo do not show any correlation with dissolved Mn concentrations in either the 16N transect or the Arabian Sea, despite presumably high rates of Mn oxide formation (Lewis and Luther 2000). Second, suspended particulate matter samples from both the upper 400 m of the 9N 2001 profile and the California Coastal Margin showed no correlation between particulate Mo and Mn (Tuit 2003 Chapter 5). This is very different from sediment trap results from the Mexican coast and Santa Barbara basin which both show correlations between particulate Mo and Mn oxides (Nameroff 1996; Zhang 1999; Zheng et al. 2000). Though we cannot preclude Mn oxidation affecting Mo dissolved concentrations there is no indication of in situ Mo cycling with Mn oxides in the profiles measured for this study.

3.4.5 Interaction with Coastal sediments

Mo is enriched in anoxic sediments and there is evidence that with variations in bottom water redox conditions, anoxic sediments can act as both a source and sink for Mo. The mechanisms controlling these processes are complex and the subject of current debate. Molybdenum enrichment appears to occur primarily at the sediment water interface and in pore waters rather than by a water column process (Francois 1988; Helz and Adelson 1997). The mechanism of enrichment might be a two stage process, possibly linked to sulfide availability (Erickson and Helz 2000; Helz and Adelson 1997; Zheng et al. 2000). Initial Mo enrichment occurs at 0.1μM H_2S but precipitation increases rapidly at porewater concentrations greater than 100 μM (Zheng et al. 2000). Mo in sediments is likely associated with FeS phases or organic matter at lower sulfide concentrations but

may be directly precipitated as $Mo(IV)S_2$ at the higher sulfide concentrations. However, if the sediment is exposed to higher oxygen concentrations Mo can dissolve and flux back out into bottom waters during burn down events.

Interactions with coastal sediment have been shown to give rise to significant benthic fluxes of Mo to and from seawater. The flux of Mo into sediments has been estimated from porewater profiles to be approximately 150 nmol Mo m^{-2} day^{-1} below sill depth in Santa Barbara basin (Zheng et al. 2000). Benthic flux chamber data from the oxygen minimum zone on the western coast of Mexico were between 0 and 1900 nmol Mo m^{-2} day^{-1} into the sediment (Nameroff 1996). Mo can also be released from sediments. Zheng et al. (2000) have recently shown fluxes of Mo from porewaters of up to 690 nmol Mo m^{-2} day^{-1} above sill depths in Santa Barbara Basin. An estimate of 14000 nmol Mo m^{-2} day^{-1} for the maximum burial flux of Mo into sediments can be calculated from assuming maximum sedimentation rate (0.5 cm yr^{-1}), minimum dry bulk density (0.1 g cm^{-3}) and a maximum Mo concentration (200 μg g^{-1}). Fluxes out of sediments might be slightly higher depending on the length of enrichment, and the depth and speed of oxic burndown, but must be proportional.

It is an open question whether Mo fluxes into sediments are large enough to affect bottom water concentrations of dissolved Mo. Santa Barbara bottom water as measured by Zheng (1999) was 126±5.7 nM (salinity normalized), significantly enriched in Mo relative to salinity and relative to North Atlantic water sample (115±4 nM,n=7) run as a control. Both the Santa Barbara bottom waters and North Atlantic samples are enriched relative to the Sargasso Sea and Santa Barbara bottom waters analyzed in this study.

These data are slightly at odds with the Zheng (1999) sediment flux data, which showed Mo fluxes in to the sediments below sill depth. However it is noteworthy that the methods employed by Zheng (1999) were designed to resolve large pore water gradients in Mo concentration. This method has not been rigorously shown to have the precision and accuracy required to resolve subtle difference in seawater Mo concentrations. The enrichment in Santa Barbara bottom waters can be interpreted as the result of the fluxing on authigenic Mo out of pore waters.

Zheng et al. (2001) suggested that release of Mo from sediments might be related to rates of basin ventilation possibly controlled by ENSO variations. El Niño events pile up hot water against the coast, which suppresses upwelling. It is this upwelled cold dense water that usually spills over the sills of the borderland basins supplies the bottom waters with oxygen. Thus during El Nino events the California Borderland Basins become more oxygen depleted. Normal or La Niña conditions can increase upwelling and basin ventilation. Sediment redox conditions respond to changes in bottom water redox condition though there may be a time lag between ventilation events and diffusive burn down into sediments (Reimers et al. 1996).

The California borderland basin profiles from this study were collected in July 2001 during normal conditions. The 5 depths sampled from the bottom waters of Santa Barbara Basin are depleted relative to waters from similar depths outside the basin. Using the Zheng et al. (2001) Mo sediment fluxes and the area (300 km^2) and volume (29 km^3) of Santa Barbara Basin below the sill depth, the amount of Mo removed from bottom waters is approximately 0.002% of the total Mo per day. Given basin water residence times of

between 290 and 2200 days (Berelson et al. 1987; Hammond et al. 1990; Vangeen et al. 1995) this flux would result in total depletions of 0.58 to 4.4%, which is the opposite of the trend see in the water by Zheng (2000) but similar to the 1.2% depletion seen in our data.

The relationship of sediment redox conditions to ENSO variations can be extended to coastal sediments underlying the OMZ along the coast of Mexico and Peru. Investigations of the depth of the OMZ along the coast of Peru show that El Nino by piling warmer less dense water along the coast depresses the OMZ as well as the thermocline (Morales et al. 1999). The OMZ response lags behind the thermocline response by about three months and the effect seems to move progressively down the coast. The effect of this phenomena is to expose sediments that were anoxic to elevated oxygen concentrations and initiate oxidative burn down. This would liberate Mo, similar to what is seen in the above sill depth Santa Barbara basin cores (Zheng et el. 2000). During Normal or La Nina conditions the OMZ rises again and anoxic sediments once again scavenge Mo from the water column. This mechanism could lead to both enrichment and depletion of the water column as seen in the profiles from the Pacific. Figure 3.18 shows the date of sample collection for each Pacific profile versus equatorial sea surface temperature, an indicator for El Nino. All of the enriched profiles were collected during or soon after El Nino events while the depleted stations were collected during normal to La Niña conditions.

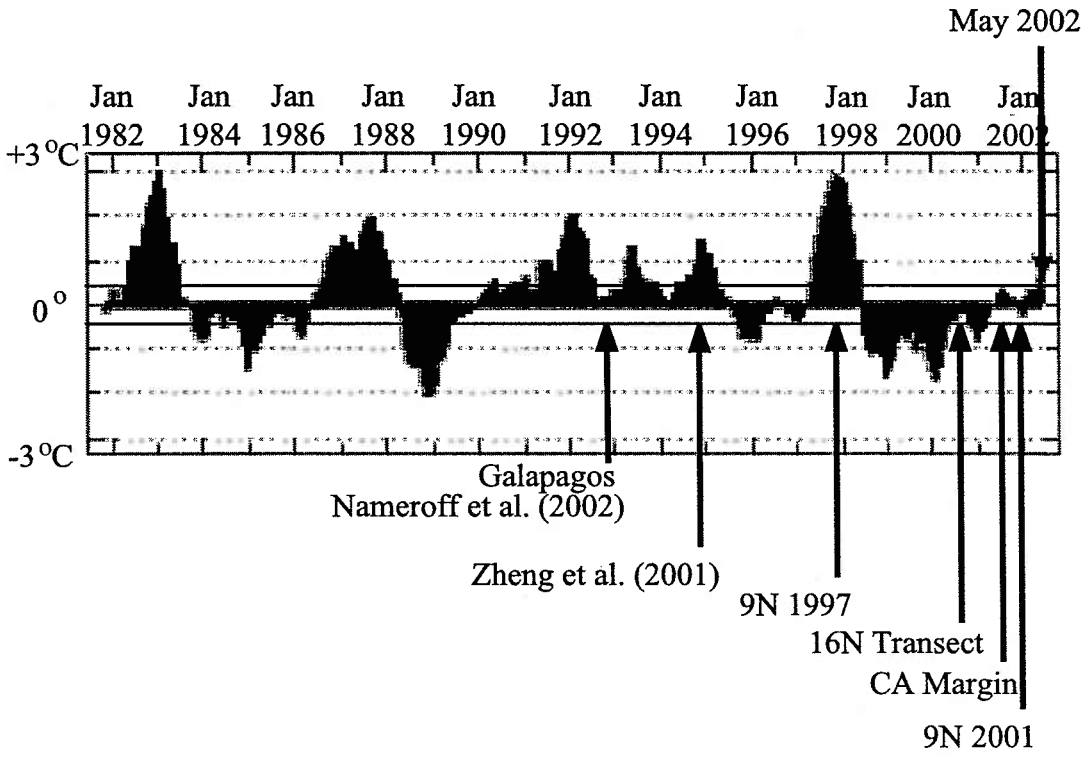

Figure 3.18 Historic Equatorial Pacific sea surface temperature graph for the last 2 decades. Horizontal black lines indicate the normal range in temperature. Peaks above the line indicate El Nino conditions, below the line La Nina conditions. Collection times of Pacific profiles are indicate with arrows. Profiles depleted for Mo were collected during normal to La Nina conditions. Profiles enriched in Mo were collected during or soon after El Nino conditions.

Although it is conceptually appealing to invoke sediment redox changes associated with ENSO variations to explain the temporal variations in Mo concentration documented an the 9N site, it is not clear that such a feature could persist 500 to 2000 km off the coast where these profiles were collected (Figure 3.2,Table 3.2). The time scale for transport of a concentration anomaly is 9 to 30 months based on horizontal diffusion (10^6 to 10^8 cm^2 s^{-1} :Dunne and Murray, 1999). These timescales would be substantially decreased by advection of waters off shore. Surface drifter data averaged from 1979 to 2000 indicate that all of these profiles were located in regions with primarily westward flowing surface currents with advection velocities range from 0 to 20 cm s^{-1} (Johnson, 2001). Vertical diffusion works against horizontal advection and diffusion smoothing out concentration anomalies. Estimates of vertical diffusion rates range from 0.1cm^2 s^{-1} (Ledwell, 1993) to 1-2 cm^2 s^{-1} (Munk, 1966). A vertical diffusion rate of 1 cm^2 s^{-1} can smooth out a 5 nM peak to below detection limits in 1-2 months.

To explore more quantitatively the relative effects of horizontal diffusion, vertical diffusion and horizontal advection we designed a simple forward time center step numerical model to solve the equation

$$\frac{dC}{dt} = D_v \frac{dC^2}{d^2z} + D_h \frac{dC^2}{d^2y} + v_h \frac{dC}{dy}$$

Where C is concentration of Mo, t is time, z is depth and y is lateral distance. The grid is set up as a horizontal slice with a depth of 300 m and a length of 3000 km. Grid spacings were every 10 m depth and 20 km distance. A constant peak of 5 nM was imposed between 50 and 100 meters of the left side of the grid representing a flux of Mo

out of the sediments. 5 nM was the maximum enrichment in the Galapagos and 9N 1997 profiles. D_v, D_h, and v_h are the vertical diffusion, horizontal diffusion and horizontal advection constants. 6 model cases were run for 6 months varying horizontal diffusion and advection (Table 3.6).

Table 3.6 Model cases

Horizontal Advection Horizontal Diffusion	0 cm s^{-1}	10 cm s^{-1}	20 cm s^{-1}
10^6 cm^2 s^{-1}	1	3	5
10^8 cm^2 s^{-1}	2	4	

This model demonstrates that it is possible to transport a concentration anomaly any where from 200-2700 km offshore in 6 months (Figure 3.19), but the sediment flux implied but the concentration anomaly and the advection is too large. Given a 5 nmol kg^{-1} enrichment and an advection rate of 10 cm s^{-1} the flux out of the sediments would be approximately $4.3 \cdot 10^7$ nmol Mo m^{-2} d^{-1}, 5 orders of magnitude larger than previous fluxes measured. Unlike an enclosed basin, on an open shelf, water may simply move away from the coast too fast to develop a deviation in dissolved Mo. To enrich or deplete coastal waters it would be necessary to either vary advection rates to allow a pool of water to stagnate and build up a Mo signature or radically increase Mo fluxes.

3.4.6. The Nutrient/Scavenged/Conservative Paradigm

The Pacific Mo profiles do not fit easily into the nutrient/scavenged/conservative paradigm that classifies most elements in marine chemistry. This theory is based

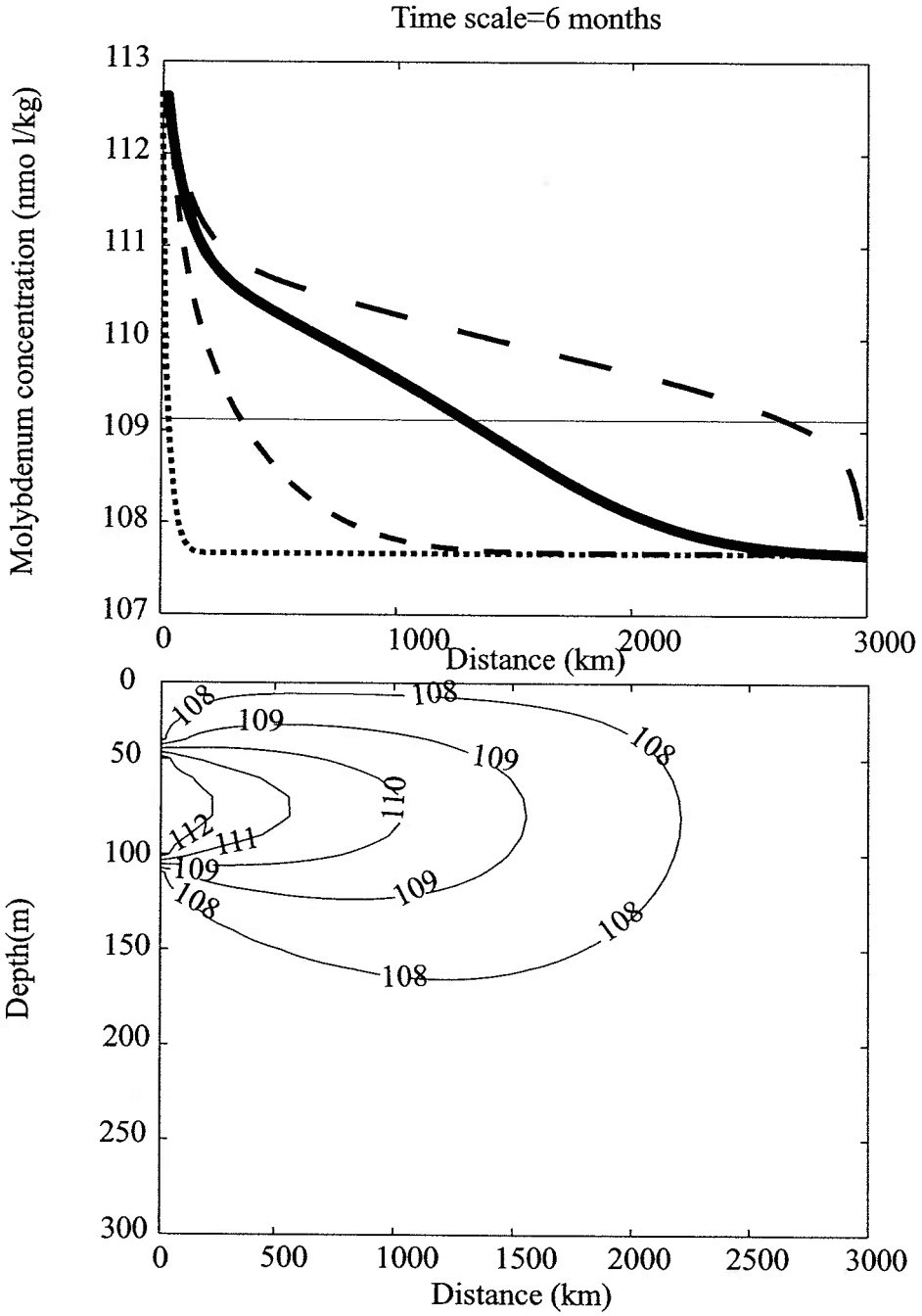

Figure 3.19 Plot of results for 2 dimension forward time center step advection diffusion model used to determine whether Mo concentration anomalies could be advected off shore. A) Plot of concentration at 50m depth for case 1 (thin dotted line: Dh=106 cm2 s-1, vh=0 cm s-1) case 2 (small dashed line: Dh=108 cm2 s-1, vh=0 cm s-1) case 3 (thick line: Dh=108 cm2 s-1, vh=10 cm s-1) case 4 (large dashed line: Dh=106 cm2 s-1, vh=20 cm s-1) B) Contour plot of Mo concentration for case3.

primarily on a vertical, one dimensional view of the water column using surface or deep water depletions to indicate nutrient uptake by organisms at the surface or scavenging of particle reactive elements at depth. Some elements, most famously Fe, are affected by both processes and thus declared hybrid. This vertical view is superimposed on the global conveyor belt to yield enrichments or depletions in deepwater concentrations as water masses age. Mo, though an essential micronutrient, does not show nutrient like uptake in surface water nor does scavenging by particles in the water column appear to be important. Yet the data indicate that Mo may not be a conservative element either. Lateral processes in the upper water, which are not accounted for in the classical view, may play a significant role in Mo distributions. It is important, when re-evaluating the marine chemistry of Mo, to take into account lateral variations.

3.5 Conclusions

This survey of Mo behavior in the global ocean demonstrates that salinity normalized Mo concentrations do not appear to be uniform through out the world ocean and therefore Mo may not be classified as a strictly conservative element. Dissolved Mo distributions did not show any evidence suggesting uptake by organisms in regions that were characterized by N-fixation or denitrification, implying that, despite Mo's crucial role in these enzymatic processes, dissolved Mo is not a tracer for these processes. Water column Mn cycling does not appear to exert a strong influence on the vertical distribution of Mo in the water column. Non-conservative behavior in the California Borderland Basin bottom water profiles indicate that benthic uptake of Mo can produce resolvable

depletions in dissolved Mo inventory. The cause of Mo enrichments in the Eastern Tropical Pacific is enigmatic. While the absolute magnitude of the enrichment is similar to the depletion observed in the CA basins the flux of Mo out of the sediments required to support this enrichment far out into the open ocean seems unreasonably large. Some combination of processes may be required.

3.6 References

Berelson, W. M., M. R. Buchholtz, D. E. Hammond, and P. H. Santschi. 1987. Radon Fluxes Measured with the Manop Bottom Lander. Deep-Sea Research Part a-Oceanographic Research Papers **34:** 1209-1228.

Berrang, P. G., and E. V. Grill. 1974. The effect of manganese oxide scavenging on molybdenum in Saanich Inlet, British Columbia. Marine Chemistry **2:** 125-148.

Bertine, K. K., and K. K. Turekian. 1973. Molybdenum in marine deposits. Geochimica et Cosmochimica Acta **37:** 1415-1434.

Capone, D. G. 2001. Marine nitrogen fixation: what's the fuss? Current Opinion in Microbiology **4:** 341-348.

Capone, D. G., and J. P. Montoya. 2001. Nitrogen fixation and denitrification, p. 501-515, Methods in Microbiology, Vol 30. Methods in Microbiology. ACADEMIC PRESS INC.

Codispoti, L. A., and T. T. Packard. 1980. Denitrification Rates in the Eastern Tropical South-Pacific. Journal of Marine Research **38:** 453-477.

Collier, R. W. 1984. Particulate and Dissolved Vanadium in the North Pacific-Ocean. Nature **309:** 441-444.

---. 1985. Molybdenum in the Northeast Pacific-Ocean. Limnology and Oceanography **30:** 1351-1354.

Colodner, D., J. Edmond, and E. Boyle. 1995. Rhenium in the Black Sea; comparison with molybdenum and uranium. Earth and Planetary Science Letters **131:** 1-15.

Crusius, J., S. E. Calvert, T. Pedersen, and D. Sage. 1996. Rhenium and molybdenum enrichments in sediments as indicators of oxic, suboxic and sulfidic conditions of deposition. Earth and Planetary Science Letters **145:** 65-78.

Dean, W. E., D. Z. Piper, and L. C. Peterson. 1999. Molybdenum accumulation in Cariaco Basin sediment over the past 24 k.y.; a record of water-column anoxia and climate. Geology (Boulder) **27:** 507-510.

Deutsch, C., N. Gruber, R. M. Key, J. L. Sarmiento, and A. Ganachaud. 2001. Denitrification and N-2 fixation in the Pacific Ocean. Global Biogeochemical Cycles **15:** 483-506.

Emerson, S. R., and S. S. Huested. 1991. Ocean Anoxia and the Concentrations of Molybdenum and Vanadium in Seawater. Marine Chemistry **34:** 177-196.

Erickson, B. E., and G. R. Helz. 2000. Molybdenum(VI) speciation in sulfidic waters: Stability and lability of thiomolybdates. Geochimica Et Cosmochimica Acta **64:** 1149-1158.

Falkowski, P. G., R. T. Barber, and V. Smetacek. 1998. Biogeochemical controls and feedbacks on ocean primary production. Science **281:** 200-206.

Francois, R. 1988. A study on the regulation of the concentrations of some trace metals (Rb, Sr, Zn, Pb, Cu, V, Cr, Ni, Mn and Mo) in Saanich Inlet sediments, British Columbia, Canada. Marine Geology **83:** 285-308.

Gruber, N., and J. L. Sarmiento. 1997. Global patterns of marine nitrogen fixation and denitrification. Global Biogeochemical Cycles **11:** 235-266.

Hammond, D. E., R. A. Marton, W. M. Berelson, and T. L. Ku. 1990. Ra-228 Distribution and Mixing in San-Nicolas and San-Pedro Basins, Southern California Borderland. Journal of Geophysical Research-Oceans **95:** 3321-3335.

Helz, G. R., and J. M. Adelson. 1997. Geochemical methods for investigating past changes in Chesapeake Bay. 35.

Hem, J. D. 1978. Redox Processes at Surfaces of Manganese Oxide and Their Effects on Aqueous Metal-Ions. Chemical Geology **21:** 199-218.

Johnson, K. S., K. H. Coale, W. M. Berelson, and R. M. Gordon. 1996. On the formation of the manganese maximum in the oxygen minimum. Geochimica Et Cosmochimica Acta **60:** 1291-1299.

Landry, M. R., and D. L. Kirchman. 2002. Microbial community structure and variability in the tropical Pacific. Deep Sea Research Part II: Topical Studies in Oceanography **49:** 2669-2693.

Lewis, B. L., and G. W. Luther. 2000. Processes controlling the distribution and cycling of manganese in the oxygen minimum zone of the Arabian Sea. Deep-Sea Research Part Ii-Topical Studies in Oceanography **47:** 1541-1561.

Lipschultz, F., and N. J. P. Owens. 1996. An assessment of nitrogen fixation as a source of nitrogen to the North Atlantic Ocean. Biogeochemistry **35:** 261-274.

Martin, J. H., and G. A. Knauer. 1973. Elemental Composition of Plankton. Geochimica Et Cosmochimica Acta **37:** 1639-1653.

Michaels, A. F. and others 1996. Inputs, losses and transformations of nitrogen and phosphorus in the pelagic North Atlantic Ocean. Biogeochemistry **35:** 181-226.

Morales, C. E., S. E. Hormazabal, and J. L. Blanco. 1999. Interannual variability in the mesoscale distribution of the depth of the upper boundary of the oxygen minimum layer off northern Chile (18-24S): Implications for the pelagic system and biogeochemical cycling. Journal of Marine Research **57:** 909-932.

Morford, J. L., and S. Emerson. 1999. The geochemistry of redox sensitive trace metals in sediments. Geochimica et Cosmochimica Acta **63:** 1735-1750.

Morris, A. W. 1975. Dissolved molybdenum and vanadium in the northeast Atlantic Ocean. Deep-Sea Research and Oceanographic Abstracts **22:** 49-54.

Morrison, J. M., L. A. Codispoti, S. Gaurin, B. Jones, V. Manghnani, and Z. Zheng. 1998. Seasonal variation of hydrographic and nutrient fields during the US JGOFS Arabian Sea Process Study. Deep-Sea Research Part Ii-Topical Studies in Oceanography **45:** 2053-2101.

Morrison, J. M. and others 1999. The oxygen minimum zone in the Arabian Sea during 1995. Deep-Sea Research Part Ii-Topical Studies in Oceanography **46:** 1903-1931.

Nameroff, T. J. 1996. Suboxic trace metal geochemistry and paleo-record in continental margin sediments of the eastern tropical North Pacific. University of Washington, Seattle, WA, United States.

Naqvi, S. W. A. 1994. Denitrification Processes in the Arabian Sea. Proceedings of the Indian Academy of Sciences-Earth and Planetary Sciences **103:** 279-300.

Orcutt, K. M. and others 2001. A seasonal study of the significance of N2 fixation by Trichodesmium spp. at the Bermuda Atlantic Time-series Study (BATS) site. Deep-Sea Research Part II: Topical Studies in Oceanography **48:** 1583-1608.

Prange, A., and K. Kremling. 1985. Distibution of dissolved molybdenum, uranium and vanadium in Baltic Sea waters. Marine Chemistry **16:** 259-274.

Raven, J. A. 1988. The Iron and Molybdenum Use Efficiencies of Plant-Growth with Different Energy, Carbon and Nitrogen-Sources. New Phytologist **109:** 279-287.

Saito, M. A. 2001. The biogeochemistry of cobalt in the Sargasso Sea. DAI **62:** 01.

Sanudo-Wilhelmy, S. A. and others 2001. Phosphorus limitation of nitrogen fixation by Trichodesmium in the central Atlantic Ocean. Nature **411:** 66-69.

Shaw, T. J. 1988. The early diagenesis of transition metals in nearshore sediments. University of California, San Diego, La Jolla, CA, United States.

Shaw, T. J., J. M. Gieskes, and R. A. Jahnke. 1990. Early diagenesis in differing depositional environments; the response of transition metals in pore water. Geochimica et Cosmochimica Acta **54:** 1233-1246.

Sirocko, F. 1995. Abrupt change in monsoonal climate: evidence from the geochemical composition of Arabian Sea sediments. University of Kiel.

Sohrin, Y., K. Isshiki, and E. Nakayama. 1989. Simultaneous determination of tungsten and molybdenum in sea water by catalytic current polarography after preconcentration on a resin column. Analytica Chimica Acta **218:** 25-35.

Sprent, J. I., and J. A. Raven. 1985. Evolution of Nitrogen-Fixing Symbioses. Proceedings of the Royal Society of Edinburgh Section B- Biological Sciences **85:** 215-237.

Steinberg, D. K., C. A. Carlson, N. R. Bates, R. J. Johnson, A. F. Michaels, and A. H. Knap. 2001. Overview of the US JGOFS Bermuda Atlantic Time-series Study (BATS): a decade-scale look at ocean biology and biogeochemistry. Deep Sea Research Part II: Topical Studies in Oceanography **48:** 1405-1447.

Stiefel, E. I. 1996. Molybdenum bolsters the bioinorganic brigade. Science **272:** 1599-1600.

Sunda, W. G., and S. A. Huntsman. 1988. Effect of Sunlight on Redox Cycles of Manganese in the Southwestern Sargasso Sea. Deep-Sea Research Part a-Oceanographic Research Papers **35:** 1297-1317.

Tebo, B. M., and S. Emerson. 1986. Microbial Manganese(Ii) Oxidation in the Marine-Environment - a Quantitative Study. Biogeochemistry **2:** 149-161.

Vangeen, A., D. C. McCorkle, and G. P. Klinkhammer. 1995. Sensitivity of the Phosphate-Cadmium-Carbon Isotope Relation in the Ocean to Cadmium Removal by Suboxic Sediments. Paleoceanography **10:** 159-169.

Wehrli, B., G. Friedl, and A. Manceau. 1995. Reaction rates and products of manganese oxidation at the sediment-water interface, p. 11-134. *In* C. P. Huang, C. R. O'Melia and J. J. Morgan [eds.], Aquatic Chemistry: Interfacial and interspecies processes. ACS Adv. Chem.

Zhang, Y. 1999. The marine geochemistry of germanium, molybdenum and uranium; the sinks. Columbia University, , United States.

Zheng, Y., R. F. Anderson, A. van Geen, and J. Kuwabara. 2000. Authigenic molybdenum formation in marine sediments; a link to pore water sulfide in the Santa Barbara Basin. Geochimica et Cosmochimica Acta **64:** 4165-4178.

CHAPTER 4. DIEL VARIATION OF MOLYBDENUM AND IRON IN MARINE DIAZOTROPHIC CYANOBACTERIA

Abstract

Measurements of Mo:C and Fe:C in cultures of two N_2 fixing cyanobacteria, *Crocosphaera watsonii* strain WH8501and *Trichodesmium erythraeum* strain IMS101 are equivalent to estimated metal carbon ratios based on growth rate and the metal use efficiency of nitrogenase, the enzyme responsible for N_2 fixation. *Crocosphaera*, a single-celled, nocturnal N_2 fixer, showed a 3-8 fold increase in Mo and a 2 fold increase Fe cellular concentrations at night in response to nitrogen fixation activity. N_2 assimilation can account for almost the entire Mo pool measured in the cells suggesting that these organisms were not expressing other Mo enzymes or storing Mo. In conjunction with the large diel variation in Mo cellular concentrations, this implies that *Crocosphaera* synthesizes its entire nitrogenase pool anew each night. In contrast, cultures of *Trichodesmium* a filamentous, diurnal N_2 fixing cyanobacteria, did not show diel variations in Mo or Fe carbon ratios, or cellular concentrations. *Trichodesmium* Mo cellular concentrations were about 30% higher than required to support N_2 assimilation rates. Cultures maintained an internal pool of Mo even when not fixing N_2. *Trichodesmium* colonies collected from the field had Mo:C ratios tenfold larger than measured in culture and far in excess of what is needed to fix N_2 at rates normally measured in the field. *Trichodesmium* appears to maintain an internal pool of Mo, possibly as additional Mo-containing enzymes or simply stored within the cell. This result does not support the use of particulate Mo concentrations to estimate N_2 fixation rates.

4.1. Biological utilization of molybdenum

Nitrogen fixation, the conversion of N_2 gas into bioavailable forms, is an important source of nitrogen for primary production in the oligotrophic ocean (Capone et al. 1997; Karl et al. 1997). Nitrogen fixation is catalyzed by the nitrogenase complex, a metal rich enzyme containing 2 mol Mo and 42-58 mol Fe per mol complex (Eady and Smith 1979). Recent studies have focused on Fe as a potentially limiting nutrient for both photoautotrophic growth and for N_2 fixation in the marine environment {Berman-Frank, 2001 #156;Kustka, 2002 #730;Falkowski, 1998 #168;Sunda, 1995 #174}. Despite Mo's role in nitrogenase, at 107 nM in seawater (Collier 1985) Mo is unlikely to be

limiting (Paulsen et al. 1991), and it has been largely ignored. There are currently no available data constraining the Mo content of marine diazotrophs. In this study we report the results of Mo and Fe analyses of marine cyanobacteria grown in laboratory culture and collected in the open ocean. These data are used to 1) document changes in cellular metal concentration over diel cycles and 2) estimate the fraction of cellular Mo and Fe inventories that are bound in the nitrogenase complex. The Mo data were collected as part of a larger effort to evaluate the potential for using particulate Mo concentrations in suspended particulate matter to estimate water column nitrogen fixation rates.

The two cyanobacterial strains studied were a single celled, nocturnal diazotroph, *Crocosphaera watsonii* strain WH8501, and a non-heterocystous, filamentous, diazotroph, *Trichodesmium erythraeum* strain IMS101. *Trichodesmium* fixes N maximally at the mid-point of the day period, concurrently with photosynthesis. It protects the nitrogenase enzyme from deactivation by O_2 evolved from photosynthesis by spatially separating N_2 fixation and photosynthesis (Berman-Frank et al. 2001b). In contrast, *Crocosphaera,* a single-celled organism, temporally separates photosynthesis and N_2 fixation, fixing N_2 only in the dark. Comparing diel patterns of Mo and Fe cellular concentrations for *Crocosphaera* and *Trichodesmium*, provides an opportunity to investigate how the different N_2 fixation strategies employed by these two marine diazotrophs influence metal cycling.

Trichodesmium has dominated the study of open ocean N_2 fixation since it was hypothesized to fix N_2 (Dugdale et al. 1961). It forms macroscopic colonies (1-1000 μm) and large scale blooms abundant enough to be visible from space (Carpenter et al. 1992;

Hood et al. 2002; Subramaniam et al. 2002). There is however a discrepancy between N_2 fixation estimates based on direct estimates of *Trichodesmium* abundance and activity and those based on indirect mass balance arguments, suggesting that there may be other unquantified sources of fixed N to surface waters (Capone 2001). There is evidence that unicellular N_2 fixing cyanobacteria maybe widely distributed in the marine environment, up to 10^3 cells per mL (Campbell et al. 1997; Neveux et al. 1999; Wasmund et al. 2001). Recent research has suggested that single-celled diazotrophic cyanobacteria, such as *Crocosphaera*, are potentially significant sources of fixed N (Waterbury and Willey 1988; Zehr et al. 2000; Zehr et al. 2001). Zehr et al. (2001) showed that at the HOT station there are multiple strains of single-celled diazotrophic cyanobacteria (2.0-10 μm size class), several closely related to *Crocosphaera* WH8501. Zehr et al. (2001) also measured at HOT, maximal levels of the messenger RNA of nitrogenase , an indicator of enzyme activity, at night and $^{15}N_2$ fixation rates consistent with those measured for *Crocosphaera* WH8501 growth on N_2 in laboratory culture. By measuring Mo and Fe in *Crocosphaera* as well as *Trichodesmium*, we expand our knowledge of a potentially important but otherwise under investigated marine diazotroph.

4.2. Methods and Materials

4.2.1 Bacterial Strains.

Trichodesmium erythraeum strain IMS101 is the most extensively studied *Trichodesmium* species (Berman-Frank et al. 2001a; Capone et al. 1997; Mulholland and Capone 2000a). The *Crocosphaera watsonii* strain WH8501 has been previously

described as *Synechocystis* sp. strain WH8501 (Rippka et al. 2001; Waterbury and Rippka 1989; Zehr et al. 2001). Both species were maintained in culture at the Woods Hole Oceanographic Institution and isolated as described elsewhere (Paerl et al. 1994; Waterbury and Rippka 1989). All cultures were verified as axenic by direct microscopic observation and by lack of heterotrophic growth in a marine broth medium (Waterbury et al. 1986).

4.2.2 Culture Conditions

Stock cultures of *Crocosphaera* and *Trichodesmium* were maintained on a 3/4 Sargasso seawater based medium. Sargasso seawater collected on cruises of opportunity and stored in the dark was successively filtered through 1.0 and 0.22 μm Millipore membrane filters and then "sterilized" by heating in a microwave oven to boiling in Teflon bottles (Keller et al. 1988). Sargasso Seawater was diluted to 75% strength with sterile Milli-Q water. The medium was amended with nutrients and trace metals (Table 4.1). All cultures were Fe-replete with a final log free iron concentration (log[Fe']) of –7.5. Total Mo concentrations were 97 nM, within 10% of seawater concentrations. All nutrient and trace metal additions were purchased from Sigma and tissue culture tested. Nutrient and trace metal stocks were sterilized either by filtration or autoclave before being added to the 3/4 Sargasso seawater base. Stock cultures were grown in Polycarbonate (Nalgene) flasks cleaned by successive washes in Micro (International Products Corporation Burlington, N.J.) and then 0.5 N trace-metal grade HCl followed by repeated rinses with Milli-Q water. Cultures were grown on a 14:10 hr light-dark cycle using white fluorescent lamps at 30.0 μEin $m^{-2}s^{-1}$ and at a temperature of 28°C.

Trichodesmium stock cultures were continuously gently stirred while Crocosphaera cultures were shaken gently daily to resuspend cells.

Table 4.1. Culture Medium

Nutrients	**Final Concentration (mol L^{-1})**
Phosphoric Acid	8×10^{-6}
EDTA	5×10^{-7}
Fe(III)citrate	5×10^{-8}
Citric Acid	1×10^{-5}
Trace metals	
$MnSO_4$	1×10^{-7}
$ZnCl_2$	1×10^{-8}
$NaMoO_4$	1×10^{-8}
$CoCl_2$	1×10^{-10}
$NiCl_2$	1×10^{-10}
$NaSeO_3$	1×10^{-10}

4.2.3 Experimental Conditions

Growth experiments were conducted in 1.5-L Nalgene polycarbonate culture chamber with an internally suspended magnetic stir bar. The culture vessel was cleaned with Micro and 0.05 N HCl. As with stock cultures, cells were incubated at 28°C on a 14-10 hr light:dark cycle. Cells were grown as batch cultures to late log phase. Growth rate for *Crocosphaera* was monitored by cell counts using epifluorescent illumination. For Trichodesmium cell growth rate was determined from trichome length. This was possible because the culture grew as single trichomes throughout the experiment rather than forming colonies. Cell counts for both species were determined once a day at the

time of maximum N_2 fixation and whenever sub-samples for acetylene reduction rate incubation or metal analysis were collected.

4.2.4 Nitrogen Fixation Rates

Nitrogen Fixation rates were measured using the acetylene reduction method (Capone 1993) using a ratio of 4:1 for the conversion of acetylene reduction to N_2 reduction. Between 10 and 20 mL aliquots of culture were sealed into Micro and 0.05 N HCl cleaned 60 mL Nalgene Polycarbonate bottles fitted with Teflon coated silicone septa. 6 mL of head space was removed and replaced with 6 mL acetylene. Sub-samples are incubated for 1.5-2 hrs at growth irradiance and temperature. Ethylene production was measured on a Shimadzu GC-8 gas chromatograph with a flame ionization detector and quantified relative to an ethylene standard. Results are reported as nmol N_2 reduced per min per cell.

4.2.5 Fe and Mo cellular concentration determination

Fe and Mo concentrations were measured in three *Crocosphaera* and two *Trichodesmium* experiments. Cell samples were taken over 2-3 diel cycles at times of maximum and minimum N_2 fixation as determined by simultaneous acetylene reduction rate measurements. Additionally samples of field populations of *Trichodesmium erythraeum* and *Trichodesmium theibautii* were collected on two cruises in the Atlantic, one at the Bermuda Atlantic Time Series (BATS) site in September, 2000 and the other from a survey of the sub-tropical Atlantic on the R/V Seward Johnson May, 2001. Colonies in the upper 10 m were collected via plankton tow, hand-picked into sterile Sargasso seawater to rinse and reduce carryover of non-*Trichodesmium* contaminants.

Both *Crocosphaera* and *Trichodesmium* cultures and *Trichodesmium* field samples were collected by gently (<5 inches Hg vacuum) filtering a known volume of culture or, in the case of field samples, a known number of colonies onto an acid cleaned (10% Seastar HCl at 60°C overnight) 47 mm polycarbonate membrane filters (Osmotics) using an acid cleaned Teflon filter holder. *Crocosphaera* was collected using 0.2 μm pore size while *Trichodesmium's* larger size allowed use of 5.0 μm filter. Prior to use filters are rinsed in the filter holder with sterile seawater or media to neutralize the filter after storage in a dilute Seastar HCl solution (pH 2). Filters were then frozen at –20°C for transport and later analysis.

Metal Analyses: Filter digestion and metal analyses are described in detail in (Chapter 2 Tuit 2003). Briefly, metal samples were treated by refluxing with 950 μl HNO_3 and 50 μl HF at 120°C for 4hrs in a closed Teflon vial to dissolve particulate matter and cells (Cullen and Sherrell 1999). Leachate solutions were diluted 10-fold and stored for analysis. Stored solutions were analyzed on the WHOI Finnegan Element ICP-MS. Fe and Mo concentrations in all samples were determined via isotope dilution (ID). For field samples of picked *Trichodesmium* colonies Fe, Mo, Al, Rb, and Mn were also determined via standard addition (SA). Al, Rb and Mn were not measured in cultures because dust contamination and Mn oxide formation were assumed to be minimal. Mo contributions from sea salt carryover on filters were corrected using procedural blanks. ID analyses of Mo and Fe had better precision and were used for all calculations (Figure 4.1). SA analyses of Mn, Al and Rb allowed the evaluation of possible contributions of

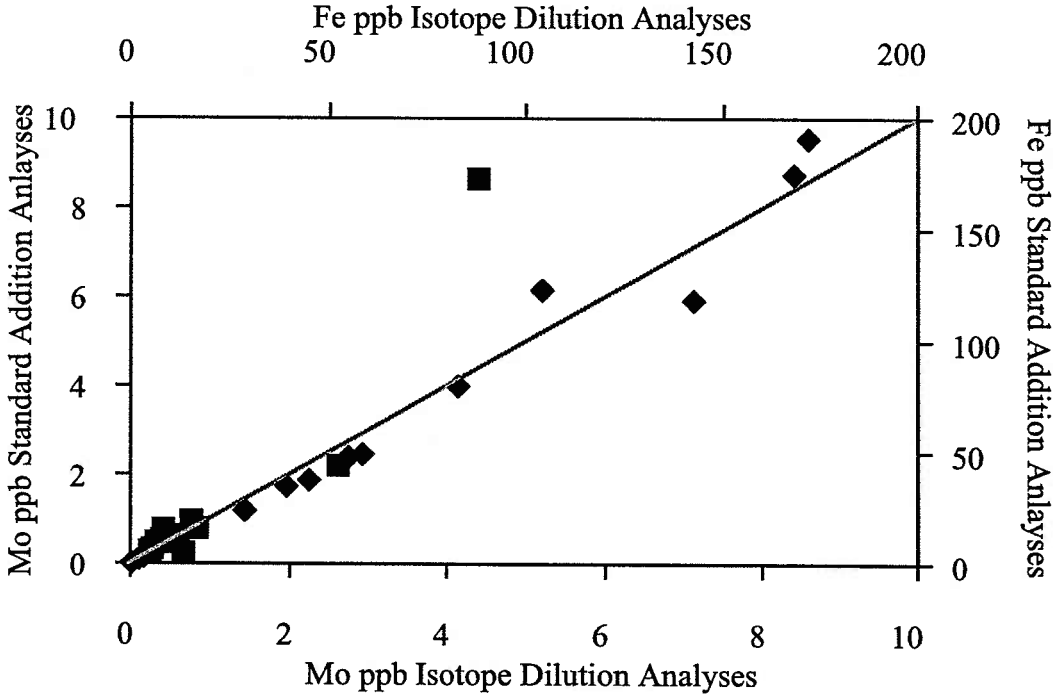

Figure 4.1 Comparison of Standard Addition (SA) and Isotope Dilution (ID) analyses of Mo (diamonds) and Fe (squares) in picked Trichodesmium samples. Most samples fall along the 1:1 line showing good agreement between analytical techniques.

Mo and Fe from crustal sources (Al), Mn oxides and from seawater salts (Rb) assuming average molar ratios to Fe and Mo in these sources. A Fe:Al ratio of 0.841 g g^{-1} and a Mo:Al ratio of 23.8 μg g^{-1} were used to estimate crustal contributions (Taylor and McLennan, 1985). Seawater dissolved Fe concentrations were assumed to be negligible but a Mo:Rb ratio of 0.093 g g^{-1} was used to make a sea salt correction (Spencer et al. 1970). Mn concentrations in the colonies were below detection limits. Contributions from crustal sources were negligible for Mo, and sea salt Mo corrections averaged 1%. Crustal contributions averaged 10% for Fe. This does not account for extracellular authigenic $Fe(OH)_3$ which may also contribute to the Fe measurements.

Media blanks that take into account possible Mo and Fe metal contributions from culture media, seawater and filter apparatus were measured as procedural blanks separately for each experiment. For *Crocosphaera* Mo media blanks average 10% of total analyte (ng Mo/filter) but were as high as 60% for non N_2 fixing samples where cellular metal concentrations were very low. Similarly for Fe media blank averaged 15% but reached as high as 40% for non-N_2 fixing samples. For Trichodesmium media blanks averaged 12% of total analyte for Mo and Fe.

CHN Analyses: Samples of cultures for CHN analysis were collected by filtering 50-100 mL of culture onto an ashed GF/F filter, or an acid cleaned PC filter. PC filters were used initially because of concerns that the differences in retention pore sizes of GF/F and PC filters might make metal and nutrient samples non-comparable. PC filters and cells were transferred to Petri dishes and covered with ethanol. Cells were gently scraped off with a Teflon coated spatula and then transferred in ethanol to a tin boat and

dried down for CHN analysis. This procedure has been shown to be quantitative (Kujawinski 2000). Picked Trichodesmium samples were collected by filtering a known number of colonies in a known volume of sterile seawater. Samples were analyzed at the VIMS Analytical Service Center on an Exeter Analytical CE-440 CHN Analyzer. Procedural Media blanks were determined by filtering 50-100 mL of sterile media or sterile seawater. Media blanks were always <10% for C and <5% for N. Metal, C and N were compared to each other by normalizing to mg dry weight (*Crocosphaera* 1 and 2; *Trichodesmium* 1) or by mL of culture filtered (*Crocosphaera* 3 and 4).

4.3. Results

4.3.1 Crocosphaera *Experiments*

Four total *Crocosphaera* experiments were performed measuring Mo and Fe cellular concentration, Fe:C and Mo:C ratios and nitrogen fixation rate over 2-3 diel cycles. Cell counts of late log phase batch culture for Experiments 1, 2, and 4 gave a doubling time of 1.5 days, the maximal growth rate observed for this organism. Experiment 3 was found to have entered stationary phase by the end of the experiment exhibiting a decreased doubling time of 2.8 days. The N_2 fixation activity of experiments 2-4 was monitored by acetylene reduction. The N_2 fixation rates calculated from acetylene reduction rate measurements in sub-samples of the main batch cultures were systematically smaller than N_2 assimilation rate required to support the growth rate determined in the culture vessel at the N cellular concentrations measured (Table 4.2).

While acetylene reduction data clearly delineate diel patterns of N_2 fixation, they provide only a minimum estimate of N_2 fixation and culture growth rates.

Table 4.2. A comparison of cell and N based growth rates and *Crocosphaera*

Experiment	Cell-based Growth rate[a] (day^{-1})	N-based Growth rate[b] (day^{-1})	N assimulation rate[c] (fmol N $cell^{-1}$ day^{-1})	N fixation rate[d] (fmol N $cell^{-1}$ day^{-1})
1	0.47		4.6	
2	0.46	0.199	2.1	2.4
3	0.25	0.025	5.2	0.8
4	0.48	0.033	13	1.5

[a]Rates were determined directly from cell counts.
[b]Rates were calculated from cellular N concentration (fmol $cell^{-1}$) and N fixation rate (fmol N $cell^{-1}$ day^{-1}) measured by acetylene reduction.
[c]Rates were calculated from cell growth rate (day^{-1}) and cellular N concentration (fmol $cell^{-1}$) of culture measured in culture vessel.
[d]Rates were measured by acetylene reduction assay in 20 mL incubation.

Analytical results from Crocosphaera culture experiments are presented in Table 4.3. There was a consistent diel variation in Mo cellular concentrations of 3-8 fold that was in phase with N_2 fixation rates (Figure 4.2, left panels). N_2 fixation rates were not measured in experiment 1and the low Mo cellular concentrations and Mo:C ratios suggest that the culture was not sampled during the peak of N_2 fixation. Mo:C ratios also exhibited clear diel variations of a similar magnitude (8-10 fold). Fe cellular concentrations also show a 2.4 to 3.3-fold increase during nitrogen fixation (Figure 4.2, right panels) with a 9 to 4 fold increase in Fe:C ratios. In experiment 4 diel variations are not apparent. Fe:C ratios and Fe cellular concentrations are extremely large compared to the other *Crocosphaera* experiments though they were not out side the range measured for *Trichodesmium*

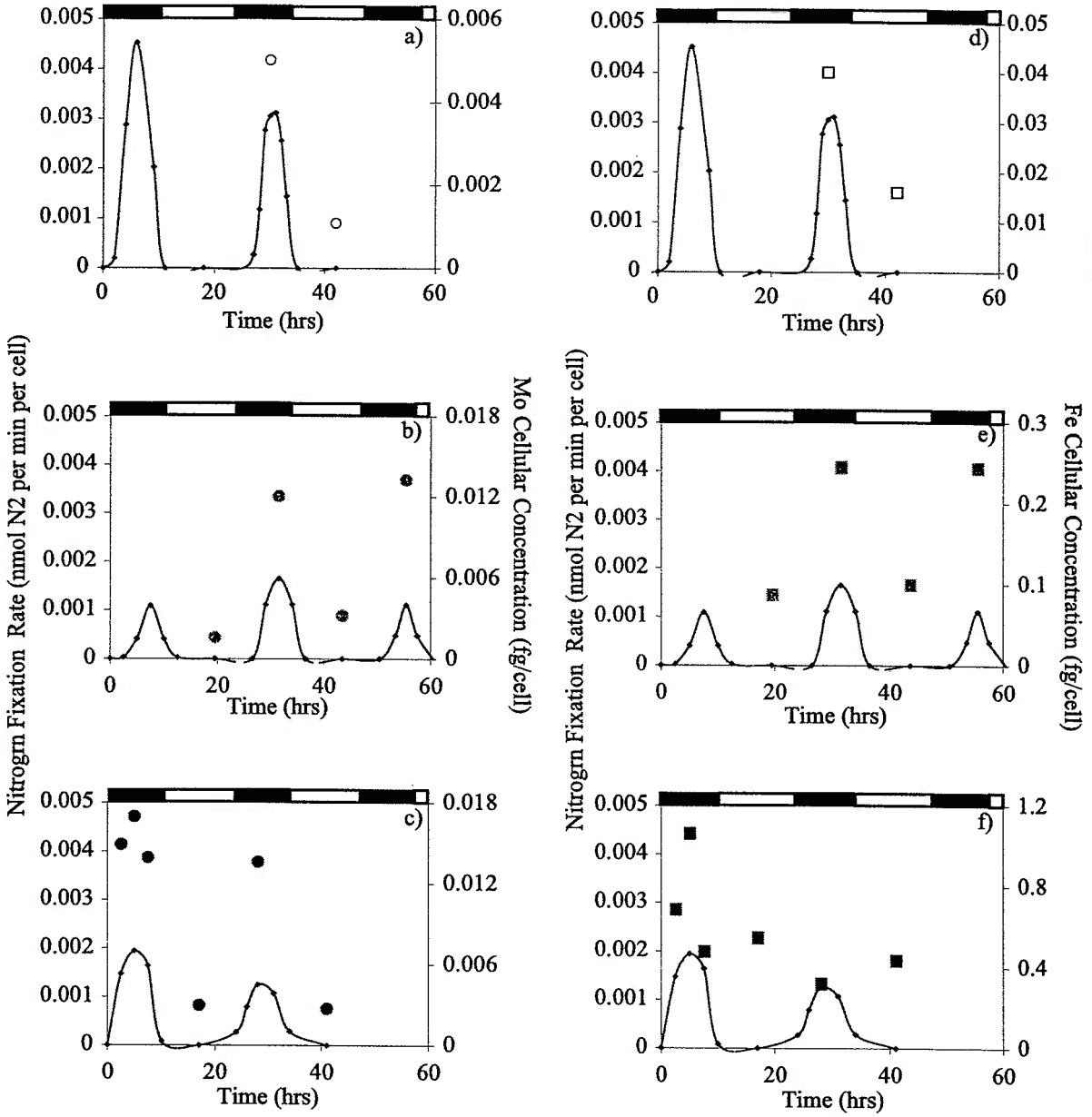

Figure 4.2 Diel variations in N2 fixation rate (lines) compared to Mo (a-c) and Fe (d-f) cellular concentrations in fg cell-1 for Crocosphaera experiments 2 (a and d), 3 (b and e) and 4 (c and f). N2 fixation rates are shown on the same scale for all experiments. Cellular concentrations are correlated with N2 fixations in all cases except for experiment 4 Fe analyses (f) where high Fe concentrations due to contamination obscures all other variations.

Table 4.3. Fe and Mo cellular concentrations and ratios for *Crocosphaera spp.* grown on a 14:10 light:dark schedule

Sample	Time[a] hr	Cellular Concentrations Fe fg/cell	Mo fg/cell	Ratios Fe:C µmol mol^{-1}	Mo:C µmol mol^{-1}	Fe:Mo mol mol^{-1}	C:N mol mol^{-1}
Experiment 1							
C5 N_2 fixing	**30**	0.013	0.0013	7.3	0.45	16.2	8.14
C10	**42**	0.004	0.0004	0.76	0.04	16.9	7.49
Experiment 2							
C9 N_2 fixing	**30**	0.040	0.0050	12.0	0.88	13.7	8.65
C2	**42**	0.016	0.0011			25.3	
Experiment 3							
Mo1 N_2 fixing	**5**						9.75
Mo2	**17**	0.087	0.0016	5.5	0.06	94.1	10.08
Mo3 N_2 fixing	**29**	0.244	0.0121	19.9	0.57	34.8	9.56
Mo4	**41**	0.099	0.0032	6.5	0.10	55.2	10.10
Mo5 N_2 fixing	**53**	0.243	0.0133	27.1	0.86	31.5	11.37
Experiment 4[c]							
2M N_2 fixing	**2.5**	0.685	0.0149	51.3	0.65	79.0	9.47
3M N_2 fixing	**5**	1.061	0.0170	96.7	0.90	107.4	7.26
4M N_2 fixing	**7.5**	0.477	0.0139	44.4	0.75	58.8	5.90
6M	**17**	0.546	0.0030	43.0	0.14	316.4	7.13
9M N_2 fixing	**28**	0.3	0.0136	30.8	0.77	40.1	7.88
12M	**41**	0.434	0.0027	27.8	0.10	274.5	7.49
Ave(s.d.) N_2 fixing[b]		0.14 (0.12)	0.011(0.005)	15.8(11.3)	0.70(0.27)	24.1(14.2)	8.6(1.8)
Ave(s.d.)[b]		0.06 (0.05)	0.003(0.001)	4.2(3.1)	0.08(0.04)	54.7(38.6)	8.8(1.5)

[a]Indicates time of sample collection, elapsed time measured from start of the dark period. Periods of N_2 fixation indicated. [b]Averages of Fe cellular concentrations and ratios do not include experiment 4. [c]Experiment 4 was possibly contaminated for Fe.

(Kustka et al. 2002). We suspect that these high Fe levels obscured diel Fe cycling in this experiment. The contrast in Fe results between experiment 4 and the earlier experiments suggested that there was a Fe contamination problem. Fe:Mo ratios of experiments 2 and 3 were lower in the N_2 fixing samples than photosynthesizing samples. In the N_2 fixing

samples Fe:Mo ratios approached the 21-29 Fe:Mo molar ratio predicted by the stoichiometry of nitrogenase.

The difference in magnitude between cellular concentration and metal:carbon ratio daily variation was due to diel variation of the carbon and nitrogen pool in *Crocosphaera* (Waterbury and Valois, unpublished data). This could be seen in experiment 3 samples 2M-4M by the decrease in C:N over the course of the night period as N was added by N_2 fixation and glycogen reserves built up during the day were depleted to fuel N_2 fixation. *Crocosphaera* also has a partially synchronized cellular division, though cell division occurs throughout the day and night, approximately one third of the cells divide at 10 am (Waterbury and Valois, unpublished data). The diel variation in both Fe and Mo however was too large to be an artifact of cell division, which could cause at most a 1.3 fold variation in metal cellular content.

4.3.2 Trichodesmium

The cell doubling time for Trichodesmium experiment 1 was about 1.4 days, the maximum observed in the Waterbury lab for axenic cultures. Experiment 2 showed a suppressed growth rate, which may be the result of a small amount of heterotrophic contamination. The cell doubling and nitrogen based doubling times disagreed for experiment 1 (Table 4.4). Estimates of growth rate of Trichodesmium presented in the literature have an extremely wide range (Mulholland and Capone 2000b). Estimates of carbon based doubling times are generally much faster than N_2 fixation based doubling time calculated from N_2 fixation rates determined by acetylene reduction (Mulholland and Capone 2000b). This discrepancy is analogous to the differences between cell-based

and nitrogen based doubling times documented in the *Crocosphaera* and *Trichodesmium* experiments reported here. In field samples it has been proposed that this discrepancy might be a

Table 4.4. A comparison of cell and N based growth rates for *Trichodesmium*.

Experiment	Cell-based Growth rate[a] (day^{-1})	N-based Growth rate[b] (day^{-1})	N assimilation rate[c] (fmol N $cell^{-1}$ day^{-1})	N fixation rate[d] (fmol N $cell^{-1}$ day^{-1})
1	0.505	0.019	272	15
2	0.096			16

[a]Rates were determined directly from cell counts.
[b]Rates were caluclated from cellular N concentration (fmol $cell^{-1}$) and N fixation rate (fmol N $cell^{-1}$ day^{-1}) measured by acetylene reduction.
[c]Rates were calculated from cell growth rate (day^{-1}) and cellular N concentration (fmol $cell^{-1}$) of culture measured in culture vessel.
[d]Rates were measured by acetylene reduction assay in 20 mL incubation.

result of Trichodesmium using alternate sources of N, such as NH_4^+ or glutamate (Mulholland and Capone 2000b). However, in an axenic culture, it is likely that the discrepancy was simply an inability to get a reliable estimate of N_2 fixation from acetylene reduction rates.

The *Trichodesmium* experiment 1 showed a possible correlation in Mo:C molar ratios in phase with N_2 fixation rate (Figure 4.3 and Table 4.5), however this correlation did not appear in experiment 2. Fe:C ratios did not show significant correlation with N_2 fixation rate in either experiment. Average C:N molar ratios for both experiments were low and stable at 6.20±0.43. Average Fe:Mo molar ratios are 34.0± 15.7, and in most cases were within or slightly higher than the 21 to 29 mol Fe per mol Mo calculated for the nitrogenase complex. Field samples of *Trichodesmium* did not show a strong diel variation in either Fe or Mo (Table 4.6). Average C:N molar ratios for the field samples

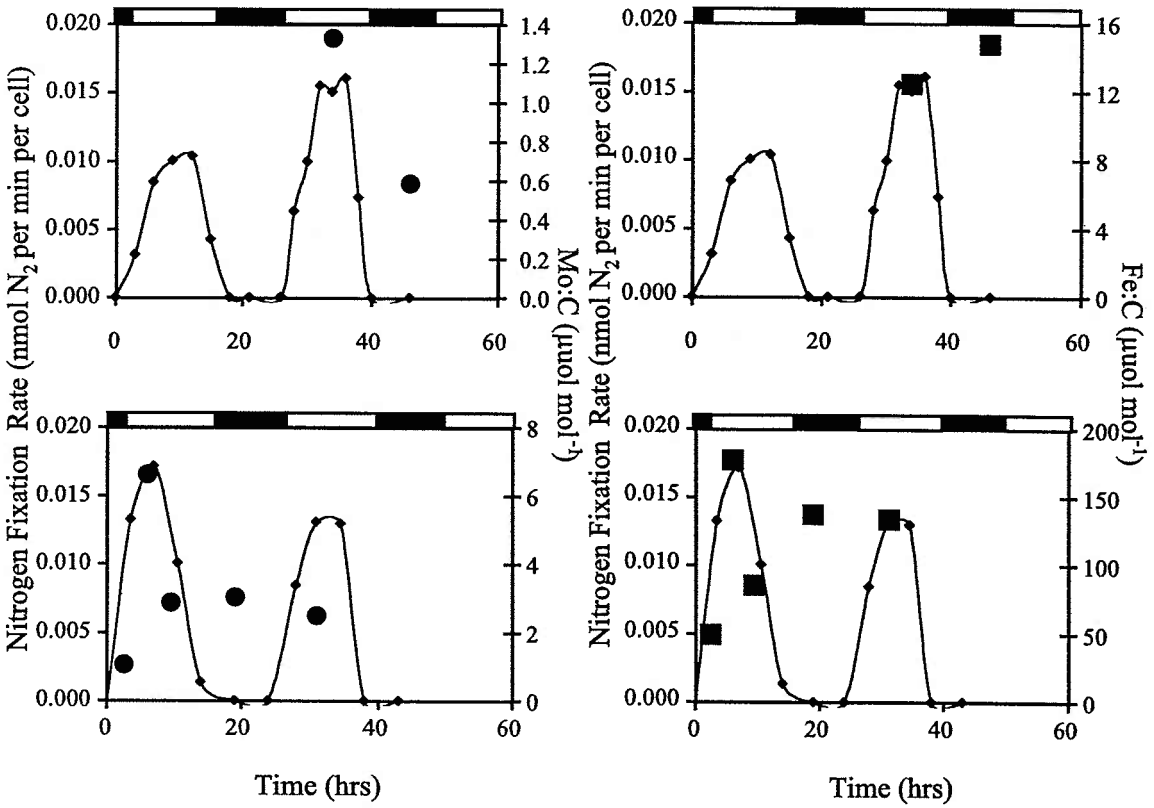

Figure 4.3 Trichodesmium diel cycles of N2 fixation (lines) compared to Mo:C (a; circles) and Fe:C (b; squares) ratios for experiment 1. Mo:C shows a 2-fold diel variation in phase with nitrogenase activity, but Fe:C ratios do not show significant variation.

Table 4.5. Fe and Mo cellular concentrations and ratios for *Trichodesmium spp.* grown on a 14:10 light:dark schedule

Sample	Time[a] hr	Fe	Mo	Fe:C	Mo:C	C:N	Fe:Mo
		fg/cell		μmol mol^{-1}			mol mol^{-1}
Experiment 1							
TD N_2 fixing	**34**	2.37	0.44	12.4	1.33	6.54	9.3
TL	**46**	2.94	0.20	14.7	0.58	6.64	25.3
Experiment 2							
2M N_2 fixing	**2.5**			49.3	1.04	6.32	47.3
3M N_2 fixing	**6**			176.7	6.62	6.06	26.7
4M N_2 fixing	**9.5**			84.7	2.87	5.51	29.6
6M	**19**			138.2	3.02	6.53	45.7
9M N_2 fixing	**31**			133.7	2.47	5.79	54.1
12M	**42**						
Average (1 s.d.)				87.1 (64.2)	2.56 (2.02)	6.20 (0.43)	34.0 (15.7)

[a]Indicates time of sample collection, elapsed time measured from start of the light period. Periods of N_2 fixation indicated.

Table 4.6. Trichodesmium Field Samples collected in the N. Atlantic.

	Fe:C	Mo:C	C:N	Fe:Mo
	μmol/mol		mol:mol	
BATS, September 1999				
10:00	45.3	19.8	7.84	2.3
14:00	79.1	2.6[a]	7.48	30.5[a]
14:00	49.8	17.8	7.81	2.8
01:00	51.7	8.6	9.66	6.0
R/V Seward Johnson, May 2001				
Sta. 01 12:00	74.1	22.7	6.26	3.3
Sta. 02 03:00	85.9	8.6	6.59	9.9
Sta. 03 21:00	51.8	53.6	6.55	1.0
Sta. 04 09:00	160.6	38.5	12.64	4.2
Sta. 04 13:00			6.32	
Sta. 07 12:00	1008.9[a]	36.4	6.85	27.7[a]
Sta. 08 12:00			6.8	
Sta. 28 14:00	48.7	24.6	6.66	2.0
Sta. 30 22:00			6.82	
Sta. 32 16:00	13.8	14.7	6.25	0.9
Average (1 s.d.)	66.1 (39.0)	22.5 (15.1)	7.1 (0.9)	3.6 (2.9)

[a]Outlying values not included in the average

were equivalent to those measured in culture. Fe:Mo ratios of field samples however were much lower than seen in culture. This was not driven by an decrease in Fe, Fe:C ratios of cultured and field samples are equivalent within error, but by a large increase in Mo, as seen by the tenfold increase in Mo:C ratio compared to culture samples.

Berman-Frank et al. (2001a) measured the Fe:C ratio of *Trichodesmium* grown at a range of free iron concentrations(Table 4.7). They report an average Fe:C (μmol:mol) of 168±23 for *Trichodesmium* grown at a similar free Fe as used in cultures in the present

Table 4.7. Comparison of *Trichodesmium* Fe:C and C:N ratios in culture and field samples from this and other studies. Free Fe concentration of the culture media shown when known.

		Fe:C		C:N		Reference
Cultures						
Growth Stage	**pFe'**	**μmol mol^{-1}**	**1 sd**	**mol mol^{-1}**	**1 sd**	
Log	-7.5	87	64	6.2	0.4	[a]
Log	-10.78	13	9.9	12.0	1.0	[b]
Log	-9.88	30	2.7	8.9	1.0	[b]
Log	-9.4	33	1.8	9.0	0.3	[b]
Log	-7.86	48	2.2	16.0	2.0	[b]
Log	-7.8	168	23	12.0	4.0	[b]
Log	replete			6.2	0.2	[c]
Lag	replete			9.1	1.3	[c]
Stationary	replete			7.9	2.1	[c]
Field Samples						
Location	**Year**					
N. Atlantic	00	66	39	7.2	1.0	[a]
Australia	99	575	265	6.1	0.7	[b]
Caribbean	88	326	127			[d]
Atlantic	96	36				[e]
Pacific	90-91			6.4	0.4	[f]

[a]This Study [b](Berman-Frank et al. 2001a) [c](Mulholland and Capone 2001) [d](Rueter et al. 1992) [e](Sanudo-Wilhelmy et al. 2001) [f](Letelier and Karl 1996)

study (log[Fe']=-7.8). However, Berman-Frank et al. (2001a) report as much 65 % of the Fe associated with *Trichodesmium* cells in these samples is extra-cellular, which brings their culture Fe:C down to 69 μmol Fe mol^{-1} C. For field samples the total range in Fe:C ratios is from 20 to >500 (Kustka et al. 2002). Berman-Frank, et al. (2001a) reported Fe:C numbers of 450±242 μmol Fe per mol C for handpicked colonies collected in shelf waters off Australia. These overlap with the earlier ratios of Rueter et al. (1992): 326±127 μmol Fe per mol C from the Caribbean. It is likely however that both of these estimates include large proportions of extra-cellular Fe from Fe oxyhydroxides. *Trichodesmium* collected from the Atlantic more recently (Sanudo-Wilhelmy et al. 2001) had Fe:C ranging from 22-72 μmol Fe per mol C which overlaps with the range in field data from the Atlantic reported here.

4.4. Discussion

4.4.1 Metal Use Efficiency of Nitrogenase

This is the first study to present data on the diel variations of Mo and Fe cellular concentrations of marine diazotrophic cyanobacteria. However, cellular concentration does not give us any information about how much of the metal in the cell is required by nitrogenase as opposed to the metal required by other enzymes or stored unused by the organism. The fraction of cellular Mo and Fe used by the nitrogenase enzyme can be estimated from the Metal Use Efficiency (MUE) of nitrogenase, or the amount of N_2 reduced per minute per fg nitrogenase bound metal.

The MUE is calculated from the molecular weight, metal requirements and specific activity of nitrogenase by the equation

$$MUE = SA \times \frac{1 \text{ mol } N_2}{4 \text{ mol } C_2H_2} \times \frac{mg}{10^{12} fg} \times \frac{1}{Q} \times \frac{M_{FeMo}}{M_M} \quad (1)$$

Where SA is the specific activity of nitrogenase, M_{FeMo} is the molecular weight of FeMo protein of nitrogenase, Q is the Fe or Mo content of the nitrogenase complex, and M_M is the molecular weight of Fe or Mo.

This approach has been used previously to estimate the Fe use efficiency of nitrogenase, the mol N_2 reduced per min per fg nitrogenase bound Fe (Kustka et al. 2002; Raven 1988; Sanudo-Wilhelmy et al. 2001; Sprent and Raven 1985). Using the specific activities of the FeMo protein of nitrogenase isolated from a variety of heterotrophs, including *Azotobacter vinelandii*, Sanudo-Wilhelmy et al. (2001) calculate a range of 5.60×10^{-8} to 1.83×10^{-8} nmol N_2 reduced per min per fg enzymatic Fe. We chose to recalculate the Fe use efficiency for several reasons. The Sanudo-Wilhelmy et al. (2001) calculations do not take into account the temperature at which the specific activity of nitrogenase was measured. A range of 25 to 30° C in temperature can lead to a 33% variation in specific activity (Burns 1979). Sanudo-Wilhelmy et al. (2001) also use an older data set for the specific activity. The specific activity of an isolated enzyme is highly dependent on how well the enzyme was purified and how the protein concentration was determined. These techniques have improved with time, generally increasing estimates of specific activity, and thus the calculated values of MEU.

To calculate the Fe and Mo use efficiency of nitrogenase we used data derived from enzyme isolated from the heterotrophic soil bacterium *Azotobacter vinelandii*, the most well studied nitrogenase. Comparable data is not available for nitrogenase isolated from cyanobacteria. We cannot preclude the possibility that the specific activity or metal requirements of nitrogenase produced by marine diazotrophs differs significantly from the parameters determined for nitrogenase produced by heterotrophic diazoatrophs. However, Zehr et al. (2001) have modeled the Fe protein of nitrogenase from *Trichodesmium* nifH sequences and find significant similarity in structural features with Fe protein isolated from *Azotobacter vinelandii* suggesting that these parameters may apply to cyanobacteria as well. The specific activity of the FeMo protein of *Azotobacter vinelandii* is 2200-2400 nmol C_2H_2 min^{-1} per mg FeMo at 30°C (Anderson and Howard, 1984). Corrected for the temperature at which these cultures were grown (28°C) this becomes 1870-2040 nmol C_2H_2 min^{-1} per mg FeMo (Burns 1979). The molecular weight of the *Azotobacter vinelandii* FeMo protein is 230-270Kda (Anderson and Howard, 1984) and the Fe and Mo content of the *Azotobacter vinelandii* nitrogenase complex is 2 mol Mo and 54-58 mol Fe per mol nitrogenase complex (Eady and Smith 1979). The ratio of acetylene to N_2 reduced is approximately a 4:1 mol C_2H_2 mol^{-1} N_2 for most N_2 fixing bacteria (Capone and Montoya 2001). Using these values we calculated a Fe use efficiency of nitrogenase of $3.94 \pm 1.04 \times 10^{-8}$ nmol N_2 reduced per min per fg enzymatic Fe, which falls within the 1.83×10^{-8} to 5.60×10^{-8} nmol N_2 reduced per min per fg enzymatic range of Sanudo-Wilhelmy et al. (2001). The Mo use efficiency is $6.46 \pm 1.32 \times 10^{-7}$ nmol N_2 reduced per min per fg enzymatic Mo.

The MUE can be used to 1) predict nitrogenase bound metal cellular concentrations based on nitrogen fixation or assimilation rate and 2) estimate the nitrogenase bound metal:C ratio of a cell based on growth rate and C:N ratio. There are several assumptions implicit in using these MUE's to investigate *Trichodesmium* and *Crocosphaera* cultures. As discussed above the nitrogenase of the cyanobacteria *Trichodesmium* and *Crocosphaera* are assumed to be similar to that of the heterotrophic soil bacterium *Azotobacter vinelandii*. All growth is assumed to be supported by N_2 fixation with no fixed N source. This is likely a good assumption for axenic cultures growing exponentially in media with no added N. It may also be a good assumption for field populations of *Crocosphaera,* which maintained maximal rates of N_2 fixation in culture despite nitrate and urea additions of up to 20 μM (unpublished data). *Trichodesmium*, however, has been shown to suppress N_2 fixation in the presence of fixed N sources (Mulholland et al. 2001), thus estimates of nitrogenase bound metal:C ratios for field populations may be over estimates.

Theoretical estimates of nitrogenase bound metal:carbon ratios were calculated by dividing the cell-based growth rate by the metal use efficiency of the enzyme and dividing again by the C:N ratio, yielding an estimate of the amount of enzyme-bound metal that is required by an organism. Given the growth rate in culture for both *Trichodesmium* and *Crocosphaera*, 0.5 day^{-1} at 28°C, and respective C:N ratios of 6.2 and 9.0, the estimated Nitrogenase-Mo:C ratios were 0.29 and 0.42 μmol Mo mol^{-1} C, respectively. These ratios are an estimate of the minimum Mo requirement based only on the Mo bound in the nitrogenase enzyme. They are also averaged over a 24 hr day rather

than the 10-14 hr period when N_2 fixation takes place, which would raise estimates by about 2 fold. The average Mo:C for the *Crocosphaera* cultures (0.71±0.27μmol Mo mol^{-1} C: Table 4.3) is within a factor of 2 of the theoretical estimate. *Trichodesmium* measured Mo:C in culture (2.56±2.02 μmol Mo mol^{-1} C: Table 4.5) are 4 to 9 fold higher than estimated Mo demand based on nitrogenase requirements but average Mo:C of the field *Trichodesmium* samples is almost a 100-fold greater than Nitrogenase-Mo:C (22.5±15.1 μmol Mo mol^{-1} C: Table 4.6).

A similar estimate made for Nitrogenase-Fe:C gives 11.8 and 8.1 μmol Fe mol^{-1} C for *Trichodesmium* and *Crocosphaera*, respectively. This estimate does not take into account Fe needed for other enzymatic processes including the Fe needed for carbon fixation by photosynthesis. These processes have been estimated to cost 0.9 mol Fe mol^{-1} C s^{-1} (Raven 1988; Sanudo-Wilhelmy et al. 2001). Adding this to the Fe budget increases estimates of Fe:C ratios to 16.6 μmol Fe mol^{-1} C for *Trichodesmium*. This estimate is at the low end of the range of Fe:C ratios seen in both the cultures (87.1±64.2μmol Fe mol^{-1} C: Table 4.5) and the natural populations sampled for this study as well as the data available in the literature (Kustka et al. 2002). *Crocosphaera* temporally separates N_2 fixation (night) and photosynthesis (day). Thus assuming nitrogenase dominates Fe demand at night and the photosynthetic apparatus dominates the daytime Fe demand, the enzymatic Fe:C estimates are 8.1 and 4.8 μmol Fe mol^{-1} C, for N_2 fixation period and light period, respectively. These are within error of measured culture samples for the light period (4.2 ± 3.1 mol Fe mol^{-1} C: Table 4.3) and N_2 fixation period (15.8±11.3 mol Fe mol^{-1} C: Table 4.3).

The agreement between theoretical estimates of Fe:C and Mo:C based on metal use efficiency estimates and those measured in culture experiments implies that a very large fraction of the total pool of measured Fe and Mo is bound in active nitrogenase enzyme. This is illustrated graphically in Figures 4.4 and 4.5, which show a comparison of measured cellular concentrations of Fe and Mo versus predicted cellular quantities required for the rate of N assimilation assuming all growth is supported by N_2 fixation. For both *Trichodesmium* and *Crocosphaera* predicted Mo cellular concentrations during N_2 fixation match very well with those independently measured in the cells. *Crocosphaera* Mo cellular concentrations measured in non N_2 fixing samples are all uniformly low, but the Trichodesmium sample is comparatively high. This implies that while *Crocosphaera* releases nearly all of its Mo back into the media, *Trichodesmium* maintains a pool of Mo even when it is not actively fixing N_2. Due to the high solubility of Mo in oxic seawater, it is more likely that this pool of Mo is sequestered internally rather than being adsorbed or bound extracellularly to the trichomes. The only other Mo enzyme known to be present in cyanobacteria is nitrate reductase, but nitrate reductase has a much higher specific activity than nitrogenase and is thought to require less Mo than nitrogenase for similar growth rates (Raven 1988; Sanudo-Wilhelmy et al. 2001; Sprent and Raven 1985). In a nitrate free medium it is even less likely to contribute significantly to the internal Mo pool. Mo is most probably associated either with a preserved pool of nitrogenase or another storage form.

Crocosphaera experiments 2 and 3 measured Fe cellular concentrations are close to the 1:1 line. Again this supports the interpretation that much of the cellular Fe

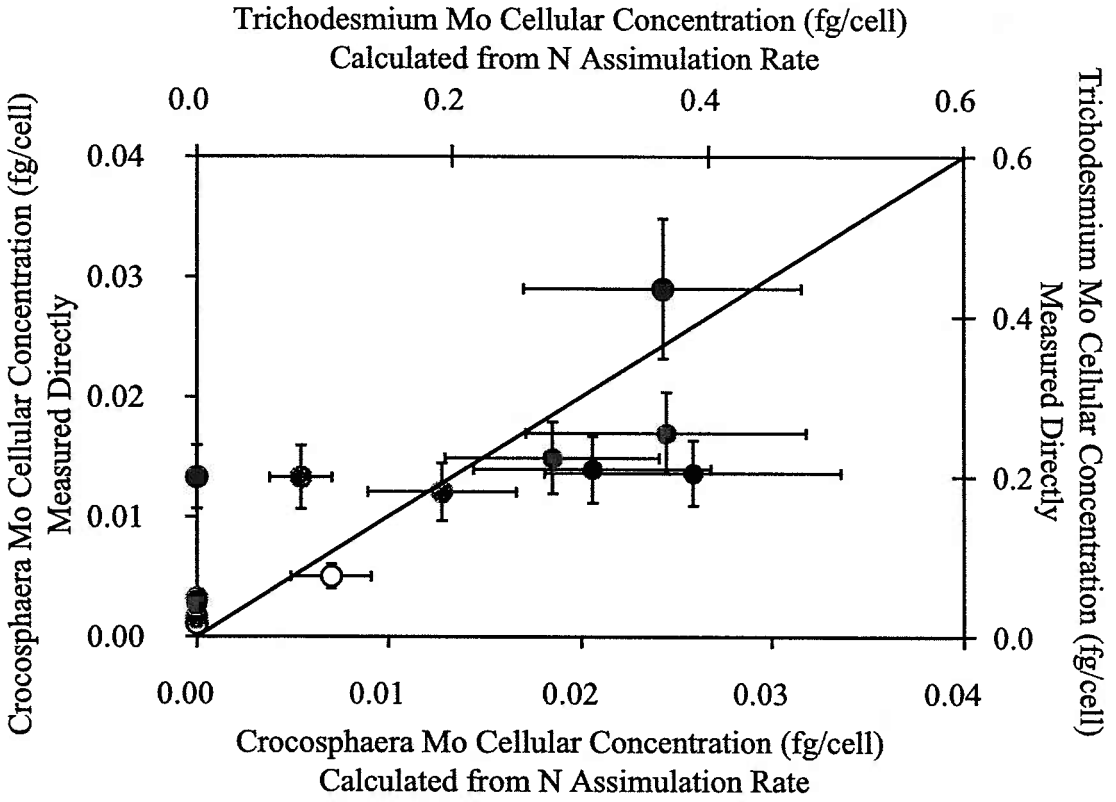

Figure 4.4 A comparison of measured Mo cellular concentrations for Crocosphaera experiments 2 (open circles), 3 (light grey circles) and 4 (dark grey circles) and Trichodesmium experiment 1 (black circles) with cellular concentrations predicted from N assimilation rate and Mo use efficiency of nitrogenase. Y-axis error bars are based on measurement error. X-axis error bars are based on the range of Mo use efficiencies calculated for nitrogenase isolated from Azotobacter vinelandii. Most samples fall within error of the 1:1 line implying that most of the Mo measured in the cells is present as nitrogenase. Crocosphaera cell samples collected during periods of no N2 fixation all approach detection limits for measured Mo concentrations, however Trichodesmium shows a significant Mo concentrations in non N2 fixing cells implying that these cells store Mo or utilize it in another enzyme system during the night period.

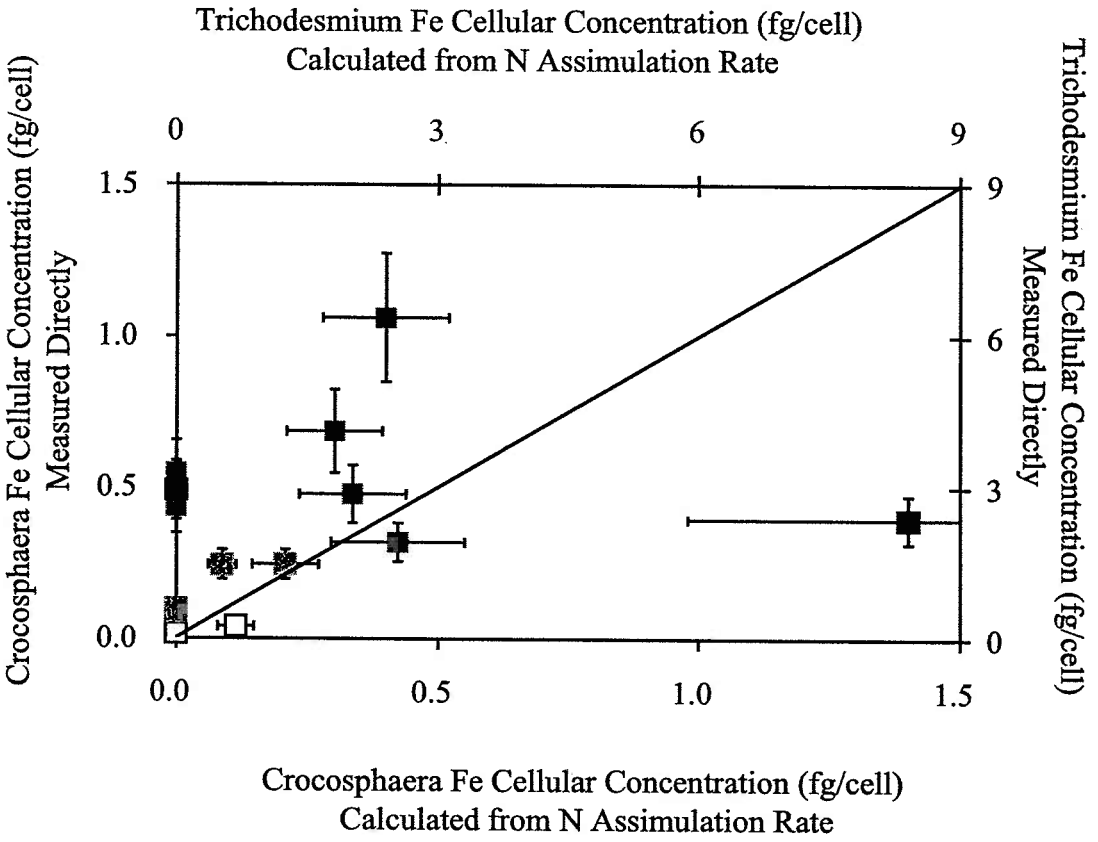

Figure 4.5 A comparison of measured Fe cellular concentrations for Crocosphaera experiments 2 (open squares), 3 (light grey squarea) and 4 (dark grey squares) and Trichodesmium experiment 1 (black sqares) with cellular concentrations predicted from N assimilation rate and Mo use efficiency of nitrogenase. Y-axis error bars are based on measurement error. X-axis error bars are based on the range of Fe use efficiencies calculated for nitrogenase isolated from Azotobacter vinelandii. Most samples fall within error of the 1:1 line implying that most of the Fe measured in the cells is present as nitrogenase. Crocosphaera cell samples collected during experiment 4 have excessmeasured Fe likely due to contamination of these samples. Trichodesmium has constant Fe cellular quotas which are lower than the Fe predicted from N assimilation rates. This suggests that the nitrogenase enzyme of Trichodesmium may be slightly more Fe efficient than Azotobacter vinelandii.

inventory in *Crocosphaera* is bound in active nitrogenase. However *Crocosphaera* experiment 4 shows enrichment for Fe that may be associated with Fe contaminations of the sample or extra cellular Fe. *Trichodesmium* in experiment 1 surprisingly have much lower Fe concentrations than predicted using metal use efficiencies based on *Azotobacter vinelandii*. This implies that nitrogenase enzyme of *Trichodesmium* may be more metal efficient. Confirmation of this finding, by isolation and measurement of Trichodesmium nitrogenase is crucial to our understanding of marine nitrogen fixation.

4.4.2 Crocosphaera

The strong diel cycling seen in both Fe and Mo that is correlated with N_2 fixation rate supports the theory that *Crocosphaera* synthesizes nitrogenase de novo each night. Whether nitrogenase degradation during the day is an intentional process recycling the component metals and proteins for use elsewhere in the cell or is an unintentional byproduct of the photosynthetic production of O_2, which inhibits nitrogenase, is unknown. Experiments 2 and 3 with reliable Fe data showed Fe cycling as well as Mo cycling. These cultures were Fe-replete and it is unknown whether this phenomena would occur at environmentally relevant Fe concentrations. The diel cycling supports theoretical estimates that the nitrogenase enzyme complex requires more Fe than the photosynthetic apparatus active during the day period. Fe:C ratios measured in photosynthesizing samples (4.2±0.3 μmol Fe mol^{-1} C) are similar to those estimated for photosynthesis with no Fe demand associated with N_2 fixation (4.8 μmol Fe mol^{-1} C).

Based on the average size (2 μm diameter) and spherical shape of *Crocosphaera*, and measured cellular metal concentrations we have estimated cellular metal

concentrations on a unit volume basis. The intracellular concentration of Mo is approximately 1.1 to 42 μM, always greater than 10 fold seawater concentrations (0.1 μM). The intracellular concentration of Fe is 19 to 1000 μM, enriched 5 orders of magnitude above seawater. However at reasonable cell abundances, 10^6 cells L^{-1} *Crocosphaera* requires only 0.12 pmol Mo L^{-1} and 2.4 pmol Fe L^{-1} compared to typical seawater concentrations of 107 nM Mo and 0.1 nM Fe. Thus these organisms are likely to account for a relatively small fraction of the total Fe and Mo inventory in seawater.

However, N_2 fixing organisms may account for a significant fraction of the particulate Mo budget. The metal concentrations of these cells assuming the dry weight is about 0.45% C average 2.4 ppm Mo when nitrogen fixing compared to 0.2 ppm Mo during photosynthesis. This is similar to the estimated Mo crustal abundance of 2 ppm (Taylor and McLennan 1985). The average dust flux and the particulate Al inventory in the upper 100m of the Sargasso Sea is small (6.7 nmol Al L^{-1}: (Jickells 1999)). This results in a Mo dust inventory of 0.045 pmol Mo L^{-1}, significantly smaller than the 0.12 pmol particulate Mo L^{-1} calculated above and suggests that Mo enrichment in suspended particulate matter may be a good indicator of N_2 fixation provided cellular requirements for other enzymes and contributions associated with Mn oxides are small.

4.4.3 Trichodesmium

A significant amount of data constraining the elemental composition of Trichodesmium is accumulating in the literature, particularly for C, N, and Fe (Table 4.6). Two recent articles reported C:N ratios in cultures of IMS101 of 5-11 (Mulholland and Capone, 2001) and 8-16 (Berman-Frank et al., 2001) The Berman-Frank et al.(2001)

paper represented cultures grown under a range of Fe concentrations, but saw no correlation of C:N:P ratio with Fe availability or quota. The Mulholland and Capone (2001) paper measured C:N over the life of a culture. They witnessed the lowest C:N ratios during log phase growth and the higher ratios during lag, stationary stages. This suggests that lower C:N ratios maybe a good indication of the health of a culture. Field measurements of C:N ratios in Trichodesmium from the North Atlantic and North Pacific are generally low, ranging from 4.7 to 7.3 (Berman-Frank et al. 2001a; Karl and Tien 1992; Kustka et al. 2002; Letelier and Karl 1998; Lewis et al. 1988; Mague et al. 1977; Mccarthy and Carpenter 1979). Both the culture work and field data presented in this study fell on the low end of the C:N spectrum. Our cell count based doubling times are faster than most reported in the literature (Mulholland and Capone 2000b).

The Fe:C ratios for our both field and culture data sets are at the lower end of the range of reported values and are most similar to the values for N. Atlantic colonies reported by Kutska et al. (2001) (Table 4.7). This study does not evaluate the possibility of extracellular Fe, but the lowest Fe:C ratios in the combined field and culture data set (Table 4.6) are in agreement with estimates of enzyme requirements, suggesting that any extracellular Fe contribution must be small. The Fe:Mo ratios of the cultures were within error of the Fe:Mo ratio of the nitrogenase complex. However, the Fe:Mo ratios of the field samples were much lower (Table 4.6). This was driven by an increase in the Mo content of field populations.

There are two possible explanations for the increased Mo concentration in the field samples, either natural populations of *Trichodesmium* have additional enzymatic

uses for Mo or natural populations of *Trichodesmium* are indulging in luxury consumption of Mo. Nitrate reductase is currently the only other Mo enzyme identified in *Trichodesmium*. *Trichodesmium* has been shown to regulate the relative amounts of nitrogenase and nitrate reductase in the cells based on the amount of fixed nitrate in the growth media at the beginning of the day period (Mulholland et al. 2001). The levels of nitrate in the surface waters from which these cells were collected are unknown. As discussed above, the problem with this argument is that the specific activity of nitrate reductase is much higher than nitrogenase, thus growth on nitrate likely requires less Mo than growth on N_2 (Raven 1988; Sanudo-Wilhelmy et al. 2001). If the increased Mo concentration in the field samples is due to an enzymatic demand the enzyme is unknown.

Alternatively, *Trichodesmium* could be reacting to some form of nutrient stress by taking up more Mo than necessary of growth. The culture, unlike oligotrophic surface waters, is a nutrient rich environment with plenty of Fe and P. Fe stress is unlikely for these field samples, Fe:C quotas, which have been shown to be a good indicator of Fe stress (Berman-Frank et al. 2001), do not differ significantly from the Fe-replete cultures. Phosphate limitation has been hypothesized for the North Atlantic (Sanudo-Wllhelmy et al. 2001; Wu et al. 2000) and may be more important. Phosphate and molybdate are both oxyanions though of slightly different size, but if all phosphate channels are wide open some Mo may be taken up as well. In either case these results, unlike *Crocosphaera*, do not support the use of particulate Mo concentration to estimate the rate of nitrogen fixation.

Molybdate is most similar to sulfate anion and sulfate channels have been shown to allow Mo uptake in *Azotobacter vinelandii* and other heterotrophic soil bacteria. In the marine system, where sulfate concentrations are up to 28 mM, sulfate has been proposed to limit Mo uptake and thus nitrogen fixation. However, N_2 fixation of marine diazoatrophs appear unaffected by competition with sulfate (Paulsen et al. 1991). These data do not support the sulfate limitation of Mo uptake hypothesis(Cole et al. 1986; Howarth et al. 1988). Trichodesmium appears to take up 100 fold more Mo than it requires for N_2 fixation. And the diel up take and release of Mo seen in both Crocosphaera and Trichodesmium cultures does not suggest that Mo is hard for them to acquire. Evidence from the recently sequenced *Trichodesmium* genome (DOE-JGI) indicates a homologue of the modEABC molybdenum transport system identified in *Azotobacter vinelandii* and *E.coli*. This suggests that *Trichodesmium* has a highly selective way to take up molybdenum, unlikely to be significantly inhibited by sulfate.

4.5. Conclusions

Both of *Crocosphaera* and *Trichodesmium* use Mo and Fe with remarkable efficiency. Estimates of metal cell quotas based on theoretical metal use efficiency agree with measured cellular concentrations, implying that nitrogenase utilizes a significant fraction of both Fe and Mo cellular pools. *Crocosphaera* shows significant cycling of Mo and Fe in response to N_2 fixation. This suggests that the nitrogenase complex in *Crocosphaera* is synthesized de novo each night and broken down each day with no attempt to conserve cellular pools of Fe or Mo. In contrast, *Trichodesmium* maintains a likely internal pool of Mo during non N_2 fixing periods and does not release Fe from the

cells. The differences in strategies employed by these organisms to manage cellular inventories of metals is likely due to their contrasting N_2 fixation strategies.

Crocosphaera culture data suggests that Mo enrichment of particulates may provide a tracer of N_2 fixation, but the large differences in Mo:C ratios of cultured and collected of Trichodesmium implies that other factors may significantly alter Mo cellular concentrations in natural populations. These issues will need to be understood before Mo enrichment can be used to estimate N_2 fixation.

4.6. References

Anderson, G.L., and J.B. Howard. 1984. Reactions with the Oxidized Iron Protein of Azobacter- Vinelandii Nitrogenase – Formation of a 2fe Center. Biochemistry **23**: 2118-2122.

Berman-Frank, I., J. T. Cullen, Y. Shaked, R. M. Sherrell, and P. G. Falkowski. 2001a. Iron availability, cellular iron quotas, and nitrogen fixation in Trichodesmium. Limnology and Oceanography **46:** 1249-1260.

Berman-Frank, I. and others 2001b. Segregation of nitrogen fixation and oxygenic photosynthesis in the marine Cyanobacterium trichodesmium. Science **294:** 1534-1537.

Burns. 1979. The nitrogenase system from azotobacter activation energy and divalent cation requirement. Biochimica Et Biophysica Acta **171:** 253-259.

Campbell, L., H. Lui, H. A. Noalla, and D. Vault. 1997. Annual variability of phytoplankton and bacteria in the subtropical North Pacific Ocean at station Aloha during the 1991-1994 ENSO event. Deep Sea Research Part I: Oceanographic Research Papers **44:** 167-192.

Capone, D. G. 1993. Determination of nitrogenase activity in aquatic samples using the acetylene reduction procedure, p. 621-631. *In* P. F. Kemp, B. F. Sherr, E. B. Sherr and J. J. Cole [eds.], Hanbook of methods in aquatic microbial ecology. Lewis Publishers.

---. 2001. Marine nitrogen fixation: what's the fuss? Current Opinion in Microbiology **4:** 341-348.

Capone, D. G., and J. P. Montoya. 2001. Nitrogen fixation and denitrification, p. 501-515, Methods in Microbiology, Vol 30. Methods in Microbiology. ACADEMIC PRESS INC.

Capone, D. G., J. P. Zehr, H. W. Paerl, B. Bergman, and E. J. Carpenter. 1997. Trichodesmium, a globally significant marine cyanobacterium. Science **276:** 1221-1229.

Carpenter, E. J., D. G. Capone, and J. G. Rueter. 1992. Marine pelagic cyanobacteria: Trichodesmium and other diazotrophs. Marine pelagic cyanobacteria: Trichodesmium and other diazotrophs, Published by Kluwer; NATO Advanced Science Institutes Series C: Mathematical & Physical Sciences, 362, ISBN 0792316142.

Cole, J. J., R. W. Howarth, S. S. Nolan, and R. Marino. 1986. Sulfate Inhibition of Molybdate Assimilation by Planktonic Algae and Bacteria - Some Implications for the Aquatic Nitrogen-Cycle. Biogeochemistry **2:** 179-196.

Collier, R. W. 1985. Molybdenum in the Northeast Pacific-Ocean. Limnology and Oceanography **30:** 1351-1354.

Cullen, J. T., and R. M. Sherrell. 1999. Techniques for determination of trace metals in small samples of size-fractionated particulate matter: phytoplankton metals off central California. Marine Chemistry **67:** 233-247.

Dugdale, R. C., D. W. Menzel, and J. H. Ryther. 1961. Nitrogen Fixation in the Sargasso Sea. Deep Sea Research Part II: Topical Studies in Oceanography **7:** 297-300.

Eady, R. R., and B. E. Smith. 1979. Physico-chemical properties of nitrogenase and its components, p. 399-490. *In* R. W. E. Hardy, F. Bottomley and R. C. Burns [eds.], A treatise on dinitrogen fixation. Wiley-Interscience.

Falkowski, P. G., R. T. Barber, and V. Smetacek. 1998. Biogeochemical controls and feedbacks on ocean primary production. Science **281:** 200-206.

Hood, R. R., A. Subramaniam, L. R. May, E. J. Carpenter, and D. G. Capone. 2002. Remote estimation of nitrogen fixation by Trichodesmium. Deep-Sea Research Part Ii-Topical Studies in Oceanography **49:** 123-147.

Howarth, R. W., R. Marino, and J. J. Cole. 1988. Nitrogen-Fixation in Fresh-Water, Estuarine, and Marine Ecosystems .2. Biogeochemical Controls. Limnology and Oceanography **33:** 688-701.

Jickells, T. D. 1999. The inputs of dust serived elements to the Sargasso Sea; a synthesis. Marine Chemistry **68:** 5-14.

Karl, D., R. Letelier, L. Tupas, J. Dore, J. Christian, and D. Hebel. 1997. The role of nitrogen fixation in biogeochemical cycling in the subtropical North Pacific Ocean. Nature **388:** 533-538.

Karl, D. M., and G. Tien. 1992. Magic - a Sensitive and Precise Method for Measuring Dissolved Phosphorus in Aquatic Environments. Limnology and Oceanography **37:** 105-116.

Keller, M. D., W. K. Bellows, and R. R. L. Guillard. 1988. Microwave Treatment for Sterilization of Phytoplankton Culture Media. Journal of Experimental Marine Biology and Ecology **117:** 279-283.

Kujawinski, E. B. 2000. The effect of protozoan grazers on the cycling of polychlorinated biphenyls (PCBs) in marine systems, Marine Chemistry and Geochemistry. MIT/Woods Hole Oceanographic Joint Program in Oceanography.

Kustka, A., E. J. Carpenter, and S. A. Sanudo-Wilhelmy. 2002. Iron and marine nitrogen fixation: progress and future directions. Research in Microbiology **153:** 255-262.

Letelier, R. M., and D. M. Karl. 1996. Role of Trichodesmium spp. in the productivity of the subtropical North Pacific Ocean. Marine Ecology Progress Series **133:** 263-273.

---. 1998. Trichodesmium spp. physiology and nutrient fluxes in the North Pacific subtropical gyre. Aquatic Microbial Ecology **15:** 265-276.

Lewis, M. R., O. Ulloa, and T. Platt. 1988. Photosynthetic Action, Absorption, and Quantum Yield Spectra for a Natural-Population of Oscillatoria in the North-Atlantic. Limnology and Oceanography **33:** 92-98.

Mague, T. H., F. C. Mague, and O. Holmhansen. 1977. Physiology and Chemical Composition of Nitrogen-Fixing Phytoplankton in Central North Pacific Ocean. Marine Biology **41:** 213-227.

McCarthy, J. J., and E. J. Carpenter. 1979. Oscillatoria (Trichodesmium) Thiebautii (Cyanophyta) in the Central North-Atlantic Ocean. Journal of Phycology **15:** 75-82.

Mulholland, M. R., and D. G. Capone. 2000a. The nitrogen physiology of the marine N2-fixing cyanobacteria Trichodesmium spp. Trends in Plant Science **5:** 148-153.

---. 2000b. The nitrogen physiology of the marine N-2-fixing cyanobacteria Trichodesmium spp. Trends in Plant Science **5:** 148-153.

---. 2001. Stoichiometry of nitrogen and carbon utilization in cultured populations of Trichodesmium IMS101: Implications for growth. Limnology and Oceanography **46:** 436-443.

Mulholland, M. R., K. Ohki, and D. G. Capone. 2001. Nutrient controls on nitrogen uptake and metabolism by natural populations and cultures of Trichodesmium (Cyanobacteria). Journal of Phycology **37:** 1001-1009.

Neveux, J., F. Lantoine, and D. Vaulot. 1999. Phycoerythrins in the southern tropical and equatorial Pacific Ocean: evidence for new cyanobacterial types. Journal of Geophysical Research, B, Solid Earth and Planets **104:** 3311-3321.

Paerl, H. W., L. E. Prufertbebout, and C. Z. Guo. 1994. Iron-Stimulated N-2 Fixation and Growth in Natural and Cultured Populations of the Planktonic Marine Cyanobacteria Trichodesmium Spp. Applied and Environmental Microbiology **60:** 1044-1047.

Paulsen, D. M., H. W. Paerl, and P. E. Bishop. 1991. Evidence That Molybdenum-Dependent Nitrogen-Fixation Is Not Limited by High Sulfate Concentrations in Marine Environments. Limnology and Oceanography **36:** 1325-1334.

Raven, J. A. 1988. The Iron and Molybdenum Use Efficiencies of Plant-Growth with Different Energy, Carbon and Nitrogen-Sources. New Phytologist **109:** 279-287.

Rippka, R., R. W. Castenholz, J. B. Waterbury, and M. Herdman. 2001. Form-genus V. Cyanothece, p. 501. *In* G. M. Garrity [ed.], Bergy's manuel of systematic bacteriology. Springer.

Rueter, J. G., D. A. Hutchins, R. W. Smith, and N. L. Unsworth. 1992. Iron nutrition of Trichodesmium., p. 289-306. *In* E. J. Carpenter, D. G. Capone and J. G. Rueter [eds.], Marine Pelagic Cyanobacteria: Trichodesmium and Other Diazotrophs. Kluwer Academic Publishers.

Sanudo-Wilhelmy, S. A. and others 2001. Phosphorus limitation of nitrogen fixation by Trichodesmium in the central Atlantic Ocean. Nature **411:** 66-69.

Sanudo-Wllhelmy, S. A. and others 2001. Phosphorus limitation of nitrogen fixation by Trichodesmium in the central Atlantic Ocean. Nature **411:** 66-69.

Sprent, J. I., and J. A. Raven. 1985. Evolution of Nitrogen-Fixing Symbioses. Proceedings of the Royal Society of Edinburgh Section B- Biological Sciences **85:** 215-237.

Subramaniam, A., C. W. Brown, R. R. Hood, E. J. Carpenter, and D. G. Capone. 2002. Detecting Trichodesmium blooms in SeaWiFS imagery. Deep-Sea Research Part Ii-Topical Studies in Oceanography **49:** 107-121.

Sunda, W. G., and S. A. Huntsman. 1995. Iron Uptake and Growth Limitation in Oceanic and Coastal Phytoplankton. Marine Chemistry **50:** 189-206.

Tuit, C. B. 2002. The Marine Biogeochemistry of Molybdenum, Marine Geology and Geophysics. MIT/Woods Hole Oceanographic Joint Program in Oceanography.

Wasmund, N., M. Voss, and K. Lochte. 2001. Evidence of nitrogen fixation by non-heterocystous cyanobacteria in the Baltic Sea and a re-calculation of a budget of nitrogen fixation. Marine Ecological Progress Serial **214:** 1-14.

Waterbury, J. B., and R. Rippka. 1989. Subsection I. Order *Chroococcaloes*, p. 1728-1746. *In* J. T. Stanley [ed.], Bergy's manuel of systematic bacteriology. Williams and Wilkins.

Waterbury, J. B., S. W. Watson, F. W. Valois, and D. G. Franks. 1986. Biological and Ecological Characterization of the Marine Unicellular Cyanobacterium *Synechococcus*, p. 71-120. *In* T. Platt and W. K. W. Li [eds.], Photosynthetic Picoplankton. Dept. of Fisheries and Oceans.

Waterbury, J. B., and J. M. Willey. 1988. Isolation and Growth of Marine Planktonic Cyanobacteria. Methods in Enzymology **167:** 100-105.

Wu, J. F., W. Sunda, E. A. Boyle, and D. M. Karl. 2000. Phosphate depletion in the western North Atlantic Ocean. Science **289:** 759-762.

Zehr, J. P., E. J. Carpenter, and T. A. Villareal. 2000. New perspectives on nitrogen-fixing microorganisms in tropical and subtropical oceans. Trends in Microbiology **8:** 68-73.

Zehr, J. P. and others 2001. Unicellular cyanobacteria fix N-2 in the subtropical North Pacific Ocean. Nature **412:** 635-638.

CHAPTER 5. MOLYBDENUM CONCENTRATION IN SUSPENDED PARTICULATE MATTER

Abstract

The data presented here represent some of the first measurements of Mo in suspended particulate matter. Particulate Mo concentrations, corrected for sea salt and terrestrial contributions, ranged between 0.65 and 51 pmol L^{-1}. Mo:C ratios ranged from 0.14 to 55 μmol:mol. Results implied that increased Mo:C ratios of particulate matter are indicators of microbial processes catalyzed by Mo-containing enzymes. Regions of N_2 fixation and denitrification, processes catalyzed by Mo-containing enzymes, have elevated particulate Mo concentrations. Measured particulate Mo concentrations from the surface Sargasso Sea far exceed the Mo required to produce measured N_2 fixation rates by up to 3 orders of magnitude, implying that there may be additional Mo demands in this region not associated with active N_2 fixation. Denitrification rates estimated from particulate Mo from the Pacific oxygen minimum zone are 2 orders of magnitude higher than in situ nitrate reduction measurements, implying enzymatic demand does not control particulate Mo concentrations. Particulate Mo concentrations do not correlate with particulate Mn, suggesting that water column Mn oxides do not scavenge Mo. Additional Mo-containing enzymes or particulate phases must be invoked to explain the particulate distribution of Mo.

5.1 Introduction

Molybdenum is an important micronutrient in phytoplankton and bacteria yet little is known about its concentration in marine phytoplankton or suspended particulate matter (SPM). Mo is closely linked to the nitrogen cycle via its role in nitrogenase, assimilatory nitrate reductase, and respiratory nitrate reductase enzymes. In addition, the DMSO dehydrogenase enzyme may be an important use of Mo in the marine system (Stiefel 1993). Measurements of particulate Mo in the existing literature are based on outdated analytical methods and are close to detection limits (Martin and Knauer 1973). The extremely high concentration of Mo in seawater (107 nM) is a significant challenge when trying to evaluate relatively small particulate concentrations.

Very few analyses of Mo in SPM or phytoplankton are available. The concentration of Mo in average phytoplankton had been estimated at 2ppm or approximately 0.11 μmol Mo:mol C(Martin and Knauer 1973), which is similar to the concentration of Mo in upper continental crust (Taylor and Mclennan 1985), A measurement of Mo in marine SPM from the Bay of Bengal gives a concentration of 5.5 ppm or 2.48 μmol Mo:mol C, assuming that C is approximately 45% of the dry weight (Babu et al. 1984).

Recent unpublished measurements of Mo:C ratios in cultures of individual diatoms and cyanobacteria have yielded some interesting results (Table 5.1). The highest measured Mo:C ratios are in N_2 fixing cyanobacteria grown without a source of fixed N. *Crocosphaera*, a single celled N_2 fixing cyanobacterium, shows a tight correlation with N_2 fixation activity and a 3-8 fold increase in Mo cellular concentration when N_2 fixing (Tuit 2003, Chapter 4). Under these conditions organisms are forced to synthesize the nitrogenase enzyme, which, though it has a similar Mo:enzyme molar ratio to the nitrate reductase enzyme, has a much lower specific activity. Thus more enzyme is required to support the N demand. N_2 fixing cyanobacteria species grown on nitrate and thus expressing the assimilatory nitrate reductase enzyme, have extremely low Mo:C ratios. Mo:C ratios of diatoms grown on nitrate have much higher Mo:C ratios than seen in cyanobacterium grown under similar conditions, which may be due to additional Mo-containing enzymes such as DMSO dehydrogenase. This culture work implies that in marine organisms Mo cellular concentration is coupled to Mo enzyme use. These data

suggest that Mo:C ratios in suspended particulate matter may be influenced by use of Mo-containing enzymes.

Table 5.1. Metal Carbon ratios of Phytoplankton.

	N source	Mo (ppm)[b]	Mo:C (µmol:mol)	Fe (ppm)[b]	Fe:C (µmol:mol)
Diatoms					
Ditylum brightwelli[a]	NO_3^-	1.29	0.36	17.8	8.53
Thalassiosira excentrica[a]	NO_3^-	0.93	0.26	182	87.1
Thalassiosira weissflogii[a]	NO_3^-	0.83	0.23	40.7	19.4
Nitzschia brevirostris[a]	NO_3^-	1.23	0.34	157	75
Cyanobacteria					
Anabena spp. [a]	NO_3^-	0.12	0.033	4.1	1.96
Cyanothece spp. [a]	NO_3^-	0.039	0.011	2.91	1.39
Trichodesmium spp. field samples[c,d]	N_2	80.8	22.5 ± 15.1	138	66.1±39.0
Trichodesmium spp. culture samples[c]	N_2	9.2	2.56 ± 2.02	182	87.11±64.62
Crocosphaera watsonii (Night) [c,f]	N_2	2.5	0.70 ± 0.27	197	15.75±11.34
Crocosphaera watsonii (Day) [c]	N_2	0.28	0.08 ± 0.04	10.4	4.23±3.1
Denitrifying bacteria					
Marinobacter spp. growing on O_2	NH_4^+	0.04	0.01 ± 0.002	142	68±20
Marinobacter spp. growing on NO_3^-	NH_4^+	1.72	0.48 ±0.11	56.5	27±10

[a] Quigg et al. (pers. com.).
[b]Mo and Fe concentrations in ppm were estimated from the metal carbon ratio by assuming C accounts for 45% of the dry weight of the organisms.
[c]Tuit (2003). ± is equivalent to ± 1 standard deviation..
[d]Trichodesmium colonies were collected from the Sargasso Sea in May, 2000.
[f]Crocosphaera spp. fixes nitrogen only at night and shows a large diel variation in Mo concentrations.

Respiratory nitrate reductase, which catalyzes the first step in the denitrification pathway, is also a Mo-containing enzyme. It supports bacterial growth using nitrate as an electron sink instead of oxygen. Facultative denitrifying bacteria, which can grow on either oxygen or nitrate, show increased Mo:C ratios when using nitrate instead of oxygen. The Mo:C ratio of *Marinobacter hydrocarbanoclaticus* (formerly *Pseudomonas nautica* (Sproer et al. 1998)) increases from 0.01 to 0.48 µmol:mol (Tuit 2003, Appendix

1). These experiments suggest that particulate Mo:C ratios will be enriched in regions where denitrification is important, such as stratified basins and the oxygen minimum zones of the Pacific and Arabian Sea.

Results from the nitrate reduction and N_2 fixation culture experiments indicate that Mo:C is linked to Mo enzyme use. Mo in the molybdate form, likely the most common form in seawater, is not particle reactive. Thus it is reasonable to assume that much of the Mo in suspended particulate matter will be associated with biogenic demands. These data lend themselves to the hypothesis that elevated Mo:C ratios in suspended particulate matter could be used as a tracer of Mo enzyme activity. The goal of this chapter is to determine whether suspended particulate matter in regions of denitrification and N_2 fixation have elevated Mo:C ratios relative to terrestrial or bulk phytoplankton and whether these enrichments can be used to estimate N_2 fixation or denitrification rates.

Mo cycling with authigenic Mn oxides is another possible mechanism for enriching Mo in suspended particulate matter, which could obscure the Mo enzymatic signal. Mo has been shown to be enriched in Mn oxides from stratified basins (Berrang and Grill 1974), sediments and sediment pore waters (Shaw et al. 1990; Shimmfield and Price 1986), and in Mn crusts and nodules (Manheim 1974; Shimmfield and Price 1986). Many marine Mn oxides have a Mo:Mn molar ratio of 1.1×10^{-3} (Manhiem, 1974; Shimmfield and Price, 1986.). This corresponds to an effective concentration of roughly 1000 ppm Mo in pure MnO_2. These studies imply that Mn oxides could substantially influence the distribution of particulate Mo. Sediment trap data from the California

Borderland Basins (Zheng et al. 2000)suggest that Mo cycling with Mn in coastal sinking particles may be significant. However a similar study from the Western Mexican Margin (Nameroff et al. 2002) did not find a correlation of Mn and Mo within the OMZ.

The mechanism of Mo incorporation into Mn oxides is unknown, but may differ with different mechanisms of Mn oxidation. The mechanisms that drive the Mn cycle in the upper portion of the open ocean (i.e. photo-reduction: (Johnson et al. 1996), and microbially mediated oxidation: (Moffett and Ho 1996)), differ dramatically from autocatalytic Mn oxidation (Hem 1978) which causes a substantial amount of Mn oxidation in sediments. Thus the large Mo/Mn ratios cited above may not be representative of microbially produced open ocean Mn oxides. There is to date no data on the concentration of Mo in microbially produced Mn oxides. The Zheng (2000) sediment trap study that indicated a Mo:Mn relationship did not address whether the Mn oxides were microbially produced authigenic particles or resuspended sediments. It remains to be established how Mn cycling influences the water column distribution of particulate Mo.

In order to determine whether or not there is significant Mo enrichment in suspended particulate matter related to Mo enzyme use, the potential role of Mo scavenging by Mn oxides must be evaluated. To accomplish both these goals, I collected SPM from surface waters of the Sargasso Sea and a profile of the upper water column and the Bermuda Atlantis Time Series Site (BATS), a region of strong nitrogen fixation. Study sites from the California Borderland Basin region and a Pacific site at 9 50 N 104 18 W allow the evaluation of both Mo association with denitrification

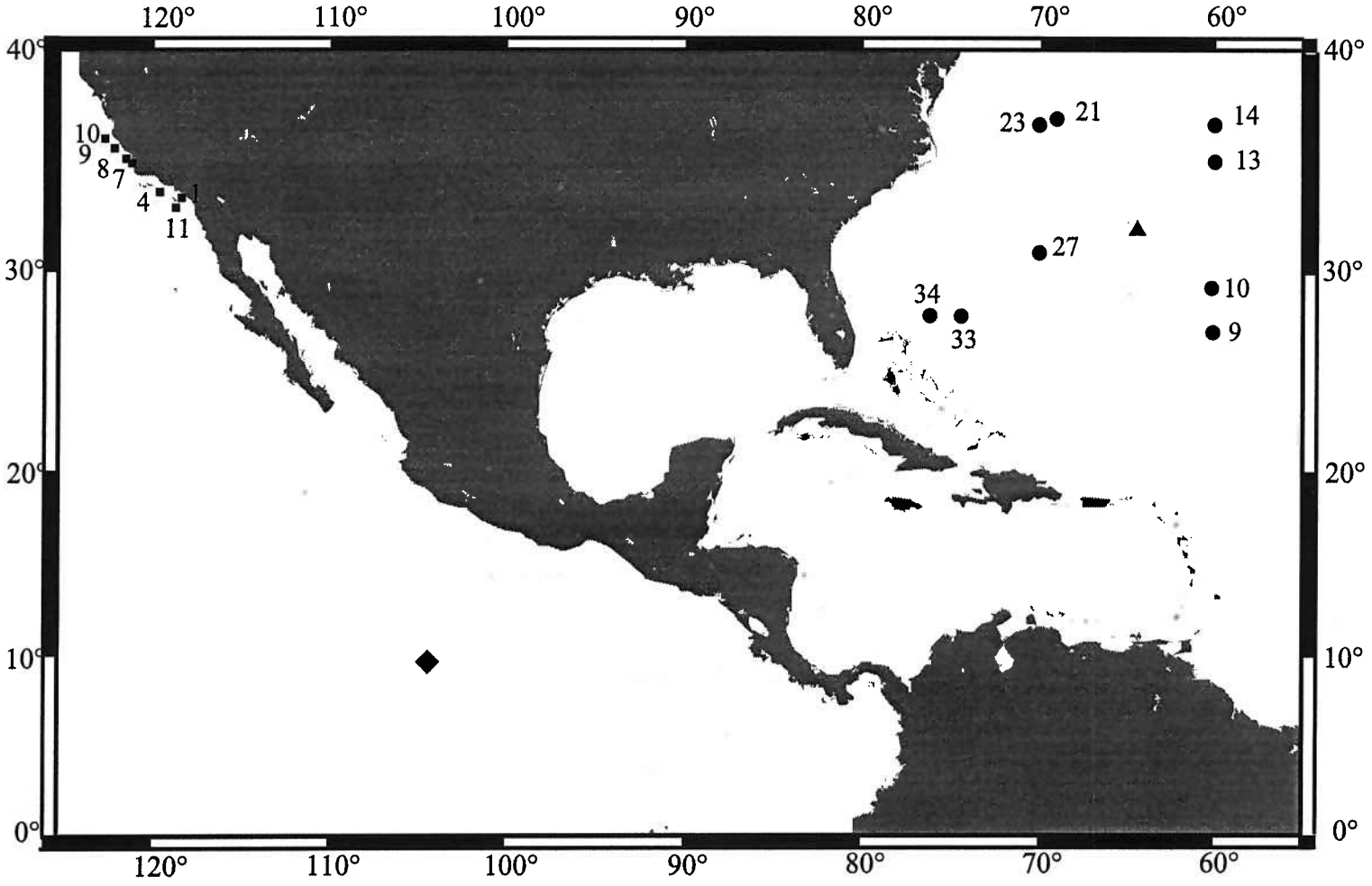

Figure 5.1 Station Location map for SPM samples listed in Table 5.2 including the California Borderland Basin (squares), the 9°N Pacific profile (diamond), the BATS profile (triangle) and the Sargasso Sea Surface Samples (circles)

in oxygen depleted water as well as the association of Mo with authigenic Mn oxides in oxygen depleted waters. These study sites are described in depth below (Figure 5.1).

5.2 Methods

5.2.1. Study sites

BATS. A three depth SPM profile was collected in September 1999 (R/V Weatherbird) from the BATS (32 10N 64 30W) station (Figure 5.1). This station had a 100 m mixed layer and nutricline (Figure 5.2). The presence of Trichodesmium colonies in the surface waters indicates that there was active N_2 fixation at this site during sample collection. Particulate samples were collected at 10, 120 and 250 m for metal analysis. Particulate samples were collected at 10, 120 and 300 m for CHN analysis. The 250 and 300 m metal and organic samples were both well below the mixed layer and fluorescence maximum therefore they were assumed to be equivalent for the purpose of calculating metal carbon ratios.

Sargasso Sea Surface waters. A survey of Sargasso Sea surface water particulate metal concentrations was completed in May 2001 (R/V Seward Johnson) (Figure 5.1,Table 5.2). Samples were collected from depths between 35 and 15 m, well within the mixed layer for each station. The nitrate concentration within the surface waters was below detection for all of the stations (Montoya pers com.). Trichodesmium colonies were present at most stations but were much more abundant at stations south of 28° N with sea surface temperature above 23° C.

Table 5.2. Filter Blank Corrected Trace Metal Analyses.[a,b]

Location	sta	LAT	LON	Depth m	Volume L	Wire Config.[c]	Mo pmol L^{-1}	Rb pmol L^{-1}	Cu pmol L^{-1}	Mn pmol L^{-1}	Fe nmol L^{-1}	Al nmol L^{-1}	POC M	PON M	C:N
CBB	1	33 46N	118 45W	45	17.0	c	57.76	75.94	nd	bd	3.15	2.88	2.95	0.44	6.65
		33 46N	118 45W	860	54.9	c	6.36	nd	nd	nd	24.94	nd	0.64	0.08	8.50
	4	33 59N	119 45W	40	10.6	c	37.26	94.39	nd	bd	bd	bd	3.68	0.50	7.29
		33 59N	119 45W	650	555.3	c	0.84	5.13	nd	69.80	2.02	7.70	0.31	0.03	8.94
	7	35 18N	121 01W	20	11.0	c	25.96	121.62	nd	bd	bd	bd	34.42	4.79	7.19
	8	35 26N	121 26W	650	103.7	c	9.23	230.58	nd	bd	0.16	bd			
	9	35 34N	122 03W	100	25.7	c	2.04	6.45	nd	144.31	1.47	3.51			
	10	36 06N	122 35W	45	50.7	a	2.55	11.50	nd	bd	0.24	bd	2.60	0.33	7.76
		36 06N	122 35W	100	301.3	a	2.54	5.44	nd	264.14	0.40	0.96	0.71	0.09	7.57
		36 06N	122 35W	45	119.2	a	0.62	3.07	nd	bd	bd	bd	2.66	0.38	7.10
	11	33 01N	119 02W	45	233.2	c	0.79	nd	nd	nd	bd	nd	2.56	0.38	6.76
Pacific		9 50N	104 18W	10	23.8	a	14.25	52.01	24.32	bd	0.22	bd	5.29	0.81	6.57
		9 50N	104 18W	28	18.5	a	21.74	62.43	73.41	bd	4.23	bd	5.56	0.86	6.43
		9 50N	104 18W	55	87.1	a	8.29	14.69	27.01	bd	0.22	bd	1.77	0.29	6.11
		9 50N	104 18W	105	349.0	a	2.05	4.20	14.33	80.64	0.25	0.47	0.52	0.08	6.90
		9 50N	104 18W	160	474.7	a	2.79	3.21	19.96	137.08	0.39	0.42	0.44	0.05	8.50
		9 50N	104 18W	200	603.0	a	2.35	2.99	17.39	134.54	0.52	1.09	0.49	0.07	7.49
		9 50N	104 18W	290	261.9	a	7.40	14.11	60.24	22.12	1.40	5.30	0.87	0.11	7.88
		9 50N	104 18W	450	430.8	a	3.85	12.90	37.33	32.89	1.87	12.00	0.92	0.13	6.88
Sargasso	9	29 30N	60 00W	30	100.7	a	4.99	nd	nd	nd.	0.53	nd	1.12	0.13	7.98
	10	24 20N	62 00W	15	45.4	a	5.25	nd	nd	nd.	bd	nd	7.00	1.73	8.72
	13	34 45N	60 00W	15	17.0	a	12.77	157.66	nd	bd	bd	6.127			
	14	36 30N	60 00W	15	63.2	a	11.32	34.16	nd	26.66	0.44	0.196	2.77	0.34	8.25
	21	36 00N	69 00W	15	47.0	a	55.40	50.10	nd	bd	0.74	9.045	1.74	0.18	9.59
	23	36 30N	70 00W	15	71.2	a	16.68	27.07	nd	bd	0.46	2.454	1.83	0.23	7.93
	27	30 29N	70 00W	20	71.5	a	3.02	24.33	nd	bd	0.19	0.885	0.08	0.01	6.78
	33	28 30N	75 00W	20	9.5	a	52.41	477.54	nd	bd	bd	15.992	0.49	0.06	8.36
		28 30N	75 00W	20	95.8	a	8.80	13.69	nd	bd	0.43	2.796	0.49	0.06	8.36
	34	28 30N	76 30W	15	136.3	a	1.03	13.55	nd	bd	bd	2.440	1.12	0.13	
BATS		32 10N	64 30W	10	56.7	a	66.33	438.52	nd	55.35	11.10	25.03	1.79	0.15	11.56
		32 10N	64 30W	120	277.8	a	31.26	106.73	nd	1493.88	2.52	2.50	0.70	0.11	6.15
		32 10N	64 30W	250	531.6	a	24.02	103.03	nd	4221.26	7.78	7.528	0.26	0.04	7.00

[a] Below detection (bd) indicates samples whose measured concentrations were less than the filter blank.[b] Not determined (nd) indicates occasions when one or more elements were not measured for a sample. [c]Wire configurations for pump deployment shown in Figure 5.3.

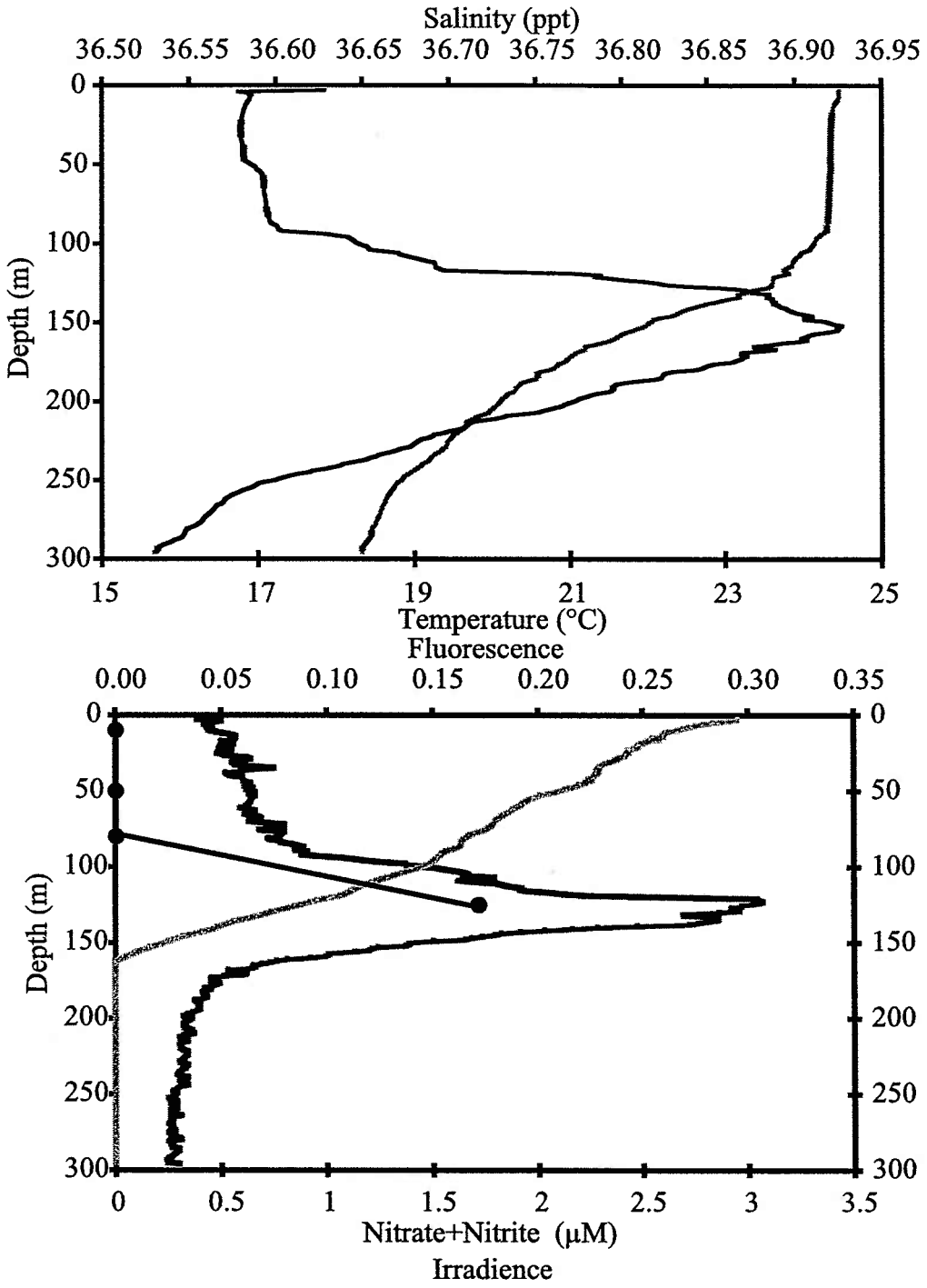

Figure 5.2 Profilesof salinity (black line), Temperature (medium gray line) Irradiance (light gray line) Fluorescence (dark gray line) and Nitrate+nitrite (black circles) from the BATS site (32 10N 64 30W).

California Borderland Basins. SPM metal and organic samples were collected from the California Borderlands Basins in July 2001 (R/V Pt. Sur). This region contains a series of stratified costal basins. Samples were collected from within San Pedro Basin (station 1) Tanner Basin (station 4) and San Nicholas Basin (station 11) as well as at a series of stations along the coast (stations 7-10). See Figure 5.1 and Table 5.2 for sample locations. Samples were collected from the fluorescence maximum (45 m) as indicative of the bulk particulate matter, below the fluorescence maximum (100m) to evaluate settling particles and from the core of the oxygen minimum zone (650 m) as a region of probable denitrification.

Eastern Tropical Pacific. A profile of SPM samples from the upper 450 m was collected from a station at the 9 50 N 104 18 W (Figure 5.1). This station had a shallow (28 m) mixed layer. The profile of relative oxygen (Figure 5.3) indicated that the upper water column was highly stratified. There was a shallow OMZ from 55 to 75 m, low and variable oxygen concentration between 75 and 280 m and a deep OMZ below 290m. The main fluorescence peak occurred at the base of the mixed layer, but on several of the casts there was also a secondary fluorescence peak within the shallow OMZ. When this was present, bacterial pigments indicated that the predominant organism in the lower florescence maximum was mostly likely a Prochlorococus species (Plumely pers com.). Nitrite showed two peaks (Figure 5.3). The shallow nitrite peak was at the base of the mixed layer. Like the fluorescence signal, this shallow peak was often split into two with a small peak in the shallow OMZ. The deep nitrite maximum was at 290 meters at the top of the deep OMZ. This was a large (2 μM nitrite) and stable feature. The nitrite

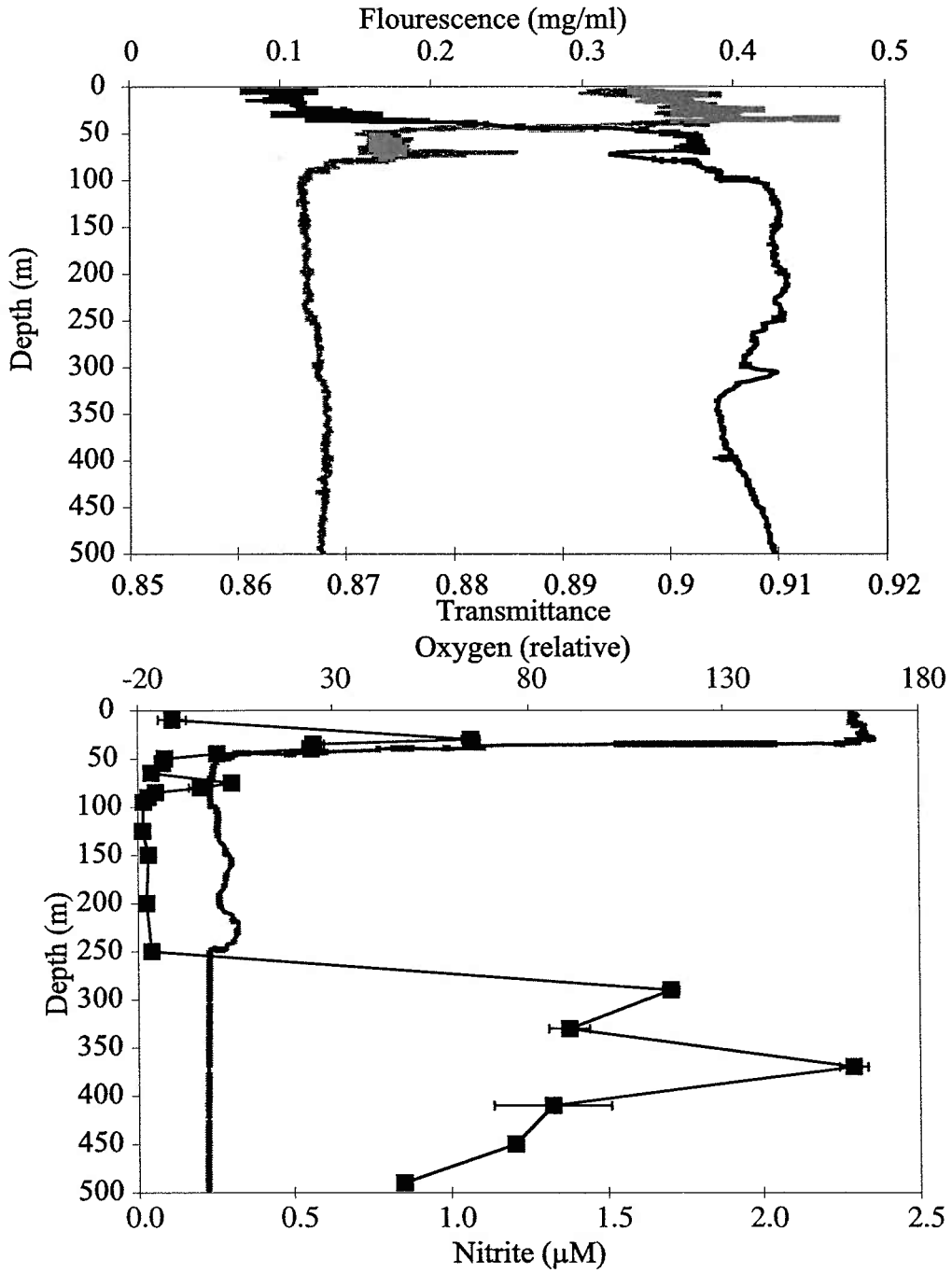

Figure 5.3 Profiles of fluorescence (light gray line), transmittance (black line), nitrite (black squares), and oxygen dark gray line) from the Eastern Equatorial Pacific site 9°50'N, 104°18'W. Oxygen values are only relative concentrations due to a faulty oxygen sensor. Notice the split shallow nitrite and fluorescence peaks at the top and within the shallow oxygen minimum.

peaks indicate that denitrification was significant at this station. There was significant nitrate (0.4 to 2.4 μM) even within the mixed layer, suggesting that N_2 fixation is likely not to be important at this station though it cannot be excluded.

5.2.2 Pump Deployment and Filter Handling at Sea

Suspended particulate matter samples were collected using the McLane Water Transfer System Large Volume Sampler (WTS 6-1-142LV08: McLane research Laboratories Inc.). Pumps consisted of three main components fixed on a stainless steel frame, the filter holder, the pump, and the electronics cylinder containing the battery (Figure 5.4). These samplers were designed to filter large volumes of seawater through a 142 mm filter when deployed from a ship either clamped directly to a hydrowire or shackled to a jacketed Kevlar or Amsteel line. For metal analyses it was preferable to use the trace metal clean Amsteel or Kevlar lines because hydrowires can be a source of metal contamination. The filter holder of the McLane WTS points upwards and is a maximum of 20 cm away from the area where the pump is clamped to the hydrowire. Pumps were deployed either singly to collect sequential organic (GF/F, Whatman ®) and metal (Supor, Gelman®) samples or two pumps were clamped side by side and deployed simultaneously. The former approach results in a slight discrepancy in the time of sample collection between Supor and GF/F samples but was unavoidable due to a limited number of pumps. Figure 5.5 shows the types of deployments used.

The pump is programmed prior to deployment using a detachable communications cable and a laptop computer loaded with the Crosscut software program. The software was used to set the time at which pumping commenced, leaving ample time

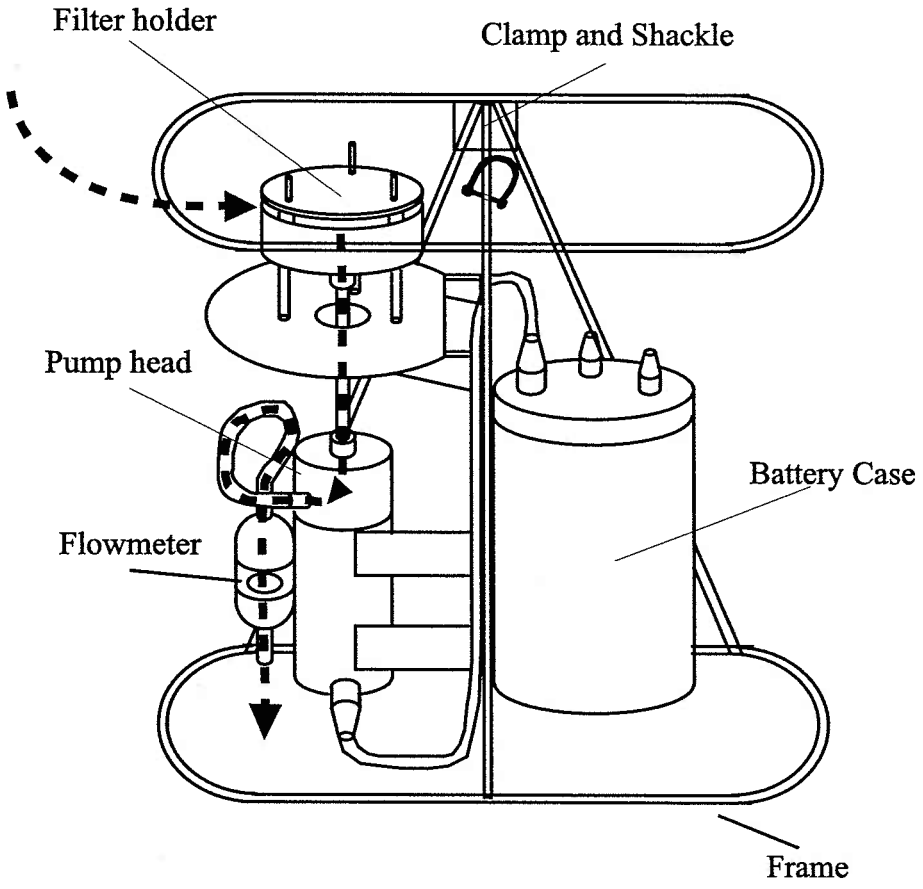

Figure 5.4 A drawing of the McLane Water Transfer System Large Volume Sampler (WTS 6-1-142LV08: McLane research Laboratories Inc.). Dotted line indicates water flow through the filter holder, the pump head and flow meter before exiting out the bottom of the frame.

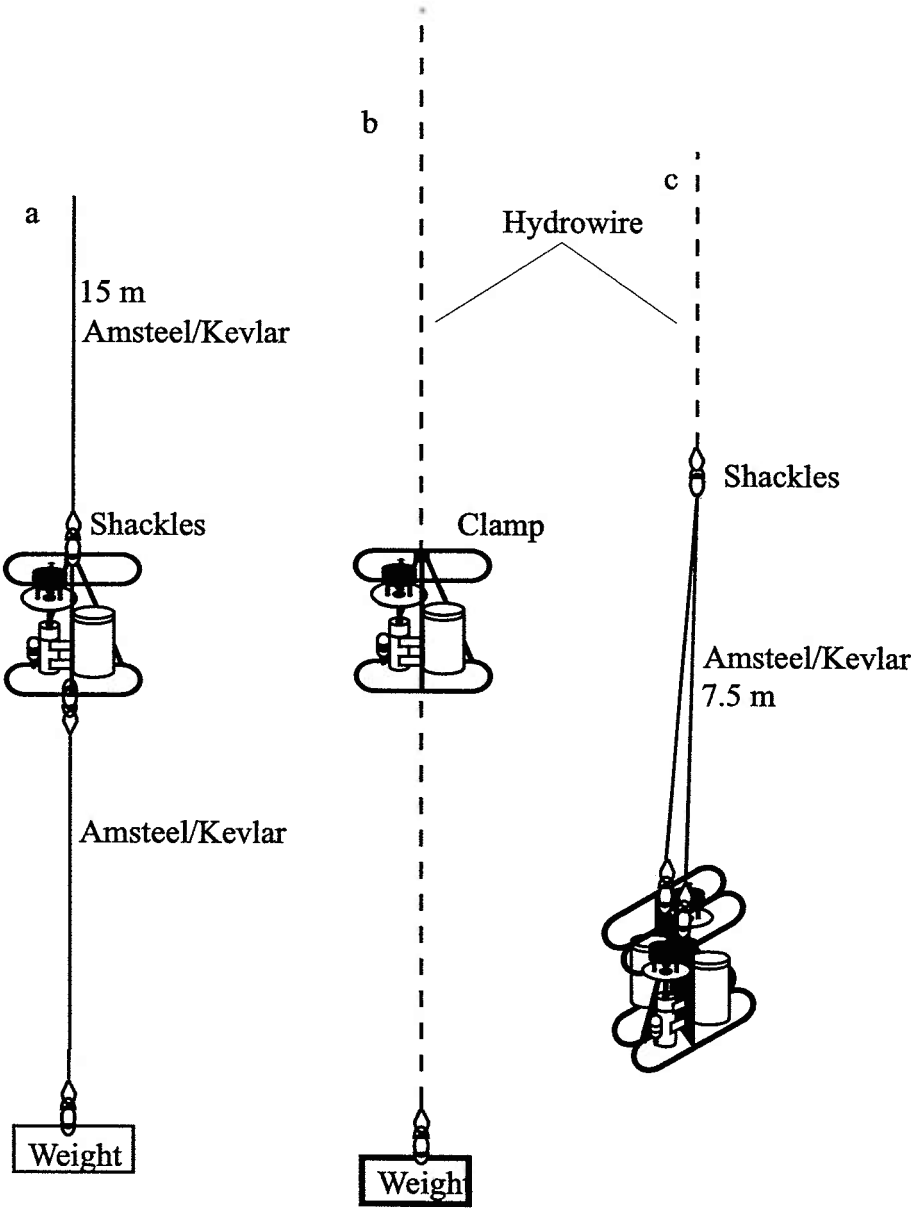

Figure 5.5 Schematic drawings of three types of pump deployments used. a) Inline shackling of the pumps on trace metal clean line (Amsteel or Kevlar). b) Clamped directly onto the hydrowire. This method had a significant metal contamination problem therefore it was used only to collect organic samples. c) Two pumps shackled together and attached to 7.5 m of trace metal clean line to take simultaneous metal and organic samples.

for deployment of the pump at the target depth and the maximum length of pumping time. The pump shut down either at the end of the specified pumping interval or sooner due to a decline in the nominal flow rate below 5 L min^{-1} or a sudden pressure drop. Clogging of the filter, trapped air bubbles in the pump lines or ship heave could all cause the pump to shutdown prematurely.

The software logged the volume of seawater filtered using an algorithm based on the configuration of the pump and the pressure drop across the filter. This algorithm works well for GF/F but consistently overestimates the volume filtered by lower flow rate filters like the Supors. Therefore a flow meter was attached to the pump out flow to independently measure volume filtered. The flow meter volume was used for all further calculations.

The flow of water through the filter and pump is illustrated in Figure 5.4. Seawater was pulled directly into the filter holder. Water flowed in large horizontal ports and through a Titanium honey–combed baffle designed to reduce turbulence. A 1mm diameter titanium mesh that screened out large particles and organisms followed and finally the primary filter (GF/F or Supor) rested on a porous HDPE frit. The pump head was made of Eralyte plastic with Teflon rotors and a titanium shaft. It was driven by a DC motor using a rare-earth magnetic coupling. The pump head was located downstream of the filter, removing the possibility of internal contamination from the pump itself and reducing the occurrence of clogging. The water outflow was routed through the flowmeter and out the bottom of the pump frame opposite the filter head to prevent recirculation.

The 142 mm filter holder was constructed of black acetyl. All plastic portions of the filter holder were cleaned with 10% HCl and Milli-Q between each deployment. Titanium pieces were simply rinsed with Milli-Q. The filter holder was always handled in a HEPA filtered flow bench and was covered with a clean plastic bag until just before deployment to eliminate shipboard dust contamination. After recovery of the pump the filter holder was immediately bagged and removed to a flow bench where the remaining water was gently (<5 mm Hg) vacuumed out of the holder before filter recovery. Resuspension and loss of material from the filter was limited by removing the extra water prior to filter recovery. Each filter was transferred to an acid cleaned 150 mm polycarbonate petri dish and stored frozen until it was analyzed.

5.2.3 Shore based Filter Analysis

Dissolved Mo associated with residual seawater can be a very significant blank when particles are collected on a high fluid retention filter. The ideal way to measure Mo:C ratios would be to measure metals and organics on the same filtered sample. However glass fiber filters (GF/F) used to sample for suspended Particulate Organic Carbon (POC) and Particulate Organic Nitrogen (PON) have a large fluid retention volume and very high metal blanks making them unsuitable for molybdenum analysis. Therefore the metal samples were collected on Supor polysulfanone filters, which have lower metal blanks and fluid retention. GF/F filters also have a higher size fraction (0.7 μm) cut off than the Supor (0.45μm) filters. This discrepancy in the filter sizes may be partially compensated by the different in loading characteristics of the filters. Supor filters have slow flow rates, clog easily and reach the minimum flow rate for the pumps

rapidly, causing the pumps shut down. In contrasts GF/F filters have higher flow rates and can pump for much longer. They generally had much higher loadings relative to the Supors. It is likely that the absolute size cut off decreased with increased filter loading. Sample analysis methods for both metal and carbon samples are described below.

GF/F filters were analyzed for POC and PON at the VIMS analytic services center. Prior to sample collection GF/F filters were ashed at 450 C for 5 hrs to remove organics. Subsections of the 142 mm GF/F filters were removed with a 25 mm diameter metal punch. They were fumed with HCl to remove carbonate material and analyzed on an Exeter Analytical CE-440 carbon/nitrogen analyzer. Duplicate analyses from the same filter were generally in agreement within 10%.

All shore based handling of the Supor filters was done in a class 100 clean room using Optima grade acid and 18 megaohm Milli-Q H_2O. Sub-sections of the Supor filters were treated by refluxing with acid to dissolve particulate matter for metals analysis after the method of Cullen and Sherrell (1999). Supor filters were cleaned prior to use by soaking overnight in 10% Optima HCl at 60 C. Filters were rinsed 4 times with Q-H_2O and finally stored in pH 2 water until ready for deployment. To analyze the loaded, frozen particulate sample, a known fraction of the filter area was removed using a stainless steel scalpel to cut the filter. An acid cleaned acrylic form was used as a cookie cutter to remove a 2.5 by 5 cm rectangle. Stainless steel scalpels have been shown not to significantly increase filter blanks (Cullen and Sherrell 1999). The piece of filter was then placed on the side of a clean 20 ml Savilex Teflon vial, loaded side out. 950 µl Optima HNO_3 and 50 µl Optima HF are added to the bottom of the vial, which was then

tightly capped, and place on a 120 C hot plate for 4 hrs. Vials were weighted before and after leaching to determine loss of acid during heating. The sample was diluted ten-fold by addition of Q-H_2O and decanted into a cleaned HDPE vial for storage until analysis.

Samples were analyzed on the WHOI Finnegan Element Inductively Coupled Plasma Mass Spectrometer (ICPMS). Two analysis methods were used (both described in detail in chapter 2 Tuit, 2003). The monoisotopic elements (Al, Mn and Rb) were measured by multi-element Standard Addition (SA) using In as an internal standard. Mo and Fe were measured by both SA and ID. Figure 5.6 compares SA and ID analyses. The relationship is generally 1:1 however there are occasional flyers with high SA concentrations.

Cu was measured by Isotope Dilution (ID) using a ^{65}Cu spike with a $Cu^{65/63}$ ratio of 294. Mass bias on Cu isotopes was corrected via comparison with bracketing standards ranged between 0.9 and 3.9 % amu^{-1}. Normal $Cu^{65/63}$ has a ratio of 0.4457. $Cu^{65/63}$ ratios of spiked samples that are between 1.8 and 70.6, result in minimal error amplification. In this study, measured $Cu^{65/63}$ ratios of spiked samples ranged from 46 to 253, leading to increases in the standard error of the measurements of up to ±60% of the on the most over spiked sample. On average, standard errors on ID Cu analyses were approximately ±7%.

5.2.4 Filter Blanks

Two types of blanks were evaluated, Filter blanks (analyses of cleaned unused filter) and Dip blanks (analyses of filters that were deployed similar to the samples but

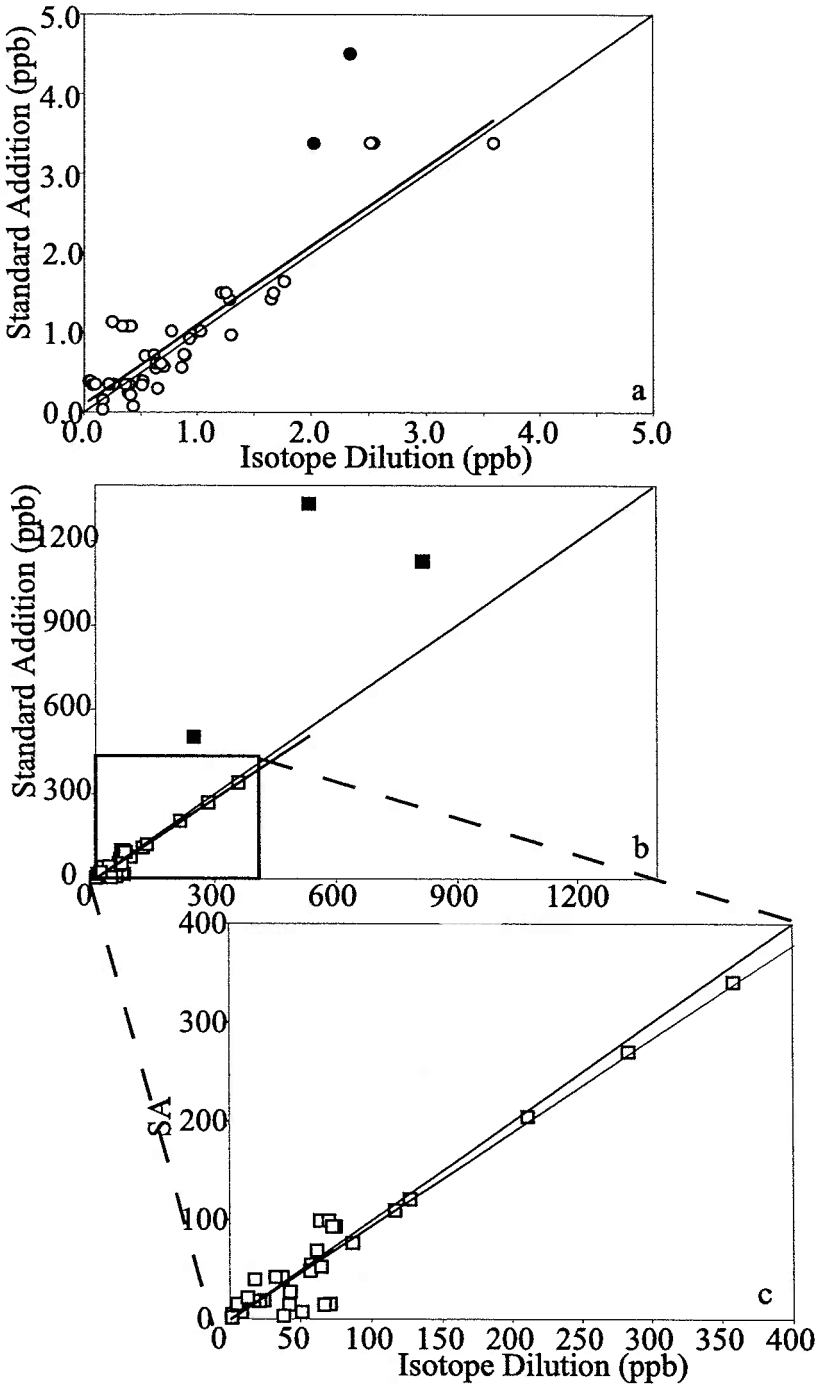

Figure 5.6 A comparison of Standard Addition and Isotope Dilution measurements of a) Mo (circles) and b) Fe (squares) concentrations in leach solutions. c) Shows expanded lower concentration Fe samples. All concentrations are in ng g-1. High concentration flyers are indicated by the filled symbols. The thin lines show 1:1 trends. Thick lines indicate regressions through the data excluding flyers. R2 values for regressions were 0.8253 and 0.9306, respectively for Mo and Fe.

without programming the pumps to turn on). The blank for the ashed GF/F filters was 1.1±0.3 μg C cm^{-2} and 0.83±0.07 μg N cm^{-2}. For POC and PON analyses a dip blank was taken from each sample location. These samples give an indication of the dissolved C and N blank of the seawater. The average dip blanks were 4.8±3.1 μg C cm^{-2} and 1.3±0.4 μg N cm^{-2} and were used to correct the sample concentrations. The average corrections were 12% on the C analyses and 22% on N, increasing up to 40% and 85%, respectively on two poorly loaded samples.

Filter blanks and Dip blanks for the metal analyses are shown in Figure 5.7. For most elements (Fe, Mn and Al) the Dip blanks are within error of the Filter blank. This is due to the fact that the dissolved concentration of the metals in seawater is very low and so does not substantially increase the filter blank concentration. Rb and Mo however have much higher and more variable dip blanks compared to the filter blanks. The high concentrations are due to high concentration of these elements in seawater, and the variability relates to the relative amount of seawater retained by the filter. This correlates with whether all of the water was evacuated from the filter holder prior to filter removal (low sea salt contribution) or not (high sea salt contribution). Because of the between sample variability for Mo and Rb and the relative agreement between the Dip and Filter blanks for the other metals, all samples except for Cu were blank corrected with the filter blank analyses. No Filter blanks were measured for Cu , so the Dip blank copper analysis from the 9 N station was used to correct Cu analyses. This is probably an acceptable assumption because like Fe, Al and Mn, Cu has very low dissolved concentrations in seawater.

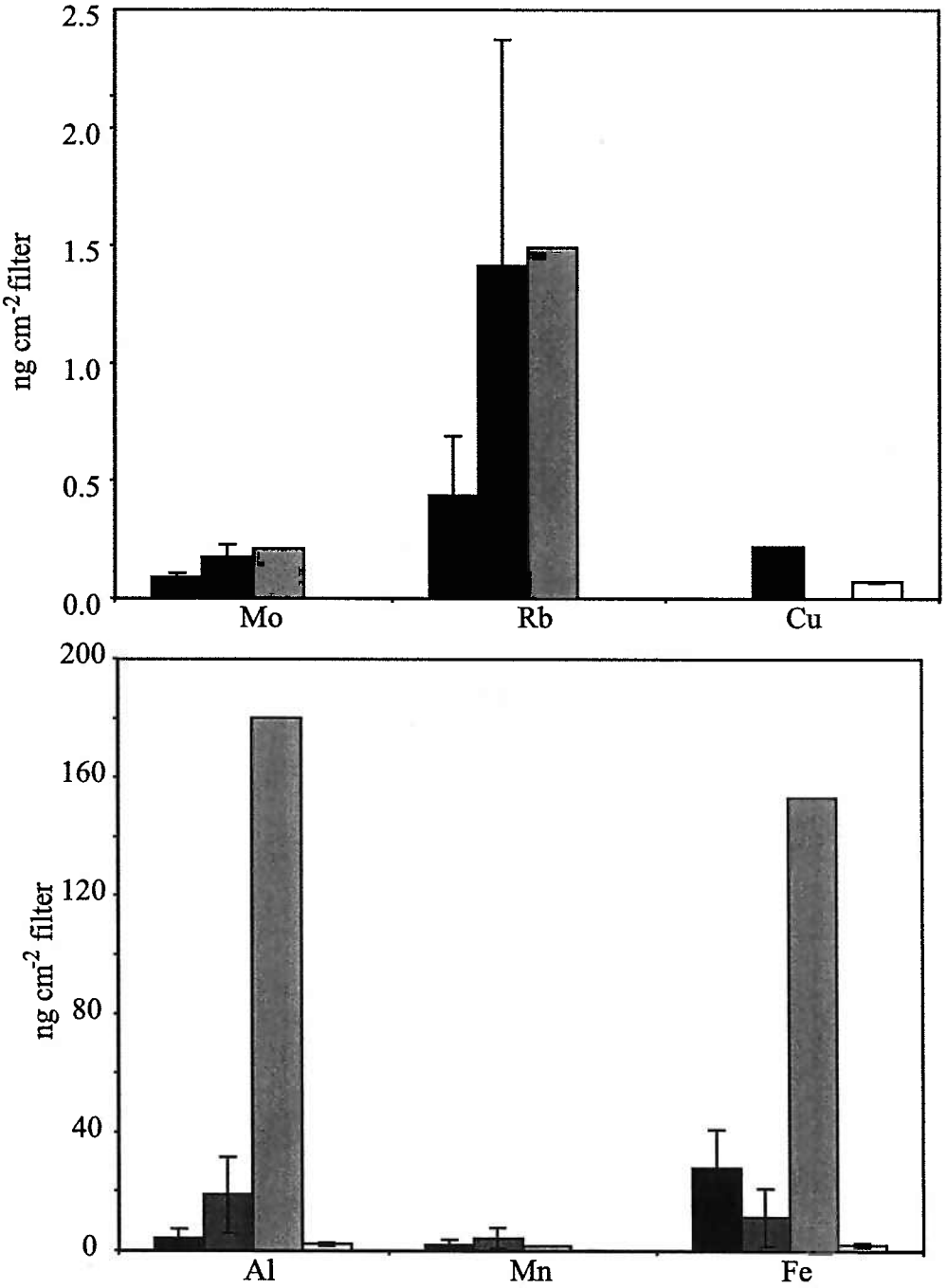

Figure 5.7 A comparison of cleaned Supor Filter blanks (black bars: n=3), Dip blanks of filters loaded and deployed on trace metal clean line but not pumped (dark gray bars: n=3), and Dip blanks deployed on the hydrowire (light gray bars:n=1) for Mo, Rb, Cu, Al, Mn, and Fe in ng (cm2 filter)-1. Error bars indicate 1sd. Filter blanks from Cullen et al (1999) (white bars: n=10) are shown for comparison for Fe, Cu, Mn, and Al.

Figure 5.7. also demonstrates why it is important to use trace metal clean techniques when collecting particulate samples. The dip blank taken for a sample deployed from a standard ships hydrowire showed extremely high Fe and Al concentrations, although Mo, Rb and Mn are all in line with the other dip blanks. Because of this contamination issue only Fe and Al samples collected from pumps suspended from Amsteel or Jacketed Kevlar line are presented.

5.3 Results

5.3.1 POC and PON

The POC and PON concentrations are listed in Table 5.2. The average C:N ratio of these samples was 7.49±0.93 mol:mol excluding both a high and a low outlier. This concentration is with error of the revised Redfield ratio of 7.3 mol:mol(Anderson and Sarmiento 1994). The Sargasso Sea and BATS station samples had lower POC and PON concentrations in the upper 100 m than either the Eastern Tropical Pacific or California borderland basin samples. POC and PON concentrations varied considerably from station to station but there were always higher concentrations of POC and PON in surface waters than waters at depth (Figure 5.8).

5.3.2 Trace Metal Analyses

The filter blank corrected trace metal analyses of each sample are listed in Table 5.2. Samples with concentrations below that of the filter blank analysis are listed as below detection. Al concentrations ranged from 1.0 to 25 nmol L^{-1}. In many of the

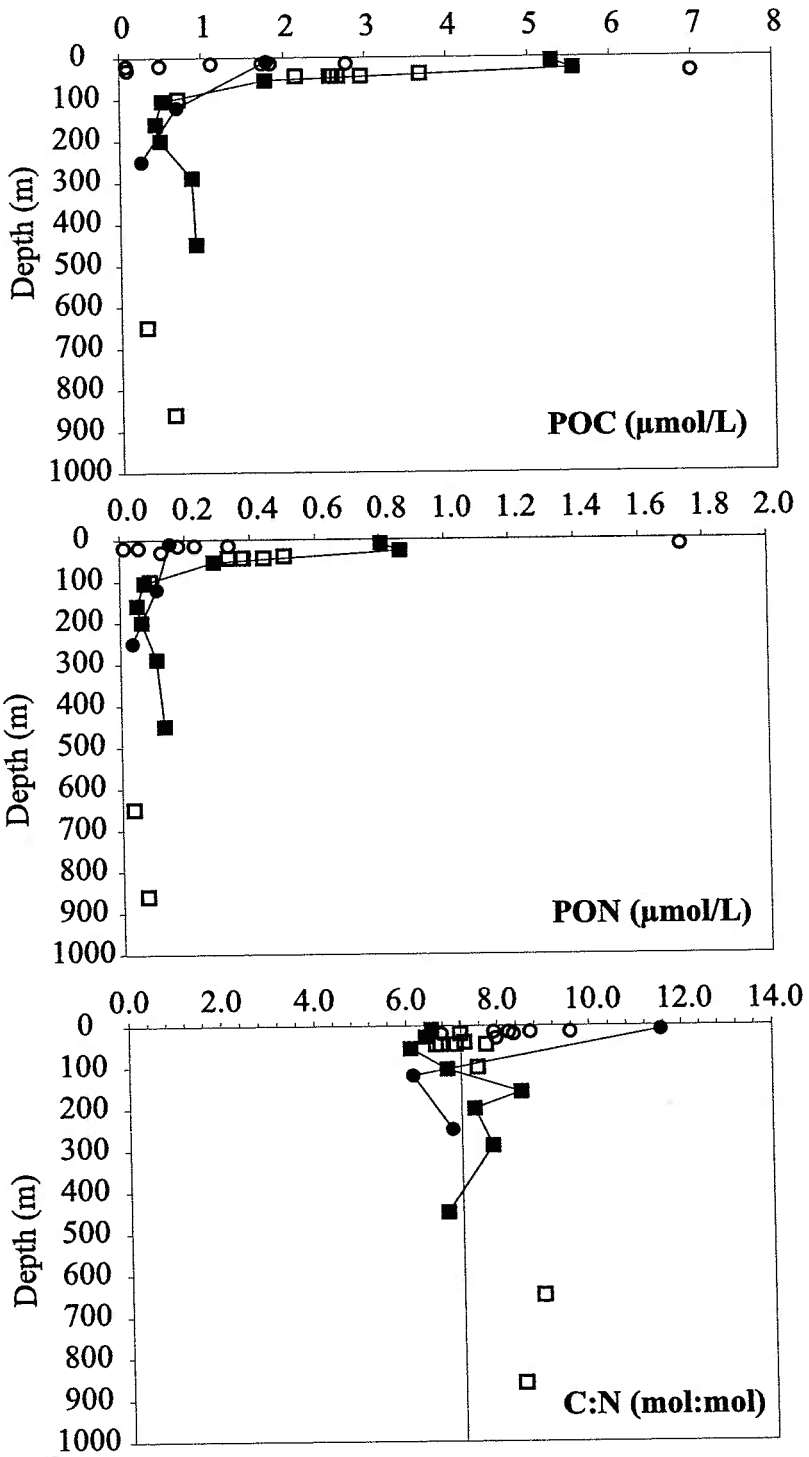

Figure 5.8 POC, PON and C:N measurements from the Eastern Tropical Pacific profile(black squares), BATS profile (black circles), California Borderland Basin samples (open squares) and the Sargasso Sea surface samples (open circles). The straight line represents the C:N Redfield ratio of 7.3 mol:mol.

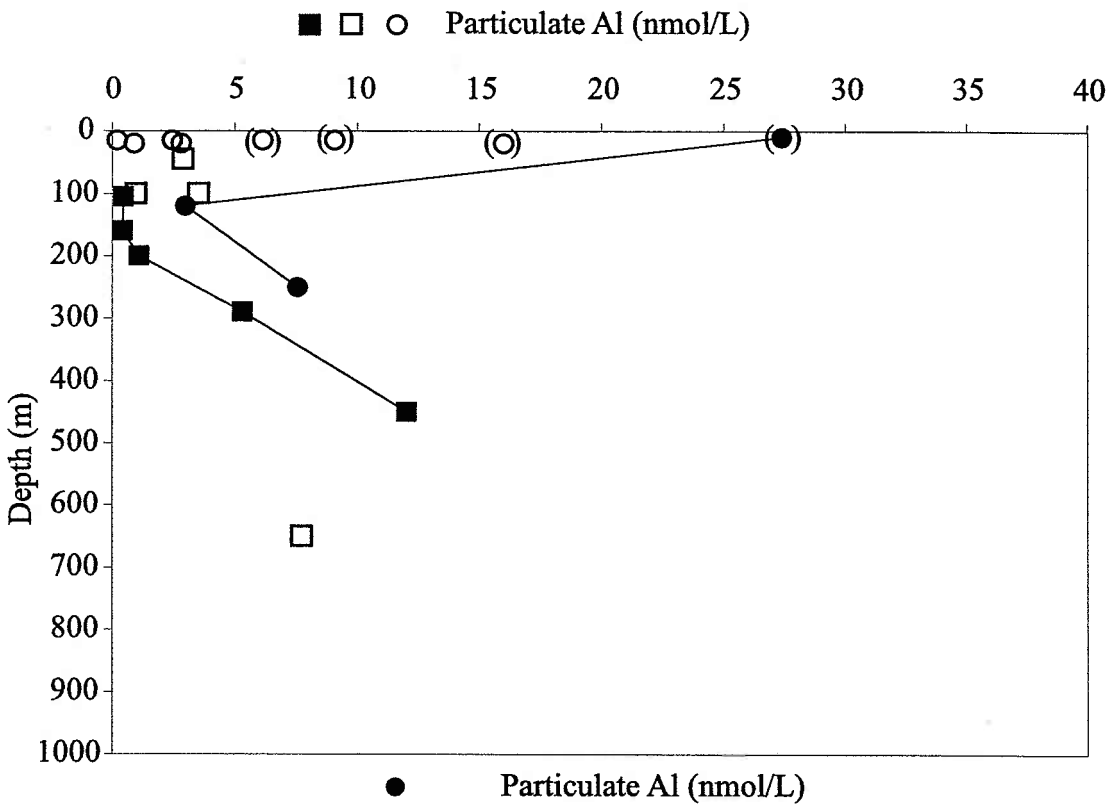

Figure 5.9 Particulate Al samples from the Eastern Tropical Pacific profile(black squares), BATS profile (black circles), California Borderland Basin samples (open squares) and the Sargasso Sea surface samples (open circles). Bracketed samples indicate surface samples that many have been contaminated during collection.

Pacific surface samples Al concentrations were below detection limits. The Al concentrations increased with depth at the Eastern Tropical Pacific site from below detection limits in the upper 100m to about 12 nmol L^{-1} at 450 m(Figure 5.9). The Al values in the OMZ (290 and 450 m) were high compared to other open ocean Pacific samples at similar depths (Martin and Knauer 1984) but not outside the range of particulate Al concentrations in more coastal waters. These deep samples were coincident with a local transmission minimum (Figure 5.3) that indicated particle concentrations at these depths were high. Despite the coastal influence very few of the California Borderland Basins samples had detectable Al. The very high particulate Al in the deep California Borderland Basin samples were collected close to the sediment water interface and likely reflect the influence of resuspended sediment. The surface Sargasso and BATS samples had several samples that exceeded 5 nmol L^{-1} and were likely contaminated. This contamination may be due to shipboard contamination and the shallow sampling depth. Also the Sargasso Sea samples were collected off the stern due to the severe weather and may have picked up contaminant particles from the ship's wake. The average surface concentration of Al, excluding the high outliers, was 1.75 nM, which is well with in the range of particulate Al concentrations measured in the Atlantic surface waters (Table 5.3).

Particulate Fe concentrations ranged from 0.16 to 24.9 nmol L^{-1} (Figure 5.10, Table 5.2). The surface samples from the Sargasso Sea had a range of 0.19 to 0.74 nmol L^{-1} with a mean of 0.46 nmol L^{-1}. The surface samples from the BATS profile at 11 nmol L^{-1} may have been contaminated for Fe as well as Al. The Sargasso Sea samples were in

the same range as recent particulate matter samples from the Atlantic (Helmers 1996; Kuss and Kremling 1999). The surface concentrations of particulate Fe in the Pacific samples were slightly higher than in the Atlantic ranging from 0.2 to 4.2 with a mean of 1.4 nmol L^{-1}. The samples were within the range of particulate Fe values reported for the northeast Pacific 0.1 to 18 nmol L (Sherrell 1989). Particulate Fe concentrations increased with depth especially within the near shore California Borderland Basin samples. For example, the very deep San Pedro Basin sample exceeded 25 nmol L^{-1} and is not shown in Figure 5.10 to avoid compressing the scale.

Table 5.3. Comparison of literature values for average trace metal concentrations in particulate matter from surface waters (0-100 m)

Location	Cu	Mn	Fe	Al	Ref.
	pmol L^{-1}	pmol L^{-1}	nmol L^{-1}	nmol L^{-1}	
Sargasso Sea, Bermuda		41.00 ± 20.28	0.47 ± 0.18	1.75 ± 1.14	[a]
East Pacific	41.58 ± 27.59	204.23 ± 84.73	1.42 ± 1.64	2.45 ± 1.33	[a]
North Atlantic	35	70	1	3.9	[b]
Northeast/Southeast /Southwest Atlantic	11	17	0.43	1.46	[c]
Tropical North Atlantic	57	64	3.98	2.89	[d]
North/Southeast Atlantic	143	128	4	6.07	[e]
Northwest Atlantic	54	200	2.17	5.93	[f]
Bermuda	6.3	34	0.32	1.2	[g]

[a] This study [b] Kuss and Kremling (1999) [c] Helmers (1996) [d] (Buatmenard and Chesselet 1979)[e](Krishnaswami et al. 1976) [f] (Wallace et al. 1977) [g](Sherrell and Boyle, 1992)

The filter blanks for Mn were a large fraction of the total Mn measured on loaded filters. This prevented meaningful determination of Mn in many of these samples. A few samples with exceptionally high filter loading, due to high particulate concentration or longer filtration times, did yield resolvable Mn concentrations. Concentrations of particulate Mn were undetectable in the upper 100 m except for the 10m BATS samples

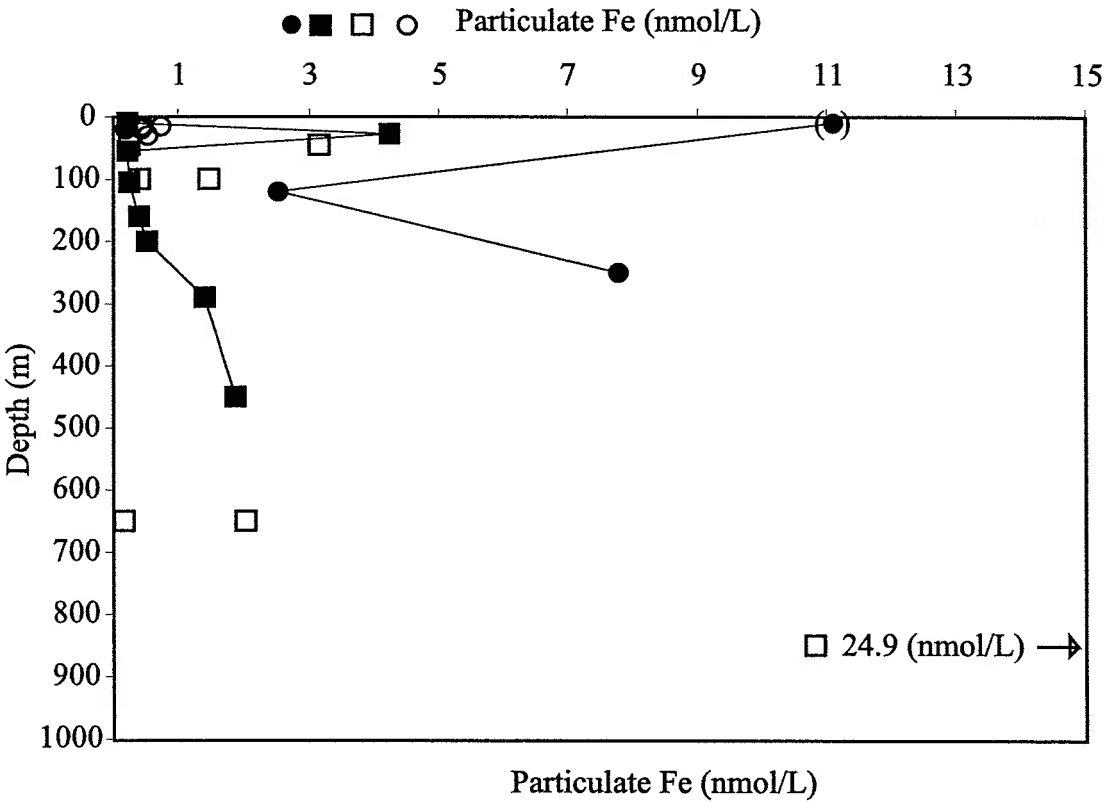

Figure 5.10 Particulate Fe samples from the Eastern Tropical Pacific profile (black squares), BATS profile (black circles), California Borderland Basin samples (open squares) and the Sargasso Sea surface samples (open circles). Arrow indicates deep sample from near the bottom of the San Nicholas Basin, the high value is likely due to sediment resuspension. Bracketed samples indicate surface samples that many have been contaminated during collection.

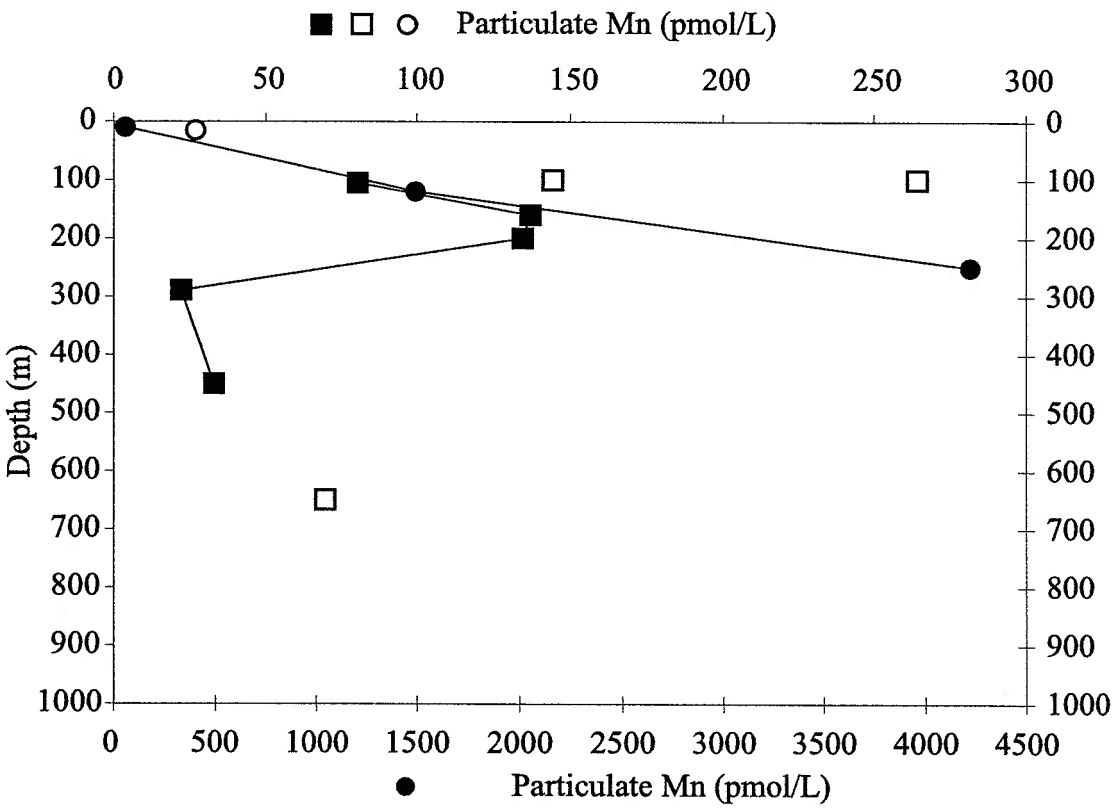

Figure 5.11 Particulate Mn samples from the Eastern Tropical Pacific profile(black squares), BATS profile (black circles), California Borderland Basin samples (open squares) and the Sargasso Sea surface samples (open circles)

and a single Sargasso Sea sample (Figure 5.11). The lack of measurable particulate Mn in surface waters was likely due to photo-reduction of Mn oxides in surface waters. This process has been shown to limit Mn oxide formation in both the Atlantic and the Pacific (Moffett 1997; Sunda and Huntsman 1988). The measurable particulate Mn samples from the Sargasso Sea are in agreement with other researchers (Table 5.3). Mn particulate concentrations at the BATS site increased with depth to 4.2 nmol L^{-1} at 250m. This was a very high Mn concentration for the Atlantic compared to other measurements of particulate Mn at BATS (Sherrell and Boyle 1992). These samples might be contaminated. Particulate Mn in the California Borderland Basin samples ranged from 70 to 264 pmol L^{-1}. At the Eastern Tropical Pacific site the particulate Mn concentration increases to depth of about 160 m then decreases sharply in the oxygen minimum zone. The absolute Mn concentrations and the shape of the profile are similar to previously reported data for suspended particulate Mn throughout the Pacific (Martin and Knauer 1984). Particulate Mn is strongly influenced by redox conditions of the water column.

Particulate Cu was measured only at the 9N site (Figure 5.12). Particulate Cu concentrations ranged from 14 to 73 pmol L^{-1} with a mean of 34 pmol L^{-1}. The average surface (<100m) particulate Cu concentration was 42 pmol L^{-1}. This concentration is similar to the particulate Cu concentration measured in the surface Sargasso Sea (Table 5.3). Copper concentrations showed a peak in the primary OMZ and rose again in the secondary OMZ. Cu and Mn were anti-correlated at the Eastern Tropical Pacific site, suggesting that Mn in this region did not control particulate Cu concentrations.

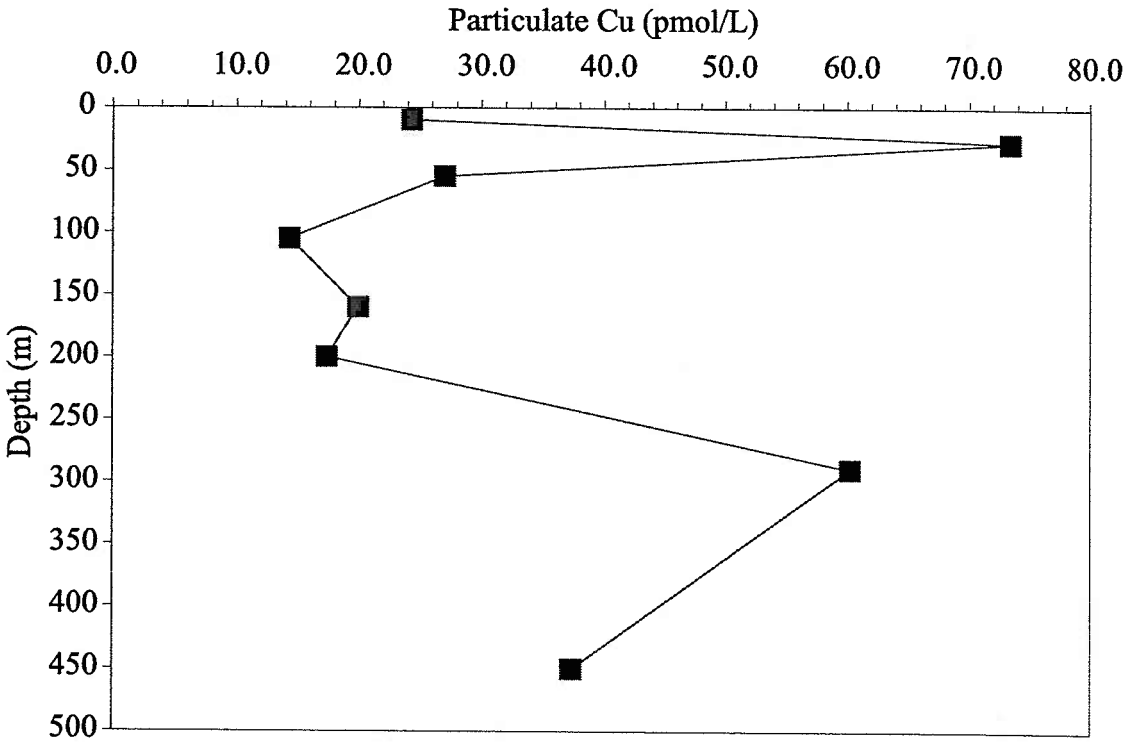

Figure 5.12 Particulate Cu profiles from the Eastern tropical Pacific, 9 50N 104 18W.

Rb and Mo concentrations were extremely variable from filter to filter. The range in measured concentrations for Rb was 3 to 477 pmol L^{-1} with a mean concentration of 73.4 pmol L^{-1}. Mo concentrations ranged from 0.62 to 68.8 with a mean of 15.72 pmol L^{-1}. The bulk measurements of Mo and Rb are not plotted because in some measurements Mo and Rb were strongly influenced by the abundance of sea salt. The section below discusses the protocol for correcting particulate Mo measurements for sea salt contributions as well as terrestrial contributions in order to determine the Mo contribution from biogenic material.

5.3.3 Determining Sample components

The collection of particulate Al, Mn and Rb in addition to Mo and Fe allows the estimation of the percentage of Mo and Fe in different particulate components as well as correction for contributions from Mo associated with residual sea salt. The purpose of these calculations was to determine the residual Mo contribution, the fraction associated with bacteria, phytoplankton, or authigenic metal oxides. To determine this fraction the measured particulate concentration must be corrected for contributions from terrestrial material and dissolved sea salts. The Mo corrections followed the format

$$Mo_{res} = Mo_{meas} - \left(Rb_{sw} \times \left[\frac{Mo}{Rb} \right]_{sw} \right) - \left(Al_{meas} \times \left[\frac{Mo}{Al} \right]_{ter} \right) \quad (1)$$

Where Mo_{meas} and Al_{meas} are the measured concentrations from Table 5.2, Rb_{sw} is the measured Rb concentration corrected for any possible terrestrial contributions (Table 5.4) and $[Mo/Rb]_{sw}$, and $[Mo/Al]_{ter}$ are the ratios of Mo to Rb in seawater, and Al in terrestrial material, respectively. The residual Mo after correcting for seawater salts and

terrestrial contributions is most likely associated with biogenic material and possibly Mn oxides. Residual Fe is likely associated with either biogenic material or with Fe oxyhydroxides.

The first step is to correct Rb, Mo, Mn, Cu and Fe for the contributions from terrestrial material, predominantly dust, which is represented by the concentration of particulate Al. Using the ratio of metal to aluminum in Upper Continental Crust (Taylor and Mclennan 1985) as a global average of terrestrial material and the measured particulate Al concentration it is possible to calculate the terrestrial contribution to the other metals. This assumes that Al in dust is not subject to scavenging or dissolution. This may be a faulty assumption since Al has been shown to dissolve in seawater and be redistributed to biogenic opaline phases (Murray and Leinen 1996). Ti has been proposed as a better tracer of terrestrial input but given that Ti is used in the construction of this filter holder this was not available to us. The terrestrial contributions calculated from Al are listed in Table 5.4 along with what percentage of the total measured particulate metal they represent. Samples in which Al concentrations were below detection were assumed to have negligible terrestrial contributions for all metals.

The terrestrially derived contributions varied between study sites and depths, as well as metals. The terrestrial contributions to Mo and Cu are always less than 10% of the measured concentrations. Terrestrial Rb corrections were generally under 25% of the measured Rb with the exception of two OMZ samples from the Pacific (4-21:68% and 7-5-16:42%).

However, Mn and Fe both had very high terrestrial contributions. In most of the surface Sargasso samples and the deeper Pacific samples the calculated terrestrial contribution accounts for over 100% of the measured Fe or Mn concentration. For Mn

Table 5.4. Terrestrial Contributions Calculated from the Particulate Aluminum Concentration

				Terrestrial Rb		Terrestrial Mo		Terrestrial Fe		Terrestrial Mn		Terrestrial Cu	
Sample	**sta**	**(m)**	**Al[c] pM**	**pM**	**%[a]**	**pM**	**%[a]**	**pM**	**%[a]**	**pM**	**%[a]**	**pM**	**%[a]**
UCC Metal:Al (mol:mol)[b]				0.000456		0.0000072		0.218		0.00380		0.00014	
CBB	1	45	2878	1.31	1.73	0.02	0.04	628	19.94	10.94		0.39	
		860	nd										
	4	40	bd										
		650	7702	3.51	68.53	0.06	6.67	1680	83.08	29.27	41.94	1.05	
	7	20	bd										
	8	650	bd										
	9	100	3511	1.60	24.84	0.03	1.25	766	52.18	13.35	9.25	0.48	
	10	45	bd										
		100	965	0.44	8.09	0.01	0.28	211	52.16	3.67	1.39	0.13	
		45	bd										
	11	45	nd										
Pacific		10	bd										
		28	bd										
		55	bd										
		105	468	0.21	5.08	0.00	0.17	102	41.16	1.78	2.21	0.06	0.45
		160	420	0.19	5.96	0.00	0.11	92	23.44	1.60	1.16	0.06	0.29
		200	1094	0.50	16.71	0.01	0.34	239	46.24	4.16	3.09	0.15	0.86
		290	5303	2.42	17.14	0.04	0.52	1157	82.57	20.16	91.13	0.73	1.21
		450	11998	5.47	42.42	0.09	2.26	2617	139.69	45.61	138.68	1.64	4.40
Sargasso	9	30	nd										
	10	15	nd										
	13	15	*6127*	2.79	1.77	0.04	0.35	1336		23.29		0.84	
	14	15	196	0.09	0.26	0.00	0.01	43	9.65	0.74	2.79	0.03	
	21	15	*9044*	4.13	8.23	0.07	0.12	1973	267.84	34.38		1.24	
	23	15	2454	1.12	4.14	0.02	0.11	535	115.31	9.33		0.34	
	27	20	885	0.40	1.66	0.01	0.21	193	102.53	3.36		0.12	
	33	20	*15992*	7.29	1.53	0.12	0.22	3488		60.79		2.19	
		20	2796	1.28	9.31	0.02	0.23	610	140.37	10.63		0.38	
	34	15	2440	1.11	8.21	0.02	1.72	532		9.27		0.33	
BATS		10	*2503*	12.5	2.85	0.20	0.29	5974	53.81	104.11	188.10	3.75	
		125	2500	1.36	1.27	0.02	0.07	650	25.80	11.33	0.76	0.41	
		250	7528	3.43	3.33	0.05	0.24	1642	21.11	28.62	1.52	1.03	

[a] Percent correction on the total particulate concentration (Table 5.2) [b] UCC trace metal to Al ratios from Taylor and McLennan (1985) [c] Samples with Al concentrations below detection limits were assumed to have negligible terrestrial contributions.

this is likely a function of limited formation of authigenic Mn oxides due to photoreduction in surface water, or to low oxygen concentrations that dissolves all Mn not associated with detrital material. For Fe in the surface Sargasso samples authigenic phases, oxides or biota, did not appear to be significantly in excess of detrital Fe. Since any authigenic Fe is determined by difference between measured Fe and terrestrial components (based on Al concentration) it is highly dependent on the Fe:Al ratio chosen for the calculation. The estimates presented here are based on average crustal concentrations, which have lower Fe:Al ratios than the shale or loess based ratios often used to make terrestrial corrections. Thus the above estimates, low as they are, are the maximum residual Fe estimates. Previous measurements of Fe in SPM show that both the Atlantic and Pacific have particulate Fe:Al ratios very similar to crustal concentrations (Landing and Bruland 1987; Sherrell and Boyle 1992).

While terrestrial dust is of little importance to the total Mo concentration, the dissolved seawater contributions can be a very large fraction of the total. Rinsing the filter and particles prior to analysis might reduce this contribution of dissolved seasalts. However, rinsing of SPM runs the risk of rupturing cells and decreasing the Mo signal as well as possibly introducing contamination for Mo and the other metals. We chose instead to use Rb concentration as a tracer of the sea salt contribution. Rb and Mo are relatively conservative in seawater with dissolved concentrations of 1.2 μmol kg^{-1} and 107.6 nmol kg^{-1}, respectively. The Mo:Rb ratio in seawater is essentially a constant at 0.0824 mol Mo: mol Rb. The Rb concentration in the filters derived from seawater

Table 5.5. Calculation of Residual Metal Concentrations and Metal Carbon Ratios

Location	sta	(m)	Mo_{meas} pM	Rb_{sw}[a] pM	Mo_{sw}[b] pM	% meas	Mo_{ter} pM	% meas	Mo_{res}[c] pM	Mo_{res}:C mol:mol	Fe_{res}[d] nM	Fe_{res}:C mol:mol	Mn_{res}[d] pM	Mn_{res}:C mol:mol	Cu_{res}[d] pM	Cu_{res}:C mol:mol
CBB	1	45	57.76	74.62	6.15	10.65	0.02	0.04	51.59	17.49	2.52	854				
		860	6.36						6.36	9.97	24.94	39073				
	4	40	37.26	94.39	7.78	20.88			29.48	8.02						
		650	0.84	1.61	0.13	16.99	0.06	6.67	0.65	2.08	0.34	1095	40.5	130		
	7	20	25.96	121.6	10.02	38.60			15.94	0.46						
	8	650	9.23	230.6	19.00	205.83			<0		0.16					
	9	100	2.04	4.8	0.40	19.82	0.03	1.25	1.61		5.72					
	10	45	2.55	11.5	0.95	37.19			1.60	0.62						
		100	2.54	5.0	0.41	16.25	0.01	0.28	2.12	2.98	0.70		131.0			
		45	0.62	3.1	0.25	40.92			0.36	0.14	0.24	94				
	11	45	0.79						0.79	0.31	0.19	271	260.5	365		
Pacific		10	14.25	52.0	4.29	30.07			9.97	1.88					24.3	5
		28	21.74	62.4	5.14	23.67			16.59	2.99					73.4	13
		55	8.29	14.7	1.21	14.61			7.08	4.00	0.22	41			27.0	15
		105	2.05	4.0	0.33	16.09	0.00	0.17	1.71	3.28	4.23	761			14.3	27
		160	2.79	3.0	0.25	8.93	0.00	0.11	2.54	5.77	0.22	122			19.9	45
		200	2.35	2.5	0.21	8.75	0.01	0.34	2.14	4.33	0.15	279	78.9	151	17.2	35
		290	7.40	11.7	0.96	13.09	0.04	0.52	6.40	7.32	0.30	680	135.5	308	59.5	68
		450	3.85	7.4	0.61	16.27	0.09	2.26	3.15	3.43	0.28	563	130.4	264	35.7	39
Sargasso	9	30	4.99				0.00	0.00	4.99	53.22	0.24	279	2.0	2		
	10	15	5.25													
	13	15	12.77	154.9	12.76	100.24	0.04	0.35	<0							
	14	15	11.32	34.1	2.81	24.79	0.00	0.01	8.52	3.08	0.53	5683				
	21	15	55.40	46.0	3.79	6.85	0.07	0.12	51.54	29.68						
	23	15	16.68	25.9	2.14	12.83	0.02	0.11	14.53	7.92						
	27	20	3.02	23.9	1.97	65.53	0.01	0.21	1.04	12.51	0.40	145	25.9	9		
	33	20	52.41	470.2	38.75	74.10	0.12	0.22	13.54	27.49						
		20	8.80	12.4	1.02	11.65	0.02	0.23	7.76	15.74						
	34	15	1.03	12.4	1.02	101.24	0.02	1.72	<0							
BATS		10	68.80	426.0	35.10	51.17	0.20	0.29	33.50	18.70	5.97	3335				
		120	32.54	105.4	8.68	26.70	0.02	0.07	23.84	34.21	14.43	20720	1484	2130		
		250	22.53	99.6	8.21	36.51	0.05	0.24	14.27	55.00			1861	7173		

aRbsw=Rbmeas(Table 5.3)-Rbter(Table 5.4) bMosm= Rbsw*0.0824. cMores= Momeas(Table 5.2)- Mosm-Moter(Table 5.4) dMeeasured metal concentrations (Table 5.2) minus terrestrial metal concentrations (Table 5.3)

(Rb_{sw}) can be calculated by subtracting Rb_{ter} from Rb_{meas}. Rb_{sw} and the ratio of Mo:Rb in seawater can be used to calculate the contribution of sea salts to the Mo concentration of each filter. Using Rb_{meas} instead of Rb_{sw} increases the seawater corrections on Mo on average less than 2%. The seawater Mo fraction had a very large range depending on the amount of seawater remaining in the filter when it was removed from the filter holder and the particulate loading of the filter. The Rb based sea salt correction is listed for each sample in Table 5.5. For most samples the correction is between 7 and 40%, but there were three samples where the seawater correction accounted for >100% and these samples tended to be poorly loaded and were not used in subsequent calculations.

Figure 5.13 illustrates how each correction described above affects the particulate concentrations in the profiles from the Eastern Tropical Pacific and BATS sites. Now that the residual or biogenic component of particulate Fe, Cu, Mn, and Mo has been calculated, these data can be used to evaluate whether enzymatic Fe, Cu and Mo demand or association with Mn oxides can account for Mo enrichments in SPM over crustal values.

5.4 Discussion

5.4.1. Mo and Nitrogen Fixation: Sargasso Sea Samples

The calculated Mo_{res}:C , Fe_{res}:C and F_{res}:Mo_{res} ratios can be compared to the Mo:C ratios measured in culture and field samples of N fixing cyanobacteria. The average Mo_{res}:Carbon ratio for the Atlantic samples was 24.71±16.36 μmol:mol. This value is very high when compared to cultured organisms (Table 5.1), including cultured

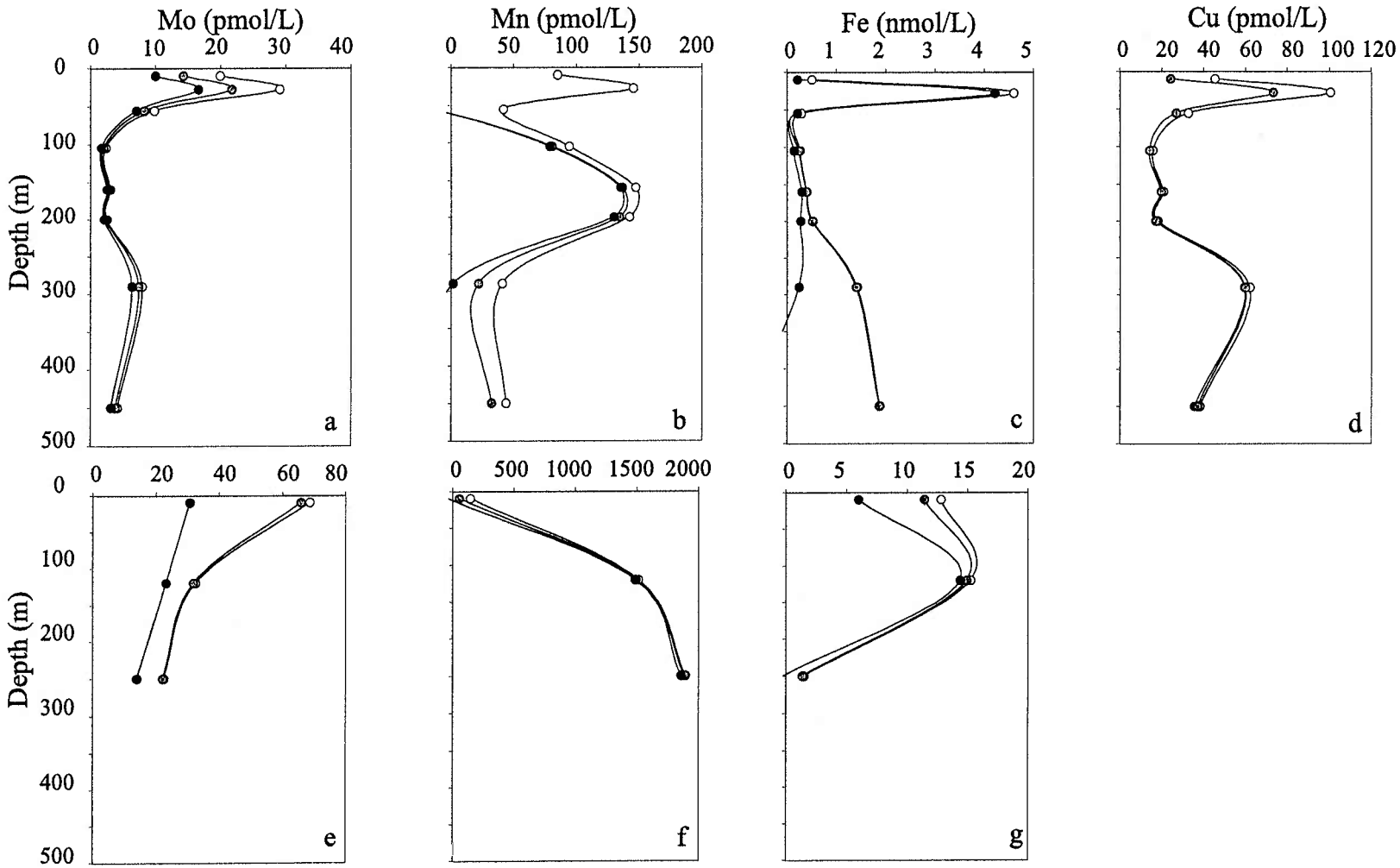

Figure 5.13 A demonstration of how filter blank, terrestrial and sea salt corrections effect profiles of Mo (a,e), Cu (d), Fe (c,g), and Mn (b,f) from the Eastern Tropical Pacific site (a-d) and BATS site (e-g). Measured concentrations (white circles) filter blank corrected concentrations (light gray circles) and Terrestrial corrected concentrations (dark gray circles) are shown for all the metals. Sea salt corrections (black circles) are shown for Mo samples as well.

Trichodesmium, but it is equivalent to Trichodesmium colonies collected from Sargasso surface waters both by Tuit (2003) and Kutska (10-50 μmol:mol: pers com.). The Pacific samples Mo_{res}:C surface ratios were lower than seen in the Sargasso at 3.68±4.16 μmol:mol. The surface waters of the Atlantic were universally depleted in nitrate, while the Pacific samples contained measurable nitrate and ammonia concentrations in surface waters. These results imply that the Mo:C ratios of the Atlantic are reflecting a different process than the Pacific samples, possibly associated with nitrogen limitation. However, the Mo:C ratios of SPM from both locations greatly exceed Mo:C ratios of cultured organisms. From where does this extra Mo in the field samples come? The Mo enrichment of natural samples could be caused by an unknown Mo enzymatic demand in Trichodesmium, possibly DMSO dehydrogenase. The presence of DMSO or other Mo enzymes has not been evaluated in Trichodesmium but DMSO dehydrogenase is an important enzyme in the marine system (Stiefel 1996). There could also be another organism present with a large Mo demand. DMS production is especially important in cocolithophores (Burkill et al. 2002) whose Mo requirements have not been evaluated in this study. However if the increased particulate Mo is associated with another organism it would have to be one closely associated with Trichodesmium colonies, which have similar Mo:C ratios. Alternatively the Mo enrichment could be due to an undetermined authigenic phase. Mn oxides are a possibility, but given the extremely low Mn concentrations in the surface Sargasso samples this does not seem likely. Fe oxides are also too low in concentration to be a significant carrier for Mo. Finally, the Mo enrichment of Trichodesmium field samples and SPM samples could be due luxury

uptake of Mo by Trichodesmium triggered by some factor (nutrient limitation, predation, etc) not experienced in the cultures.

Though the very high particulate Mo concentrations measured in this study are unlikely to be entirely associated with active N_2 fixation, data from cultured N_2 fixing organisms along with estimates of N_2 fixation rate can be used to calculate and approximate particulate Mo concentration needed to support N_2 fixation in the Sargasso Sea. Since the 1960 s there have been a wide range of estimates of N_2 fixation in the oceans (Capone 2001; Karl et al. 2002) (Table 5.6). These estimates are based on both indirect methods that use ^{15}N or N:P ratio mass balance to estimate an N_2 fixation rate averaged over broad areas and time frames, and direct methods, based on measured N_2 fixation rates for specific organisms, usually acetylene reduction measurements on Trichodesmium, and estimates of that organisms abundance. The direct N_2 fixation rate estimates represent snap shots from specific times and locations that may not be equivalent to when these particulate samples were collected. Also these measurements are inherently difficult and there is some indication from laboratory measurements that acetylene measurements may underestimate N_2 fixation rates in Trichodesmium (Tuit 2003, Chapter 4.) Complimentary N_2 fixation rate (^{15}N) measurements (Montoya Lab) were made during the Sargasso Sea cruise, which will allow directly comparison with theses samples, however that data is not yet available. In the mean time these N_2 fixation estimates provide a rough comparison.

Using the metal use efficiency of nitrogenase (5.6 pmol Mo d $(\mu mol\ N)^{-1}$ and 152 pmol Fe d $(\mu mol\ N)^{-1}$ at 25 °C: calculation of metal use efficiency explored in depth in

Tuit 2003, Chapter 4) we can use the N_2 fixation rates to calculate a particulate Mo concentration for the upper 20 m. Assuming 25°C surface waters and that N_2 fixation occurs only in the upper 20 m gives a maximum particulate metal concentration based on N_2 fixation.

Table 5.6. Calculated Mo and Fe required to support estimated N_2 Fixation rates (after Capone 2001).

Direct	Date	Method	Areal N fixation µmol N m^{-2} d^{-1}	1sd	Mo pmol L^{-1}	Fe nmol L^{-1}	Ref
Trichodesmium/tropical regions							
N Pacific: HOT/ALOHA	1990-92	AR, 3:1[i]	85	49	0.024	0.00065	a
Arabian Sea, 7-10 N	May '95	AR, 3:1[i]	35	7.4	0.010	0.00027	b
Arabian Sea @ 10 N	May '95		99	25	0.028	0.00075	c
SW N Atlantic, 0 -17 N	Apr '96	AR, 3:1[i]	258	98	0.072	0.00196	c
SW N Atlantic, 7 -27 N	Oct '96	AR, 3:1[i]	206	63	0.057	0.00157	c
Richelia/Hemiaulus							
SW N Atlantic, 7 -27 N	Oct '96	AR, 3:1[i]	3110	1315	0.867	0.02365	d
Indirect/Mass Balance							
N Atlantic		Extr	2100		0.585	0.01597	e
N Pacific: HOT/ALOHA		mass balance/N:P	93		0.026	0.00071	a
N Pacific: HOT/ALOHA		mass balance/^{15}N	137		0.038	0.00104	a
N Atlantic		N*	197		0.055	0.00150	f
Pacific		mass balance	107		0.030	0.00081	g
Sargasso Particulates					1.04-51.4	0.19-0.74	h

[a](Karl et al. 1997) [b](Capone et al. 1998) [c](Capone 2001) [d](Carpenter et al. 1999) [e](Carpenter et al. 1997) [f](Gruber and Sarmiento 1997) [g](Deutsch et al. 2001) [h]This Work [i]Acetylene reduction method for measuring N fixation using a 3:1 Acetylene:N_2 ratio.

The estimated particulate Fe required by N_2 fixation is less than 0.02 nmol L^{-1} much lower than measured particulate Fe concentrations. The filter blank corrected Fe samples (0.19-0.74 nmol L^{-1}) are in agreement with other recent measurements of

particulate Fe in the surface Atlantic (Helmers 1996; Kuss and Kremling 1999). This suggests that there is plenty of total Fe in surface waters to support N_2 fixation, though only a very small fraction of this Fe is likely to be bioavailable. Most of the particulate Fe is probably present as Fe oxides or in other refractory phase. Terrestrial contributions account for almost all of the filter blank corrected Fe concentration in surface water. The measured particulate Mo concentrations far exceed the estimates from N_2 fixation (Table 5.5 and 5.6). These measurements imply that Mo concentration in particulate matter and Mo:C ratios cannot be used to quantify N_2 fixation. Elevated Mo:C ratios and particulate matter Mo concentrations do seem to indicate regions were N_2 fixation is taking place but the scatter in the data is too great to provide a meaningful measure of N_2 fixation

5.4.1 Mo and Mn oxides

Studies of trace metals in SPM have demonstrated that Mn oxides can influence distributions of other trace metals (Cu, Ni)(Noriki et al. 1997). Despite the strong relationship of Mo and Mn oxides in sediments, crust and nodules, there are no positive correlation between Mo and Mn in these samples. Mo and Cu are anti-correlated with Mn throughout the upper 500m of the Eastern Tropical Pacific (Figure 5.14). This suggests that Mo is not incorporated into authigenic Mn oxides. Authigenic Mn oxides are generally formed by microbial precipitation of amorphous Mn oxide on an organic matrix, which encapsulates a microbe. They form at depths below the euphotic zone where the finely dispersed authigenic Mn oxides are subject to photodegradation. Alternatively, the formation of sedimentary Mn oxides, crust and nodules are likely predominantly controlled by autocatalytic Mn oxide precipitation where the presence of

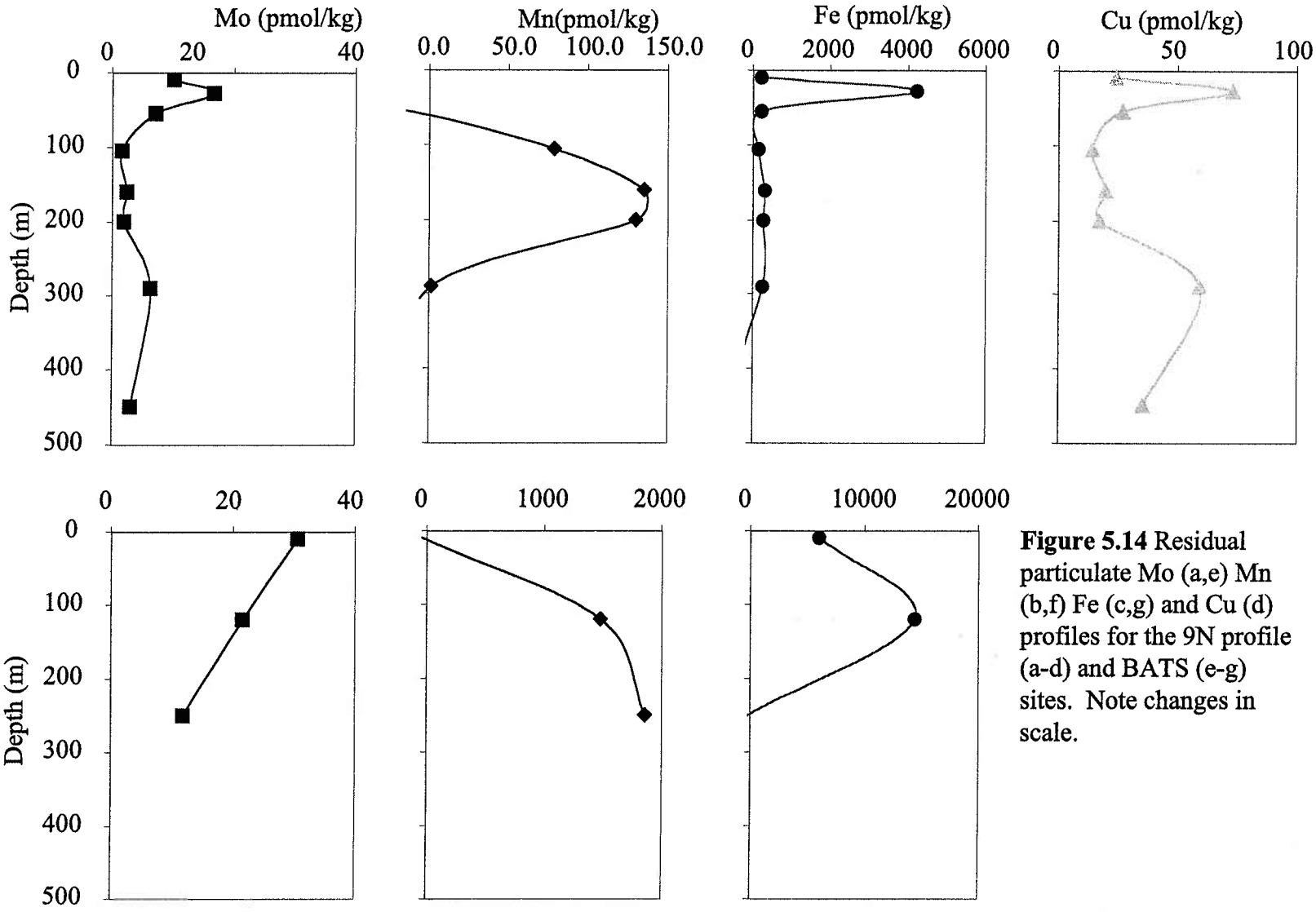

Figure 5.14 Residual particulate Mo (a,e) Mn (b,f) Fe (c,g) and Cu (d) profiles for the 9N profile (a-d) and BATS (e-g) sites. Note changes in scale.

partially crystalline Mn oxides causes Mn oxidation to occur more rapidly (Hem 1978). Mn oxidizing bacteria may have a much smaller catalytic role in regions where there are high concentrations of solids. The anti-correlation of Mo and Mn in the 9N SPM profile when compared to the high enrichments of Mo in sedimentary Mn oxides and nodules suggests that a precipitation mechanism may have a role in determining the Mo concentration of Mn oxides.

The method of Mo incorporation into Mn oxides is a long standing mystery. Mo could be incorporated via a microbial co-precipitation pathway. Several metals have been shown to be co-precipitated with Mn in microbially catalyzed Mn oxides but the lack of Mo correlation with Mn through the 9N profile suggests that Mo is not one of them. It is likely not a simple scavenging mechanism. Mn oxides have a predominately negative surface charge in seawater thus they are very efficient at scavenging cations but molybdate, the most likely form of Mo in seawater, is an oxyanion and should not be scavenged. Mo isotopes show similar fractionation effects in Mn oxides produced abiotically in the laboratory and in Mn oxide nodules (Anbar pers. com.) providing additional evidence that the mechanism of Mo incorporation into Mn oxides is not likely to be microbially mediated.

5.3.4 Mo and Cu and Denitrification

Denitrification like N_2 fixation requires a Mo-containing enzyme. Mo:C ratios measured in diatoms and denitrifying bacteria show that phytoplankton and bacteria utilizing either assimilatory or respiratory nitrate reductase have elevated Mo:C ratios. Cu can be involved in two steps of the denitrification pathway. Nitrite reductase, which is

responsible for the reduction of NO_2^- to NO can use either Cu or Fe. Nitrous oxide reductase, which catalyzes the reduction of N_2O to N_2, is a Cu-only enzyme. If the denitrifying bacteria present were using the Cu nitrite reductase, or nitrous oxide reductase, it is probable that areas of denitrification would see increases in particulate Cu as well as Mo.

Figure 5.14a compares the residual particulate metal concentrations through the denitrification zones of the Eastern Pacific profiles. The seawater and terrestrial contributions do not affect the shape of these profiles. The Cu and Mo particulate profiles are very similar. Both metals have a shallow maximum associated with the fluorescence peak at 28 m; this peak is shallower than the shallow nitrite maximum at 50 m. A deeper Mo and Cu maximum at 300 m was coincident with the deep nitrite maximum (Figure 5.3). This implies that the increased Mo and Cu may be related to increased Mo and Cu enzymatic demand by denitrification.

The Mo:C and Cu:C profiles also have a peak at the deep nitrite maximum (Table5.5). However, the Mo:C ratio at the deep nitrite maximum was 7.3 μmol Mo:mol C, much higher than has been measured for marine denitrifying bacteria grown on nitrate in culture (0.48μmol Mo:mol C: Table 5.1). This requires that there must be other forms of particulate Mo present in addition to the nitrate reductase demand. Possible phases include other Mo enzymes or, if the OMZ be strong enough to allow the production of sulfide, thiomolybdates that are easily scavenged by organic matter (Helz et al. 1996).

If particulate Mo in the OMZ is driven by increased Mo demand by denitrifying organisms, Mo particulate concentration may provide a new way to estimate in situ

nitrate reduction rates. In situ denitrification rates are extremely difficult to measure. Using the specific activity of nitrate reductase, or the rate of nitrate reduction per mg enzyme per min, it is possible to estimate the rate of nitrate reduction from the particulate Mo concentration. The specific activity (SA) of nitrate reductase (NAR) for a range of denitrifying bacteria is 27 to 60 mol NO_3^- reduced min^{-1} mg^{-1} nitrate reductase (Table A1.1). The molecular weight (MWt) of nitrate reductase is between 172 and 230 kDa, the molar ratio of Mo to nitrate reductase is 1. Considering only the 300 m depth (6.4 pmol L^{-1} Mo),

(2)

$$\frac{6.4\text{pmolMo}}{\text{L}} \times \frac{1\text{molMo}}{10^{12}\text{pmolMo}} \times \frac{1\text{molNar}}{1\text{molMo}} \times \text{MWt}\frac{\text{gNAR}}{\text{molNAR}} \times \frac{10^3\text{mgNAR}}{\text{gNAR}} \times \text{SA}\frac{\text{mmolNO}_3^-}{\text{min} \bullet \text{mgNAR}} \times \frac{1440\text{min}}{\text{day}} \times \frac{10^3\text{nmolNO}_3^-}{\text{mmolNO}_3^-}$$

which is equal to 42800 to 127000 nmol NO_3^- L^{-1} day^{-1}. This 100 to 350 times higher than nitrate reduction measurements for the Eastern Tropical Pacific, which range from 12 to 400 nmol NO_3^- day^{-1} L^{-1} (Cline and Richards 1972; Codispoti and Christensen 1985; Lipschultz and Owens 1996). The estimated nitrate reduction rate for this sample is likely an upper bound. It does not account for the lower temperatures at depth, which could cause less efficient enzyme activity or a non-nitrate reductase Mo pool. It also assumes enzyme saturation. Nitrate concentrations at this depth were only 29 μM, compared to 10mM generally used to grow denitrifying bacteria in culture. Both limited access to substrate and lower temperatures can decrease enzyme reaction rate. Still these data do not support the use of particulate Mo to provide estimates of denitrification rate.

5.5 Conclusions

These data are the first systematic measurements of particulate Mo in the marine system. Mo does not appear to be scavenged by microbially produced Mn oxides, despite its strong association with Mn oxides in sediments. This suggests that the enzymatic mechanism that catalyzes microbial Mn oxidation, the predominant mechanism of Mn oxidation in the water column, can exclude Mo, while the autocatalytic Mo oxidation which is important in sediments mechanism cannot. Mo:C ratios range from 0.14 to 55 μmol Mo:mol C. Regions of N_2 fixation have the highest mean Mo:C concentrations. Mo:C also show a slight increase in regions of denitrification. However, the concentration of Mo in particulate matter far exceeds nitrogenase or nitrate reductase enzymatic demand and requires the presence of other Mo phases.

5.6 References

Anderson, L. A., and J. L. Sarmiento. 1994. Redfield Ratios of Remineralization Determined by Nutrient Data-Analysis. Global Biogeochemical Cycles **8:** 65-80.

Babu, S. K., M. V. K. Murthy, and D. Satyanarayana. 1984. Preconcentration and Photometric Estimation of Molybdenum in Seawater, Particulate Matter and Sediments of Visakhapatnam (Bay of Bengal). Marine Environmental Research **11:** 305-317.

Berrang, P. G., and E. V. Grill. 1974. The effect of manganese oxide scavenging on molybdenum in Saanich Inlet, British Columbia. Marine Chemistry **2:** 125-148.

Buatmenard, P., and R. Chesselet. 1979. Variable Influence of the Atmospheric Flux on the Trace-Metal Chemistry of Oceanic Suspended Matter. Earth and Planetary Science Letters **42:** 399-411.

Burkill, P. H. and others 2002. Dimethyl sulphide biogeochemistry within a coccolithophore bloom (DISCO): an overview. Deep-Sea Research Part Ii-Topical Studies in Oceanography **49:** 2863-2885.

Capone, D. G. 2001. Marine nitrogen fixation: what's the fuss? Current Opinion in Microbiology **4:** 341-348.

Capone, D. G. and others 1998. An extensive bloom of the N2-fixing Cyanobacterium trichodesmium erythraeum in the central Arabian Sea. Marine Ecology Progress Series **172:** 281-292.

Carpenter, E. J., H. R. Harvey, B. Fry, and D. G. Capone. 1997. Biogeochemical tracers of the marine cyanobacterium Trichodesmium. Deep-Sea Research Part I-Oceanographic Research Papers **44:** 27-38.

Carpenter, E. J., J. P. Montoya, J. Burns, M. R. Mulholland, A. Subramaniam, and D. G. Capone. 1999. Extensive bloom of a N2-fixing diatom/cyanobacterial association in the tropical Atlantic Ocean. Marine Ecology Progress Series **185:** 273-283.

Cline, J. D., and F. A. Richards. 1972. Oxygen Deficient Conditions and Nitrate Reduction in Eastern Tropical North-Pacific Ocean. Limnology and Oceanography **17:** 885-900.

Codispoti, L. A., and J. P. Christensen. 1985. Nitrification, Denitrification and Nitrous-Oxide Cycling in the Eastern Tropical South-Pacific Ocean. Marine Chemistry **16:** 277-300.

Cullen, J. T., and R. M. Sherrell. 1999. Techniques for determination of trace metals in small samples of size-fractionated particulate matter: phytoplankton metals off central California. Marine Chemistry **67:** 233-247.

Deutsch, C., N. Gruber, R. M. Key, J. L. Sarmiento, and A. Ganachaud. 2001. Denitrification and N-2 fixation in the Pacific Ocean. Global Biogeochemical Cycles **15:** 483-506.

Gruber, N., and J. L. Sarmiento. 1997. Global patterns of marine nitrogen fixation and denitrification. Global Biogeochemical Cycles **11:** 235-266.

Helmers, E. 1996. Trace metals in suspended particulate matter of Atlantic Ocean surface water (40 degrees N to 20 degrees S). Marine Chemistry **53:** 51-67.

Helz, G. R. and others 1996. Mechanism of molybdenum removal from the sea and its concentration in black shales: EXAFS evidence. Geochimica Et Cosmochimica Acta **60:** 3631-3642.

Hem, J. D. 1978. Redox Processes at Surfaces of Manganese Oxide and Their Effects on Aqueous Metal-Ions. Chemical Geology **21:** 199-218.

Johnson, K. S., K. H. Coale, W. M. Berelson, and R. M. Gordon. 1996. On the formation of the manganese maximum in the oxygen minimum. Geochimica Et Cosmochimica Acta **60:** 1291-1299.

Karl, D., R. Letelier, L. Tupas, J. Dore, J. Christian, and D. Hebel. 1997. The role of nitrogen fixation in biogeochemical cycling in the subtropical North Pacific Ocean. Nature **388:** 533-538.

Karl, D. and others 2002. Dinitrogen fixation in the world's oceans. Biogeochemistry **57:** 47-109.

Krishnaswami, S., D. Lal, and B. L. K. Somayajulu. 1976. Investigations of Gram Quantities of Atlantic and Pacific Surface Particulates. Earth and Planetary Science Letters **32:** 403-419.

Kuss, J., and K. Kremling. 1999. Spatial variability of particle associated trace elements in near-surface waters of the North Atlantic (30 degrees N/60 degrees W to 60

degrees N/2 degrees W), derived by large-volume sampling. Marine Chemistry **68:** 71-86.
Landing, W. M., and K. W. Bruland. 1987. The Contrasting Biogeochemistry of Iron and Manganese in the Pacific-Ocean. Geochimica Et Cosmochimica Acta **51:** 29-43.
Lipschultz, F., and N. J. P. Owens. 1996. An assessment of nitrogen fixation as a source of nitrogen to the North Atlantic Ocean. Biogeochemistry **35:** 261-274.
Manheim, F. T. 1974. Chap. 42. Molybdenum. *In* K. H. Wedepohl [ed.], Handbook of Geochemistry. Springer-Verlag.
Martin, J. H., and G. A. Knauer. 1973. Elemental Composition of Plankton. Geochimica Et Cosmochimica Acta **37:** 1639-1653.
---. 1984. Vertex - Manganese Transport through Oxygen Minima. Earth and Planetary Science Letters **67:** 35-47.
Moffett, J. W. 1997. The importance of microbial Mn oxidation in the upper ocean: a comparison of the Sargasso Sea and equatorial Pacific. Deep-Sea Research Part I-Oceanographic Research Papers **44:** 1277-1291.
Moffett, J. W., and J. Ho. 1996. Oxidation of cobalt and manganese in seawater via a common microbially catalyzed pathway. Geochimica Et Cosmochimica Acta **60:** 3415-3424.
Murray, R. W., and M. Leinen. 1996. Scavenged excess aluminum and its relationship to bulk titanium in biogenic sediment from the central equatorial Pacific Ocean. Geochimica Et Cosmochimica Acta **60:** 3869-3878.
Nameroff, T. J., L. S. Balistrieri, and J. W. Murray. 2002. Suboxic trace metal geochemistry in the Eastern Tropical North Pacific. Geochimica et Cosmochimica Acta **66:** 1139-1158.
Noriki, S., T. Shiribiki, H. Yokomizo, K. Harada, and S. Tsunogai. 1997. Copper and nickel in settling particle collected with sediment trap in the western North Pacific. Geochemical Journal **31:** 373-382.
Shaw, T. J., J. M. Gieskes, and R. A. Jahnke. 1990. Early diagenesis in differing depositional environments; the response of transition metals in pore water. Geochimica et Cosmochimica Acta **54:** 1233-1246.
Sherrell, R. M. 1989. The Trace Metal Geochemistry of Supended Oceanic Particulate Matter, p. 211, Joint Program in Oceanography and Oceanographic Engineering. Woods Hole Oceanographic Institution/Massachuseets Institute of Technology.
Sherrell, R. M., and E. A. Boyle. 1992. The Trace-Metal Composition of Suspended Particles in the Oceanic Water Column near Bermuda. Earth and Planetary Science Letters **111:** 155-174.
Shimmfield, G. B., and N. B. Price. 1986. The Behavior of molybdenum and manganese during early sediment diagenesis-offshore Baja California, Mexico. Marine Chemistry **19:** 261-280.
Sproer, C., E. Lang, P. Hobeck, J. Burghardt, E. Stackebrandt, and B. J. Tindall. 1998. Transfer of Pseudomonas nautica to Marinobacter hydrocarbonoclasticus. International Journal of Systematic Bacteriology **48:** 1445-1448.
Stiefel, E. I. 1993. Molybdenum Enzymes, Cofactors, and Chemistry - an Introductory Survey. Acs Symposium Series **535:** 1-19.

---. 1996. Molybdenum bolsters the bioinorganic brigade. Science **272:** 1599-1600.
Sunda, W. G., and S. A. Huntsman. 1988. Effect of Sunlight on Redox Cycles of Manganese in the Southwestern Sargasso Sea. Deep-Sea Research Part a-Oceanographic Research Papers **35:** 1297-1317.
Taylor, S. R., and S. M. McLennan. 1985. The Continental Crust: its composition and evolution, 1st ed. Blackwell Scientific Publications.
Wallace, G. T., G. L. Hoffman, and R. A. Duce. 1977. Influence of Organic-Matter and Atmospheric Deposition on Particulate Trace-Metal Concentration of Northwest Atlantic Surface Seawater. Marine Chemistry **5:** 143-170.
Zheng, Y., R. F. Anderson, A. van Geen, and J. Kuwabara. 2000. Authigenic molybdenum formation in marine sediments; a link to pore water sulfide in the Santa Barbara Basin. Geochimica et Cosmochimica Acta **64:** 4165-4178.

CHAPTER 6. SYNTHESIS AND CONCLUSIONS

6.1 Introduction

There is a paradigm in marine chemistry that classifies element behavior in seawater as conservative, scavenged or nutrient based on their water column profiles and the differences in deep water concentrations between basins (Nozaki 1996). In this classification scheme conservative elements, with their high concentrations, invariant profiles and extreme solubility, are generally considered to have relatively uninteresting chemical behavior. The classification of Mo as conservative has led to a lack of interest in pursuing its marine biogeochemistry, despite its well known biological roles.

The hypothesis that Mo, when measured with sufficient precision, would be shown to be non-conservative in seawater was the impetus for this work. Focusing on Mo's involvement with enzymes catalyzing portions of the nitrogen cycle, this research has attempted to evaluate the role of organisms in the distribution of Mo. This data presents the most precise measurements of Mo to date in seawater, marine phytoplankton and bacteria and suspended particulate matter. The conclusion drawn from these studies set the stage for a reexamination of the marine biogeochemistry of Mo in the oceans.

6.2 Specific conclusions/contributions of this thesis

In Chapter 2, methods were described to measure Mo in seawater, phytoplankton and marine particulate matter. The Isotope Dilution (ID) method, with errors on triplicate analyses of only 0.5% (1sd), significantly improves on techniques thus far employed in

the literature(Collier 1985; Morris 1975; Nameroff et al. 2002; Sohrin et al. 1999). The methods for measuring Mo, simultaneously with several other elements (Fe, Mn, Rb and Al), in cells and particulate matter provides a precise and accurate technique that overcomes interferences from molecular and isobaric species. These methods are applicable to the low level Mo concentrations found in many natural samples. Both the seawater and particulate Mo methods are tools that may be easily applied to future studies.

In chapter 3, the high precision Mo seawater method was applied to a survey of water column profiles from the Pacific Ocean and the Sargasso and the Arabian Seas. This study demonstrates that salinity normalized Mo concentrations are not uniform through out the world ocean and therefore Mo cannot be classified as a conservative element. Profiles from the Eastern Equatorial Pacific show near surface dissolved phase concentrations that deviate from the salinity trend by up to 5%. Uptake of Mo by organisms and scavenging of Mo by Mn oxides were both examined as possible mechanisms for causing these deviations in the dissolved Mo distribution but neither mechanism requires enough Mo to deplete the dissolved phase. Depletions of Mo in the bottom waters of the California Borderland Basin profiles indicate that benthic uptake of Mo can produce resolvable depletions in dissolved Mo inventory. However simple advection diffusion calculations, suggests that the flux of Mo in or out of the sediments required to support the propagation of these features far out into the open ocean is unreasonably large. Further work is needed to derive a mechanism to explain dissolved Mo distribution in the Eastern Equatorial Pacific.

In Chapter 4, the Mo and Fe cellular concentrations and Mo:C and Fe:C ratios were measured in two N_2 fixing cyanobacteria over several diel cycles. The organisms studied were *Crocosphaera watsonii* strain WH8501,a single celled, nocturnal diazotroph, and *Trichodesmium erythraeum* strain IMS101, a non-heterocystist, filamentous, diurnal diazotroph. The Fe:C ratio of cultured *Trichodesmium* was in agreement with *Trichodesmium* colonies collected from the field, and literature values for cultured (pFe 7.8 to 7.5) and collected *Trichodesmium*. The current estimate for Fe:C in *Trichodesmium* ranges from 20 to 100 μmol Fe: mol C. The Fe:C ratio of *Crocosphaera* was established. Fe:C ratios correlate with N_2 fixation activity, when photosynthesizing conditions Fe:C ranged from 0.7 to 6.5 μmol Fe:mol C, while under N_2 fixing conditions Fe:C increased to between 7.3 to 27.1 μmol Fe:mol C.

The cellular inventories of Mo in *Crocosphaera* also correlates with N_2 fixation activity. The enzyme nitrogenase, responsible for the conversion N_2 into bioavailible nitrogen, requires large amounts of Mo and Fe. In *Crocosphaera*, estimates of metal cell quotas based on theoretical metal use efficiency of nitrogenase agree with measured cellular concentrations, implying that nitrogenase utilizes a significant fraction of Mo cellular pools and that the nitrogenase complex is synthesized de novo each night. In contrast, *Trichodesmium* maintains a likely internal pool of Mo during non-N_2 fixing periods. The different strategies employed by these organisms in response to Mo may be a result of the different nitrogen fixation strategies they use. *Crocosphaera* is a single celled organism, to protect its nitrogenase enzyme from photosynthetically derived oxygen it fixes nitrogen only at night. *Trichodesmium*, on the other hand, is a filamentous

organism, it appears to spatially separate the processes and may be able to store some quantity of enzyme even when it is not in use. Alternatively *Trichodesmium* may be using Mo for another purpose. This hypothesis is supported by the extremely high Mo concentrations measured in Trichodesmium colonies collected from the field.

Crocosphaera culture data suggests that Mo enrichment of particulates may provide a tracer of N fixation, but the large differences in Mo:C ratios of cultured and collected *Trichodesmium* implies that other factors may significantly alter Mo cellular concentrations in natural populations. These issues will need to be understood before Mo enrichment can be used to estimate N_2 fixation.

In Chapter 5, a survey of suspended particulate matter samples from the Pacific and Sargasso represent some of the first reliable measurements of Mo in marine particulate matter. There was no correlation between particulate Mo and Mn implying, that unlike sedimentary Mn oxides, water column Mn oxides do not scavenge Mo. This result may be due to different methods of Mn oxidation in the water column (microbial catalyzed oxidation (Sunda and Huntsman 1988)) and the sediments (autocatalytic oxdation (Hem 1977)). Residual particulate Mo concentrations, corrected for sea salt and terrestrial contributions, exhibited a wide range in Mo:C ratios 0.14 to 55 μmol:mol. In general the measured ratios, exceed those measured in cultures of denitrifying bacteria (0.01-0.4 μmol:mol), nitrogen fixing cyanobacteria, (0.08 to 2.4 μmol:mol) and diatoms (0.30 μmol:mol, Quigg, pers com.) Estimates of nitrate reduction rates based on particulate Mo concentrations in the OMZ of the Eastern Tropical Pacific are 2 orders of magnitude higher than in situ measurements of nitrate reduction in the Pacific. Measured

particulate Mo concentrations from the surface Sargasso Sea far exceed the Mo required to produce estimated N_2 fixation rates but are in agreement with Mo:C ratios measured in Trichodesmium colonies collected on the same cruise. These results imply that Mo enzymatic Mo demand for neither nitrogenase nor dissimilatory nitrate reducatase is a significant influence on the particulate distribution of Mo.

And finally, in Appendix 1, an experiment examined the variation in Mo:C ratio for cultures of the marine facultative denitrifying bacterium *Marinobacter hydrocarbanoclaticus* grown on nitrate or oxygen as a terminal electron sink. Mo:C ratios of cultures growing anaerobically on nitrate had Mo:C ratios 5 fold higher than when growing on oxygen. The Mo cellular concentrations are in good agreement with required enzymatic Mo based on the specific activity of dissimilatory nitrate reductase isolated from several species of *Pseudomonas*. These results suggest that increased Mo:C ratios in suspended particulate matter, particularly at depth, may be a good indication of the presence of marine denitrifying bacteria.

6.3 Wider implications of this research

Molybdenum is demonstrably non-conservative in the Eastern Equatorial Pacific, yet it fits none of the mechanisms by which elements are classified in the scavenged/nutrient/conservative paradigm. Mo's non-conservative behavior is likely to be related to processes occurring in mid-depth waters, and on only small regional scales. Increasingly it has become clear that this classification scheme does not adequately

describe observed profiles for many elements, and so-called "hybrid" distributions are used to describe profiles (see for example (Donat and Bruland 1988)).

There has been a recurrent debate in the marine nitrogen fixation literature on whether the high concentration of sulfate (28 mM) in seawater can inhibit the uptake of molybdate, the most likely form of Mo in seawater and thus limit nitrogen fixation(Cole et al. 1986; Paulsen et al. 1991). Two lines of evidence suggest that these organisms are not limited for Mo. First, the rapid release of Mo when the enzyme is not in use implies that these organisms do not have trouble acquiring Mo. Second, the Mo:C ratios measured in field samples far exceed the Mo requirements for N_2 fixation. Recent sequencing of the *Trichodesmium* genome (DOE-JGI) revealed that *Trichodesmium* contains a homologue of the Mo transport similar to the one found in *E. coli* also supports this conclusion.

6.4 Suggestions for future research

There are multiple avenues of Mo biogeochemistry to be explored. The mechanism causing non-conservative Mo behavior in the Eastern Equatorial Pacific is still unknown. A more extensive model of water mass movement may be required to determine where and how the non-conservative Mo signature forms. If it is related to fluxes from sediments due to variations in the depth of the oxygen minimum then Mo variations may provide a conservative tracer of mid depth water mass flow. This would be a critical compliment to surface floater data in a very complex region of ocean currents.

There are very few measurements of Mo flux to and from sediments. Uptake by anoxic sediments has been shown to influence Mo concentrations in bottom waters of enclosed basins. But while sediments might react rapidly to changes in bottom water redox conditions, the water column represents a temporally and spatial averaged signal that might lag significantly behind basin ventilation events. A focused study of a single basin may help to elucidate the connect between sediment flux and bottom water concentrations

Mo concentration has been evaluated in only a small number of species under a limited range of conditions. The cultures examined in this work were all grown under nutrient replete conditions, circumstances only rarely if ever encountered by organisms in situ. Repeating these experiments under nitrogen, phosphate or Fe limited conditions is critical to applying the culture results to the natural environment.

6.5 References

Cole, J. J., R. W. Howarth, S. S. Nolan, and R. Marino. 1986. Sulfate Inhibition of Molybdate Assimilation by Planktonic Algae and Bacteria - Some Implications for the Aquatic Nitrogen-Cycle. Biogeochemistry **2:** 179-196.

Collier, R. W. 1985. Molybdenum in the Northeast Pacific-Ocean. Limnology and Oceanography **30:** 1351-1354.

Donat, J. R., and K. W. Bruland. 1988. Direct Determination of Dissolved Cobalt and Nickel in Seawater by Differential Pulse Cathodic Stripping Voltammetry Preceded by Adsorptive Collection of Cyclohexane-1,2-Dione Dioxime Complexes. Analytical Chemistry **60:** 240-244.

Hem, J. D. 1977. Reactions of metal ions at surfaces of hydrous iron oxide. Geochimica et Cosmochimica Acta **41:** 527-536.

Morris, A. W. 1975. Dissolved molybdenum and vanadium in the northeast Atlantic Ocean. Deep-Sea Research and Oceanographic Abstracts **22:** 49-54.

Nameroff, T. J., L. S. Balistrieri, and J. W. Murray. 2002. Suboxic trace metal geochemistry in the Eastern Tropical North Pacific. Geochimica et Cosmochimica Acta **66:** 1139-1158.

Nozaki, Y. 1996. A fresh look at Elements Distribution in the North Pacific. Eos.
Paulsen, D. M., H. W. Paerl, and P. E. Bishop. 1991. Evidence That Molybdenum-Dependent Nitrogen-Fixation Is Not Limited by High Sulfate Concentrations in Marine Environments. Limnology and Oceanography 36: 1325-1334.
Sohrin, Y., M. Matsui, and E. Nakayama. 1999. Contrasting behavior of tungsten and molybdenum in the Okinawa Trough, the East China Sea and the Yellow Sea. Geochimica et Cosmochimica Acta 63: 3457-3466.
Sunda, W. G., and S. A. Huntsman. 1988. Effect of Sunlight on Redox Cycles of Manganese in the Southwestern Sargasso Sea. Deep-Sea Research Part a-Oceanographic Research Papers 35: 1297-1317.

Appendix 1: Variations in trace metal cellular concentrations in *M. hydrocarbanoclaticus* in response to growth on nitrate and oxygen.

A1.1 Introduction

Nitrate reductase is a molybdopterin enzyme that catalyzes the reduction of NO_3^- to NO_2^-. There are two major forms of the enzyme, assimilatory nitrate reductase which is responsible for the uptake and assimilation of nitrate as a nitrogen source, and respiratory (also called dissimilatory) nitrate reductase which allows organisms to use nitrate as a terminal electron sink in the absence of oxygen. Respiratory nitrate reductase catalyzes the initial step in the denitrification pathway, which ultimately converts nitrate into gaseous N_2O or N_2. Both types of nitrate reduction are globally important processes influencing the environment and climate both indirectly, through the limitation of primary production and controlling the removal of bioavailable nitrogen from the marine system and directly, through production of the green house gas N_2O(Mancinelli 1996).

Nitrate reductase is a ubiquitous enzyme, present both in prokaryotes and eukaroytes. It is likely to be the most common use of Mo in marine organisms(Stiefel 1993; Stolz and Basu 2002). The amount of Mo required by phytoplankton and heterotrophic bacteria to support nitrate reductase activity is unknown. The enzyme has a very high specific activity; μmol NO_3^{-1} min^{-1} mg $enzyme^{-1}$ as opposed to the nmol N_2 min^{-1} mg $enzyme^{-1}$ rate measured for nitrogenase, the enzyme responsible for N_2 fixation. It is likely that only a very small amount of Mo is required as assimilatory nitrate reductase to support growth on nitrate. Phytoplankton utilizing nitrate and thus requiring the Mo-containing nitrate reductase enzyme have low Mo:C ratios (0.30 μmol:mol: Quigg pers com.) On the other hand respiratory nitrate reductase, which provides all of

the energy for anaerobic growth of denitrifying organisms, may have larger Mo:C ratios due to the need to reduce greater amount of nitrate. If Mo cellular concentration or Mo:C ratios correlate with nitrate reduction rate, Mo in particulate material may provide a tracer of denitrification activity in the marine environment

To test how Mo cellular concentrations change under growth by denitrification, a facultative marine denitrifying bacterium, *Marinobacter hydrocarbanoclaticus* (formerly *Pseudomonas nautica* (Sproer et al. 1998) was grown aerobically on oxygen and anaerobically on nitrate. Mo, Fe and Cu cellular concentrations and carbon ratios were measured under both conditions. All of these metals may be affected by the transition from growth on oxygen to growth on nitrate (Moura and Moura 2001). Nitrate reductase contains both Fe and Mo. The Fe:Mo ratio of the enzyme ranges from 13 to 21 mol:mol (Baumann et al. 1996; Blumle and Zumft 1991; Carlson et al. 1982; Correia et al. 2001; Ishizuka et al. 1984; Krause and Nealson 1997). Cu can be involved in enzymes responsible for two other steps in the denitrification pathway; nitrite reductase has both CuFe and Fe-only versions while nitrous oxide dehydrogenase has only been isolated as a Cu enzyme(Moura and Moura 2001). Cu cellular concentration may give us additional information on the subsequent denitrification steps. Nitrate reduction rates were calculated for the anaerobic culture and compared to the specific activity of nitrate reductase isolated from other denitrifying bacteria. This allows the estimation of what fraction of the measured Mo concentrations is related to nitrate reductase activity.

A1.2 Methods

M. hydrocarbanoclaticus strain 617 was obtained from the American type culture collection. *M. hydrocarbanoclaticus* is a facultative marine denitrifying bacterium that

has been isolated from the water column near Hawaii and contaminated sediments in the Mediterranean (Sproer et al. 1998). All cultures were grown on a 3/4th Sargasso seawater based medium amended to a final concentration of 12 mM nitrate, 3 mM ammonia, 0.2 mM phosphate, 0.18% (w/v) sodium lactate and 50 nM Fe(III)citrate.

Aerobic and Anaerobic stock cultures were prepared from *M. hydrocarbanoclaticus* colonies grown on nitrate agar plates. All cultures were incubated at approximately 31°C on a reciprocal shaker at 96 rpm. Aerobic stocks were grown in 250 ml Erlenmeyer flask containing 100 ml of medium. All glass and plastic ware used in medium preparation and experiments was acid cleaned. Anaerobic stocks were incubated in 150 ml serum flasks containing 120 ml of media and sealed with red rubber stoppers and aluminum crimps. Anaerobic conditions were obtained by bubbling nitrogen through the media for at least 30 minutes, flushing the serum flasks with nitrogen and anaerobically dispensing the media. Culture growth was determined by optical density at 450 nm. Stock cultures were grown under aerobic or anaerobic conditions for at least 10 doubling times before they were used. An inoculum from a late log phase culture was added to initialize both experiments.

The aerobic experiment was performed in duplicate. Two 1.8 L Fernbochs containing 500 mL of medium each were inoculated with 5 ml aliquots of aerobic preculture. Samples were taken every 2 hours for nitrate and nitrite analyses and absorbance measurements. The cultures were harvested in late log phase growth by centrifugation (5000 rpm, 15°C, 15 minutes). The cells were resuspended and homogenized on a vortex mixer. Known fractions of the cell suspensions were filtered for carbon and metal analyses. Metal samples were filtered onto a 0.22 μm an acid-

cleaned polycarbonate membrane filter (method described in Chapter 2). Filters were folded in half and placed in an acid cleaned petri dish and frozen for storage. Carbon samples were collected on ashed GFF filters. Cell counts of the Carbon filtrate indicate that less than 1% of the cells were lost through the GFF filter.

The anaerobic experiment was initiated by inoculating 8 (A-H) 150 ml serum flasks containing 120 ml of anaerobic medium with 3 ml of the anaerobic preculture. Growth rate was determined for each replicate by absorbance. Absorbance to cell count relationship for anaerobic cultures were determined for one of the replicates. Two replicates were used to monitor nitrate and nitrite concentrations. At late log phase growth the cultures were harvested by centrifugation. The six replicates were paired together prior to centrifugation based on similar growth rates in order to have enough material for metal and carbon analysis. This resulted in triplicate metal and carbon analyses. Metal and Carbon samples were collected using the same procedure as the aerobic samples.

The assumption in both of the above experiments was that the difference in metal concentrations reflected changes in the internal cellular pool. However changes in redox conditions can also cause changes in the extracellular adsorption of metals to cell surfaces. For instance Fe forms Fe oxyhydroxides that can adhere to cells under oxic conditions. To test this problem a batch of cells was grown aerobically to late log phase and harvested via centrifugation. An aliquot of these cells was harvested as a control and measured for metal concentrations. Another aliquot was autoclaved to kill the cells, and another was poisoned with sodium azide, a metabolic inhibitor that interferes with electron transport. These cell suspensions were inoculated into anaerobically prepared

150 ml serum-flask containing 120 ml of anaerobic media with 8 mM nitrate and 8 mM nitrite to mimic media conditions at the end of an anaerobic experiment. These cells were incubated at 30°C and 96 rpm for 6 hours and then harvested for metal analyses.

Nitrate and nitrite in the media samples were measured on a SKALAR SANplus Continuous Flow Analyzer. Carbon and nitrogen analyses of the GFF filters were determined on an Exeter Analytical CE-440 C/N analyzer. Metal filter analysis procedures are described in depth in Chapter 2 and Chapter 5. Filters were leached to dissolve cells. Mo, Cu and Fe were measured via isotope dilution ICP-MS. Media blanks for metals and organic analyses were measured. Media blanks were always less than 11% on Cu, 13% on Fe and 22% on Mo. Though carbon and nitrogen media blanks were high (<33 and <42 %, respectively) due to residual media on the samples and the mM levels nitrate, ammonia and lactate in the media, they were consistent (1sd ±7.5%).

A1.3 Results and Discussion

The result of the test for changes in extracellular metal concentrations due to changes in redox conditions is shown in Figure A1.1. Neither the Azide nor the Autoclaved sample showed any cellular growth. The concentration of nitrite in each sample after the incubation was similar to an un-inoculated control. Neither treatment had a significant effect on the Mo concentration of the cells. Azide and Autoclave treated cells have Mo concentrations equivalent the aerobic control cells. Iron shows a slight enrichment in the azide treated sample, but a huge (6-fold) enrichment in the autoclaved cells compared to the initial aerobic control. Similarly the Cu analyses showed large 3.5 fold enrichment in the autoclave sample, but no response in the azide treated samples.

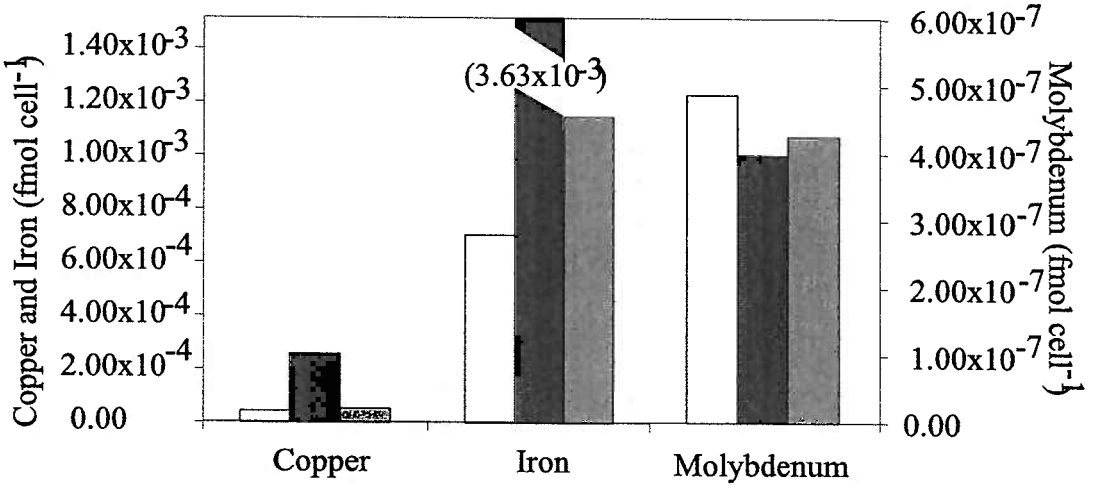

Figure A1.1 Cu, Fe and Mo cellular concentrations in cells of M. hydrocarbanoclaticus grown aerobically (white bars) and incubated in anaerobic media following one of two treatments to inhibit cellular growth (dark grey bars)50 minutes in the autoclave or (light grey bars) addition of sodium azide to inhibit growth.

The large increases of Fe and Cu in the autoclaved sample were likely due to metal contamination from the autoclave itself. These results suggest that the redox changes in the media do not effect the extracellular concentration of Mo or Cu but may have a slight effect on Fe.

The aerobic experiment (Figure A1.2) had a doubling time of 1.2 hrs. The anaerobic experiment (Figure A1.3) had an average doubling time of 2.13 hrs. Bonin et al. (1992) measured doubling times for *M. hydrocarbanoclaticus* on both oxygen (1.5 hr) and nitrate (3 hrs). The Bonin et al. (1992) cultures were grown at 30°C while the experiments presented here were measured at approximately 31°C, which may account for the more rapid growth rates seen in these samples.

No nitrate was consumed during the course of the aerobic experiment. Nitrite remained undetectable throughout the experiment. *M. hydrocarbanoclaticus* uses ammonia as its nitrogen source for both aerobic and anaerobic growth. Nitrate is reduced as a terminal electron acceptor, and only when oxygen is limited.

The anaerobic experiment had produced approximately 1.5 mM of nitrite when the experiment was terminated. There was a long delay in the production of nitrite, which may be due to contamination by trace amounts of oxygen in the media (Figure A1.3). Trace oxygen contamination would be expected to increase growth rate. This effect may not be observed however if it occurred only in the early part of the experiment, before the cell density was high enough for reliable absorbance measurements. The replicate analyses of the nitrate samples are too variable to demonstrate unambiguously whether this culture was producing nitrous oxide. This could be demonstrated if the nitrate+nitrite concentration of the final samples were

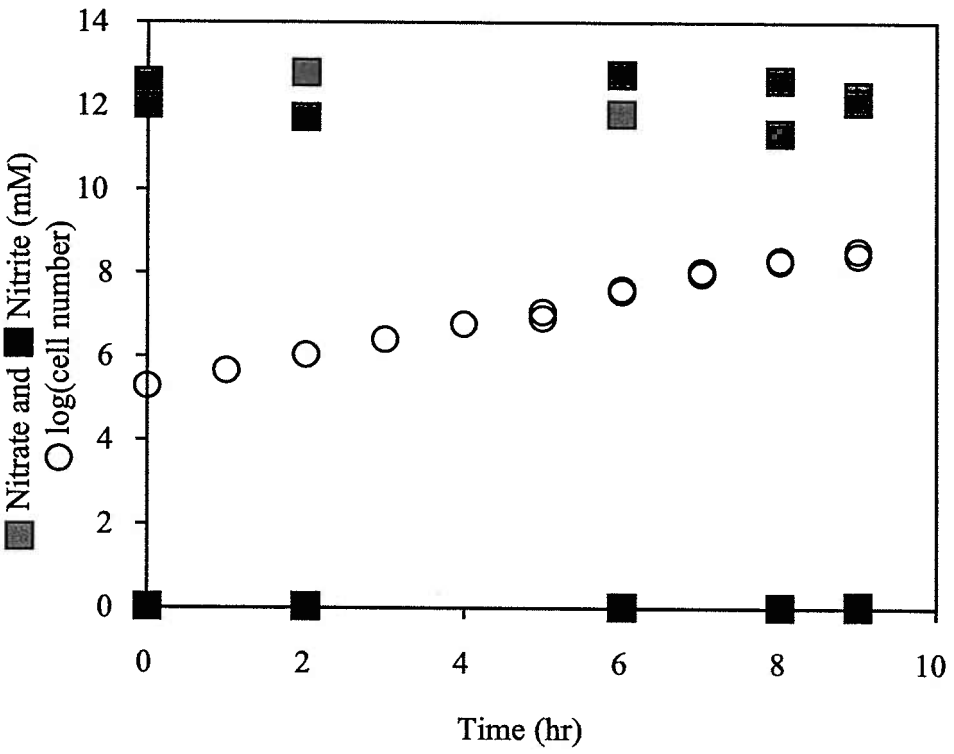

Figure A1.2 Aerobic cultures of M. hydrocarbanoclaticus showing Log(Cell number) Nitrite (mM) and Nitrate (mM) concentrations.

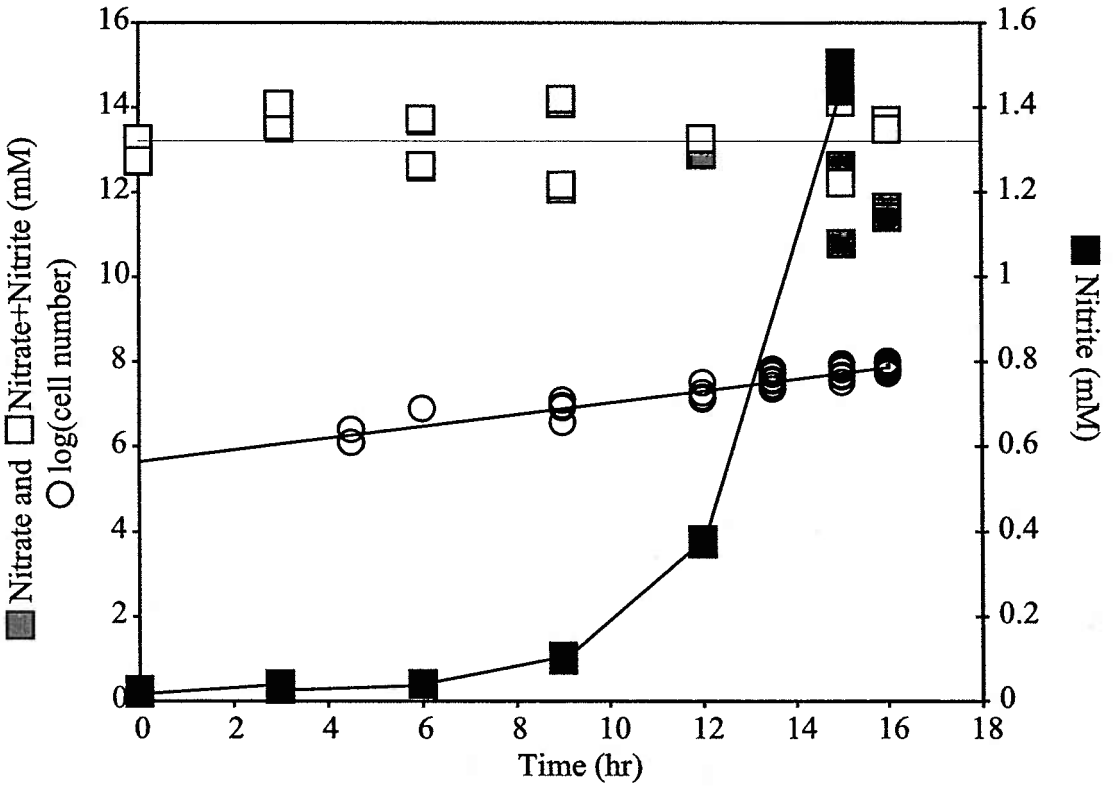

Figure A1.3 Anaerobic cultures of M. hydrocarbanoclaticus showing Log(Cell number) Nitrite (mM) and Nitrate (mM) and Nitrate+Nitrite concentrations

significantly less than the initial nitrate concentrations. Nitrous oxide production in these cultures cannot be proved or precluded.

Metal ratios of the aerobic and anaerobic cells are shown in Figure A1.4. Fe:C ratios were slightly higher in the aerobic experiments. This could be the effect of increased internal demand under oxic conditions. Extracellular Fe oxyhydroxide precipitation under oxic conditions might also contribute, but aerobic cells exposed to oxygen limited conditions did not show a decrease in Fe concentration when implying that the increased Fe is intracellular. Error bars on the replicate aerobic analyses are such that it is impossible to determine a difference between the aerobic and anaerobic experiments for Cu:C ratios. The lack of increased Cu ratios in the anaerobic experiment suggests that either *M. hydrocarbanoclaticus* utilizes significant Cu enzymes during aerobic growth, that insufficient concentrations of nitrite reductase and nitrous oxide dehydrogenase were synthesized or that *M. hydrocarbanoclaticus* produces the Fe-only form of nitrite reductase and did not produce nitrous oxide dehydrogenase. The nitrite concentration in the experiment was increasing exponentially when these cells were harvested and there was no significant depletion of the nitrate+nitrite concentration supporting the interpretation that only small amounts of nitrite reductase were present.

The Mo:C ratios are unambiguously higher in the anaerobic cultures. The 5-fold increase indicates that initiation of nitrate reduction was can significantly affect Mo:C ratios. At 0.48 μmol:mol the Mo:C ratio in anaerobic *M. hydrocarbanoclaticus* is slightly higher than the Mo:C ratio of diatoms grown on nitrate (0.29 μmol:mol Quigg et al in prep.) but lower that seen in N_2 fixing cyanobacteria (0.71 to 1.33 μmol:mol Tuit 2003: Chapter 4) The Fe:Mo ratio in the anaerobic samples (58 mol:mol) is much lower

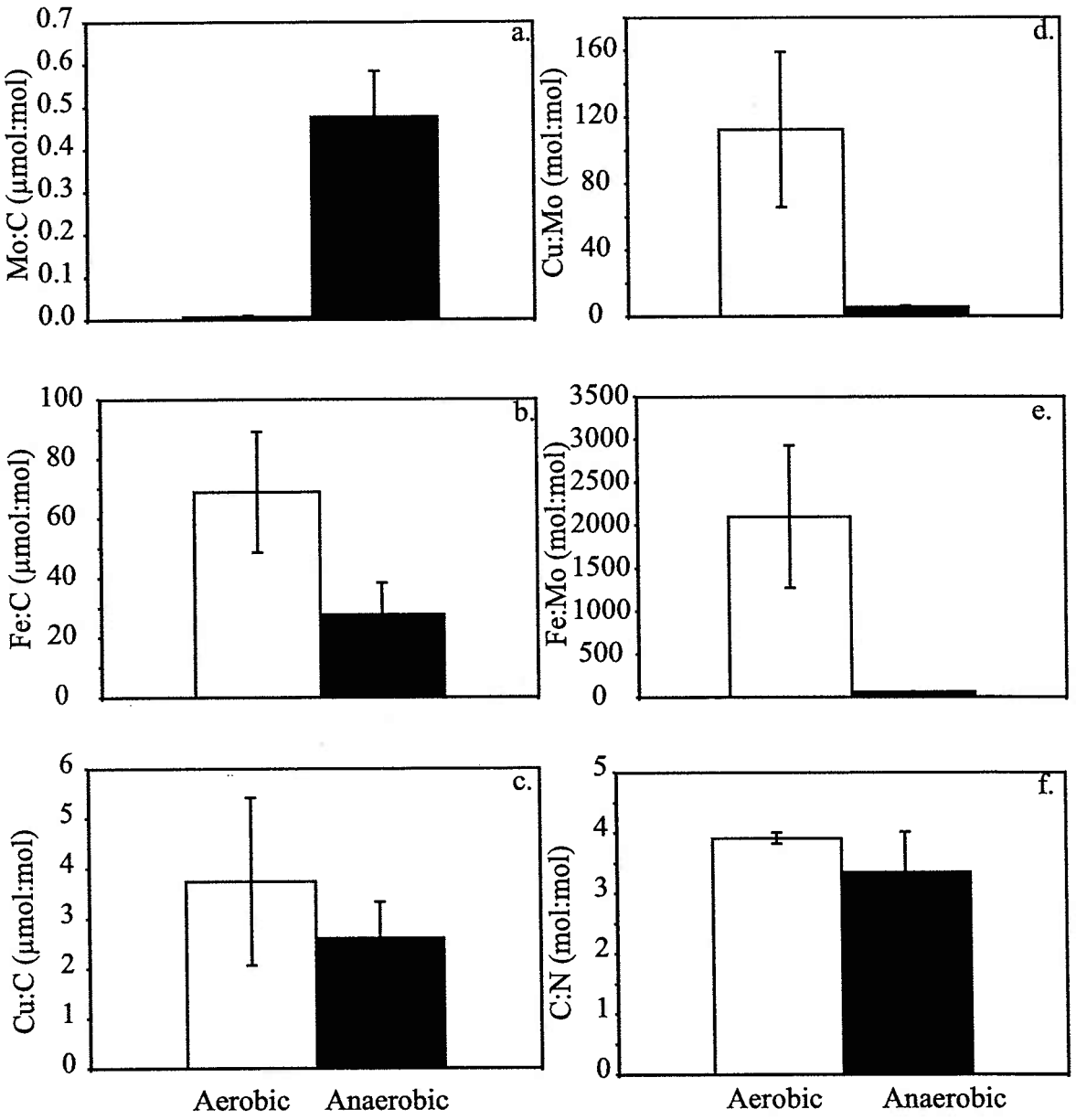

Figure A1.4 Cellular ratios of aerobic (white bars) and anaerobic (black bars) for a) Mo:C (µmol:mol), b) Fe:C (µmol:mol), c) Cu:C (µmol:mol), d) Cu:Mo (mol:mol), e) Fe:Mo (mol:mol), e) C:N (mol:mol). Error bars are one standard deviation for aerobic (n=2) and anaerobic (n=3). (mol:mol), e) Fe:Mo (mol:mol), f) C:N (mol:mol). Error bars are one standard deviation for aerobic (n=2) and anaerobic (n=3).

than in the aerobic samples (2100 mol:mol) but is still 3-5 fold higher than the Fe:Mo ratio seen in nitrate reductase enzymes (Table A1.1) This is reasonable because Fe is involved in many other enzymes, but it suggests that nitrate reductase makes up a significant fraction of the physiological utilized Fe pool under nitrate reducing conditions.

If nitrous oxide production is negligible, then the rate of nitrate reduction is equivalent to the rate of nitrite production. The nitrite production rate for the anaerobic experiment was $9.25\pm0.78\times10^{-14}$ μmol min^{-1} cell. *M. hydrocarbanoclaticus* nitrate reductase has been isolated. It is a membrane bound respiratory nitrate reductase with a molecular weight of approximately 201 kDa (Correia et al. 2001). The Mo concentration per cell ($1.21\pm0.17\times10^{-5}$ fmol $cell^{-1}$) and molecular weight of nitrate reductase can be used to convert the measured nitrite production rate into a putative enzyme activity of 38.1 ± 6.3 μmol min^{-1} mg $protein^{-1}$, via the equation,

$$A = \frac{NAR\left(\frac{\mu mol\ NO_3^{-2}\ reduced}{min \times cell}\right)}{[Mo]\left(\frac{fmol}{cell}\right)\times10^{-15}\left(\frac{mol\ Mo}{fmol\ Mo}\right)\times\left(\frac{1}{1}\right)\left(\frac{mol\ protein}{mol\ Mo}\right)\times MWt\ protein\left(\frac{g}{mol}\right)\times10^{3}\left(\frac{mg}{g}\right)}$$

Where NAR is the rate of nitrate reduction, [Mo] is the concentration of Mo in the anaerobic cells and MWt is the molecular weight of nitrate reductase. This equation assumes that all Mo in the cell is associated with nitrate reductase. Table A1.1 lists some of the data available for membrane bound respiratory nitrate reductase isolated from several other denitrifying bacteria. The enzyme activity measured in this experiment is in agreement with the specific activities listed Table A1.1. It is also consistent with nitrate

reductase activities measured in other *M. hydrocarbanoclaticus* experiments (Bonin and Gilewicz 1991). It suggests that most if not all of the Mo in *M. hydrocarbanoclaticus* under anaerobic conditions is associated with nitrate reductase.

Table A1.1. Membrane-bound respiratory nitrate reductase enzymatic Characteristics.

Organism		Molecular weight (kDa)	Mo:Fe (mol:mol)	Specific Activity (μmol min^{-1} mg^{-1})	Ref
M. hydrocarbanoclaticus		201			[a]
S. putrefaciens		210	1:14	31 to 60	[b]
Ps stuzeri		172	1:13	27	[c]
Ps. aeruginosa		220	1:21	50	[d]
Ps. denitrificans	**NR1**	220 to 230	1:14	36-48	[e]
	NR2	190 to 200	1:13	42-58	[e]

[a]This Study [b](Krause and Nealson 1997) [c](Blumle and Zumft 1991) [d](Godfrey et al. 1984) [e](Ishizuka et al. 1984)

A1.4 Conclusion

This experiment indicates that Mo:C ratios and Mo concentrations are 5 fold enriched in *M. hydrocarbanoclaticus* when growing anaerobically. The Mo:C ratios are slightly higher than diatoms growing on nitrate but lower than N_2 fixing cyanobacteria suggesting that the presence of respiratory denitrifying bacteria may lead to increased Mo:C ratios in suspended particulate matter. The good agreement between Mo based nitrate reductase efficiency calculated here and those measured in cultures of other denitrifiers, suggests that most if not all of the Mo in denitrifying bacteria is used in nitrate reductase. This implies that, in regions where other biological or inorganic Mo–containing phases are less significant, particularly in oxygen minimum zones where denitrification drives most of the carbon remineralization, the particulate Mo concentration of particulate matter may provide an additional estimate nitrate reduction rate.

A1.5 References

Baumann, B., M. Snozzi, A. J. B. Zehnder, and J. R. vanderMeer. 1996. Dynamics of denitrification activity of Paracoccus denitrificans in continuous culture during aerobic-anaerobic changes. Journal of Bacteriology **178:** 4367-4374.

Blumle, S., and W. G. Zumft. 1991. Respiratory Nitrate Reductase from Denitrifying Pseudomonas- Stutzeri, Purification, Properties and Target of Proteolysis. Biochimica Et Biophysica Acta **1057:** 102-108.

Bonin, P., and M. Gilewicz. 1991. A Direct Demonstration of Co-Respiration of Oxygen and Nitrogen-Oxides by Pseudomonas-Nautica - Some Spectral and Kinetic-Properties of the Respiratory Components. Fems Microbiology Letters **80:** 183-188.

Carlson, C. A., L. P. Ferguson, and J. L. Ingraham. 1982. Properties of Dissimilatory Nitrate Reductase Purified from the Denitrifier Pseudomonas-Aeruginosa. Journal of Bacteriology **151:** 162-171.

Correia, C. and others 2001. Spectroscopic characterization of the membrane nitrate reductase isolated from Pseudomonas nautica. Journal of Inorganic Biochemistry **86:** 186-186.

Godfrey, C., C. Greenwood, A. J. Thomson, R. C. Bray, and G. N. George. 1984. Electron-Paramagnetic-Resonance Spectroscopy Studies on the Dissimilatory Nitrate Reductase from Pseudomonas-Aeruginosa. Biochemical Journal **224:** 601-608.

Ishizuka, M., T. Toraya, and S. Fukui. 1984. Purification, Properties and Limited Proteolysis of Nitrate Reductase from Pseudomonas-Denitrificans. Biochimica Et Biophysica Acta **786:** 133-143.

Krause, B., and K. H. Nealson. 1997. Physiology and enzymology involved in denitrification by Shewanella putrefaciens. Applied and Environmental Microbiology **63:** 2613-2618.

Mancinelli, R. L. 1996. The nature of nitrogen: an overview. Life Support & Biosphere Science: International Journal of Earth Space **3:** 17-24.

Moura, I., and J. J. G. Moura. 2001. Structural aspects of denitrifying enzymes. Current Opinion in Chemical Biology **5:** 168-175.

Sproer, C., E. Lang, P. Hobeck, J. Burghardt, E. Stackebrandt, and B. J. Tindall. 1998. Transfer of Pseudomonas nautica to Marinobacter hydrocarbonoclasticus. International Journal of Systematic Bacteriology **48:** 1445-1448.

Stiefel, E. I. 1993. Molybdenum Enzymes, Cofactors, and Chemistry - an Introductory Survey. Acs Symposium Series **535:** 1-19.

Stolz, J. F., and P. Basu. 2002. Evolution of nitrate reductase: molecular and structural variations on a common function. Chembiochem: a European Journal of Chemical Biology **3:** 198-206.

Appendix 2: Data Tables For Molybdenum Sea Water Analyses

A2.1 Arabian Sea Profile (19 10N 67 10E) JGOFS P4 N7 July 1995 R/V Tommy G. Thompson [a]

Sample	Depth	Mo	1 sd	n	Filter	Collec-tion	Salinity	Mo Salinity norm-alized	Temper-ature	Oxygen	Flouro-meter	Trans-misson	NO_3^-	NO_2^-	PO_4^{3-}	Mn
	m	nmol/kg				method	ppt	nmol/kg	°C	mmol/kg	mg/kg		µM	µM	µM	nM
643	10	113.26	0.00	3	UnF	CTD	36.6990	108.01	24.73	165.84	1.300		7.02	0.27	0.75	2.97
639	50	112.81	0.00	3	UnF	CTD	36.5250	108.10	23.43	136.31	0.028		11.26	0.03	1.11	1.62
635	100	112.25	0.45	3	UnF	CTD	36.4790	107.70	20.05	6.81	0.021		23.62	0.01	2.18	0.88
234	140	111.00	0.49	2	UnF	CTD	36.0100	107.89	17.68	0.81	0.157		20.39	1.72	2.35	
631	190	110.54	0.12	2	UnF	CTD	35.9710	107.56	15.44	1.08	0.259		17.60	3.50	2.45	5.58
629	250	110.86	0.30	2	UnF	CTD	35.8760	108.15	14.39	0.80	0.295		19.34	3.01	2.48	5.50
627	300	111.13	0.65	2	UnF	CTD	35.8520	108.49	13.81	0.76	0.289		22.65	1.72	2.53	3.94
626	350	110.36	0.31	2	UnF	CTD	35.8610	107.71	13.26	0.80	0.314		23.80	1.43	2.59	3.08
625	400	110.24	0.43	2	UnF	CTD	35.8120	107.75	12.76	0.80	0.323		25.22	1.01	2.64	4.08
624	450	108.94	0.33	2	UnF	CTD	35.7600	106.63	12.38	1.03	0.335		26.41	0.74	2.67	
623	500	110.80	0.85	2	UnF	CTD	35.7150	108.58	0.00	0.00	0.000					5.37
	550								11.93	0.76	0.332		28.00	0.51	2.71	4.59
621	600	109.86	0.83	2	UnF	CTD	35.6170	107.96	11.48	0.89	0.327		29.64	0.23	2.74	4.14
618	800	108.42	0.08	2	UnF	CTD	35.5000	106.89	9.97	1.43	0.322		34.81	0.00	2.89	3.20
616	1000	109.42	0.22	2	UnF	CTD	35.3490	108.34	8.46	4.47	0.333		38.20	0.00	3.01	0.98
606	2000	106.35	0.11	2	UnF	CTD	34.8420	106.83	3.18	88.29	0.000		38.40	0.00	0.00	
654	3000	106.63	0.41	2	UnF	CTD	34.7440	107.42	1.81	127.68	0.000		37.41	0.00	2.61	
650	16	113.23	0.10	2	F	Go-Flo	36.6970	108.00	27.98	196.41	0.451		0.28	0.00	0.29	
647	51	112.18	0.43	3	F	Go-Flo	36.5250	107.50	24.49	165.84	0.615		9.75	0.07	0.82	
645	88	112.75	0.42	3	F	Go-Flo	36.5000	108.12	23.76	139.59	0.253		10.88	0.05	1.07	

[a]Samples provided by Chris Measures and Sue Vink

A2.2 Sargasso Sea Profile (25 60N 70 04W) March 1998 R/V Oceanus 318[a]

Sample	Depth	Mo	1 sd	n	Filter	Collection	Salinity	Mo Salinity normalized	Temperature	Oxygen	Flouro-meter	Transmisson	NO_3^-	NO_2^-	PO_4^{3-}	Mn
	m	nmol/kg				method	ppt	nmol/kg	°C	mmol/kg	mg/kg		µM	µM	µM	nM
10	10	112.67	0.20	3	F	Go-Flo	36.5842	107.79	24.43	4.04	0.044		0.00			
20	20	113.20	0.47	3	F	Go-Flo	36.5807	108.31	24.37	4.00	0.053					
30	30	113.02	0.00	1	F	Go-Flo	36.5801	108.13	24.36	3.89	0.057					
40	40	111.58	0.00	1	F	Go-Flo	36.5816	106.75	24.35	3.78	0.054					
50	50	112.69	0.26	2	F	Go-Flo	36.5856	107.81	24.35	3.77	0.063		0.00			
70	70	112.36	0.00	1	F	Go-Flo	36.5942	107.47	24.33	3.93	0.063					
	80												0.00			
90	90	112.79	0.00	1	F	Go-Flo	36.6015	107.86	24.30	3.70	0.091					
110	110	112.62	0.00	1	F	Go-Flo	36.6835	107.45	23.89	3.74	0.169					
	125												1.72			
130	130	112.56	0.00	1	F	Go-Flo	36.8743	106.84	23.32	3.87	0.286					
150	150	113.49	0.13	2	F	Go-Flo	36.9197	107.59	22.03	3.96	0.139					
200	200	111.94	0.00	1	F	Go-Flo	36.7724	106.55	20.11	4.01	0.036					
300	300	112.43	0.48	2	F	Go-Flo	36.5308	107.72	18.33	4.33	0.030					

[a]Nitrate data provided by Kent Cavender-Bares

A2.3Transect 2 (16 00N 150 00W) June 2000 R/V Roger Revelle [a]

Sample	Depth m	Mo nmol/kg	1 sd	n	Filter	Collection method	Salinity ppt	Mo Salinity norm-alized nmol/kg	Temperature °C	Oxygen mmol/kg	Flouro meter mg/kg	Trans-misson	NO_3^- µM	NO_2^- µM	PO_4^{3-} µM	Mn nM
02-02-24	23	105.21	0.14	3	F	CTD	34.5786	106.50	24.84	182.95	0.129	92.59	0.18	0.00	0.18	
02-02-23	43	105.67	0.77	2	F	CTD	34.5785	106.96	24.84	185.31	0.131	92.60	0.00	0.00	0.00	
02-02-22	63	105.15	0.76	2	F	CTD	34.5786	106.44	24.84	185.02	0.138	92.58	0.17	0.00	0.17	
02-02-21	82	105.02	0.29	3	F	CTD	34.6394	106.12	24.67	187.86	0.162	92.59	0.00	0.00	0.00	
02-02-20	103	105.55	0.18	2	F	CTD	35.0458	105.41	22.30	201.09	0.211	92.58	0.09	0.00	0.09	
02-02-19	122	106.29	2.58	2	F	CTD	34.8757	106.67	20.51	198.38	0.364	92.54	0.21	0.08	0.21	
02-02-18	142	107.13	0.70	2	F	CTD	35.0090	107.10	20.18	194.66	0.288	92.82	0.19	0.07	0.19	
02-02-17	162	105.43	0.13	3	F	CTD	34.9215	105.66	18.94	186.08	0.199	93.06	0.31	0.03	0.31	
02-02-16	182	105.48	0.10	2	F	CTD	34.6382	106.59	16.57	181.91	0.151	93.22	0.56	0.00	0.56	
02-02-15	202	103.35	0.21	2	F	CTD	34.3669	105.25	14.33	181.05	0.133	93.27	0.61	0.01	0.61	
02-02-14	226	103.42	0.35	3	F	CTD	34.1981	105.85	12.39	182.63	0.128	93.35	1.09	0.00	1.09	
02-02-13	251	104.12	0.02	2	F	CTD	34.1667	106.65	10.79	173.69	0.125	93.37	1.43	0.00	1.43	
02-02-12	277	103.50	0.63	2	F	CTD	34.1654	106.02	10.02	154.33	0.133	93.38	1.99	0.00	1.99	
02-02-11	321	104.74	0.01	2	F	CTD	34.3713	106.66	9.57	59.22	0.148	93.32	2.38	0.00	2.38	
	351								8.51	71.20	0.140	93.36	2.55	0.00	2.55	
	400								8.11	31.48	0.142	93.36	2.80	0.00	2.80	
	450												2.90	0.00	2.90	
	500								7.21	14.95	0.144	93.38	3.01	0.00	3.01	
	550												3.07	0.00	3.07	
	600								6.29	16.68	0.141	93.43	3.12	0.00	3.12	
	650												3.14	0.00	3.14	
	700								5.62	18.29	0.137	93.46	3.20	0.00	3.20	
	750												2.97	0.00	2.97	

A2.3Transect 2 continued.

Sample	Depth m	Mo nmol/kg	1 sd	n	Filter	Collection method	Salinity ppt	Mo Salinity norm-alized nmol/kg	Temperature °C	Oxygen mmol/kg	Flouro meter mg/kg	Trans-misson	NO_3^- µM	NO_2^- µM	PO_4^{3-} µM	Mn nM
	800								4.98	28.92	0.134	93.48	3.18	0.00	3.18	
	900								4.16	40.21	0.136	93.51	3.18	0.00	3.18	
	1000								3.54	50.29	0.141	93.53	3.17	0.00	3.17	
	1500								2.82	66.47	0.135	93.55	3.01	0.00	3.01	
02-02-20	103	107.07	0.00	1	UnF	CTD	35.0458	106.93								
02-08-19	122	106.54	0.00	1	UnF	CTD	34.8757	106.92								
02-02-15	202	104.04	0.00	1	UnF	CTD	34.3669	105.96								

[a]Samples provided by Brian Popp and Eric DeCarlo

A2.4Transect 4 (16 00N 119 00W) June 2000 R/V Roger Revelle[a]

Sample	Depth	Mo	1 sd	n	Filter	Collection	Salinity	Mo Salinity norm-alized	Temperature	Oxygen	Flouro meter	Trans-misson	NO_3^-	NO_2^-	PO_4^{3-}	Mn
	m	nmol/kg				method	ppt	nmol/kg	°C	mmol/kg	mg/kg		µM	µM	µM	nM
04-02-22	21	104.24	0.00	1	F	CTD	34.5633	105.55								
04-13-17	23	104.54	0.03	2	F	CTD	34.5584	105.88	25.19	186.93	0.135	92.41	0.37	0.00	0.18	
04-13-16	42	105.19	0.28	3	F	CTD	34.5965	106.42	23.77	191.35	0.160	92.42	0.08	0.00	0.20	
04-02-19	81	104.61	1.42	2	F	CTD	34.5777	105.89	21.83	206.61	0.189	92.60				
04-02-18	101	102.94	0.15	2	F	CTD	34.2111	105.32	18.34	204.62	0.343	92.51	0.87	0.08	0.38	
04-02-17	125	103.68	0.15	2	F	CTD	34.2461	105.96	15.69	97.69	0.264	92.84	21.28	0.03	1.88	
04-13-06	152	105.66	0.00	1	F	CTD	34.4565	107.33	13.42	32.91	0.167	93.07	24.98	0.00	2.28	
04-02-15	175	105.65	0.30	2	F	CTD	34.6911	106.59	12.90	8.87	0.166	93.13	26.60	0.02	2.55	
04-02-14	199	105.12	0.37	2	F	CTD	34.7040	106.02	12.16	7.03	0.169	93.11	26.66	0.01	2.60	
04-13-05	226	105.63	0.58	2	F	CTD	34.7006	106.54	11.58	4.50	0.169	92.90	28.55	0.06	2.67	
04-13-04	252	105.47	0.44	2	F	CTD	34.6614	106.50	11.08	5.56	0.168	93.09	29.59	0.00	2.68	
04-02-11	300	105.79	0.12	2	F	CTD	34.6469	106.87	10.52	5.54	0.165	93.04	25.93	0.00	2.65	
04-13-03	302	105.56	0.06	2	F	CTD	34.6326	106.68	10.37	4.48	0.166	93.07	30.15	0.00	2.77	
04-02-09	524	105.53	0.46	2	F	CTD	34.5154	107.01	7.48	8.45	0.149	93.11	37.30	0.00	3.06	
04-02-08	697	105.11	0.09	2	F	CTD	34.5122	106.60	6.05	7.22	0.148	93.19	42.19	0.00	3.30	
04-02-04	1197	104.85	0.12	2	F	CTD	34.5622	106.18	3.74	38.20	0.149	93.29	44.23	0.00	3.25	
04-02-02	1795	104.77	0.66	2	F	CTD	34.6185	105.92	2.48	74.66	0.139	93.36	41.90	0.00	3.01	
04-02-14	199	106.46	0.00	1	UnF	CTD	34.7040	107.37								
04-02-18	101	103.92	0.00	1	UnF	CTD	34.2111	106.31								
04-02-19	81	104.77	0.00	1	UnF	CTD	34.5777	106.05								
04-02-22	21	104.55	0.00	1	UnF	CTD	34.5633	105.87								
04-13-06	152	105.24	0.61	2	UnF	CTD	34.4565	106.90								
04-13-16	42	105.90	0.00	1	UnF	CTD	34.5965	107.13								

[a]Samples provided by Brian Popp and Eric DeCarlo

A2.5Transect 5 (16 00N 107 00W)June 2000 R/V Roger Revelle [a]

Sample	Depth m	Mo nmol/kg	1 sd	n	Filter	Collec-tion method	Salinity ppt	Mo Salinity norm-alized nmol/kg	Temper-ature °C	Oxygen mmol/kg	Flouro-meter mg/kg	Trans-misson	NO_3^- µM	NO_2^- µM	PO_4^{3-} µM	Mn nM
5-2-23	11	105.59	0.05	3	F	CTD	34.4902	107.15	28.78	177.82	0.163	92.37	0.36	0.00	0.20	
5-2-21	20	104.41	0.14	3	F	CTD	34.4905	105.96	28.76	182.18	0.170	92.34	0.07	0.00	0.20	
5-2-20	44	105.04	0.55	3	F	CTD	34.7350	105.85	25.88	197.84	0.352	91.63	4.16	0.15	0.70	
5-2-19	54	104.58	0.11	2	F	CTD	34.4907	106.12								
5-2-18	65	105.96	0.47	2	F	CTD	34.5846	107.23	18.36	34.74	0.341	92.70	25.37	0.16	2.17	
5-2-17	74	106.20	0.64	2	F	CTD	34.6197	107.37								
5-2-16	84	105.14	0.32	2	F	CTD	34.6392	106.23	15.57	9.64	0.221	93.05	15.57	0.03	2.47	
5-2-15	104	105.61	0.58	2	F	CTD	34.7029	106.52								
5-2-14	129	106.24	0.11	3	F	CTD	34.7447	107.02								
5-2-13	154	106.40	0.00	1	F	CTD	34.7587	107.14	12.43	-2.54	0.183	92.86	12.49	3.23	2.63	
5-2-12	203	107.33	1.17	3	F	CTD	34.7404	108.13	11.58	-3.08	0.176	92.94	13.24	2.53	2.67	
5-2-11	303	104.20	0.38	3	F	CTD	34.6875	105.14								
5-2-09	489	105.90	0.37	3	F	CTD	34.5707	107.22	7.96	-5.45	0.159	93.28	33.51	0.19	3.14	
5-2-08	651	104.96	0.44	2	F	CTD	34.5518	106.32								
	901								4.86	-3.40	0.155	93.31	0.00	0.00	0.00	
5-2-05	1099	104.49	0.12	2	F	CTD	34.5617	105.81	4.08	9.90	0.150	93.35	45.45	0.00	3.39	
	1300								3.51	25.28	0.152	93.37	44.66	0.00	3.29	
	1496								3.06	41.57	0.146	93.40	43.63	0.00	3.18	
	1696								2.70	56.06	0.146	93.42	42.72	0.00	3.09	
	1997								2.22	81.79	0.137	93.46	41.02	0.00	2.93	
5-2-23	11	104.91	0.00	1	UnF	CTD	34.4902	106.46								
5-2-21	20	104.92	0.00	1	UnF	CTD	34.4905	106.47								
5-2-20	44	103.22	0.72	2	UnF	CTD	34.7350	104.00								

A2.5Transect 5 continued.

Sample	Depth m	Mo nmol/kg	1 sd	n	Filter	Collec-tion method	Salinity ppt	Mo Salinity norm-alized nmol/kg	Temper-ature °C	Oxygen mmol/kg	Flouro-meter mg/kg	Trans-misson	NO_3^- µM	NO_2^- µM	PO_4^{3-} µM	Mn nM
5-2-19	54	105.72	0.00	1	UnF	CTD	34.4907	107.28								
5-2-18	65	106.11	0.00	1	UnF	CTD	34.5846	107.38								
5-2-17	74	105.91	0.00	1	UnF	CTD	34.6197	107.08								
5-2-16	84	106.39	0.83	2	UnF	CTD	34.6392	107.50								
5-2-15	104	106.09	0.00	1	UnF	CTD	34.7029	107.00								
5-2-14	129	104.97	0.93	1	UnF	CTD	34.7447	105.74								
5-2-13	154	107.47	0.00	1	UnF	CTD	34.7587	108.22								
5-2-12	203	106.78	0.00	2	UnF	CTD	34.7404	107.58								
5-2-11	303	106.23	0.00	1	UnF	CTD	34.6875	107.18								
5-2-09	489	105.19	0.00	1	UnF	CTD	34.5707	106.49								
5-2-08	651	106.54	0.00	1	UnF	CTD	34.5518	107.93								
5-2-05	1099	104.74	0.52	2	UnF	CTD	34.5617	106.06								

[a]Samples provided by Brian Popp and Eric DeCarlo

A2.6Transect 6 (15 00N 98 00W) June 2000 R/V Roger Revelle [a]

Sample	Depth	Mo	1 sd	n	Filter	Collec-tion	Salinity	Mo Salinity norm-alized	Temper-ature	Oxygen	Flouro-meter	Trans-misson	NO_3^-	NO_2^-	PO_4^{3-}	Mn
	m	nmol/kg				method	ppt	nmol/kg	°C	mmol/kg	mg/kg		µM	µM	µM	nM
6-2-24	13	103.16	0.35	3	F	CTD	34.1293	105.80	28.57	181.17	0.190	92.19	0.39	0.00	0.19	
6-2-22	23	101.65	0.41	3	F	CTD	34.1344	104.23	28.55	183.78	0.203	92.17	0.31	0.01	0.24	
6-2-21	32	104.41	0.97	2	F	CTD	34.3196	106.48	28.54	178.73	0.250	91.02	8.40	0.94	1.09	
6-2-20	43	105.65	0.14	3	F	CTD	34.5736	106.95	22.60	123.24	0.854	90.84	0.00	0.00	0.00	
6-2-19	52	105.33	0.31	2	F	CTD	34.6087	106.52	18.93	43.03	0.606	92.49	28.04	0.20	2.39	
6-2-18	63	105.01	0.00	1	F	CTD	34.7114	105.89	16.05	6.32	0.254	93.11	0.00	0.00	0.00	
6-2-17	73	104.91	0.12	2	F	CTD	34.7478	105.67	15.42	3.35	0.218	93.33	0.00	0.00	0.00	
6-2-16	92	106.35	0.35	2	F	CTD	34.7961	106.97	14.19	0.74	0.370	92.42	0.00	0.00	0.00	
6-2-15	152	105.08	0.43	2	F	CTD	34.8064	105.66	12.54	-0.42	0.161	92.81	29.31	1.08	2.51	
6-2-14	202	104.02	0.05	2	F	CTD	34.7741	104.70	11.79	-1.06	0.173	92.90	0.00	0.00	0.00	
	251								11.26	-1.67	0.174	92.80	27.87	1.90	2.64	
	301								10.52	-2.08	0.179	92.80	0.00	0.00	0.00	
6-2-11	351	106.04	0.15	2	F	CTD	34.6731	107.04	9.86	-2.60	0.181	92.83	26.12	1.94	2.89	
6-2-09	495	104.64	0.11	3	F	CTD	34.5970	105.86	7.95	-3.86	0.170	93.09	31.67	0.93	3.16	
6-2-08	699	104.93	0.02	2	F	CTD	34.5562	106.27	6.13	-5.47	0.153	93.30	41.85	0.00	2.97	
	998								4.66	1.09	0.158	93.26	0.00	0.00	0.00	
6-2-05	1098	104.63	0.65	2	F	CTD	34.5636	105.95	4.28	8.55	0.150	93.27	29.31	1.08	2.51	
6-2-04	1297	104.43	0.39	2	F	CTD	34.5828	105.69	3.60	25.19	0.149	93.32	0.00	0.00	0.00	
	1497								3.16	40.38	0.140	93.29	44.07	0.00	3.22	
6-2-02	1697	103.74	0.00	1	F	CTD	34.6151	104.90	2.81	53.12	0.145	93.23	42.99	0.00	3.13	
	1896								2.43	70.95	0.139	93.32	41.87	0.00	3.01	
6-2-24	13	103.78	0.00	1	UnF	CTD	34.1293	106.43								
6-2-22	23	104.84	0.00	1	UnF	CTD	34.1344	107.50								

A2.6Transect 6 continued.

Sample	Depth	Mo	1 sd	n	Filter	Collec-tion	Salinity	Mo Salinity norm-alized	Temper-ature	Oxygen	Flouro-meter	Trans-misson	NO_3^-	NO_2^-	PO_4^{3-}	Mn
	m	nmol/kg				method	ppt	nmol/kg	°C	mmol/kg	mg/kg		µM	µM	µM	nM
6-2-21	32	105.85	0.00	1	UnF	CTD	34.3196	107.95								
6-2-20	43	106.26	0.00	1	UnF	CTD	34.5736	107.57								
6-2-17	73	107.09	0.00	1	UnF	CTD	34.7478	107.87								
6-2-16	92	109.66	0.00	1	UnF	CTD	34.7961	110.30								
6-2-14	202	105.76	0.00	1	UnF	CTD	34.7741	106.45								
6-2-11	351	105.78	0.00	1	UnF	CTD	34.6731	106.78								
6-2-09	495	105.46	0.00	1	UnF	CTD	34.5970	106.69								

[a]Samples provided by Brian Popp and Eric DeCarlo

A2.7 Galapagos (1S 95W) November 2001 R/V Knorr

Sample	Depth	Mo	1 sd	n	Filter	Collec-tion	Salinity	Mo Salinity norm-alized	Temp-erature	Oxygen	Flouro-meter	Trans-misson	NO_3^-	NO_2^-	PO_4^{3-}	Mn
	m	nmol/kg				method	ppt	nmol/kg	°C	mmol/kg	mg/kg		µM	µM	µM	nM
3	3	110.20	0.00	3	UnF	CTD	34.9400	110.39	21.54	4.78	0.230		10.74	0.20		
10	10	107.90	0.00	3	UnF	CTD	34.9390	108.09	21.45	4.69	0.250		10.73	0.26	0.42	
20	20	109.70	0.00	3	UnF	CTD	34.9390	109.89	21.36	4.59	0.250		10.89	0.24	0.51	
30	30	109.50	0.00	3	UnF	CTD	34.9500	109.66	21.02	4.45	0.300		11.06	0.27	0.65	
40	40	113.20	0.00	3	UnF	CTD	35.0190	113.14	19.93	4.05	0.380		12.44	0.34	0.51	
50	50	109.70	0.00	3	UnF	CTD	35.0840	109.44	19.01	3.36	0.350		15.78	0.60	0.71	
65	65	108.90	0.00	3	UnF	CTD	35.0640	108.70	16.59	2.37	0.300		21.10	0.74	0.97	
80	80	108.60	0.00	3	UnF	CTD	35.0210	108.53	14.77	1.99	0.260		23.84	0.77	1.18	
95	95	106.60	0.00	3	UnF	CTD	34.9970	106.61	14.18	1.96	0.170		24.98	0.26		

A2.7 Galapagos continued.

Sample	Depth	Mo	1 sd	n	Filter	Collec-tion	Salinity	Mo Salinity norm-alized	Temp-erature	Oxygen	Flouro -meter	Trans-misson	NO_3^-	NO_2^-	PO_4^{3-}	Mn
	m	nmol/kg				method	ppt	nmol/kg	°C	mmol/kg	mg/kg		µM	µM	µM	nM
110	110	110.00	0.00	3	UnF	CTD	34.9440	110.18	13.91	2.05	0.110		25.42	0.15	1.21	
125	125	111.00	0.00	3	UnF	CTD	34.9500	111.16	13.46	2.31	0.060		24.12	0.00	1.35	
140	140	110.60	0.00	3	UnF	CTD	34.9350	110.81	13.31	2.33	0.030		23.87	0.00	1.40	
160	160	112.70	0.00	3	UnF	CTD	34.9240	112.95	13.15	2.07	0.010		26.31	0.00	1.44	
180	180	109.30	0.00	3	UnF	CTD	34.9160	109.56	13.05	1.53	0.010		29.18	0.00	1.50	
200	200	106.90	0.00	3	UnF	CTD	34.9100	107.18	12.91	1.39	0.010		30.20	0.00	1.56	
230	230	107.60	0.00	3	UnF	CTD	34.8940	107.93	12.75	1.50	0.000		30.59	0.00	1.50	
260	260	107.00	0.00	3	UnF	CTD	34.8870	107.35	12.59	1.46	0.000		30.78	0.00	1.68	
290	290	108.50	0.00	3	UnF	CTD	34.8700	108.90	12.18	0.85	0.000		33.99	0.00	1.82	
330	330	107.60	0.00	3	UnF	CTD	34.7680	108.32	10.80	0.78	0.000		35.74	0.00	1.87	
380	380								9.92	1.07	0.000		36.67	0.00	1.99	
450	450	106.50	0.00	3	UnF	CTD	34.6550	107.56	8.69	1.42	0.000		37.89	0.00	2.00	
600	600	107.60	0.00	3	UnF	CTD	34.5880	108.88	7.22	1.64	0.000		40.51	0.00	2.00	
800	800	107.95	0.92	3	UnF	CTD	34.5540	109.34	5.69	1.91	0.000		41.39	0.00	2.58	

A2.8 9N 1997 (9 49N 104 15W) December 1997 R/V Atlantis 3-11

Sample	Depth	Mo	1 sd	n	Filter	Collection	Salinity	Mo Salinity normalized	Temperature	Oxygen	Flouro-meter	Transmisson	NO_3^-	NO_2^-	PO_4^{3-}	Mn
	m	nmol/kg				method	ppt	nmol/kg	°C	mmol/kg	mg/kg		µM	µM	µM	nM
3-11-25 15	12	102.02	0.00	1	UnF	CTD	33.4416	106.78	28.35	170.82		87.99				
3-11-25 14	32	106.40	0.00	1	UnF	CTD	33.6198	110.76	27.10	156.34		87.90				
3-11-25 6	62	111.06	0.00	1	UnF	CTD	34.8594	111.51	14.77	4.83		89.70				
3-11-25 13	72	107.70	0.31	2	UnF	CTD	34.8801	108.07	13.84	5.17		89.78				
3-11-24 7	82	108.59	0.00	1	UnF	CTD	34.8602	109.02	13.95	5.40		89.93				
3-11-25 5	97	107.68	0.66	2	UnF	CTD	34.8866	108.03	13.10	10.71		89.85				
3-11-25 16	121	106.41	0.00	1	UnF	CTD	34.8733	106.79	12.76	14.76		89.93				
3-11-25 11	141	107.35	0.18	2	UnF	CTD	34.8571	107.79	12.48	18.80		89.98				
3-11-24 6	141	0.00	0.00	1	UnF	CTD	34.8431		12.54	18.21		90.08				
3-11-25 10	162	109.17	0.88	3	UnF	CTD	34.8419	109.67	12.18	23.47		90.02				
3-11-24 5	201	107.46	0.00	1	UnF	CTD	34.8082	108.05	11.63	26.45		90.08				
3-11-24 15	240	109.48	0.00	1	UnF	CTD	34.7956	110.12	11.14	18.18		90.03				
3-11-24 14	281	106.25	0.58	2	UnF	CTD	34.7845	106.90	10.83	11.46		90.00				
3-11-24 4	319	108.18	0.00	1	UnF	CTD	34.7693	108.89	10.49	7.93		90.02				
3-11-24 13	400	107.67	0.00	1	UnF	CTD	34.7340	108.49	9.69	-0.28		90.09				
3-11-03 5	460	107.12	0.42	3	UnF	CTD			0.00	0.00		0.00				
3-11-24 16	460		0.00	1	UnF	CTD	34.6876		8.80	-1.08		89.85				
3-11-25 4	461		0.00	1	UnF	CTD	34.6860		8.80	-0.91		89.93				
3-11-24 3a	520	107.42	0.00	1	UnF	CTD	34.6527	108.50	8.00	-0.97		89.83				
3-11-24 11	601	107.57	0.00	1	UnF	CTD	34.6352	108.70	7.17	-1.02		89.97				
3-11-24 10	799	108.22	0.00	1	UnF	CTD	34.6168	109.42	5.61	4.58		90.13				
3-11-24 3b	999	109.01	1.07	2	UnF	CTD	34.6265	110.19	4.72	20.81		90.19				
3-11-25 15	12	102.79	0.00	1	F	CTD	33.4416	107.59								
3-11-25 14	32	107.15	0.00	1	F	CTD	33.6198	111.55								

A2.8 9N 1997 continued

Sample	Depth	Mo	1 sd	n	Filter	Collec-tion	Salinity	Mo Salinity norm-alized	Temper-ature	Oxygen	Flouro -meter	Trans-misson	NO_3^-	NO_2^-	PO_4^{3-}	Mn
	m	nmol/kg				method	ppt	nmol/kg	°C	mmol/kg	mg/kg		µM	µM	µM	nM
3-11-25 6	62	110.47	1.45	2	F	CTD	34.8594	110.92								
3-11-25 5	97	109.55	1.86	2	F	CTD	34.8866	109.91								
3-11-25 10	162	95.00	1.41	2	F	CTD	34.8419									
3-11-25 4	461	107.37	0.00	1	F	CTD	34.6860	108.34	27.88	197.08						

A2.9 9N 2001 (9 49N 104 15W) December 2001 R/V Atlantis 7-5

Sample	Depth	Mo	1 sd	n	Filter	Collec-tion	Salinity	Mo Salinity norm-alized	Temper-ature	Oxygen	Flouro-meter	Trans-misson	NO_3^-	NO_2^-	PO_4^{3-}	Mn
	m	nmol/kg				method	ppt	nmol/kg	°C	mmol/kg	mg/kg		µM	µM	µM	nM
7-5-08 24	11	102.25	0.12	2	F	CTD	33.7407	106.07	27.72	177.41	0.455		0.33	0.06	2.93	
7-5-08 23	16	102.09	0.71	2	F	CTD	33.7945	105.73	27.71	179.92	0.415		0.84	0.05	2.93	
7-5-08 22	21	102.92	0.00	1	F	CTD	33.7992	106.57	27.69	175.14	0.394		2.26	0.16	3.06	
7-5-08 21	31	104.32	0.76	2	F	CTD	34.0375	107.27	25.85	70.15	0.363		15.26	1.76	3.28	
7-5-08 20	40	105.62	0.19	2	F	CTD	34.5532	106.99	19.56	28.24	0.259		25.30	0.67	3.34	
7-5-08 19	51	107.41	0.50	2	F	CTD	34.7354	108.23	16.30	-0.93	0.179		31.01	0.73	3.38	
7-5-08 18	60	105.94	0.38	2	F	CTD	34.8235	106.48	14.40	-2.65	0.140		32.23	0.08	3.39	
7-5-08 17	71	105.96	0.16	2	F	CTD	34.8459	106.43	13.81	-2.91	0.144		33.20	0.06	3.27	
7-5-08 16	81	107.78	0.27	2	F	CTD	34.8572	108.22	13.46	-2.98	0.139		33.99	0.09	3.33	
7-5-08 15	90	106.45	0.04	2	F	CTD	34.8568	106.89	13.21	-2.72	0.120		34.63	0.06	3.30	
7-5-08 14	102	104.74	0.07	3	F	CTD	34.8518	105.18	13.07	-2.22	0.118		34.97	0.03	3.18	
7-5-04 24	120	107.36	0.24	4	F	CTD	34.8270	107.89	12.64	-1.39	0.116		36.13	0.02	2.57	

A2.9 9N 2001 continued.

Sample	Depth m	Mo nmol/kg	1 sd	n	Filter	Collec-tion method	Salinity ppt	Mo Salinity norm-alized nmol/kg	Temper-ature °C	Oxygen mmol/kg	Flouro-meter mg/kg	Trans-misson	NO_3^- µM	NO_2^- µM	PO_4^{3-} µM	Mn nM
7-5-08 13	120			1	F	CTD	34.8380		12.79	-0.35	0.118		35.14	0.02	3.12	
7-5-04 23	140	105.98	0.15	2	F	CTD	34.8011	106.59	12.30	5.14	0.116		35.90	0.02	2.55	
7-5-04 22	160	105.31	0.00	1	F	CTD	34.7855	105.96	11.92	4.39	0.119		36.23	0.02	2.56	
7-5-04 21	180	105.01	0.44	2	F	CTD	34.7726	105.70	11.68	9.85	0.118		35.94	0.00	2.58	
7-5-04 20	200	105.94	0.00	1	F	CTD	34.7634	106.66	11.48	8.90	0.120		36.27	0.00	2.60	
7-5-04 19	220	106.42	0.01	3	F	CTD	34.7583	107.16	11.36	0.84	0.121		36.48	0.00	2.61	
7-5-04 18	240	105.36	0.43	2	F	CTD	34.7490	106.12	11.13	-3.93	0.122		34.97	0.00	2.29	
7-5-04 17	260	105.27	0.35	2	F	CTD	34.7407	106.05	10.96	-4.10	0.126		34.47	0.19	1.78	
7-5-04 16	290	105.39	0.05	2	F	CTD	34.7168	106.25	10.49	-4.22	0.128		29.06	2.53	0.70	
7-5-04 15	318	105.54	0.42	2	F	CTD	34.6884	106.49	10.04	-4.40	0.129		29.44	2.08	0.59	
7-5-04 14	350	104.43	0.72	2	F	CTD	34.6577	105.46	9.50	-4.55	0.128					
7-5-04 13	380	104.86	0.59	2	F	CTD	34.6291	105.98	8.85	-4.73	0.126		33.65	0.54	0.52	
7-5-05 22	450	104.86	0.28	3	F	CTD	34.6055	106.06	7.97	-5.23	0.128		34.96	0.88	2.91	
7-5-05 23	450				F	CTD	34.6055		7.96	-5.23	0.124		35.47	0.19	2.93	
7-5-05 20	500	104.63	0.49	2	F	CTD	34.5918	105.87	7.40	-5.54	0.124		38.76	0.56	2.80	
7-5-05 19	600	104.87	0.57	2	F	CTD	34.5722	106.17	6.31	-5.94	0.121		45.26	0.02	2.62	
7-5-05 18	800	104.71	0.36	2	F	CTD	34.5619	106.04	5.06	10.20	0.116		48.17	0.02	2.64	
7-5-05 17	1000	104.77	0.84	2	F	CTD	34.5706	106.07	4.35	24.42	0.116		47.78	0.02	2.61	
7-5-05 16	1492	104.99	0.32	2	F	CTD	34.6122	106.17	3.01	56.14	0.114		45.49	0.02	2.63	
7-5-05 14	2380	105.48	0.98	2	F	CTD	34.6716	106.47	1.85	106.17	0.105		42.06	0.02	2.60	
7-5-18G	10	103.31	2.17	2	F	Go-Flo	33.5800	107.68	0.04		0.481		0.66	0.04	0.48	
7-5-04G	20	102.91	2.26	2	F	Go-Flo	33.6090	107.17	0.16		0.642		2.88	0.16	0.64	
7-5-16G	20	103.09	1.70	2	F	Go-Flo	33.6090	107.36	0.02		0.313		0.72	0.02	0.31	

A2.9 9N 2001 continued.

Sample	Depth	Mo	1 sd	n	Filter	Collec-tion	Salinity	Mo Salinity norm-alized	Temper-ature	Oxygen	Flouro-meter	Trans-misson	NO_3^-	NO_2^-	PO_4^{3-}	Mn
	m	nmol/kg				method	ppt	nmol/kg	°C	mmol/kg	mg/kg		µM	µM	µM	nM
7-5-19G	20	101.29	0.00	1	F	Go-Flo	33.6090	105.48	0.05		0.484		0.86	0.05	0.48	
7-5-01G	28	100.42	0.00	1	F	Go-Flo	33.8250	103.91	0.08		0.552		1.63	0.08	0.55	
7-5-02G	28	101.99	0.00	1	F	Go-Flo	33.8250	105.54	0.06		0.568		1.98	0.06	0.57	
7-5-03G	28	103.50	2.68	2	F	Go-Flo	33.8250	107.10	0.07		0.404		1.37	0.07	0.40	
7-5-12G	28	101.97	0.00	1	F	Go-Flo	33.8250	105.51	0.09		0.768		4.50	0.09	0.77	
7-5-09G	44	106.84	0.00	1	F	Go-Flo	34.4450	108.56	0.00		2.147		24.31	0.00	2.15	
7-5-17G	45	105.04	0.00	1	F	Go-Flo	34.4450	106.73	1.09		2.341		26.14	1.09	2.34	
7-5-20G	65	105.92	0.55	2	F	Go-Flo	34.8100	106.50	0.02		2.528		31.63	0.02	2.53	
7-5-14G	75	105.29	0.00	1	F	Go-Flo	34.8450	105.76	0.02		2.541		32.83	0.02	2.54	
7-5-08G	88	105.68	0.10	2	F	Go-Flo	34.8450	106.15	0.03		2.580		32.73	0.03	2.58	
7-5-13G	105	105.67	0.08	2	F	Go-Flo	34.8500	106.13	0.02		2.518		34.98	0.02	2.52	
7-5-06G	120	107.08	1.79	3	F	Go-Flo	34.8400	107.57	0.02		2.586		34.76	0.02	2.59	
7-5-07G	140	105.26	0.40	2	F	Go-Flo	34.8100	105.83	0.00		2.599		35.10	0.00	2.60	
7-5-15G	165	105.64	0.00	1	F	Go-Flo	34.7900	106.28	0.00		2.593		35.71	0.00	2.59	
7-5-05G	200	105.83	0.00	1	F	Go-Flo	34.7700	106.53	0.02		2.538		34.48	0.02	2.54	
7-5-10G	330	105.04	0.42	2	F	Go-Flo	34.6750	106.03	0.38		2.786		29.41	1.61	3.13	
7-5-11G	380	105.22	0.12	2	F	Go-Flo	34.6400	106.31	1.61		3.132		32.66	0.38	2.79	

A2.10 Santa Barbara Basin (34 13N 120 02W) July 2001 R/V Pt. Sur

Sample	Depth	Mo	1 sd	n	Filter	Collec-tion	Salinity	Mo Salinity norm-alized	Tempe r-ature	Oxygen	Flouro -meter	Trans-misson	NO_3^-	NO_2^-	PO_4^{3-}	Mn
	m	nmol/kg				method	ppt	nmol/kg	°C	mmol/kg	mg/kg		µM	µM	µM	nM
5a-29-5	540	103.44	0.00	1	F	CTD	34.2300	105.76								
5a-29-4	550	102.92	0.05	2	F	CTD	34.2300	105.24								
5a-29-3	560	102.73	0.06	2	F	CTD	34.2300	105.04								
5a-29-2	570	103.06	0.27	2	F	CTD	34.2300	105.38								
5a-29-1	580	103.10	0.22	2	F	CTD	34.2300	105.41								

A2.11 San Nicholas (33 01N 119 03W) July 2001 R/V Pt. Sur

Sample	Depth	Mo	1 sd	n	Filter	Collec-tion	Salinity	Mo Salinity norm-alized	Temper -ature	Oxygen	Flouro -meter	Trans-misson	NO_3^-	NO_2^-	PO_4^{3-}	Mn
	m	nmol/kg				method	ppt	nmol/kg	°C	mmol/kg	mg/kg		µM	µM	µM	nM
11-25-9	1620	104.37	0.80		2F	CTD	34.5000	105.88								
11-25-7	1660	104.02	0.76		2F	CTD	34.5000	105.53								
11-25-5	1700	103.98	0.14		2F	CTD	34.5000	105.49								
11-25-3	1730	102.72	0.12		2F	CTD	34.5000	104.21								
11-25-1	1750	103.83	0.80		2F	CTD	34.5000	105.33								

A2.12 San Pedro Basin (33 35N 118 32W) July 2001 R/V Pt. Sur

Sample	Depth	Mo	1 sd	n	Filter	Collec-tion	Salinity	Mo Salinity norm-alized	Tempe r-ature	Oxygen	Flouro -meter	Trans-misson	NO_3^-	NO_2^-	PO_4^{3-}	Mn
	m	nmol/kg				method	ppt	nmol/kg	°C	mmol/kg	mg/kg		µM	µM	µM	nM
4 17 12	5	104.03	0.69	2	F	CTD	33.6300	108.27								
4-17-11	25	102.57	0.13	2	F	CTD	33.6000	106.85								
4-17-10	40	101.61	0.72	2	F	CTD	33.4700	106.25								
4-17-09	60	102.75	0.00	1	F	CTD	33.6500	106.87								
4-17-08	90	103.49	0.00	1	F	CTD	33.8100	107.14								
4-17-07	150	103.75	0.00	1	F	CTD	34.0200	106.74								
4-17-06	225	103.78	0.00	1	F	CTD	34.0500	106.67								
4-17-05	300	105.30	0.00	1	F	CTD	34.1900	107.80								
4-17-04	450	104.82	0.00	1	F	CTD	34.2800	107.02								
4-17-03	550	104.81	0.00	1	F	CTD	34.3300	106.86								
4-17-02	650	104.77	0.00	1	F	CTD	34.3600	106.73								
4-17-01	750	105.90	0.00	1	F	CTD	34.3900	107.78								
4-16-12	900	105.29	0.00	1	F	CTD	34.4400	107.00								
4-16-03	1480	104.69	0.00	1	F	CTD	34.4800	106.27								
4-16-02	1490	105.07	1.01	2	F	CTD	34.4800	106.65								
4-16-01	1500	105.48	0.30	2	F	CTD	34.4800	107.07								

A2.13 Tanner Basin (32 59N 119 45W) July 2001 R/V Pt. Sur

Sample	Depth	Mo	1 sd	n	Filter	Collec-tion	Salinity	Mo Salinity norm-alized	Temper-ature	Oxygen	Flouro-meter	Trans-misson	NO_3^-	NO_2^-	PO_4^{3-}	Mn
	m	nmol/kg				method	ppt	nmol/kg	°C	mmol/kg	mg/kg		µM	µM	µM	nM
1-06-12	5	105.02	0.09	2	F	CTD	33.5900	109.43								
1-06-11	15	101.60	1.81	2	F	CTD	33.5800	105.90								
1-06-10	30	102.43		1	F	CTD	33.4900	107.05								
1-06-09	45	102.82		1	F	CTD	33.4900	107.46								
1-06-07	90	103.19		1	F	CTD	33.6800	107.23								
1-06-06	145	104.25		1	F	CTD	34.0100	107.28								
1-06-05	225	103.60		1	F	CTD	34.1200	106.27								
1-06-04	300	104.76		1	F	CTD	34.2000	107.21								
1-05-09	520	104.25		1	F	CTD	34.3200	106.31								
1-05-07	610	104.76		1	F	CTD	34.3400	106.78								
1-05-05	710	104.04		1	F	CTD	34.3700	105.95								
1-06-03	840	105.83		1	F	CTD	34.3800	107.74								
1-06-02	850	103.75		1	F	CTD	34.3900	105.59								
1-05-02	860	103.71	0.08	3	F	CTD	34.3900	105.55								
1-06-01	870	105.83		1	F	CTD	34.3900	107.71								
1-05-01	880	104.44	0.62	2	F	CTD	34.3900	106.30								

Appendix 3 Statistical Analysis of Mo concentrations in seawater

A t test was used to determine whether the average concentration of Mo in each profile varied significantly from the average seawater concentrations of Mo (107.6 nmol kg^{-1}). A normal distribution was assumed for each profile. Filtered and unfiltered samples from the same profiles were treated as separate populations.

The t statistic is computed by

$$t = \frac{X - \mu_0}{s\sqrt{1/n}}$$

Where X is the mean of the profile, μ_0 is the hypothetical mean concentration of Mo in seawater (107.6 nmol kg^{-1}), n is the number of depths measured in the profile and s is the standard deviation of the profile.

The hypothesis being test is

$$H_0: \mu_1 \leq \mu_0$$

Against the alternative

$$H_1: \mu_1 > \mu_0$$

The null hypothesis states that the mean of the profile is equal or less than 107.6 nmol kg^{-1}, while the alternative hypothesis is that the profile is greater than 107.6 nmol kg^{-1}. The Critical value for the t test are determined from the degrees of freedom, v=n-1, and the selected level of significance, α=5%. Tables of critical values of t can be found in (Kellaway 1968). Where t greater than the critical value H_0 can be rejected, leaving the H_1 which indicates that the concentration of the profile is greater than the average

seawater value of Mo. If t is less than the critical value then the only conclusion possible is that there is no evidence that the concentration of the profile is greater then 107.6 nmol kg^{-1}. Note that this is not saying that it is less then 107.6 nmol kg^{-1}, only that ther is nothing to suggest that it is greater.

The t test above only considered the positive portion of a normal distribution. It can be turned around to consider the negative side of a normal distribution using the equation

$$t = \frac{\mu_0 - X}{s\sqrt{1/n}}$$

This equation tests the hypothesis

$$H_0: \mu_1 \geq \mu_0$$

Against the alternative

$$H_1: \mu_1 < \mu_0$$

Now the null hypothesis states that the mean of the profile is equal or greater than 107.6 nmol kg^{-1}, while the alternative hypothesis is that the profile is less than 107.6 nmol kg^{-1}.

For this negative t test, a t greater than the critical value indicates that the concentration of the profile is less than 107.6 nmol kg^{-1}. If t is less than the critical value then the only conclusion possible is that there is no evidence that the concentration of the profile is less then 107.6 nmol kg^{-1}.

Table A3.1 shows the results of positive and negative t tests for all of the dissolved Mo profiles present in Chapter 3 (Tuit 2003). Samples where t is greater than the critical value are shown in bold. These data support comparisons of standard error of

population (Figure 3.10). Profiles with bold negative t test have average values less than average seawater. These include the 16 N transect profiles except for the unfiltered samples from station 2, the 9N 2001 profile and all of the Borderland Basin profiles. If the Borderland Basin profiles are compared to average Mo concentrations above the sill depth, rather than average seawater, only the Santa Barbara and San Nicholas Basins are significantly depleted. Profiles with bold positive t test have average values greater than average seawater. These include the Galapagos and 9N 1997 profiles. The Sargasso and Arabian Sea profiles were neither greater than nor less than the average seawater values.

Table A3.1 Results of t test comparing profiles to average seawater Mo concentrations (107.6 nmol kg^{-1}.)

	Filtered	X	s	n	Critical value	Positive t test	Negative t test
Profiles							
Transect 6	F	106.0	0.8	17	1.746	-8.791	**8.791**
	UnF	107.2	0.6	8	1.895	-2.303	**2.303**
Transect 5	F	106.5	0.6	15	1.761	-7.038	**7.038**
	UnF	106.8	1.0	15	1.761	-3.090	**3.090**
Transect4	F	106.3	0.5	17	1.746	-10.244	**10.244**
	UnF	106.6	0.6	7	1.943	-4.332	**4.332**
Transect 2	F	106.1	0.7	14	1.771	-8.483	**8.483**
	UnF	106.9	0.7	4	2.353	-2.173	2.173
9N 2001	F	106.5	0.7	31	1.697	-9.581	**9.581**
Galapagos	UnF	109.3	1.7	22	1.721	**4.357**	-4.357
9N 1997	F	109.7	1.7	5	2.132	**2.656**	-2.656
	UnF	108.8	1.4	21	1.725	**3.588**	-3.588
Sargasso Sea	F	107.5	0.5	12	1.796	-1.159	1.159
Arabian Sea	F	107.9	0.3	3	2.920	1.048	-1.048
	UnF	107.8	0.6	16	1.753	0.717	-0.717
Santa Barbara below sill	F	105.4	0.3	5	2.132	-19.272	**19.272**
San Nicholas below sill	F	105.3	0.6	5	2.132	-8.388	**8.388**
Tanner above sill	F	107.1	0.6	13	1.782	-3.872	**3.872**
Tanner below sill	F	106.7	0.4	3	2.92	-4.379	**4.379**
San Pedro above sill	F	107.0	1.0	11	1.812	-2.302	**2.302**
San Pedro below sill	F	106.6	1.1	5	2.132	-2.250	**2.251**

Table A3.21 Results of t test comparing California Borderland Basin profile below sill depth the average above sill depth concentrations (107.0 nmol kg^{-1}.)

	Filtered	X	s	n	Critical value	Positive t test	Negative t test
Santa Barbara below sill	F	105.4	0.3	5	2.132	-13.667	**13.667**
San Nicholas below sill	F	105.3	0.6	5	2.132	-6.029	**6.029**
Tanner above sill	F	107.1	0.6	13	1.782	0.486	-0.486
Tanner below sill	F	106.7	0.4	3	2.920	-1.462	1.462
San Pedro above sill	F	107.0	1.0	11	1.812	-0.041	0.041
San Pedro below sill	F	106.6	1.1	5	2.132	-0.871	0.871

A3.1 References

Kellaway, F. W. 1968. Penguin-Honeywell book of Tables, p. 75. Penguin Books Ltd.